uOttawa

L'Université canadienne
Canada's university

FACULTÉ DES ÉTUDES SUPÉRIEURES ET POSTOCTORALES

uOttawa

L'Université canadienne
Canada's university

FACULTY OF GRADUATE AND POSDOCTORAL STUDIES

Rodrigo Ivan Serna Guerrero
AUTEUR DE LA THÈSE / AUTHOR OF THESIS

M.A.Sc. (Chemical Engineering)
GRADE / DEGREE

Department of Chemical and Biological Engineering
FACULTÉ, ÉCOLE, DÉPARTEMENT / FACULTY, SCHOOL, DEPARTMENT

Triamine-grafted Pore-expanded Mesoporous Silica for Carbon Dioxide Adsorption in Closed-circuit Breathing Systems

TITRE DE LA THÈSE / TITLE OF THESIS

Sayari Abdelhamid
DIRECTEUR (DIRECTRICE) DE LA THÈSE / THESIS SUPERVISOR

CO-DIRECTEUR (CO-DIRECTRICE) DE LA THÈSE / THESIS CO-SUPERVISOR

Boguslaw Kruczek

Handan Tezel

Marten Ternan

Christopher Jones

Gary W. Slater
Le Doyen de la Faculte des etudes superieures et postdoctorales / Dean of the Faculty of Graduate and Postdoctoral Studies

Triamine-grafted pore-expanded mesoporous silica for carbon dioxide adsorption in closed-circuit breathing systems

by Rodrigo Ivan Serna-Guerrero

Thesis submitted to the

Faculty of Graduate and Postdoctoral Studies

in partial fulfillment of the requirements for the degree of

Doctorate in Philosophy

In the

Department of Chemical and Biological Engineering

University of Ottawa

© Rodrigo Serna-Guerrero, Ottawa, Canada 2010

Library and Archives Canada

Published Heritage Branch

395 Wellington Street
Ottawa ON K1A 0N4
Canada

Bibliothèque et Archives Canada

Direction du Patrimoine de l'édition

395, rue Wellington
Ottawa ON K1A 0N4
Canada

Your file Votre référence
ISBN: 978-0-494-74237-2
Our file Notre référence
ISBN: 978-0-494-74237-2

NOTICE:

The author has granted a non-exclusive license allowing Library and Archives Canada to reproduce, publish, archive, preserve, conserve, communicate to the public by telecommunication or on the Internet, loan, distribute and sell theses worldwide, for commercial or non-commercial purposes, in microform, paper, electronic and/or any other formats.

The author retains copyright ownership and moral rights in this thesis. Neither the thesis nor substantial extracts from it may be printed or otherwise reproduced without the author's permission.

AVIS:

L'auteur a accordé une licence non exclusive permettant à la Bibliothèque et Archives Canada de reproduire, publier, archiver, sauvegarder, conserver, transmettre au public par télécommunication ou par l'Internet, prêter, distribuer et vendre des thèses partout dans le monde, à des fins commerciales ou autres, sur support microforme, papier, électronique et/ou autres formats.

L'auteur conserve la propriété du droit d'auteur et des droits moraux qui protège cette thèse. Ni la thèse ni des extraits substantiels de celle-ci ne doivent être imprimés ou autrement reproduits sans son autorisation.

In compliance with the Canadian Privacy Act some supporting forms may have been removed from this thesis.

While these forms may be included in the document page count, their removal does not represent any loss of content from the thesis.

Conformément à la loi canadienne sur la protection de la vie privée, quelques formulaires secondaires ont été enlevés de cette thèse.

Bien que ces formulaires aient inclus dans la pagination, il n'y aura aucun contenu manquant.

Canada

Abstract

In the search for efficient, less energy-intensive alternatives for CO_2 capture, and inspired by the scrubbing processes using liquid amine solutions, amine groups have been incorporated onto porous supports. Our research group tailored mesoporous materials type MCM-41 by enlarging their pore size to incorporate a high content of readily available amine groups. In earlier studies, triamine-grafted pore-expanded mesoporous silica (TRI-PE-MCM-41) presented large CO_2 removal capacity combined with a fast rate of adsorption. This thesis focused on evaluating TRI-PE-MCM-41 as CO_2 adsorbent by determining a variety of adsorptive properties with the aim of gaining a deep understanding of its behavior and to outline its advantages and limitations.

The CO_2-amine chemistry in gas-solid processes was investigated under humid and dry conditions using aminopropyl-grafted pore-expanded MCM-41 silica (MONO-PE-MCM-41). To draw accurate conclusions regarding CO_2 adsorption in the presence of water vapor, an analytical method coupling thermogravimetric analysis (TGA) and mass spectrometry (MS) was developed. The CO_2/N molar ratio in dry streams was close to 0.5, consistent with the formation of carbamate and, as the relative humidity in the feed increased, the CO_2/N ratio increased up to 0.88, in line with the gradual formation of bicarbonate.

With respect to the effect of moisture on TRI-PE-MCM-41, it was found that its capacity for CO_2 in dry streams was enhanced by ca. 17% in streams with 74% relative humidity. In addition, breakthrough curve analysis using a packed-bed column was performed for CO_2 mixtures in dry and humid air. The results showed a practically infinite selectivity of TRI-PE-MCM-41 towards CO_2 over N_2 and O_2. While water vapor was also removed by TRI-PE-MCM-41, it did not adsorb competitively with CO_2.

With the aim of predicting the behavior of fixed-bed columns packed with amine-functionalized adsorbents, we developed equilibrium and kinetic models capable of describing CO_2 adsorption on TRI-PE-MCM-41 under various operating conditions. A new semi-empirical equilibrium model was developed based on the assumption that adsorption of CO_2 occurs via two independent mechanisms: (i) chemical adsorption on the amine functional groups, and (ii) physisorption on the surface of the adsorbent. To investigate the adsorption kinetics of CO_2 on TRI-PE-MCM-41, experimental data of CO_2 uptake as a

function of time at temperatures between 25 and 70 °C were fit to a series of kinetic models, namely Lagergen's pseudo-first and pseudo-second order and Avrami's kinetic models. The best fit was obtained using Avrami's model, as it provided a fractional reaction order (ca. 1.4), which has been associated with the occurrence of multiple adsorption pathways. Using the aforementioned equilibrium and kinetic models, a series of simulations of CO_2 adsorption in a column packed with amine-grafted mesoporous silica was carried out to predict breakthrough curves. The simulation results were compared with experimental data produced at various flow rates of a stream of 5% CO_2/N_2. In all cases, the predicted breakthrough time and the corresponding CO_2 uptake were in close agreement with the experimental data.

To further support the potential of TRI-PE-MCM-41 for commercial scale applications, it was necessary to demonstrate its stability throughout intensive cycling. The behavior of the adsorbent was evaluated in batch experiments, via adsorption-desorption cycling using various regeneration conditions. Using a 2^3 factorial design of experiments, the impact on the performance of the adsorbent of different levels of temperature, pressure and flow rate of purge gas during desorption was determined. It was found that all the investigated parameters have a statistically significant influence on the working adsorption capacity, but only temperature is influential with respect to desorption rate. If vacuum is applied, regeneration can be achieved at a temperature as low as 70 °C with only a 13 % penalty in terms of working adsorption capacity. It was also demonstrated that under the proper regeneration conditions, TRI-PE-MCM-41 is stable over 100 adsorption-desorption cycles.

The final chapter of this thesis dealt with the potential application of TRI-PE-MCM-41 as CO_2 scrubber in closed-circuit breathing systems, including a first evaluation in a commercial-scale setup. A comparative study between currently used soda lime and TRI-PE-MCM-41 showed that although the former has a significantly higher CO_2 uptake, it was negatively affected by high flow rates, while the former suffered a lower impact, attributed to fast adsorption kinetics. The performance of TRI-PE-MCM-41 in an anesthesia delivery unit under real operating conditions is presented. Under the current configuration, lower adsorption capacities than those at laboratory-scale testing were measured. Discussion of this low performance and recommendations for future work are included.

Résumé

Dans le but de trouver des solutions efficaces et beacoup moins consommatrices d'énergie pour la capture de CO_2, et en s'inspirant des procédés d'absorption utilisant les solutions liquides aminées, des groupements amine ont été incorporés sur des supports poreux. Notre groupe de recherche a réussis a concevoir des matériaux mésoporeux de type MCM-41 en élargissant leur taille de pore dans le but d'incorporer une quantité élevée des groupements amine, facilement accessibles. Des études antérieures ont montré que la silice mesoporeuse avec pores élargis et triamine incorporé (TRI-PE-MCM-41) présente une grande capacité et une vitesse élevée pour l'adsorption de CO_2. Cette Thèse est consacrée a l'évaluation de TRI-PE-MCM-41 comme adsorbant de CO_2 en déterminant une série de propriétés d'adsorption, afin d'approfondir la compréhension de son comportement et de déterminer ses avantages et ces inconvénients.

Dans ce travail, les interactions entre le CO_2 et les groupements amine dans un procédé gaz-solide ont été étudiées dans des conditions humides et sèches en utilisant la silice MCM-41 à pores élargies avec propylamine incorporé (MONO-PE-MCM-41). Afin d'obtenir des conclusions précises concernant l'adsorption de CO_2 en présence de vapeur d'eau, une méthode analytique couplant l'analyse thermogravimétrique (TGA) et la spectrométrie de masse (MS) a été développée. Le rapport molaire CO_2/N dans le cas de l'adsorption de CO_2 sec était proche de 0.5, correspondant à la formation de carbamate , alors qu'en présence accrue d'humidité, le taux de CO_2/N atteignait 0.88, conforme à la formation progressive du bicarbonate.

En ce qui concerne l'effet de l'humidité, la capacité d'adsorption du CO_2 sec sur TRI-PE-MCM-41 a été ameliorée de ca. 17% en presence de 74 % d'humidité relative. En outre, des courbes de perçage utilisant une colonne à lit fixe ont été obtenues pour des mélanges de CO_2 avec l'air sec et humide. Les résultats montrent une sélectivité CO_2/N_2 et CO_2/O_2 pratiquement infinie en faveur du CO_2. Bien que l'adsorption de la vapeur d'eau sur TRI-PE-MCM-41 soit significative, elle a un effect positif sur l'adsorption.

Dans le but de prédire le comportement des colonnes à lit fixes utilisant des adsorbants avec amines incoporées, des modèls d'équilibre et de cinétique capables de décrire

le comportement d'adsorption du CO_2 sur TRI-PE-MCM-41 dans diverses conditions de fonctionnement ont été développés et analysés. Le nouveau modèle d'équilibre semi-empirique développé est basé sur la supposition que l'adsorption du CO_2 a lieu selon deux mécanismes indépendants: (i) l'adsorption chimique sur les groupements fonctionnels aminés, et (ii) l'adsortion physique sur la surface de l'adsorbant. Afin d'étudier la cinétique d'adsorption du CO_2 sur TRI-PE-MCM-41, des données expérimentales d'adsorption de CO_2 en fonction du temps a différentes températures, dans une gamme de 25 a 70 °C, ont été ajustées à différentes modèles cinétiques, à savoir le modèle de Lagergen pseudo-premier et pseudo-deuxième et le modèle cinétique d'Avrami. Le meilleur ajustement a été obtenu en utilisant le modèle d'Avrami, car il a permis de fournir un ordre fractionnaire de réaction (ca. 1.4). Ce dernier a été associé à la présence de différents régimes d'adsorption. Utilisant les modèles d'équilibre et cinétiques mentionnés ci-dessus, une série de simulations d'adsorption de CO_2 dans une colonne à lit fixe en utilisant TRI-PE-MCM-41 a été effectuée pour prédire des courbes de perçage. Les résultats de simulation ont été comparés aux données expérimentales produites avec différent flux gazeux de 5% CO_2/N_2. Dans tous les cas étudiés, le temps de saturation et les capacités d'adsorption du CO_2 predis étaient en très bon accord avec les données expérimentales.

Afin de prouver le potentiel de TRI-PE-MCM-41 pour des applications à l'échelle commerciale, il était nécessaire de démonter sa stabilité durant de multiples cycles d'adsorption et de désorption. Le recyclage de l'adsorbant a été évalué en utilisant diverses conditions de régénération. Utilisant un plan factoriel d'expériences 2^3, les performances de l'adsorbant à différents niveaux de température, de pression et de flux de gaz de purge pendant la désorption, ont été déterminées. Il a été constaté que tous les paramètres étudiés ont une influence statistiquement significative sur la capacité effective d'adsorption, mais seulement la température a une influence sur la vitesse de désorption. Lorsque le vide s'applique, la régénération peut être réalisée à une température aussi basse que 70 °C avec une pénalité de seulement 13% en termes de capacité effective d'adsorption. Il a été également démontré que dans des conditions appropriées de régénération, TRI-PE-MCM-41 est stable durant plus de 100 cycles d'adsorption et de désorption.

Le chapitre final de cette thèse traite de l'application de TRI-PE-MCM-41 comme épurateur de CO_2 dans les systèmes de respiration de circuit fermé, et aussi une première

évaluation d'une installation commerciale. Une étude comparative a montré que la chaux sodée a une capacité d'adsorption de CO_2 sensiblement plus élevée que TRI-PE-MCM-41. Mais a cause de sa vitesse d'adsorption élevée, la capacité de TRI-PE-MCM-41 est beaucoup moins affectée par des débits gazeux élevés que la chaux sodée. Les performances de TRI-PE-MCM-41 dans une unité de livraison d'anesthésie dans de conditions réelles de fonctionnement sont présentées. Dans de telles conditions, des capacités d'adsorption plus faibles comparativement au test de laboratoire ont été obtenues. Une discussion concernant ces résultats ainsi que des recommandations pour des travaux futurs sont incluses.

Acknowledgements

As I was in the final stages of writing this thesis, I realized that this, like any other story, is about a girl Years ago, I found myself in Ottawa, a city I had never seen before, far away from my hometown of Pachuca in Mexico, following a beautiful girl It was then that I decided I would chase this girl at the same time that I would pursue another one of my dreams to obtain a Doctorate degree

So, it seems like it was only yesterday when I was standing at Prof Abdel Sayari's office with nothing else but a very short CV and good intentions, asking him to accept me in his research group In the distance, I understand that it was nothing short of a leap of faith he took by taking me under his supervision and for that, I will always be thankful to him In the years since, I have found his guidance invaluable and his dedication to research an example to follow I want to express my gratitude to him for all his support throughout these years

I also take this opportunity to thank my colleagues at Prof Sayari's group for all their assistance in bringing this work to life Particularly, I want to thank Youssef Belmabkhout for all the fruitful discussions and ideas that helped to improve the quality of my research To him and everyone else for offering me their friendship, I thank you

Of course, this thesis would not have been possible without the financial support of the institutions that believed in this project Thus, I wish to thank the Mexican National Council for Science and Technology (CONACYT) and the Government of Ontario for granting me scholarships throughout my Doctoral studies The National Science and Engineering Research Council also supported this work through the Collaborative Health Research Project

I also want to make a special mention to all my family To my brothers Gabriel and Fernando, for all the good times we have shared We might be far away, but you are my best friends To my parents Gabriel and Martha, whose guidance and unconditional support have allowed me to achieve every important goal in my life you know I love you and you are always in my mind

And about the girl? Worry not, my dear reader! I think she was convinced of my love after seeing me travel 3600 km just to be close to her, and we are married now Gabriela, this thesis is especially dedicated to you

Statement of Contributions of Collaborators

I hereby declare that I am the sole author of this thesis. I performed the experimental design, all experiments and the associated data analysis.

My supervisor, Prof. Abdelhamid Sayari provided continual guidance throughout this work and made editorial comments and corrections to my written work.

Enshira Da'na proposed the synthesis conditions of the aminopropyl-grafted adsorbent. She is the co-author of the manuscript presented in Chapter 4.

Dr. Youssef Belmabkhout provided assistance to obtain data from gravimetric measurements using a magnetic suspension microbalance. He is the co-author of the manuscripts presented in Chapters 5, 6 and 8.

Table of Contents

List of Figures

List of Tables

List of Symbols and Abbreviations

Symbols

A = Arrhenius preexponential factor
b = Coefficient of the Toth isotherm model (bar^{-1})
c = Dimensionless constant of the BET isotherm model
C_A = Concentration of the adsorbate in the gas phase (mol mL^{-1})
C_{Ai} = Concentrations of any gas *i* downstream a fixed bed column (mol mL^{-1})
C_{0i} = Feed concentration of gas *i* into a fixed bed column (mol mL^{-1})
C_F = Correction factor of the KJS method equal to 3 Å
D_L = Axial dispersion of the adsorbate in the gas stream (cm^2 s^{-1})
d_p = Mean pore diameter (nm)
D_S = Diffusivity within a solid (cm^2 s^{-1})
E_a = Activation energy (kJ mol-1)
F = Total molar flow (mol min^{-1})
F_D = Purge gas flow (mL min^{-1})
ΔH = Heat of adsorption at a surface coverage close to zero (kJ mol^{-1})
k_A = Avrami's model adsorption kinetic constant (s^{-1})
k_f = Pseudo-first order model adsorption kinetic constant (s^{-1})
k_s = Pseudo-second order model adsorption kinetic constant (g $mmol^{-1}$ s^{-1})
n_{adsi} = Working adsorption capacity of any gas *i* (mmol g^{-1})
n_s = Coefficient of the Toth isotherm model (mmol g^{-1})
P = Adsorbate gas pressure (bar)
P_0 = Saturation pressure (bar)
P_D = Desorption pressure (bar)
q = Adsorption capacity (mmol g^{-1})
$\Delta q(\%)$ = Normalized standard deviation
q_{AVG} = Average working adsorption capacity (mmol g^{-1})
Δq_{AVG} = Average change of adsorption capacity between cycles (mmol g^{-1})
q_b = Adsorption capacity at breakthrough (mmol g^{-1})
q_e = Amount adsorbed at equilibrium (mmol g^{-1})
q_{exp} = Experimentally measured amounts of CO_2 adsorbed (mmol g^{-1})
q_{chem} = CO_2 uptake by amine groups via chemical adsorption (mmol g^{-1})
q_m = Adsorption capacity on a monolayer (mmol g^{-1})
q_{mod} = Predicted amounts of CO_2 adsorbed (mmol g^{-1})
q_{phys} = CO_2 uptake by physisorption on the adsorbent surface (mmol g^{-1})
q_s = Amount adsorbed at partial pressure close to $P/P_0 = 1$
$q_{support}$ = Adsorption capacity of the purely siliceous mesoporous support (mmol g^{-1})
q_t = Amount adsorbed at a given point in time (mmol g^{-1})
N = Number of experimental data points available
r = Pore radius as a function of relative pressure (nm)
r_{AVG} = Average rate of desorption (mmol g^{-1} s^{-1})
r_p = Radius of a particle (nm)
R = Universal ideal gas constant (mL bar mol^{-1} K^{-1})
S = Surface area of the amine-containing adsorbent (m^2 g^{-1})

S_A = Surface area (m^2 g^{-1})
$S_{support}$ = Surface area of the purely siliceous mesoporous support (m^2 g^{-1})
t = Time elapsed since the beginning of the adsorption process (s)
t = Coefficient of the Toth isotherm model
T = Adsorption temperature (°C)
T_0 = Reference temperature (K)
t_b = Breakthrough time (s)
T_D = Desorption temperature (°C)
T_A = Adsorption temperature (°C)
T_{back} = Temperature at the back of the canister in anesthesia delivery unit (°C)
T_D = Desorption temperature (°C)
T_{front} = Temperature at the front of the canister in anesthesia delivery unit (°C)
T_{middle} = Temperature at the middle of the canister in anesthesia delivery unit (°C)
t_{ni} = Stoichiometric time corresponding to gas *i* (s)
u_s = Superficial velocity of the gas mixture (m s^{-1})
V_L = Volume of the adsorbate in the liquid state at the adsorption temperature relative to the volume of gas at standard conditions of temperature and pressure
V_m = Molar volume of the liquid adsorbate (mL mol^{-1})
V_p = Pore volume (mL g^{-1})
W = Mass of adsorbent loaded in the column (g)
Y = Statistical model's measured response
z = Column length in the axial direction (m)

α = Coefficient of the temperature-dependent form of the Toth isotherm model
β_i = Coefficients of the statistical model
γ = Surface tension (N cm^{-1})
ε = Bed void fraction
χ = Coefficient of the temperature-dependent form of the Toth isotherm model
τ = Statistical film thickness (nm)

Abbreviations
ADU = Anesthesia delivery units
DI-silane = [3-(2-aminoethylamino)propyl]trimethoxysilane
DMDA = Dimethyldecylamine
CCBS = Closed-circuit breathing systems
CTAB = Cetyltrimethylammonium bromide
IUPAC = International Union of Pure and Applied Chemistry
OMS = Ordered Mesoporous Silica
PE-MCM-41 = Pore-expanded MCM-41 silica
PE-MCM-41E = Pore-expanded MCM-41 with DMDA extracted by ethanol
PVOH = Polyvinyl alcohol
MEA = Monoethanolamine
MOF = Metal organic framework
MONO-PE-MCM-41 = Aminopropyl-grafted pore-expanded MCM-41 silica
MONO-silane = (3-aminopropyl)trimethoxysilane

MS = Mass spectrometery
PEI-PE-MCM-41 = Polyethylenemine impregnated pore-expanded MCM-41 silica
RH = Relative humidity
TGA = Thermogravimetric analysis
TLS = Translucent Liquid Sculpey ®
TMAOH = Tetramethylammonium hydroxide
TPD = Temperature programmed desorption
TRI-PE-MCM-41 = Triamine-grafted pore-expanded MCM-41 silica
TRI-PE-MCM-41(dry) = Triamine-grafted pore-expanded MCM-41 silica produced via dry grafting
TRI-PE-MCM-41B = TRI-PE-MCM-41 agglomerates produced using binder
TRI-silane = 2-[2-(3-trimethoxysilylpropylamino)ethylamino]ethylamine
TS = Temperature swing adsorption
TVS = Temperature-vacuum swing adsorption

...y así, del poco dormir y el mucho leer, se le secó el celebro,

de manera que vino a perder el juicio.

(...and what with little sleep and much reading, his brains got so dry

that he lost his wits.)

Miguel de Cervantes Saavedra,

Don Quixote

Chapter 1

Introduction

The current debate about carbon dioxide (CO_2) emissions and their impact on climate change has prompted a thorough search for more efficient alternatives to the gas separation technologies currently used in industry. While such efforts have been mainly driven by the necessity to minimize CO_2 emissions from fossil fuel combustion processes, either as end-of-the-line [Sakamoto, 2007] or in acid-gas sweetening processes [Cavenati, 2006; Schladt, 2007], some of the technologies developed are promising in other fields where carbon dioxide represents an undesired species in the process. Such is the case of closed circuit breathing systems (CCBS) used to supply oxygen in confined spaces such as submarine or aerospace travel [Ernsting, 1999]. CCBS also find applications as mobile systems to permit human activities in highly adverse environments like mining or rescue missions [Moore, 2007]. Another quite important application of CCBS is found in anesthesia delivery systems, where they are used to recycle breathing gases and expensive anesthetics, minimizing operating costs during medical interventions [Baum, 1996].

The need for a closed breathing system is a result of the low efficiency in oxygen intake by humans since only about 25% of it is used, the rest being exhaled. The role of CCBS is to minimize the use of fresh breathing gases by cycling them back into the breathing loop. To make use of the recycled gases, it is necessary to remove the exhaled carbon dioxide from the system to avoid its presence at concentrations considered hazardous in the breathing loop [Dosch, 2003]. Thus, it is compelling to have a system where CO_2 levels are maintained at a minimum, despite the fluctuations in breathing rate of the user and the inherent humidity present in these systems.

For more than 60 years, the CO_2 scrubber market for CCBS has been dominated by systems using soda lime, a calcium hydroxide-based absorbent with various contents of strong bases like NaOH or KOH whose popularity lies on its low cost [Baum, 1996]. Soda lime removes CO_2 from gas streams via a chemical reaction that produces solid carbonates, promoted by strong bases as presented in Scheme 1.1.

$$CO_2 + H_2O \longrightarrow H_2CO_3$$

$$H_2CO_3 + 2NaOH\ (or\ KOH) \longrightarrow Na_2CO_3\ (or\ K_2CO_3) + 2H_2O$$

$$Na_2CO_3\ (or\ K_2CO_3) + Ca(OH)_2 \longrightarrow CaCO_3 + 2NaOH\ (or\ KOH)$$

Scheme 1.1. Typical reaction pathway for the absorption of CO_2 on soda lime

Unfortunately, several drawbacks with respect to the use of soda lime have been identified. In the first place, for being an absorbent that reacts chemically with CO_2, it is used in a single-use-then-dispose basis, which generates large quantities of solid waste with its subsequent management costs. Further, the rate of absorption of the material decreases with time since the reaction takes place within the calcium hydroxide-carbonate interface, which moves progressively towards the center of the particle. Thus, the active material (i.e., $Ca(OH)_2$) is easily available only at the very beginning of the reaction, making it harder for the CO_2 molecules to reach the receding interface as the reaction proceeds.

Beside the aforementioned constraints related to the very nature of the soda lime absorbents, other operating problems have been encountered. It was found that the CO_2 removal capacity of soda lime absorbents is decreased in humid streams [Kobayashi, 2003]. This effect is not desirable since humidity is present in any working CCBS due to the very nature of human breathing. Furthermore, humidity is required in the gas streams of anesthesia machines to avoid irritation in the respiratory system of the patient. In addition, some safety issues have been raised with the use of soda lime scrubbers in medical applications. It has been established that due to the presence of strong bases like KOH and NaOH in soda lime, it degrades some common anesthetics, particularly chlorinated volatile products, producing what is commonly known as Compound A ($CF_2=C(CF_3)OCH_2F$) [Keijzer, 2007a; Marini, 2007]. This compound has been associated with the development of cancer in animal studies, and thus its presence in breathing systems must be avoided at all costs. The production of other undesired compounds like carbon monoxide, ethanol, formaldehyde and hydrogen in closed-circuit anesthesia machines using dry soda lime is also well documented [Wissing 2001; Laster, 2005; Dunning III, 2007; Keijzer 2007b]. To avoid the production of such poisonous compounds, a common practice has been to humidify the soda lime before loading it into the anesthesia delivery apparatus but, as mentioned before, this results in a decreased capacity for CO_2 removal. For all the above-mentioned reasons, it

is deemed necessary to develop a safer alternative to the currently used absorbent technology in CCBS.

Within the years, soda lime absorbents have undergone minor changes on its chemical composition to improve its performance, but these "new" materials present only small variations on their concentration of KOH and/or NaOH and operate under the same principle of carbonate production [Murray 1999; Mchaourab, 2001]. The alleged advantages are mainly a lower production of toxic components but some of them offer only about 50% of the CO_2 absorption capacity of regular soda lime [Ueyama, 2000; Higuchi, 2001].

To overcome the aforementioned limitations of the currently used soda lime technology, the research project hereby presented focused on an innovative approach for the removal of CO_2 in CCBS. Compared to the solid or liquid absorption systems studied by the vast majority of research groups, adsorption separation is a technology that requires a lower energy input during operation and regeneration of the scrubber material for recycling and reuse. To that aim, a novel material developed by our research group, a triamine-grafted pore-expanded mesoporous silica (TRI-PE-MCM-41) was proposed as CO_2 adsorbent. In preliminary studies, this adsorbent exhibited an adsorption performance that made it promising for CO_2 capture in many gas mixtures, including those typically found in CCBS [Harlick and Sayari, 2007]. In addition, contrary to conventional soda lime, this novel CO_2 adsorbent does not contain strong bases, and therefore it is unlikely to generate toxic byproducts.

Because of the similar conditions encountered in CCBS streams and those in flue gas, i.e., total pressure close to atmospheric and CO_2 concentrations of ca. 10%, it is expected that some of the findings in this thesis may be also useful in the development of technologies for post combustion CO_2 capture. Consequently, some of the discussion throughout this thesis also involves the performance of TRI-PE-MCM-41 for CO_2 adsorption from a flue gas treatment perspective.

1.1 Thesis Structure

This work is focused on gaining a better understanding on the characteristics of amine-functionalized materials in order to establish the potential and limitations of TRI-PE-MCM-41 as CO_2 adsorbent. It is thus a contribution toward the development of amine-

functional adsorbents for CO_2 capture. It is expected that the findings of this thesis will set a basis on which to build proper strategies for the application of the proposed adsorbent. The present thesis is organized as follows:

Chapter 2, Amine-Functionalized Pore-Expanded MCM-41: A promising adsorbent for CO_2. A general discussion on the development of ordered mesoporous materials in general, and amine-functionalized materials in particular, is provided. This chapter aims at providing the reader with a background on why the use of amine-functional mesoporous materials for CO_2 capture is attractive.

Chapter 3, Synthesis and Characterization of TRI-PE-MCM-41. This section presents a detailed explanation on the synthesis of the adsorbent and the determination of its structural and chemical characteristics. The method to successfully produce amine-functionalized materials in a hundreds-of-grams scale is described, along with appropriate agglomeration procedures.

Chapter 4, New insights into the interactions of CO_2 with amine-functionalized silica. To gain a clear understanding on the phenomena occurring between supported amines and CO_2, a series of experiments were performed to investigate the interaction mechanisms involved. An experimental method coupling thermogravimetric analysis and mass spectrometry was proposed to reliably calculate CO_2 adsorption capacity at equilibrium in humid streams. In addition, the seemingly disparate efficiencies of CO_2 adsorption on supported amines reported in literature were rationalized.

Chapter 5, Further investigations of CO_2 capture using triamine-grafted, pore-expanded mesoporous silica. A series of studies evaluating the performance of TRI-PE-MCM-41 under conditions relevant to CO_2 capture in CCBS and post-combustion streams is presented. Adsorption capacity in dry and humid mixtures at equilibrium and in fixed bed columns were calculated, along with a preliminary study on regeneration conditions including temperature swing and temperature-vacuum swing configurations.

Chapter 6, Modeling CO_2 adsorption on amine-functionalized mesoporous silica. 1. A semi-empirical equilibrium model. One of the most important characteristics of an adsorbent is its capacity at equilibrium, as it represents its full uptake potential. In this chapter, CO_2 adsorption isotherms at various temperatures in a wide range of pressure are

presented. In addition, a new semi-empirical equilibrium model capable of describing CO_2 adsorption on amine-functionalized mesoporous materials is proposed for the first time.

Chapter 7, Modeling adsorption of CO_2 on amine-functionalized mesoporous silica. 2. Kinetics and breakthrough curves. In this chapter, an in-depth study on the kinetics of CO_2 adsorption on TRI-PE-MCM-41 at various temperatures is presented, and a series of kinetic models for CO_2 adsorption on amine-functionalized materials are proposed for the first time. A comparison with polyethyleneimine-impregnated mesoporous silica is also provided. Based on the equilibrium and kinetic models proposed, CO_2 breakthrough curves were predicted at various flow rates.

Chapter 8, Influence of regeneration conditions on the cyclic performance of amine-grafted mesoporous silica for CO_2 capture: An experimental and statistical study. Since one of the main attractions of adsorption separation technologies is the possibility to regenerate the adsorbent, a study on the regeneration of TRI-PE-MCM-41 under temperature swing and temperature-vacuum swing configurations is presented. The influence of regeneration parameters, i.e., temperature, pressure and purge gas flow, on the adsorption and desorption behavior of TRI-PE-MCM-41 is presented and the possibility to regenerate it over a hundred cycles was demonstrated.

Chapter 9, Triamine-grafted pore-expanded mesoporous silica for CO_2 scrubbing in closed-circuit breathing systems. The final chapter of this thesis was devoted to the study of TRI-PE-MCM-41 as a potential replacement for soda lime in CCBS. A comparative study between the performance of TRI-PE-MCM-41 and soda lime in a fixed bed column under a variety of flow rates and stream compositions was performed. In addition, a preliminary study on the performance of TRI-PE-MCM-41 in a commercial CCBS under real operating conditions is presented.

References

J.A. Baum, *Low Flow Anaesthesia*. Ed. Butterworth-Heinemann, New York, 1996

S. Cavenati, C.A. Grande, A. Rodrigues, Removal of carbon dioxide from natural gas by vacuum pressure swing adsorption. *Energy Fuels*, 20 (2006) 2648

M.P. Dosch, *The Anesthesia Gas Machine*. Electronic version available at www.udmercy.edu/crna/agm, 2003

M.B. Dunning III, L.E. Bretscher, S.R. Arain, Y. Symkowski, H.J. Woehlck, Sevoflurane breakdown produces flammable concentrations of hydrogen. *Anesthesiology* 106 (2007) 144

J. Ernsting, Breathing systems in aerospace, *IEE Colloquium (Digest)* 60, (1999) 24

P.J.E. Harlick, A. Sayari, Applications of pore-expanded mesoporous silica. 5. Triamine grafted material with exceptional CO_2 dynamic and equilibrium adsorption performance. *Ind. Eng. Chem. Res.*, 46, 2 (2007) 446

H. Higuchi, Y. Adachi, S. Arimura, M. Kanno, T. Satoh, The carbon dioxide absorption capacity of Amsorb® is half that of soda lime. *Anesth. Analg.*, 93 (2001) 221

C. Keijzer, R.S.G.M. Perez, J.J. de Lange, Compound A and carbon monoxide production from sevoflurane and seven different types of carbon dioxide absorbent in a patient model. *Acta Anesthesiol. Scand.* 51 (2007a) 31

C. Keijzer, R.S.G.M. Perez, J.J. de Lange, Detection of carbon monoxide production as a result of the interaction of five volatile anesthetics and desiccated sodalime with an electrochemical carbon monoxide sensor in an anesthetic circuit compared to gas chromatography. *J. Clini. Monit. Computing* 21 (2007b) 257

S. Kobayashi, H. Bito, T. Katoh, S. Sato, Effect of humidity in the circuit on the CO_2 absorption capacity of Amsorb and Sodasorb II. *J. Anesth.* 17, (2003) 145

M.J. Laster, E.I. Eger II, Temperatures in soda lime during degradation of desflurane, isoflurane, and sevoflurane by desiccated soda lime. *Anesth. Analg.*, 101 (2005) 753

F. Marini, I. Bellugi, D. Gambi, M. Pacenti, S. Dugheri, L. Focardi, G. Tulli, Compound A, formaldehyde and methanol concentrations during low-flow sevoflurane anesthesia: comparison of three carbon dioxide absorbers. *Acta Anesthesiol Scand.* 51 (2007) 625

A. Mchaourab, S.R. Arain, T.J. Ebert, Lack of degradation of sevoflurane by a new carbon dioxide absorbent in humans. *Anesthesiology* 94 (2001) 1007

P. Moore, Miner protection, *Mining Magazine* 196 (2007) 35

J. M. Murray, C.W. Renfrew, A. Bedi, C.B. McCrystal, D.S. Jones, J.P.H. Fee, Amsorb: A new carbon dioxide absorbent for use in anesthetic breathing systems. *Anesthesiology* 91 (1999) 1342

Y. Sakamoto, K. Nagata, K. Yogo, K. Yamada, Preparation and CO_2 separation properties of amine-modified mesoporous silica membranes. *Microporous Mesoporous Mater.* 101 (2007) 303

M.J. Schladt, T.P. Filburn, J.J. Helble, Supported amine sorbents under temperature swing absorption for CO_2 and moisture capture. *Ind. Eng. Chem. Res.* 46 (5), pp. 1590

H. Ueyama, M. Takashina, T. Suzuki, V. Sriranganathan, T. Mashimo, Warning: Carbon dioxide absorption capacity of Amsorb was unexpectedly low in low-flow anesthesia. *Anesthesiology* 93 (2000) 1560

H. Wissing, I. Kuhn, U. Warnken, R. Dudziak, Carbon monoxide production from desflurane, enflurane, halothane, isoflurane and sevoflurane with dry soda lime. *Anesthesiology* 95 (2001) 1205

Chapter 2

Amine-functionalized, pore-expanded MCM-41: A promising adsorbent for CO_2

Since their discovery [Beck et al., 1992; Kresge et al., 1992], ordered mesoporous silicas (OMS) have drawn the attention of the scientific community in such areas as catalysis, adsorption, materials science and nanotechnology. These materials present characteristics that are highly appreciated in any catalyst, adsorbent or catalyst support like high surface area, narrow pore size distribution, large pore volume [Kruk and Jaroniec, 2001] and in some cases mechanical and thermal stability [Wu, 2001]. The distinctive characteristic of OMS is the periodic distribution of pores with sizes in the mesopore range, i.e., 2 to 50 nm according to the International Union of Pure and Applied Chemistry (IUPAC) classification. Further, there are a number of synthesis strategies to tailor their pore size without affecting significantly other structural properties. Consequently, extensive effort has been devoted to the study and exploitation of OMS. Several authoritative reviews on the synthesis, modification and applications of OMS are readily available (e.g., Sayari [1996], Sayari and Liu [1997], Stein et al., [2000], Asefa [2002], Hoffman [2006]).

In general, the synthesis of OMS consists of the hydrolysis of silica in the presence of a supramolecular template, the most common being surfactants (neutral, anionic or cationic) and polymers. Due to the wide variety of templates available and synthesis conditions, the pores in OMS can be arranged in several different geometries. MCM-41, one of the most widely studied OMS and the material explored in this work presents a 2 dimensional hexagonal arrangement of pore channels, also known as "honeycomb" pore structure [Sayari et al., 2000]. It is believed that MCM-41 pores have an almost perfectly cylindrical shape and are not interconnected, making it useful as a reference material to establish and validate theoretical adsorption-based models with experimental results [Kruk et al., 1997; Morishige and Nakamura, 2004].

Several synthesis strategies have been developed to control the pore size of MCM-41 and other silica mesophases. Changing the size of the hydrocarbon chain in alkyltrimethylammonium salts afforded MCM-41 with pores in the range of 2 to 4.5 nm. [Beck, et al., 1992; Sayari and Yang, 2000; Vartuli et al., 2001]. Pore sizes up to 7 nm can be achieved by adjusting the synthesis temperature [Corma et al., 1997; Cheng et al., 1997, Kruk et al. 1999]. To further

increase the pore opening of MCM-41, additional organic molecules have been used as expander agents either during synthesis or by post-synthesis hydrothermal treatment [Sayari et al , 1999] It has been documented that under appropriate conditions, pore sizes can be expanded up to the range of 10-20 nm. The typical steps of synthesis and post-synthesis pore expansion of MCM-41 are represented in Figure 2.1

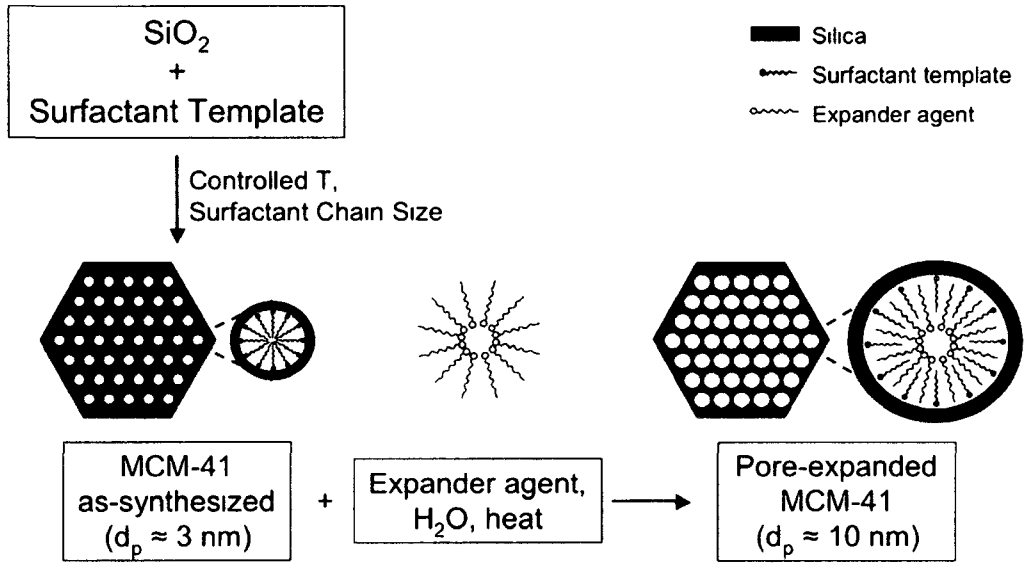

Figure 2.1 Synthesis of MCM-41 and post-synthesis hydrothermal modification

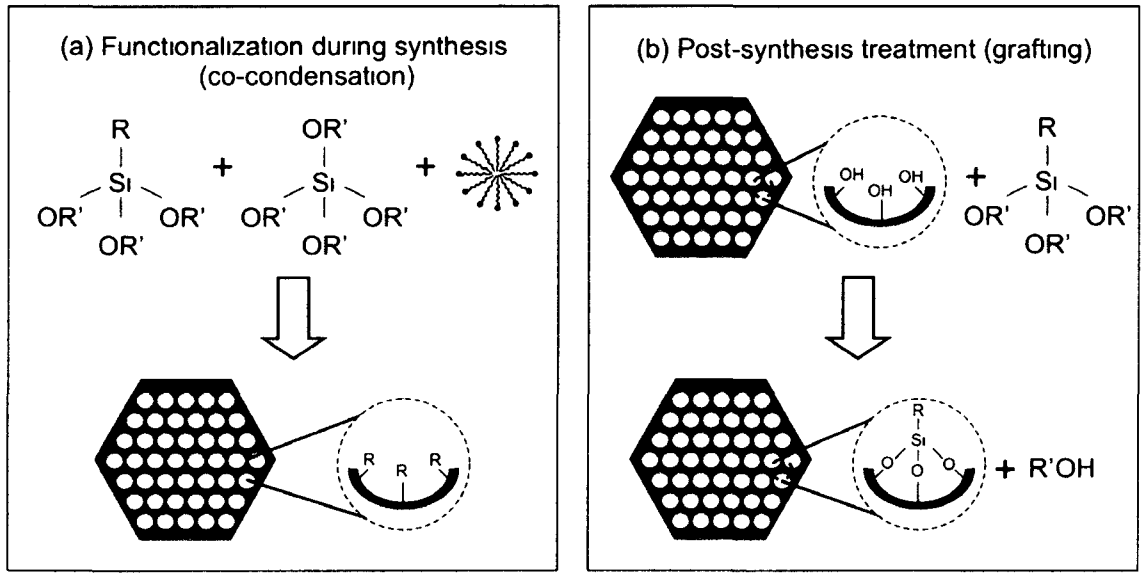

Figure 2.2 Functionalization of OMS by two main routes: grafting and co-condensation

In addition, the siliceous structure of the material permits the incorporation of organic functional groups, thus allowing the design of materials with specific surface properties [Stein et al., 2000; Sayari and Hamoudi, 2001]. This feature has been exploited in the field of adsorption to enhance or diminish the compatibility of OMS toward particular adsorbates. As represented in Figure 2.2, there are two main routes explored for the synthesis of organically functionalized MCM-41: (i) the use of organosilanes during synthesis along with the silica precursor, which results in the direct incorporation of the organic functionality onto the surface of the pore walls (Figure 2.2a), and (ii) the incorporation of organic functionalities by post-synthesis treatment, a process commonly known as grafting (Figure 2.2b). As can be seen, OMS offer the flexibility to be modified into materials with properties tuned for a particular application. Hence, there is a possibility to achieve appropriate surface properties for enhanced compatibility with CO_2.

Driven mainly by environmental concerns such as climate change, the use of adsorption-based technologies have been proposed in recent years for capture of CO_2 from gas streams [Sircar, 2002]. While the industrially used process of CO_2 absorption in liquid amines has proven efficient, it presents several drawbacks including the corrosive nature of amine solutions [Veawab et al., 1999; Li, 2008]. In addition, liquid amine scrubbing is an energy intensive process, particularly during regeneration of the CO_2-loaded solution [Feng et al., 2010]. As an alternative to liquid absorption, the use of solid adsorbents for the separation of CO_2 does not produce wastewater and the CO_2 separated can be released at high concentrations either for confinement or reuse. The adsorption separation processes proposed so far have suggested the use of zeolites, which exhibit an acceptable capacity for CO_2 [Li and Tezel, 2007]. It has been determined, however, that zeolites present a strong affinity with water, resulting in a significant decrease of CO_2 capacity in humid streams [Brandani and Ruthven, 2004].

To develop a highly efficient adsorbent for CO_2, several research groups have explored the amine-CO_2 chemistry for adsorption applications. Recently, Choi et al., [2009] published a comprehensive review on novel materials for CO_2 capture, including a detailed account on amine-functionalized adsorbents. In general, amine groups have been supported on porous solids following two methods: impregnation of liquid organic amines and grafting of amine-bearing silanes. Amine-impregnated adsorbents have produced materials with high loading of amine groups, which in some cases resulted in high adsorption capacity at equilibrium. However they present some limitations including a low stability due to the weak interactions between the

amine-functional groups and the support. In addition, amine-impregnated materials, typically containing polyethyleneimine or tetraethylenepentamine, present severe diffusion limitations at temperatures close to ambient, restricting their operation at temperatures higher than ca. 60 °C, preferably at 70-75 °C. In the case of amine-grafted materials, the organic loading is a function of the availability of surface hydroxyl groups to anchor the silane. Nevertheless, when properly designed, amine-grafted adsorbents present high rate of adsorption and an efficient use of amine functional groups even at low temperatures. Furthermore, the covalent bonding of organic groups endows these materials with improved stability, compared to their impregnated counterparts.

In an effort to obtain a suitable CO_2 adsorbent, our research group explored systematically the improvements that could be obtained by using OMS as supports of amine groups. In first place, and differently from other studies published earlier, a pore-expanded MCM-41 (PE-MCM-41) was used as support. This support exhibits a unique combination of high surface area (ca. 1000 m^2g^{-1}), large pores (up to 25 nm) and large pore volume (up to 3.6 $cm^3\ g^{-1}$). Because of its wide-open pore structure, PE-MCM-41 permitted the loading of a large number of readily available amine groups. In the work by Franchi et al. [2005], diethanolamine was loaded directly on PE-MCM-41 resulting in a higher CO_2 uptake than 13X, particularly in the presence of moisture. It was also demonstrated that the amine-impregnated silica has a better stability during adsorption-desorption cycles compared to other adsorbents and that its capacity could be restored by heating in an inert environment at 140 °C in contrast to 400 °C required for the regeneration of 13X zeolite.

Chemically bonded functional groups were subsequently studied using different amine-silanes with the aim of improving the OMS performance. Silanes with one, two and three amine groups per molecule (Figure 2.3) were grafted onto PE-MCM-41 and evaluated as CO_2 adsorbents [Harlick and Sayari, 2005]. It was found that the triamine-functionalized, pore-expanded mesoporous silica (namely, TRI-PE-MCM-41) had the highest adsorption capacity, attributed to its high density of functional groups. With the use of TRI- PE-MCM-41, it was possible to achieve higher adsorption capacities than 13X in dry streams at low concentrations (<15 mol%) of CO_2 [Harlick and Sayari, 2006].

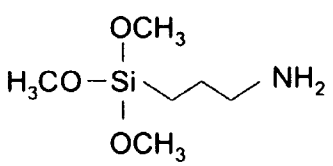

(3-Aminopropyl)trimethoxysilane

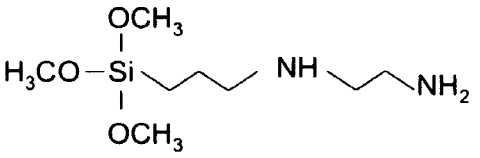

[3-(2-Aminoethylamino)propyl]trimethoxysilane

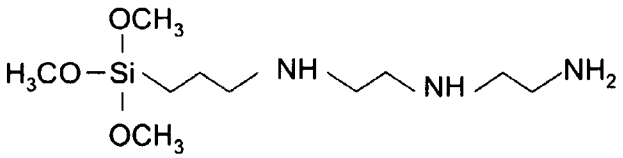

*N*¹-(3-Trimethoxysilylpropyl)diethylenetriamine

Figure 2.3 Molecular structure of amine-containing silanes

To further improve the efficiency of amine grafting, a systematic addition of water during the incorporation of functional groups was carried out. The process of grafting in the presence of small quantities of water is sometimes referred to as coating [Stein et al., 2000] since it is believed to allow the incorporation of silanes beyond a single layer on the silica surface. In the study by Harlick and Sayari, [2007] it was found that addition of water during grafting resulted indeed in higher loadings of amine groups on PE-MCM-41 (Figure 2.4a). However, beyond a certain amine loading, the CO_2 adsorption capacity began to decrease. As can be seen in Figure 2.4b, a maximum efficiency of CO_2 adsorption was obtained with the addition of approximately 0.3 cm^3 of water per gram of silica. Beyond this point, the adsorption capacity for CO_2 decreases despite the increase in amine loading. This was attributed to the polymerization of silane molecules, producing a network of organic molecules that hampers the diffusion of CO_2 molecules into the adsorption sites.

TRI-PE-MCM-41 was tested as adsorbent for dry and humid (27% relative humidity) streams containing 5% CO_2 and compared to 13X under the same conditions. While the adsorption capacity of 13X was dramatically decreased from 2.05 mmol g^{-1} in dry streams to 0.09 mmol g^{-1} in the presence of moisture, TRI-PE-MCM-41 exhibited a slightly higher capacity in humid streams than in dry streams, being 2.94 and 2.65 mmol g^{-1}, respectively.

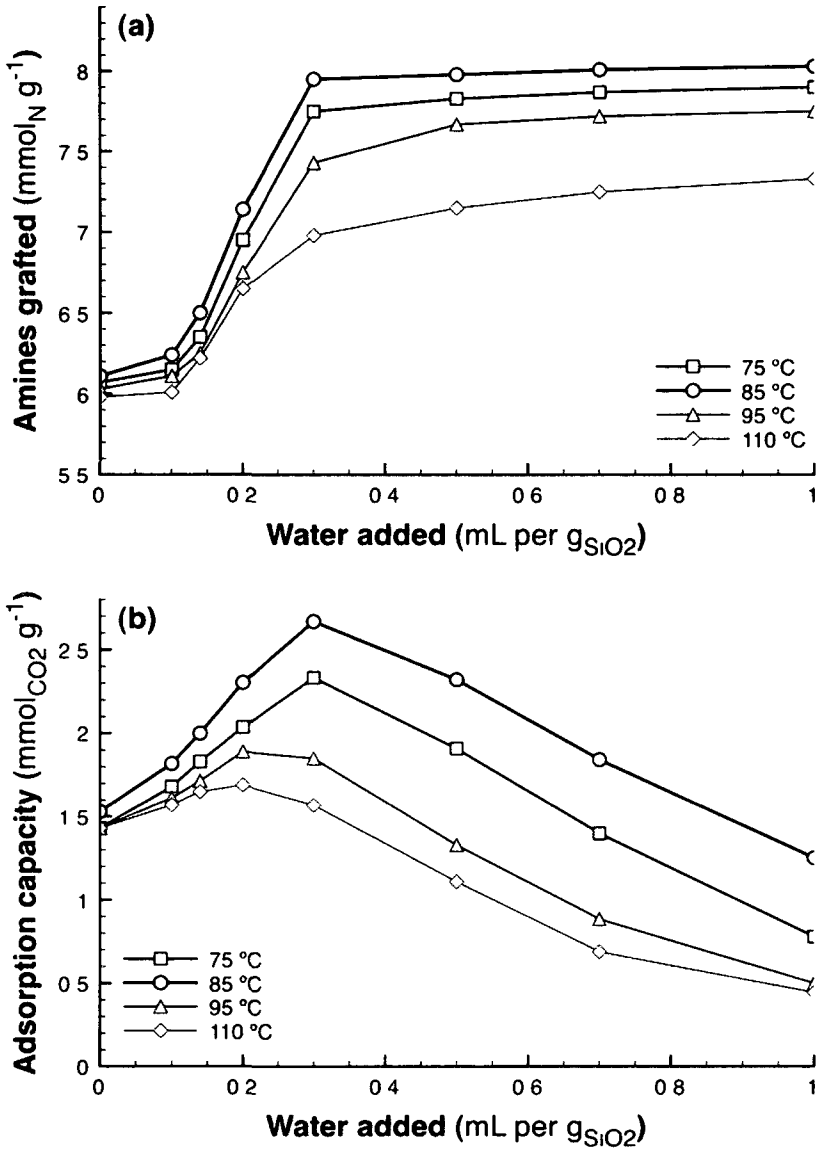

Figure 2.4 Effect of the grafting temperature and water content on (a) amount of amine grafted and (b) the adsorption capacity of 5% CO_2 in N_2 on TRI-PE-MCM-41 [Harlick and Sayari, 2007]

As a result of those studies, an optimum recipe for the production of a highly efficient and water-tolerant adsorbent was proposed, although based on trials producing approximately one gram of adsorbent per batch The present work includes in Chapter 3 a contribution toward the production of large batches (ca 0 5 kg) of TRI-PE-MCM-41 In addition, this thesis provides an in-depth study on the properties and behavior of TRI-PE-MCM-41 with the aim of establishing its potential and limitations The results obtained in this work will contribute to the

advance of CO_2 capture technologies using amine-grafted mesoporous materials, particularly for applications in closed-circuit breathing systems.

References

T. Asefa, G.A. Ozin, H. Grondey, M. Kruk, M. Jaroniec, Recent developments in the synthesis and chemistry of periodic mesoporous organosilicas *Stud. Surf. Sci. Catal.* 141 (2002) 1

J.S. Beck, J.C. Vartuli, W.J. Roth, M.E. Leonowicz, C.T. Kresge, K.D. Schmitt, C.T.W. Chu, D.H. Olson, E.W. Sheppard, S.B. McCullen, J.B. Higgins, J.L. Schlenker, A new family of mesoporous molecular sieves prepared with liquid crystal templates. *J. Am. Chem. Soc.* 144 (1992) 10834

F. Brandani, D. M. Ruthven, The effect of water on the adsorption of CO_2 and C_3H_8 on type X zeolites. *Ind. Eng. Chem. Res.* 43 (2004) 8339

C.F. Cheng, W. Zhou, D.H. Park, J. Klinowski, M. Hargreaves, L.F. Gladden, Controlling the channel diameter of the mesoporous molecular sieve MCM-41. *J. Chem. Soc. Faraday Trans.* 93, 2 (1997) 359

S. Choi, J.H. Drese, C.W. Jones, Adsorbent materials for carbon dioxide capture from large anthropogenic point sources. *ChemSusChem* 2 (2009) 796

A. Corma, Q. Kan, M.T. Navarro, J. Perez-Pariente, F. Rey, Synthesis of MCM-41 with different pore diameters without addition of auxiliary organics. *Chem. Mater.* 9 (1997) 2123

B. Feng, M. Du, T.J. Dennis, K. Anthony, M.J. Perumal, Reduction of energy requirements of CO_2 desorption by adding acid into CO_2-loaded solvent. Energy Fuels 24 (2010) 213

R.S. Franchi, P.J.E. Harlick, A. Sayari, Applications of pore-expanded mesoporous silica. 2. Development of a high-capacity, water tolerant adsorbent for CO_2. *Ind. Eng. Chem. Res.* 44 (2005) 8007

P.J.E. Harlick, A. Sayari, Amine grafted, pore-expanded MCM-41 for acid gas removal: Effect of grafting temperature, water, and amine type on performance. *Stud. Surf. Sci. Catal.* 158B (2005) 987

P.J.E. Harlick, A. Sayari, Applications of pore expanded mesoporous silica. 3. Triamine silane grafting for enhanced CO_2 adsorption. *Ind. Eng. Chem. Res.* 45 (2006) 3248

P.J.E. Harlick, A. Sayari, Applications of pore-expanded mesoporous silica. 5. triamine grafted material with exceptional CO2 dynamic and equilibrium adsorption performance. *Ind. Eng. Chem. Res.* 46 (2007) 446

F. Hoffmann, M. Cornelius, J. Morell, M. Froba, Silica-based mesoporous organic–inorganic hybrid materials. *Angew. Chem. Int. Ed.* 45 (2006) 3216

H.Y. Huang, R.T. Yang, D. Chinn, C.L. Munson, Amine-grafted MCM-48 and silica xerogel as superior sorbents for acidic gas removal from natural gas, *Ind. Eng. Chem. Res.* 42 (2003) 2427

R.A. Khatri, S.S.C. Chuang, Y. Soong, M. Gray, Carbon dioxide capture by diamine-grafted SBA-15: A combined Fourier transform infrared and mass spectrometry study. *Ind. Eng. Chem. Res.* 44 (2005) 3702

C.T. Kresge, M.E. Leonowicz, W.J. Roth, J.C. Vartuli, J.S. Beck, Ordered mesoporous molecular sieves synthesized by a liquid-crystal template mechanism. *Nature* 359 (1992) 710

M. Kruk, M. Jaroniec, A. Sayari, Application of large pore MCM-41 molecular sieves to improve pore size analysis using nitrogen adsorption measurements. *Langmuir* 13 (1997) 6267

M. Kruk, V. Antochshuk, M. Jaroniec, A. Sayari, New approach to evaluate pore size distributions and surface areas for hydrophobic mesoporous solids. *J. Phys. Chem. B* 103, 48 (1999) 10670

M. Kruk, M. Jaroniec, Characterization of modified mesoporous silicas using argon and nitrogen adsorption. *Microporous Mesoporous Mater.* 44-45 (2001) 725

Y. Li, Study on corrosion and material selection for desulphurization unit in refinery. *Petroleum Refinery Eng.* 38 (2008) 24

K. Morishige, Y. Nakamura, Nature of adsorption and desorption branches in cylindrical pores. *Langmuir* 20 (2004) 4503

P. Li, H. Tezel, Equilibirum and kinetic analysis of CO_2-N_2 adsorption separation by concentration pulse chromatography. *J. Colloid Interf. Sci.* 313 (2007) 12

A. Sayari, Periodic mesoporous materials: Synthesis, characterization and potential applications. *Stud. Surf. Sci. Catal.* 102 (1996) 1

A. Sayari, P. Liu, Non-silica periodic mesostructured materials: recent progress. *Micropor. Mater.* 12 (1997) 149

A. Sayari, Y. Yang, M. Kruk, M. Jaroniec, Expanding the pore size of MCM-41 silicas: use of amines as expanders in direct synthesis and postsynthesis procedures. *J. Phys. Chem. B.* 103

(1999) 3651

A. Sayari, S. Hamoudi, Y. Yang, I.L. Moudrakovski, J.R. Ripmeester, New insights into the synthesis, morphology, and growth of periodic mesoporous organosilicas. *Chem. Mater.* 12 (2000) 3857

A. Sayari, Y. Yang, Highly ordered MCM-41 silica prepared in the presence of decyltrimethylammonium bromide. *J. Phys. Chem. B* 104 (2000) 4835

A. Sayari, S. Hamoudi, Periodic mesoporous silica-based organic-inorganic nanocomposite materials. *Chem. Mater.* 13 (2001) 3151

S. Sircar, Pressure swing adsorption. *Ind. Eng. Chem. Res.* 41 (2002) 1389

A. Stein, B.J. Melde, R.C. Schroden, Hybrid inorganic-organic mesoporous silicates – nanoscopic reactors coming of age. *Adv. Mater.* 12 (2000) 1403

J.C. Vartuli, A. Malek, W.J. Roth, C.T. Kresge, S.B. McCullen, The sorption properties of as-synthesized and calcined MCM-41 and MCM-48. *Microporous Mesoporous Mater.* 44-45 (2001) 691

A. Veawab, P. Tontiwachwuthikul, A. Chakma, Corrosion behavior of carbon steel in the CO_2 absorption process using aqueous amine solutions. *Ind. Eng. Chem. Res.* 38 (1999) 3917

J. Wu, M.M. Abu-Omar, S.H. Tolbert, Fluorescent probes of the molecular environment within mesostructured silica/surfactant composites under high pressure. *Nano Lett.* 1 (2001) 27

F. Zheng, D.N. Tran, B.J. Busche, G.E. Fryxell, R.S. Addleman, T.S. Zemanian, C.L. Aardahl, Ethylenediamine-modified SBA-15 as regenerable CO_2 sorbent, *Ind. Eng. Chem. Res.* 44, 9, (2005) 3099

Chapter 3

Synthesis and characterization of TRI-PE-MCM-41

As explained in the preceding sections, triamine-grafted pore-expanded MCM-41 silica (TRI-PE-MCM-41) exhibited promising characteristics for the separation of CO_2 in dry and humid streams during earlier studies [Harlick and Sayari, 2006; Harlick and Sayari, 2007]. To provide further evidence on the advantages of this adsorbent, this thesis explored in depth the properties of TRI-PE-MCM-41 for its use in commercial applications, focusing on closed-circuit breathing systems (CCBS) and its potential as a replacement of the currently used soda lime-based technology. Although the synthesis of TRI-PE-MCM-41 was optimized earlier [Harlick and Sayari, 2007], the adsorbent was produced on a ca. one-gram-of-silica basis only. Therefore, it was necessary to scale-up the production of grafted mesoporous silica to obtain enough material for meaningful testing, particularly toward commercial-scale evaluation, and to provide evidence for the possibility of even larger-scale industrial production. The details on the synthesis, scale-up and characterization of TRI-PE-MCM-41 samples used in this work are presented next.

3.1 Experimental

3.1.1 Materials. The silica source used was Cab-O-Sil M-5 fumed silica from Cabot. Cetyltrimethylammonium bromide (CTAB, Aldrich) was used as structure directing agent and tetramethylammonium hydroxide (TMAOH 25%, balance water, Aldrich) for pH adjustment. The post-synthesis pore expander agent was dimethyldecylamine (DMDA 97% purity, Aldrich). The grafting agent 2-[2-(3-trimethoxysilylpropylamino)ethylamino]ethylamine (herein referred to as TRI-silane) was obtained from Sigma-Aldrich. Celvol 107® polyvinyl alcohol (PVOH) from Celanese and Translucent Liquid Sculpey® (TLS) from Polyform were used as binders. Ultra high purity grade nitrogen and certified gas mixture of 5% CO_2 balance N_2 were supplied by Linde Ltd. All reagents and gases were used without further purification.

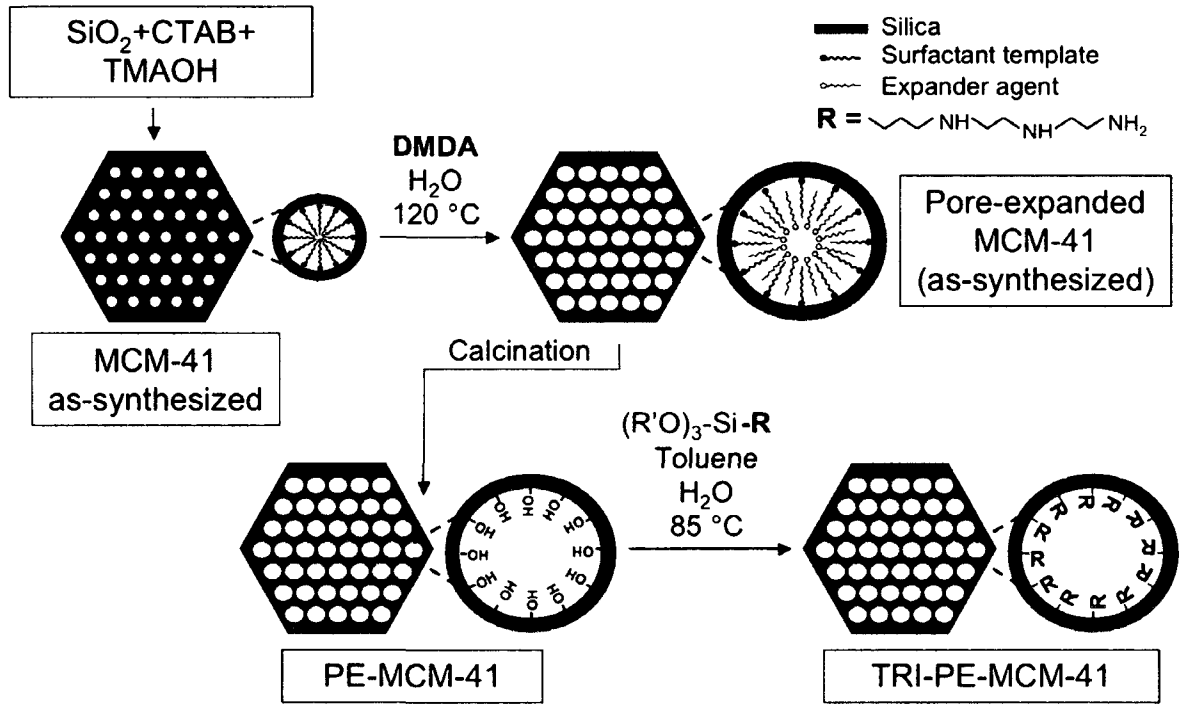

Figure 3.1 Schematic representation of TRI-PE-MCM-41 synthesis

3.1.2. Synthesis of TRI-PE-MCM-41. In the past, our research group successfully achieved the production of MCM-41 in the hundreds-of-gram scale and developed an efficient method for the hydrothermal post-synthesis pore-expansion of ca. 350 g of as-synthesized MCM-41 using an 8 L stainless steel vessel. Such method was used in this work to produce pore-expanded mesoporous silica to be used as support for the amine functional groups. A schematic representation of the procedure followed for the production of TRI-PE-MCM-41 is presented in Figure 3.1. MCM-41 silica was prepared based on a procedure described previously [Sayari et al., 1998; Sayari et al., 2000] for the synthesis of highly ordered MCM-41 as explained next. An amount of 578.6 g of TMAOH at 25% in aqueous solution was mixed with 5500 g of water under vigorous stirring in a stainless steel vessel. An amount of 820 g of CTAB was subsequently added, and stirred for 15 minutes. Afterwards, 328.4 g of Cabot Cab-O-Sil fumed silica was added. After stirring for 30 more minutes, the resulting gel was heated under autogeneous stirring at 100 °C for 40 h. The obtained material was thoroughly washed with water, filtered and dried with air at ambient temperature. Whenever required, purely siliceous MCM-41 can be produced by removing the organic template by heating at 550 °C under a flux of nitrogen, then air for 5 h.

For post-synthesis pore expansion, a sample of the as-synthesized MCM-41 (i.e., non-calcined) obtained as described above was treated based on the procedure described by Sayari et. al, [1999]. A suspension was formed by mixing 437.5 g of DMDA in 5250 g of water under vigorous stirring. An amount of 350 g of as-synthesized MCM-41 was subsequently added and the mixture was left stirring for 15 min. The resulting suspension was heated in a stainless steel reactor at a constant heating temperature of 120 °C for 72 h, time after which it was washed with water, filtered and dried in ambient air. To remove the surfactant and the expander agent, the dry powder was calcined at 550 °C under flowing nitrogen then air for 5 h. The resulting product was labeled as PE-MCM-41.

With the intention of making the synthesis process more attractive from an economical point of view, an additional step is proposed in the present work, which is the recycling of DMDA after post-synthesis expansion. Since the expander agent does not undergo any chemical change during the hydrothermal treatment, it can be potentially recuperated exploiting its particularly high hydrophobic character for reuse. Following a procedure suggested previously [Serna-Guerrero and Sayari, 2007], after the hydrothermal treatment of MCM-41, DMDA was extracted from the material using ethanol. The solid phase was subsequently separated by filtration. Addition of excess water to the filtrate gave rise to the formation of a highly hydrophobic phase containing mostly DMDA. The two well-defined phases were separated using a separation funnel. The recovered organic phase was dried using sodium carbonate. To obtain higher purity DMDA, ethanol was removed by distillation using a rotavap operating at 80 °C under vacuum.

Grafting of TRI-silane on PE-MCM-41 was based on the optimized procedure reported earlier [Harlick and Sayari, 2007]. Briefly, PE-MCM-41 was dried overnight at 120 °C in a vacuum oven and then dispersed in toluene under vigorous stirring. Precise quantities of water were then added to the mixture and left stirring for at least 1 h. TRI-silane was then added and the resulting mixture left stirring for 16 h at 85 °C. To recover the product, the mixture was filtered and washed with toluene and pentane followed by drying in a natural convection oven at 100 °C for no more than 1 h. Although the quantities of each reactant were well established in the aforementioned work (i.e., 1 g of PE-MCM-41, 250 mL of toluene, 0.3 mL of water and 3 mL of TRI-silane), they were further adjusted in the scale-up procedure, as explained in Section 3.2. Such adjustment was necessary as increasing all

reactants and solvents in the same proportion was not appropriate. For example, the method reported by Harlick and Sayari [2007], uses a very high solvent-to-silica ratio of 250 mL g^{-1}. If the solvent and reactants were increased in similar proportions, a 25 L reactor would be necessary to graft amines on 100 g of silica. Such a large amount of solvent is unacceptable from a practical and economical point of view, making it necessary lower the solvent-to-silica ratio before attempting scale-up. As a result of the increased silica concentration in the reaction mixture, further adjustments in the silica to water ratio, timing and sequence were necessary to produce a good quality adsorbent, discussed hereafter.

Since the amount of purely siliceous material produced in our laboratory using the 8 L scale reactor is ca. 300 g, our efforts at this stage of the project aimed at grafting 300 g of silica per batch. As it was intended to use the same 8 L vessel, it was required that the total volume of the mesoporous silica, the optimum amount of water, triamine silane and the solvent be less than 8 L. According to the optimum recipe, the ratio of silica:water:triamine is 1 g:0.3 ml:3 ml, which would be translated to 300 g:90 ml:900 ml in a large scale grafting. Thus, the volume of solvent would be ca. 4.5 L, equivalent to a solvent to silica ratio of 15 ml g^{-1}, in order to leave a reasonable headspace in the vessel.

The approach used for scaling up consisted on reducing systematically the solvent-to-silica ratio in small-scale synthesis inside a glass multineck flask under vapor reflux, until a material with adsorbent properties close to those regarded as optimum was obtained. Once this was achieved, synthesis on a larger scale was attempted.

In order to apply the proposed adsorbent directly into commercial CCBS, it had to be processed into pellets with dimensions and shape similar to commercial absorbents. Thus, agglomeration of TRI-PE-MCM-41 into particles of appropriate size was also studied. Previous work in our group suggested the use of PVOH as binder for amine-functionalized mesoporous silica [Franchi, 2005], since it provided suitable mechanical properties even when used at small concentrations. A series of trials using PVOH under various concentrations and solvent mixtures were produced. In addition, a polymeric ceramic binder (i.e., TLS) was explored to obtain pellets of the adsorbent with good mechanical properties while minimizing any negative impact in the adsorption performance of the material.

3.1.3 Characterization. Characterization of the synthesized materials is a necessary step to determine its structural and chemical properties. The structural properties such as surface area (S_A), pore size (d_p) and pore volume (V_p) were calculated using nitrogen adsorption-desorption data obtained on a Micromeritics ASAP 2020 volumetric apparatus. With respect to chemical properties, the total content of organic matter was determined by thermogravimetric analysis (TGA) using a TA Instruments Q-500 apparatus. Characterization of each sample was performed right after its synthesis. Each set of characterization results provided new insights on the suitability of each recipe and clues on how to improve subsequent reaction conditions, if necessary. Thus, the complementary synthesis and characterization steps were run in parallel.

Surface area (S_A) was measured using the widely accepted Brunauer-Emmett-Teller (BET) method [Gregg and Sing, 1982], based on the nitrogen adsorption data at partial pressures (P/P_0) ranging from 0.05 to 0.3, according to the following equation:

$$\frac{(P/P_0)}{q(1-P/P_0)} = \frac{1}{q_m c} + \frac{c-1}{q_m c}(P/P_0) \qquad (1)$$

where q is the amount adsorbed at equilibrium (mol g^{-1}), c is a dimensionless constant and q_m is the monolayer capacity.

Pore volume was determined using the amount of liquid nitrogen adsorbed at saturation:

$$V_p = q_s V_L \qquad (2)$$

where V_p is the pore volume, q_s is the amount adsorbed per gram of adsorbent at partial pressure close to $P/P_0 = 1$ and V_L is the volume of the adsorbate in the liquid state at the adsorption temperature relative to the volume of gas at standard conditions of temperature and pressure; for nitrogen $V_L = 1.56\times10^{-3}$ cm^3_{liquid} cm^{-3}_{gasSTP}.

Finally, the pore size distribution and mean pore diameter (d_p) were calculated using the Kruk-Jaroniec-Sayari approach to the Barret-Joyner-Halenda method, which was developed specifically for ordered mesoporous silica (OMS) using Eq. 3 [Kruk et al., 1997]:

$$r = \frac{2\gamma V_m}{RT\ln(P/P_0)} + \tau + C_F \quad (3)$$

where r is the pore size as a function of relative pressure, γ is surface tension, V_m is the molar volume of the liquid adsorbate, R is the universal gas constant, T is the absolute temperature, τ is the statistical film thickness and C_F is a correction factor equal to 3 Å.

The total content of organic material in the adsorbent was measured using TGA. Thermal degradation of the sample occurred from ambient temperature to 800 °C in N_2, then to 1000 °C in air, with ca. 2 h equilibration at 200 °C at a heating rate of 10 °C min^{-1}. The weight loss below 200 °C corresponded to the removal of any moisture or alcohol stemming from non-hydrolyzed alkoxy groups. The weight loss beyond 200 °C was used to calculate the amine loading

The TGA apparatus also permitted to screen the CO_2 adsorption capacity for each sample synthesized. Such analysis helped to determine whether further testing with a particular sample should be pursued. The possibility to program several steps during measurements is available within the TA Instruments' software. Therefore, a program was developed for an automated analysis involving activation of the adsorbent, adsorption of CO_2, removal of CO_2 and thermal degradation in a single experiment, as follows. A sample of TRI-PE-MCM-41 of ca. 50 mg was placed in the sample holder of the TGA and pretreated under flowing nitrogen at 200 °C since in separate experiments, it was demonstrated that the grafted tri-amine species are stable up to 250 °C under flowing nitrogen [Harlick and Sayari, 2006] and any adsorbed CO_2 desorbs below 140 °C. [Franchi et al., 2005]. Under such temperature, any moisture or CO_2 adsorbed from the environment was removed as well as non-hydrolyzed methoxy groups attached to the silica surface. After pretreatment, the temperature was decreased to 25 °C and the gas stream switched to a mixture containing 5% CO_2 in nitrogen, as it is the typical end-tidal concentration of CO_2 exhaled by humans in CCBS [Keller, 2005]. Under such conditions, the adsorption capacity is equivalent to the weight gain in the sample until no significant change is observed.

3.2 Results and Discussion

3.2.1 Scale-up synthesis of TRI-PE-MCM-41. As previously mentioned, the synthesis of TRI-PE-MCM-41 was performed at small scale varying the silica to solvent ratio in an attempt to develop an attractive recipe for larger scale grafting. Table 3.1 shows the various silica-to-solvent ratios explored, as well as the corresponding water concentrations for the different recipes used. The organic content of each sample measured with thermogravimetry and the adsorption capacity at 5% CO_2 balance N_2 at ambient temperature are included.

Our first attempt was to reproduce the results published previously to corroborate the accuracy of the claimed capacity. As seen in Table 3.1, the CO_2 adsorption capacity and organic content of a sample produced in 150 mL of toluene (Entry 2) was very similar those reported by Harlick and Sayari [2007]. A material with good adsorptive properties was also obtained adding the same relative amount of water when the silica (in grams) to toluene (in milliliters) ratio was reduced to 1:75 (Entry 3).

Table 3.1 Amine content and adsorption performance of TRI-PE-MCM-41 synthesized under various conditions in 250 mL glass reactor

Entry	SiO_2: toluene (g: mL)	SiO_2: H_2O (g: mL)	Amine content ($mmol_N\ g^{-1}$)	CO_2 capacity ($mmol\ g^{-1}$)	Maximum Rate of Adsorption ($mmol\ g^{-1}\ min^{-1}$)
1*	1:250	1:0.3	7.98	2.65	1.79
2	1:150	1:0.3	8.43	2.65	1.61
3	1:75	1:0.3	8.58	2.77	1.56
4	1:75	1:0.2	7.89	2.57	1.66
5	1:30	1:0.3	9.16	1.19	1.12
6	1:30	1:0.2	7.83	2.39	1.27
7	1:30	1:0.1	6.58	1.97	1.45
8	1:15	1:0.2	7.44	2.39	1.45

*Conditions reported in Harlick and Sayari [2007]

However, when the solvent-to-silica ratio decreased beyond 75 mL g^{-1} and water was kept at 0.3 mL g_{SIO2}^{-1}, the adsorption capacity deteriorated. As seen in Table 3.1, when the recipe used contained a relative amount of toluene of 30 mL per gram of silica and water

content of 0.3 mL g_{SIO2}^{-1}, the resulting material presented a CO_2 adsorption capacity of only 1.19 mmol g^{-1} (Entry 5). By using a lower concentration of water (i.e. 0.2 mL per gram of silica, Entry 6), the adsorption capacity increased to 2.39 mmol g^{-1}. Entry 7 shows the results of grafting in 30 mL of toluene but using only 0.1 mL of water per gram of silica, which resulted in a capacity of 1.97 mmol g^{-1}, a comparatively lower value than Entry 6. Thus, the optimum amount of water at lower solvent-to-silica ratios was established around 0.2 mL per gram of silica, unlike the optimum value of 0.3 mL observed with higher solvent-to-silica ratios. It is also worth mentioning that, unlike the procedure used for large solvent-to-silica content, where water was added in a single step, the addition of water into the reaction mixture was performed in five steps with the same volume allowing a 30 min stabilization period between them. This was required since a single injection of a large amount of water resulted in a material with poor adsorption capacity. A proposed explanation is that when the concentration of water is sufficiently large (as a consequence of a higher silica to solvent ratio), the water molecules are not driven into the silica surface to find a less hydrophobic environment, but may be forming a second liquid phase, thus preventing a proper interaction with the silica surface. The target silica to solvent ratio of 1 g_{SiO2}: 15 $mL_{toluene}$ (Entry 8) offered an optimum adsorption capacity with a relative water content of 0.2 mL per gram of silica.

Table 3.2 Organic content and adsorption capacity of TRI-PE-MCM-41 synthesized in a 75 mL teflon lined vessel

Entry	SiO_2: toluene (g: mL)	SiO_2: H_2O (g: mL)	Amine content ($mmol_N$ g^{-1})	CO_2 capacity (mmol g^{-1})	Maximum Rate of Adsorption (mmol g^{-1} min^{-1})
9	1:15	1:0.3	8.82	1.46	1.05
10	1:15	1:0.25	7.46	2.44	1.31
11	1:15	1:0.2	7.23	2.21	1.16

Once established the possibility to produce TRI-PE-MCM-41 using a lower relative amount of solvent, grafting in a small-scale batch reactor (75 mL volume) was studied. As

presented in Table 3.2, various relative amounts of water were explored and the performance results were very similar to those of the materials synthesized in glass flasks. Yet again, a higher adsorption capacity was obtained using 0.2 mL per gram of silica (Entry 11) with a decrease in CO_2 adsorption capacity when 0.3 mL per gram of silica was used (Entry 9). In an attempt to further optimize the recipe, water was used in a concentration of 0.25 mL per gram of silica (Entry 10). It was found that such concentration produces a material with an adsorption capacity that should be close to its highest possible, i.e., 2.44 mmol g^{-1}.

Since grafting of TRI-silane onto TRI-PE-MCM-41 using small closed reaction vessels proved to be possible, synthesis at larger scale using an 8 L stainless steel reactor was attempted. Since previous experiments suggested that the optimum concentration of water depends on the particular size of the batch and the method used for grafting, various relative amounts of water were screened. Once more, addition of water was performed in several steps to promote its interaction with the silica surface. As can be seen in Table 3.3, the best adsorption capacity in this case was obtained using 0.2 mL of water per gram of silica. Unlike the smaller scale batch synthesis, the recipe using 0.25 mL of water per gram of silica resulted in a material with a comparatively lower capacity for CO_2.

Table 3.3 Organic content and adsorption capacity of TRI-PE-MCM-41 synthesized in an 8 L stainless steel vessel

Entry	SiO_2: toluene (g: mL)	SiO_2: H_2O (g: mL)	Amine content ($mmol_N$ g^{-1})	CO_2 capacity (mmol g^{-1})	Maximum Rate of Adsorption (mmol g^{-1} min^{-1})
12	1:15	1:0.1	6.89	2.20	1.65
13	1:15	1:0.15	7.05	2.31	1.65
14	1:15	1:0.2	7.27	2.32	1.87
15	1:15	1:0.25	7.56	1.97	1.04

In summary, large scale TRI-PE-MCM-41 with an optimum adsorption capacity for CO_2 can be produced in a batch reactor using the procedure described next. After drying 300 g of TRI-PE-MCM-41 in a vacuum oven at 120 °C, the material is poured into the reactor

vessel and mixed with 4.5 L of toluene. Once a homogeneous mixture is produced, 12 mL of water is added every 30 min to a total volume of 60 mL. After a homogeneous mixture is obtained, 900 mL of TRI-silane are added under vigorous stirring. The reactor vessel is closed and left under stirring for 16 h in an oven set at a temperature of 85 °C. The resulting material is filtered and washed with copious amounts of toluene and pentane. Finally, the collected solid is dried at 100 °C in a natural convection oven for no more than 1 h.

3.2.2 Characterization. The work described above resulted in the successful synthesis of TRI-PE-MCM-41 in a scale of more than 400 g of adsorbent per batch. This was achieved by following the strategy described earlier consisting of (i) a systematic reduction of the solvent-to-silica ratio during grafting, (ii) a small scale batch synthesis using a 75 ml reactor and (iii) a larger scale batch synthesis in an 8 L batch reactor. In order to establish the quality of the adsorbent obtained with each recipe, it was necessary to characterize the structural and chemical properties of the product.

The structural properties of the materials were determined by nitrogen adsorption at 77 K and are presented in Table 3.4. Typical nitrogen adsorption isotherms of PE-MCM-41 silica before and after incorporation of functional groups are presented in Figure 3.2. The nitrogen adsorption isotherm of a typical MCM-41 sample before post-synthesis pore enlargement is also shown for comparison.

Table 3.4 Structural properties of ordered mesoporous materials

Sample	S_A (m^2 g^{-1})	V_p (cm^3 g^{-1})	d_p (nm)
MCM-41	1309 ±76	1.09 ±0.15	3.63 ±0.53
PE-MCM-41	1134 ±74	2.62 ±0.36	10.88 ±1.32
TRI-PE-MCM-41	429 ±73	1.05 ±0.13	9.57 ±0.92
TRI-PE-MCM-41*	715	2.62	9.57

*On a per-gram-of-silica basis, assuming an organic loading of ca. 40 wt%

As seen in Figure 3.2, all isotherms correspond to the Type IV according to the International Union of Pure and Applied Chemistry (IUPAC) classification, which is characteristic of mesoporous materials. The pore-expanded mesoporous silica used as

support presented significantly larger d_p and V_p than typical MCM-41, while maintaining a high S_A and a relatively narrow pore size distribution. This is the result of an effective post-synthesis pore expansion of as-synthesized MCM-41. The structural characteristics of PE-MCM-41 make it particularly attractive as support of amine-bearing molecules. Indeed, it can be expected that its large pore size and volume will permit a high loading of organic molecules without losing its porous nature due to pore blocking by excess functional groups.

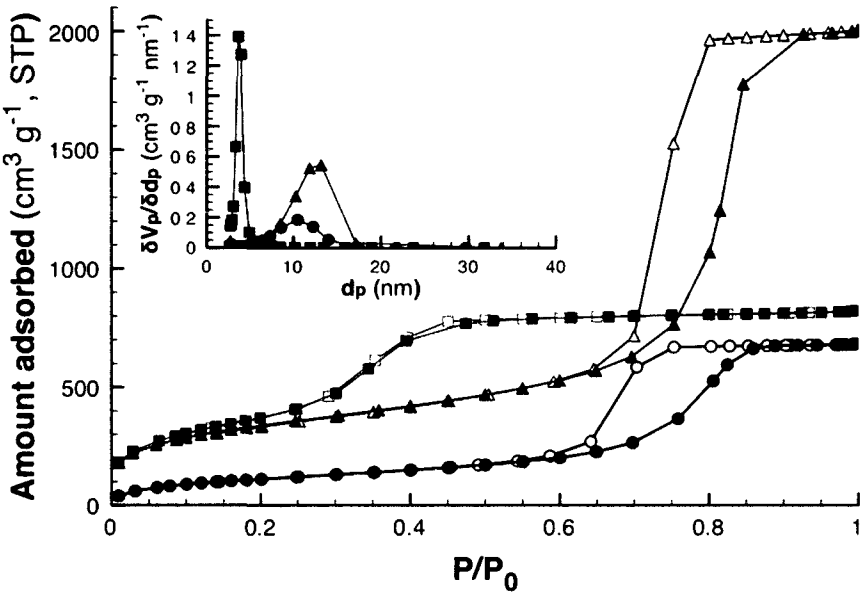

Figure 3.2 Nitrogen adsorption (closed symbols) - desorption (open symbols) isotherms of MCM-41 (squares), PE-MCM-41 (triangles) and TRI-PE-MCM-41 (circles); inset figure represents pore size distribution

A difference of 1-2 nm was observed between the pore diameter of the siliceous support and TRI-PE-MCM-41, attributed to the space occupied by the organic molecules on the surface. The functional groups in TRI-PE-MCM-41 also impacted negatively on S_A, although its value can still be considered high, being 429 m^2 g^{-1}. Most importantly, as observed in Figure 3.2, the mesoporous nature of TRI-PE-MCM-41 was maintained after the grafting process, while high amine content (ca. 7.9 mmol g^{-1}) was achieved. This is particularly attractive since the large free space offered by mesopores is generally associated with lower resistance to diffusion compared to microporous materials.

3 2 3 Recovery of Expander Agent As a further improvement of the process of pore enlargement of MCM-41, the recovery and reuse of the expander agent was investigated. ^{13}C Nuclear magnetic resonance analysis of DMDA prior to use, and the recovered DMDA before and after distillation was performed and the resulting data are presented in Figure 3.3. As seen, the peaks attributable to DMDA, particularly those at 60 and 46 ppm [Sayari et al., 1998], are present before distillation, but peaks associated with ethanol are also observed at 58 and 18 ppm After distillation, no ethanol was detected by NMR, as can be appreciated in Figure 3.3c. Indeed, the profile obtained after distillation is identical to that of virgin DMDA

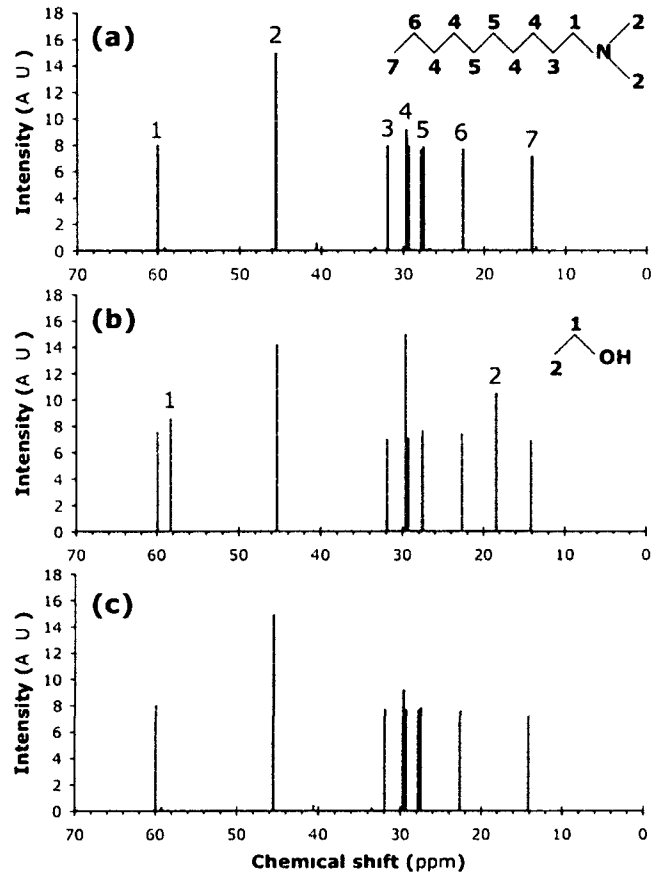

Figure 3.3 ^{13}C Nuclear magnetic resonance data for (a) DMDA virgin, (b) DMDA recuperated, (c) DMDA recovered after purification

The recovered DMDA was also used for pore expansion of as-synthesized MCM-41. The nitrogen adsorption characterization of the material produced with the recycled DMDA

is shown in Figure 3.4. As can be seen, this material presents a nitrogen adsorption isotherm and structural characteristics comparable to those of PE-MCM-41 produced with virgin DMDA, suggesting the reuse of DMDA was successfully accomplished.

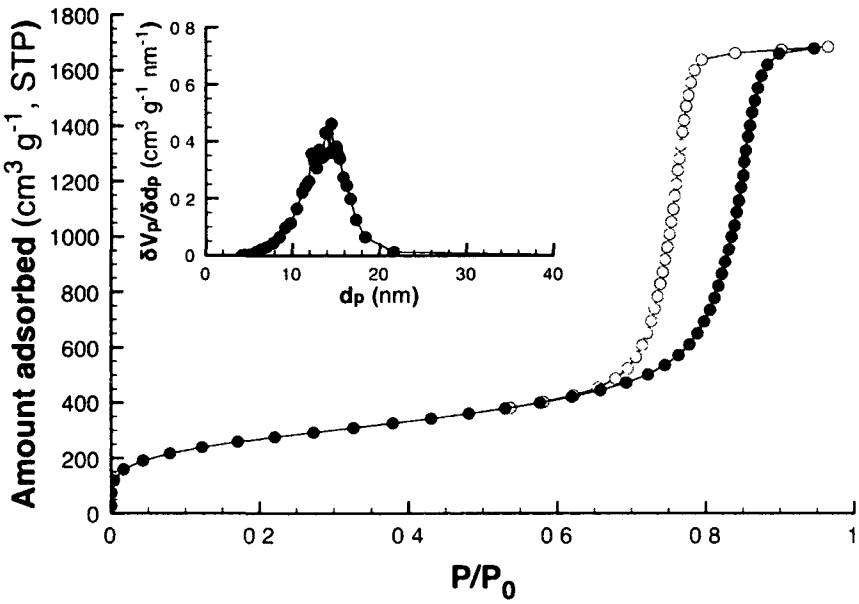

Figure 3.4 Nitrogen adsorption (closed symbols) - desorption (open symbols) isotherms of PE-MCM-41 synthesized using recycled DMDA (S_A = 1049 m^2 g^{-1}, V_p = 1.99 cm^3 g^{-1}, d_p = 13 nm)

3.2.4 Agglomeration. Particles of PE-MCM-41-based materials can be produced by pressing its powder form under a load of 450 kg cm^{-2} without a significant loss of structural properties, according to an earlier work [Serna-Guerrero and Sayari, 2007]. This procedure was followed to produce pellets for use in small, laboratory-scale fixed bed adsorption columns. A typical nitrogen adsorption isotherm of this kind of agglomerates is presented in Figure 3.5. Since these particles maintained structural properties close to their powder form and they were produced without any addition of binder components, it is expected that only minor differences will be observed with respect to their performance as CO_2 adsorbents. The structural properties and adsorption capacity of pellets produced by compression showed a strong resemblance with those of TRI-PE-MCM-41 powder.

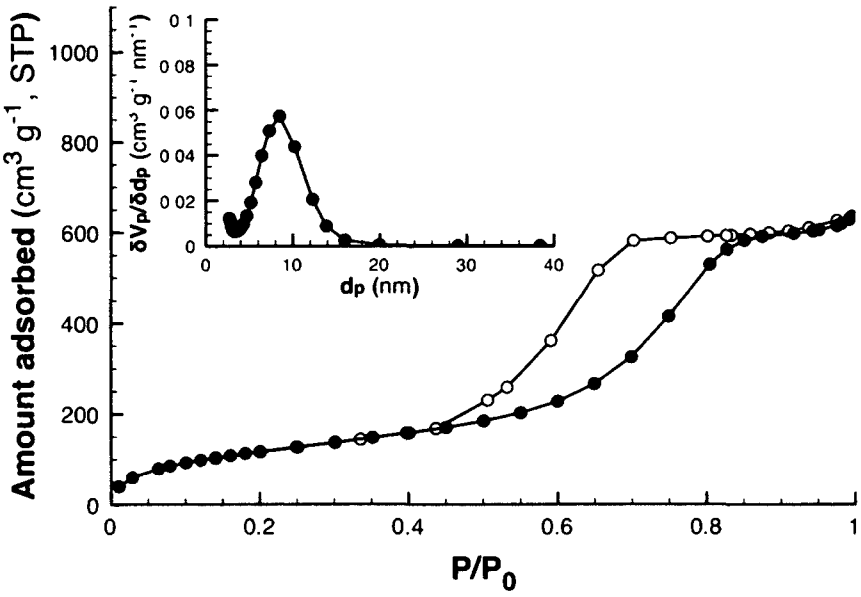

Figure 3.5 Nitrogen adsorption (closed symbols) - desorption (open symbols) isotherms of TRI-PE-MCM-41 agglomerated by compression (S_A = 389 m^2 g^{-1}; V_p = 0.83 cm^3 g^{-1}; d_p = 9.32 nm)

However, this approach is impractical when processing large amounts of powder for a commercial-scale application. Consequently, other methods were explored in order to process larger amounts of TRI-PE-MCM-41 into stable agglomerates of amine-grafted adsorbent with an acceptable adsorption performance. According to a previous study [Franchi, 2005], agglomerates of amine-dispersed mesoporous silica can be produced using PVOH as binding agent. In that work, a PVOH solution is first prepared in excess boiling water. The solution was kept boiling until enough water was evaporated to produce a 10% weight PVOH solution, which would be subsequently added to the powder material and mixed mechanically to produce a wet paste. Such paste should be malleable enough to be processed into defined shapes, followed by the removal of excess water by drying in an oven. This process was attempted for TRI-PE-MCM-41, mixing 1 g of adsorbent with 1 g of 10% PVOH aqueous solution (Recipe 1). Although particles with a defined and stable shape were obtained, a dramatic loss in adsorption capacity occurred as seen in Table 3.5. This decreasing capacity was associated with a loss in structural properties following this procedure, as presented in Figure 3.6. It is possible that the silica pore walls are hydrolized when soaked in sufficiently large amounts of liquid water, resulting in the collapse of the

pore walls [Rao et al., 2009]. Therefore, an iteration of this procedure was attempted, trying to use the lowest possible amount of water to disperse the binder homogeneously in the TRI-PE-MCM-41 particles. For Recipe 2, an amount of 0.5 mL of a more concentrated PVOH aqueous solution (12%) was mixed with 0.5 mL ethanol and the resulting solution added to 1 g of TRI-PE-MCM-41. As observed in Figure 3.6, although smaller than Recipe 1, this approach had also a negative impact on the properties of the adsorbent. It should be noted that after several trials, it was observed that a PVOH solution with higher concentration was too viscous, resembling a gelatinous phase, and that at higher ethanol content, the dissolved PVOH precipitated into an insoluble solid phase. Consequently, no lower water content could be used for agglomeration using PVOH.

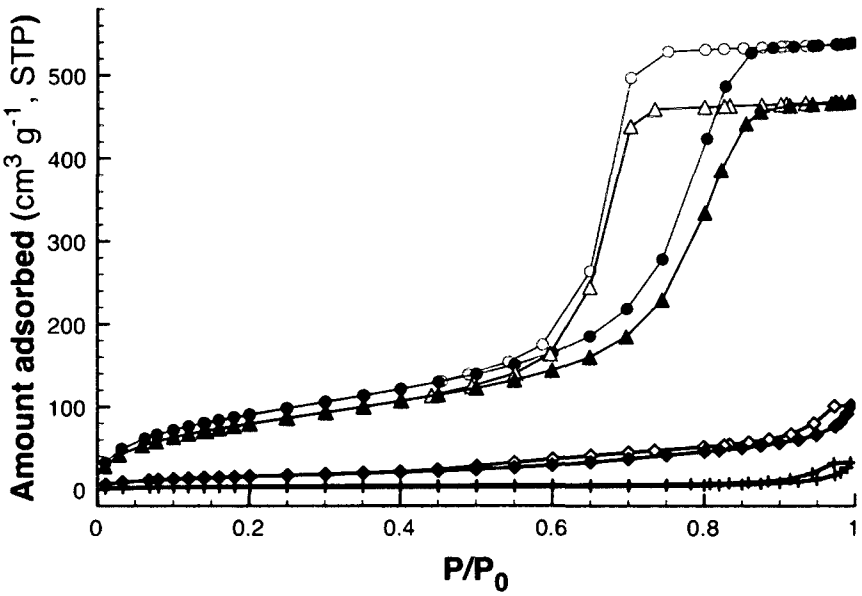

Figure 3.6 Nitrogen adsorption (closed symbols) and desorption (closed symbols) isotherms of TRI-PE-MCM-41 (circles) and agglomerates produced with Recipe 1 (crosses), Recipe 2 (diamonds), and Recipe 3 (triangles)

The next approach (Recipe 3) was to disperse TRI-PE-MCM-41 in sufficient ethanol to produce a wet paste and saturate the material with a non-aqueous solvent followed by the addition of PVOH solution. In the case of Recipe 3, an amount of 1.5 mL of ethanol was mixed with 1 g of TRI-PE-MCM-41 followed by the addition of 0.5 mL of PVOH 12% aqueous solution. The paste was then extruded and left drying overnight in air at room

temperature. As seen in Figure 3.6 and Table 3.5, Recipe 3 produced agglomerates that maintained acceptable structural properties and adsorption performance. Nevertheless, these agglomerates presented a low mechanical strength, producing large amounts of dust when handling and would break easily. Considering the restrictions offered by using a water-ethanol mixture with PVOH, a different agglomeration approach was pursued.

Table 3.5 Structural properties of TRI-PE-MCM-41 produced in large batch and agglomerates

Sample	S_A ($m^2 g^{-1}$)	V_p ($cm^3 g^{-1}$)	d_p (nm)	CO_2 capacity (mmol g^{-1})
TRI-PE-MCM-41 (large batch)	350	0.83	9.32	2.32
TRI-PE-MCM-41 (Recipe 1)	11	0.03	10.1	0.80
TRI-PE-MCM-41 (Recipe 2)	55	0.12	7.80	0.75
TRI-PE-MCM-41 (Recipe 3)	307	0.72	9.46	2.03
TRI-PE-MCM-41 (Recipe 4)	245	0.62	10.0	2.15

From the observations above, it was decided to search for a binder that did not require to be dissolved in an aqueous phase and that could produce agglomerates with good mechanical strength. For that reason, a liquid polymeric ceramic binder was chosen, namely TLS. In a typical agglomeration procedure, 1 g of ethanol was added to 1 g of TRI-PE-MCM-41 to produce a wet paste. Afterwards, 0.25 g of TLS per gram of TRI-PE-MCM-41 were added and mixed until a homogeneous paste was obtained. The resulting paste was then extruded and placed in a vacuum oven at 140 °C for not more than 1 h to cure the binder and activate the adsorbent. After curing, the binder content was determined to be ca. 12% of the final weight of the sample. The resulting particles had well defined shapes with a suitable mechanical stability. As presented in Figure 3.7 and Table 3.5, these agglomerates also maintained a suitable mesoporous structure, with a decrease in surface area and pore volume proportional to the amount of binder. Furthermore, the adsorption capacity loss was also proportional to the binder content, indicating that the polymeric binder did not affect the structural and chemical properties of the adsorbent and can be used reliably to produce TRI-PE-MCM-41 pellets.

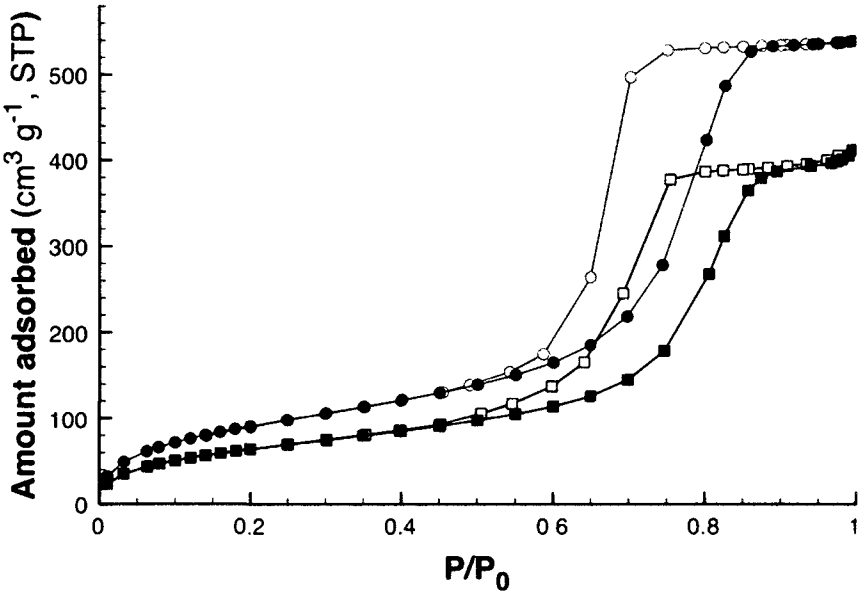

Figure 3.7 Nitrogen adsorption (closed symbols) and desorption (closed symbols) isotherms of TRI-PE-MCM-41 (circles) and agglomerates produced with Recipe 4 (squares)

3.3 Summary

This Chapter presented a study on the synthesis and characterization of TRI-PE-MCM-41 produced under various conditions. By following a systematic approach, it was possible to propose a recipe to graft TRI-silane on 300 g of PE-MCM-41 in a single batch reaction, producing a CO_2 adsorbent with good structural and adsorptive properties. Additionally, work on the agglomeration of TRI-PE-MCM-41 was presented. Compression of powder at 450 kg_f cm^{-2} produced pellets of TRI-PE-MCM-41 with minor disruption on its structural properties compared to its powder form. For agglomeration of large amounts of TRI-PE-MCM-41, however, it is suggested to produce pellets using a polymeric ceramic binder.

References

R.S. Franchi, Development of an adsorbent for CO_2 based on amine-impregnated porous supports. M. A. Sc. Thesis, University of Ottawa, Canada, 2005

R.S. Franchi, P.J.E. Harlick, A. Sayari, Applications of pore-expanded mesoporous silica. 2. Development of a high-capacity, water tolerant adsorbent for CO_2. *Ind. Eng. Chem. Res.* 44 (2005) 8007

S.J. Gregg, K.S.W. Sing, *Adsorption, Surface Area and Porosity*. Academic Press, New York, 1982

P.J.E. Harlick, A. Sayari, Applications of pore expanded mesoporous silica. 3. Triamine silane grafting for enhanced CO_2 adsorption. *Ind. Eng. Chem. Res.* 45 (2006) 3248

P.J.E. Harlick, A. Sayari, Applications of pore-expanded mesoporous silica. 5. triamine grafted material with exceptional CO_2 dynamic and equilibrium adsorption performance. *Ind. Eng. Chem. Res.* 46 (2007) 446

C. Keller, J. Brimacombe, C. Hoermann, A, Loeckinger, A. Kleinsasser, Pressure support ventilation with the Proseal® laryngeal mask airway. A comparison of sevoflurane, isoflurane and propofol. *Europ. J. Anesthesiol.* 22 (2005) 630

M. Kruk, M. Jaroniec, A. Sayari, Application of large pore MCM-41 molecular sieves to improve pore size analysis using nitrogen adsorption measurements. *Langmuir* 13 (1997) 6267

T.V.M. Rao, Y. Yang, A. Sayari, Ethane dehydrogenation over pore-expanded mesoporous silica supported chromium oxide: 1. Catalysts preparation and characterization. *J. Mol. Catal. A: Chem.* 301 (2009) 152

A. Sayari, M. Kruk, M. Jaroniec, I.L. Moudrakovski, New approaches to pore size engineering of mesoporous silicates. *Adv. Mater.* 10 (1998) 1376

A. Sayari , Y. Yang, M. Kruk, M. Jaroniec, Expanding the pore size of MCM-41 silicas: use of amines as expanders in direct synthesis and postsynthesis procedures. *J. Phys. Chem. B.* 103 (1999) 3651

A. Sayari, Y. Yang, Highly ordered MCM-41 silica prepared in the presence of decyltrimethylammonium bromide. *J. Phys. Chem. B* 104 (2000) 4835

R. Serna-Guerrero, A. Sayari, Applications of pore-expanded mesoporous silica. 7. Adsorption of volatile organic compounds. Env. Sci. Technol. 41 (2007) 4761

Chapter 4

New insights into the interactions of CO_2 with amine-functionalized silica

Ind. Eng. Chem. Res. 47 (2008) 9406-9412

Abstract.

The CO_2 – amine chemistry in gas – solid processes was investigated under both humid and dry conditions using aminopropyl-grafted pore-expanded MCM-41 silica (MONO-PE-MCM-41). To draw accurate conclusions, a set of conditions had to be met including (i) the use of an adsorbent with open pore structure and readily accessible adsorption sites, e.g. MONO-PE-MCM-41 with a mean pore size of 7.2 nm; (ii) the CO_2 concentration in the feed should be high enough to achieve saturation via chemisorption, but low enough to avoid any additional physisorption, e.g., 5% CO_2 in N_2; (iii) the use of a reliable method for the accurate measurement of CO_2/N ratio. Under such conditions, the obtained CO_2/N ratios were reminiscent of those obtained in the CO_2 scrubbing process using ethanolamine solutions. Under dry conditions, the CO_2/N ratio was close to 0.5, consistent with the formation of carbamate. Streams with relative humidity (RH) of 27, 61 and 74% were studied as well. As RH in the feed increased, CO_2/N ratio increased from 0.57 to 0.88, in line with the gradual formation of bicarbonate. As for the determination of CO_2/N ratio under dry conditions, both thermogravimetry (TG) and mass spectrometry (MS) were suitable, whereas in the presence of moisture, TG was found to drastically underestimate the CO_2 uptake. The seemingly disparate CO_2/N ratios reported in the literature for various propylamine-bearing adsorbents were rationalized on the basis of the adsorbent pore structure and/or the experimental conditions used.

4.1 Introduction

As climate change has become a topic of great interest among the scientific community as well as the general public, extensive effort has been devoted to the development of different strategies to prevent the release of "greenhouse gases" into the atmosphere [Yang et al., 2008]. Carbon dioxide (CO_2) has drawn particular attention for being the main anthropogenic

contributor to global warming. Consequently, new approaches have been proposed to overcome the limitations of the currently used liquid amine scrubbing technology which, in addition to its corrosive and toxic nature [Veawab et al., 1999], consumes large amounts of energy [Oyenekan et al., 2007]. Inspired by this technology, a number of research groups developed solid-supported amine adsorbents for CO_2 separation [Birbara et al., 2002; Sayari, 2004; Sayari and Harlick, 2006; Gray et al., 2007; Harlick and Sayari, 2007; Jones et al., 2007; Olah et al., 2008]. The adsorption approach is expected to combine the high selectivity and reversibility of the CO_2-amine chemistry and the low energy requirements to regenerate the solid adsorbent. Furthermore, unlike zeolite-based adsorbents [Brandani et al., 2004], amine-functionalized materials proved to be more tolerant to moisture, thus eliminating the need for strict control of humidity prior to adsorption.

The main guideline to develop efficient amine-functionalized CO_2 adsorbents is the use of a support such as silica with well-developed structural properties, in particular high surface area and pore volume, as well as large pore size. Since the advent of ordered mesoporous silicas, these materials with pore diameters in the nanometer range were found to be particularly attractive as adsorbents and supports [Sayari, 2003]. Consequently, amine groups have been incorporated onto mesoporous supports and tested for CO_2 adsorption under humid and dry conditions.

Based on the studies of CO_2 absorption in liquid amine solutions, the main reaction pathways between primary amines and CO_2 can be represented as shown in Scheme 4.1 [Arstad et al., 2007; da Silva et al., 2007]. Accordingly, the interaction of CO_2 with amine in a water-free environment gives rise to the formation of carbamate, a reaction that requires 2 amine groups per CO_2 molecule (i.e., $CO_2/N = 0.5$). On the other hand, when water is present, CO_2 is removed through the formation of bicarbonate. If the same chemistry applies to the gas-solid systems, the adsorption capacity for humid CO_2 on amine-functionalized materials will be double that of dry streams, as only one amine group is required per CO_2 molecule. It should be noted that the reaction pathway in Scheme 4.1 does not contemplate the production of bicarbonate through the hydrolysis of carbamate. Indeed, as it was demonstrated recently, this is mechanistically improbable to take place [da Silva et al., 2007].

$$2(RNH_2) + CO_2 \longleftrightarrow \underset{\text{carbamate}}{RNHCO_2^-RNH_3^+}$$

$$RNH_2 + CO_2 + H_2O \longleftrightarrow \underset{\text{bicarbonate}}{RNH_3^+HCO_3^-} \xleftrightarrow{RNH_2} \underset{\text{carbonate}}{(RNH_3^+)_2CO_3^{2-}}$$

Scheme 4.1 Typical reaction pathways between CO_2 and primary amines.

The production of carbamate, however, is not exclusive of environments where water is absent. It is well established that the production of carbamate is much faster than the formation of bicarbonate [Vaidya and Kenig, 2007]. Considering that carbamate is not a reaction intermediate in the generation of bicarbonate, the two possible reaction pathways between amines and CO_2 are competitive reactions with kinetics favoring the formation of carbamate. As such, for practical purposes, the pathway leading to carbamate formation is considered the limiting stoichiometry for the absorption of CO_2 in dynamic processes [Bonenfant et al., 2003; Ma'mun et al., 2007], while the production of bicarbonate is only observed when a long contact time is permitted [Böttinger et al., 2008]. To explain the formation of bicarbonate without the intermediacy of carbamate, it has been proposed that, after the first reaction pathway has produced sufficiently large amounts of carbamate, the equilibrium favors the reverse reaction resulting in the regeneration of CO_2. This would represent a macroscopic equilibrium in dry environments but, when water is available, the recovered CO_2 would have the potential to produce bicarbonate [da Silva et al., 2007; Böttinger et al., 2008]. Such reaction pathway suggests that, although bicarbonate formation is comparatively slow, if long enough contact time is allowed, the uptake of CO_2 in humid streams should correspond to a ratio of 1 mol per mol of amine. If the residence time is not long enough, a CO_2/N ratio between 0.5 and 1.0 will be obtained depending on the relative extent of the bicarbonate pathway. In the case of solid-supported amines, these scenarios may be complicated by the additional occurrence of physisorption.

Since the theoretical values of CO_2/N are well established for these mechanisms, it is proposed to use the CO_2/N ratio as criteria for the relative efficiency of the adsorbents, in addition to their actual CO_2 adsorption capacity. Further, the CO_2/N ratio is a benchmark based on quantitative results that allows the rationalization of the adsorption data published so far, as it has been produced under a wide range of experimental conditions. As reviewed by Harlick and Sayari [2007], the CO_2/N ratios reported in the literature varied within a wide

range, i.e., from 0.025 to 0.89 for dry conditions and from 0.19 to 1 in the presence of humid CO_2. This raises the question as to whether the proposed mechanisms for CO_2 adsorption are adequate and, if so, why the reported CO_2/N ratios are widely scattered. As it is important to fully understand the chemistry involved in this process for the design, development and improvement of amine-functionalized materials, the objective of the current investigation is twofold, namely to elucidate the gas-solid CO_2-amine interactions and to rationalize the wide range of CO_2/N ratios reported in the literature.

4.2 Experimental

A set of experimental conditions was chosen specifically to investigate the behavior of amines supported on porous solids in the presence of CO_2. First, the support consisted of MCM-41 type silica whose pores have been enlarged by post-synthesis hydrothermal treatment (hereby referred to as PE-MCM-41) [Sayari et al., 1999]. The exceptionally large pore size and volume of this material, even after the incorporation of an organic moiety is of major importance since other amine-modified mesoporous materials reported in the literature have exhibited a microporous structure and in some cases no porosity at all [Xu et al., 2002; Kim et al., 2005; Liu et al., 2007], most likely preventing the accessibility of amine groups. In addition, (3-aminopropyl)trimethoxy-silane was selected as grafting agent since it has a simple structure involving a single primary amine. The CO_2-supported amine interaction is thus expected to be analogous to that of the widely studied monoethanolamine (MEA) in solution. For consistency, the adsorbents referred to in this work correspond exclusively to materials with functional groups containing only primary amines, typically propylamine.

Last but not least, the use of a reliable method for the accurate measurement of CO_2 adsorption capacity, and by inference the CO_2/N ratio, should be used. In a number of studies reported in the literature, CO_2 adsorption measurements were performed using gravimetric analysis assuming that any weight change in the sample is the result of CO_2 uptake exclusively [Xu et al., 2002; Huang et al., 2003; Kim et al., 2005; Liu et al., 2007; Wang et al., 2007]. Although this is a reasonable assumption when CO_2 is adsorbed in its pure form or as a mixture with non-adsorbing gases, it may not be so when water vapor is present. In cases where adsorption of CO_2 from humid streams was measured by gravimetry, a pre-humidification step was used. It was then assumed that the amount of water pre-adsorbed on

the sample remains constant by maintaining the same relative humidity (RH) in the gas feed throughout the test and thus, any additional weight gain would correspond only to CO_2 adsorption [Knowles et al., 2005; Knowles et al., 2006]. However, it is possible that some of the pre-adsorbed water be displaced in the presence of CO_2-containing streams. Measurements using breakthrough curves, for example, may allow the determination of the adsorption capacity for different species [Hiyoshi et al., 2005], but it may underestimate the total adsorption capacity if the experimental parameters used do not permit strict equilibrium conditions to be reached. As described later, to measure the actual amount of CO_2 adsorbed in the presence of moisture a quantitative method coupling TGA and mass spectrometry (MS) was developed. Measurements of adsorption capacity using only gravimetric analysis were also performed for comparison.

4.2.1 Materials. Cab-O-Sil M-5 fumed silica from Cabot was used as the silica source. Cetyltrimethylammonium bromide (CTAB, Aldrich) and tetramethyl ammonium hydroxide (TMAOH 25%, balance water, Aldrich) were used as structure directing agent and for pH adjustment, respectively. The post-synthesis pore expander agent was dimethyldecylamine (DMDA 97% purity, Aldrich). The grafting agent used was (3-aminopropyl)trimethoxy-silane (herein referred to as MONO-silane) and was obtained from Sigma-Aldrich. Ultra high purity grade nitrogen and certified gas mixtures of CO_2 balance N_2 were supplied by BOC Canada. All reagents and gases were used without further purification.

4.2.2 Synthesis of mesoporous adsorbent. The PE-MCM-41 support was prepared in two stages based on a procedure described elsewhere [Sayari et al., 1998; Kruk et al., 2000]. An amount of 578.6 g of TMAOH 25% was diluted in 5500 g of water under vigorous stirring in an 8 L stainless steel vessel. Afterwards, CTAB (820 g) was added, and stirred for 15 minutes. Subsequently, 328.4 g of Cab-O-Sil fumed silica was added. After mixing for 30 more minutes at ambient temperature, the resulting gel was placed in an oven and stirred at 100 °C under autogenous pressure for 40 h. The obtained material was filtered, thoroughly washed with water and dried at ambient conditions. The obtained material whose pores were filled with surfactant will be designated *as-synthesized* MCM-41.

The *as-synthesized* MCM-41 underwent a pore expansion procedure consisting of a hydrothermal treatment using DMDA as expander agent [Sayari et al., 1998; Sayari et al., 1999; Serna-Guerrero and Sayari, 2007]. An emulsion was prepared by adding 437.5 g of DMDA in 5250 g of water under vigorous stirring at ambient temperature. Subsequently, 350 g of as-synthesized MCM-41 was added and the mixture was kept under stirring for 15 more minutes. The resulting suspension was heated in a stainless steel closed vessel at 120 °C under continuous stirring for 72 h. Subsequently, the material was filtered, washed with water, and dried in ambient air. The material obtained was calcined in air at 550 °C for 5 h to remove both the expander agent and the template; it will be designated PE-MCM-41. Alternatively, the expander may be selectively extracted with ethanol [Serna-Guerrero and Sayari, 2007] and separated for reuse.

Incorporation of the amine functionality was achieved via surface grafting. After drying 1 g of PE-MCM-41 in a vacuum oven at 120 °C, the material was loaded into a multi-neck glass flask containing 150 mL of toluene. Once a homogeneous mixture was produced, 0.4 mL of distilled deionized water was added and left stirring for at least 30 min. The glass flask doted with a condenser was then submerged in a silicon oil bath set at 85 °C using a temperature controlled stirring hotplate with an external temperature probe. MONO-silane (2 ml) was subsequently added to the mixture and left stirring for 16 h. The material was filtered and washed with copious amounts of toluene, then pentane. Finally, the recovered solid was dried at 100 °C in a natural convection oven for 1 h and was labeled MONO-PE-MCM-41.

4.2.3. Characterization. The structural properties of PE-MCM-41 and MONO-PE-MCM-41 were determined by nitrogen adsorption at 77 K using a Micromeritics ASAP 2020 volumetric apparatus. Prior to each analysis, the samples were degassed under vacuum at 150 °C for 5 hours. The surface area was determined by the BET method, whereas the pore size distribution was calculated using the Kruk-Jaroniec-Sayari (KJS) approach [Kruk et al., 1997]. The pore volume was calculated as the amount of liquid nitrogen adsorbed at P/P_0 = ca. 1. The organic content in the sample was determined by thermogravimetric analysis (TGA) on a TA Instruments Q-500 apparatus by increasing the temperature of the sample at a rate of 10 °C min^{-1} up to 800 °C under flowing nitrogen at 100 ml min^{-1}, followed by

complete combustion of the organic material under air at the same heating rate and gas flow up to 1000 °C. Only the weight loss above 200 °C was considered as propylamine loss [Harlick and Sayari, 2007].

4.2.4. Adsorption experiments. The CO_2 adsorption capacity was measured using the above-mentioned TGA apparatus coupled with a Pfeiffer Thermostar mass spectrometer. As represented in Figure 4.1, the TGA system was modified to be able to switch between two different gas streams entering the measurement chamber. The experimental procedure for adsorption of dry CO_2 involved the following steps: (i) activation of the adsorbent, (ii) adsorption of CO_2, (iii) temperature programmed desorption (TPD) of CO_2 and (iv) decomposition of the organic layer of the adsorbent. A sample of MONO-PE-MCM-41 of ca. 30 mg was placed in the measurement pan of the TGA and pretreated under flowing N_2 at 200 °C since it has been demonstrated that the grafted amine species are stable up to 250 °C and any CO_2 and moisture adsorbed from ambient air desorbs below 140 °C [Khatri et al., 2006]. In addition, non-hydrolyzed methoxy groups are also removed during the activation step [Harlick and Sayari, 2007]. After pretreatment, the temperature was decreased to 25 °C and the gas stream switched to a mixture containing 5% CO_2 balance N_2 at a flow rate of 100 ml min^{-1}. The flow of CO_2 mixture continued for at least 16 h to ensure that equilibrium was attained. The organic content was obtained by decomposition as described above.

For adsorption of CO_2 in humid streams, the mixture of CO_2 in N_2 was bubbled through a glass saturator containing distilled deionized water before entering the measurement chamber of the TGA, as shown in Figure 4.1. The saturator was maintained at a constant temperature with the aid of a temperature controlled water bath. To produce streams with 27, 61 and 74% RH, the temperature of the cooling bath was set at 5, 17 and 20 °C, respectively. In addition, a series of experiments were performed using a pre-hydration step. In this case, UHP nitrogen was bubbled into the water saturator, then directed to the sample-containing chamber until an apparent equilibrium was obtained. The gas flowing through the water saturator was subsequently switched to the 5% CO_2/N_2 mixture, maintaining the saturator at the same temperature and, hence, a constant RH throughout the pre-hydration and CO_2 adsorption stages. The equilibration time and the other steps of the procedure (i.e., activation, desorption and decomposition) were the same as described above for dry CO_2.

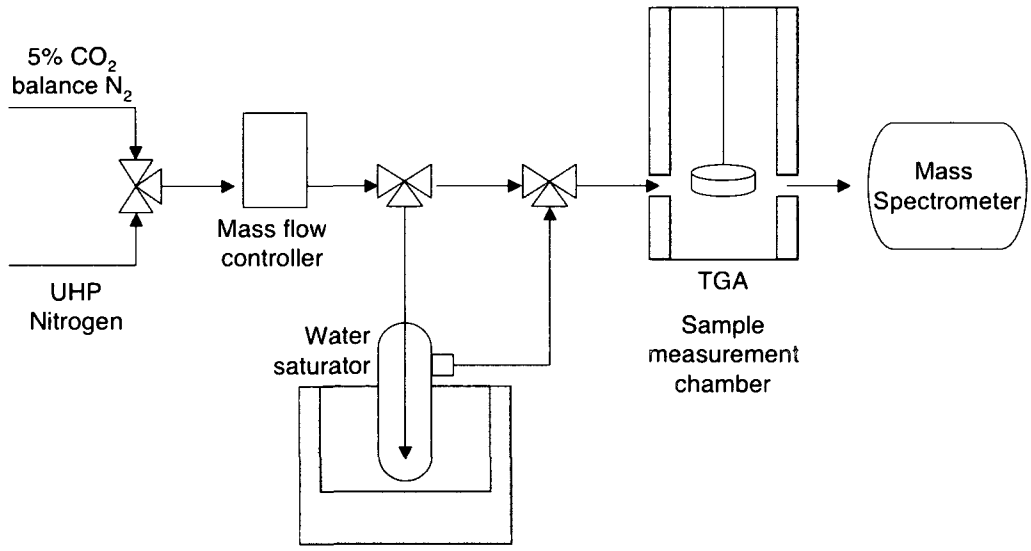

Figure 4.1 Schematic representation of the experimental setup used for adsorption measurements.

The quantification of CO_2 adsorption capacity was determined from the MS response during desorption. Calibration of the MS for CO_2 was achieved as follows. Known quantities of $CaCO_3$ were decomposed under flowing nitrogen at a heating rate of 10 °C min^{-1} in the TGA instrument while the effluent was monitored by MS. The established linear relationship between the area of the MS signal corresponding to 44 amu and the total amount of CO_2 released was used as a calibration curve to quantify the amount of CO_2 released from the adsorbent. A blank experiment (activation, CO_2 exposure and desorption) was carried out without adsorbent for the purpose of correcting the MS baseline.

In addition, adsorption isotherms for water and CO_2 were determined by gravimetry using the TGA apparatus. A sample of MONO-PE-MCM-41 was activated under the conditions described above and then cooled down to 25 °C. The gas fed to the TGA was subsequently switched to a mixture containing known concentrations of the adsorbate (i.e., CO_2 or water). In the case of CO_2, certified gas mixtures with compositions ranging from 1000 ppm to 20% CO_2 balance N_2 and UHP-grade CO_2 were used. The concentration of water was controlled with the aid of a temperature-controlled glass saturator containing distilled water in a similar manner as described previously for the humid CO_2 adsorption measurements.

4.3 Results and discussion

The nitrogen adsorption isotherms of PE-MCM-41 and MONO-PE-MCM-41 are presented in Figure 4.2. The main structural characteristics determined experimentally are listed in Table 4.1. The support exhibited pores averaging 9.9 nm in diameter and a surface area of 1124 $m^2 g^{-1}$. After grafting, the typical amine loading of MONO-PE-MCM-41 determined by TGA was 4.3 mmol g^{-1} and the mean pore size was as high as 7.2 nm. In addition, the adsorbent exhibited a relatively large surface area (ca. 420 $m^2 g^{-1}$) and pore volume (ca. 0.65 $cm^3 g^{-1}$). The presence of mesopores in the adsorbent, even after amine functionalization, is a characteristic that makes MONO-PE-MCM-41 particularly attractive. The widely open structure of surface-modified PE-MCM-41 has been associated with the efficient use of functional groups such as triamine [Harlick and Sayari, 2007] and polyamidoamine (PAMAM) dendrimer [Reynhardt et al., 2003] for adsorption and catalysis.

Table 4.1 Structural characteristics of PE-MCM-41 and MONO-PE-MCM-41

	Surface area ($m^2 g^{-1}$)	Pore volume ($cm^3 g^{-1}$)	Mean pore size (nm)	Amine content (mmol g^{-1})
PE-MCM-41	1124	2.28	9.9	-
MONO-PE-MCM-41	420	0.65	7.2	4.3

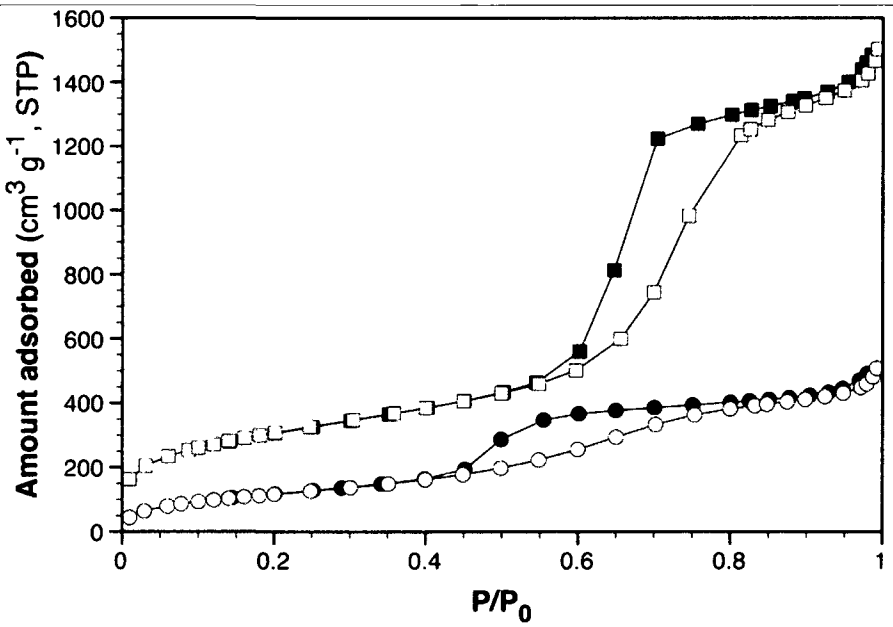

Figure 4.2 Nitrogen adsorption (open symbols) and desorption (closed symbols) isotherms at 77 K for PE-MCM-41 (squares) and MONO-PE-MCM-41 (circles)

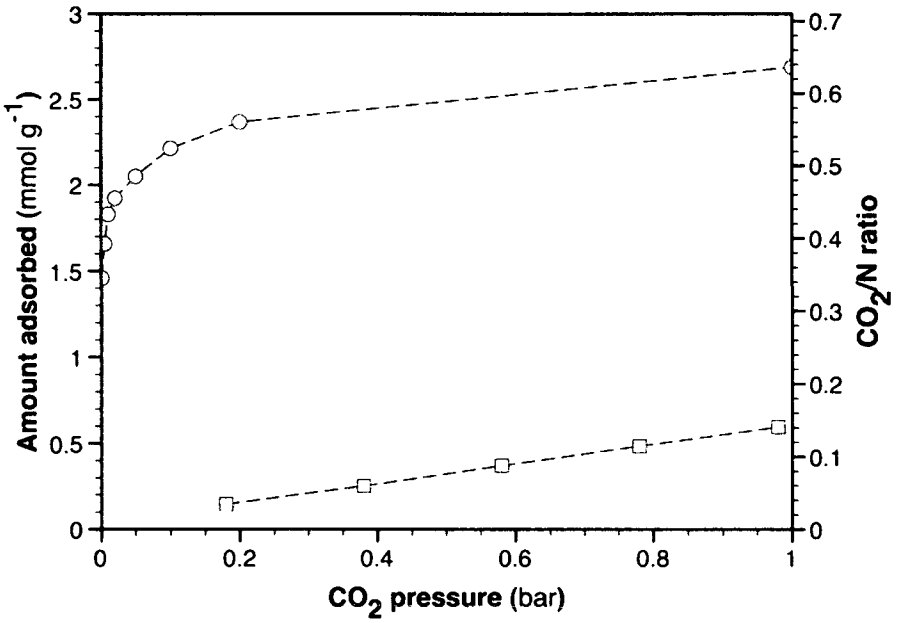

Figure 4.3 CO_2 adsorption isotherms at 25 °C on PE-MCM-41 (squares) and MONO-PE-MCM-41 (circles). The right-hand ordinate is CO_2/N ratio for MONO-PE-MCM-41 only

Figure 4.3 shows the CO_2 adsorption isotherm at 25 °C on MONO-PE-MCM-41. As seen in Figure 4.3, the comparatively low adsorption capacity of the siliceous support (PE-MCM-41) underlines the major contribution of the amine groups to the uptake of CO_2 by MONO-PE-MCM-41. As seen, the CO_2/N ratio depends on the CO_2 concentration with a stoichiometric theoretical value of 0.5 obtained at ca. 5% CO_2. It is worth mentioning that these results are in agreement with the equilibrium data observed for various amines in solution, where a typical CO_2/N ratio of 0.5 is obtained at CO_2 concentrations between 5 and 10% [Jakobsen et al., 2005; Ma'mun et al., 2007; Bahadori et al., 2008; Böttinger et al., 2008]. Lower concentrations of CO_2 may result in CO_2 uptakes below the saturation level of all available amine sites, with CO_2 becoming the limiting reactant as dictated by phase equilibrium. Using higher concentrations of CO_2 in dry streams leads to adsorption capacities corresponding to CO_2/N ratios above 0.5, which can be attributed to the occurrence of both chemical and physical adsorption. As CO_2 concentration increases however, the adsorption capacity of the purely siliceous support (PE-MCM-41) becomes significant. Based on Figure 4.3, the onset of physisorption at atmospheric pressure over the purely siliceous PE-MCM-41 occurs at a CO_2 concentration of ca. 10% and increases with the CO_2 partial pressure. It is

thus inferred that, in addition to CO_2 chemisorption, physical adsorption takes place at high CO_2 concentration as MONO-PE-MCM-41 maintained a mesoporous structure. Thus, a mixture of 5% CO_2 balance nitrogen was used to investigate the CO_2–amine chemistry, in order to minimize any contribution to the CO_2 uptake due to physical adsorption.

4.3.1 Adsorption of dry CO_2. Adsorption of CO_2 was first performed under dry conditions. As the production of carbamate is expected, the equilibrium CO_2/N ratio should be close to 0.5. The CO_2 adsorption capacity calculated for MONO-PE-MCM-41 is presented in Table 4.2. A typical desorption profile of CO_2 as determined by MS after baseline correction is presented in Figure 4.4. For comparison, the amount of adsorbed CO_2 as calculated from the weight gain determined by TGA (see Figure 4.5) is included in Table 4.2. Figures 4.4 and 4.5 also show the results of CO_2 adsorption in humid streams and are discussed with further detail in Section 4.3.2. As seen in Table 4.2 (last line), the results obtained from both methods were remarkably similar, corroborating the reliability of the quantitative analysis using mass spectrometry. It is also seen that the amount of CO_2 removed corresponds closely to the stoichiometric ratio for carbamate formation.

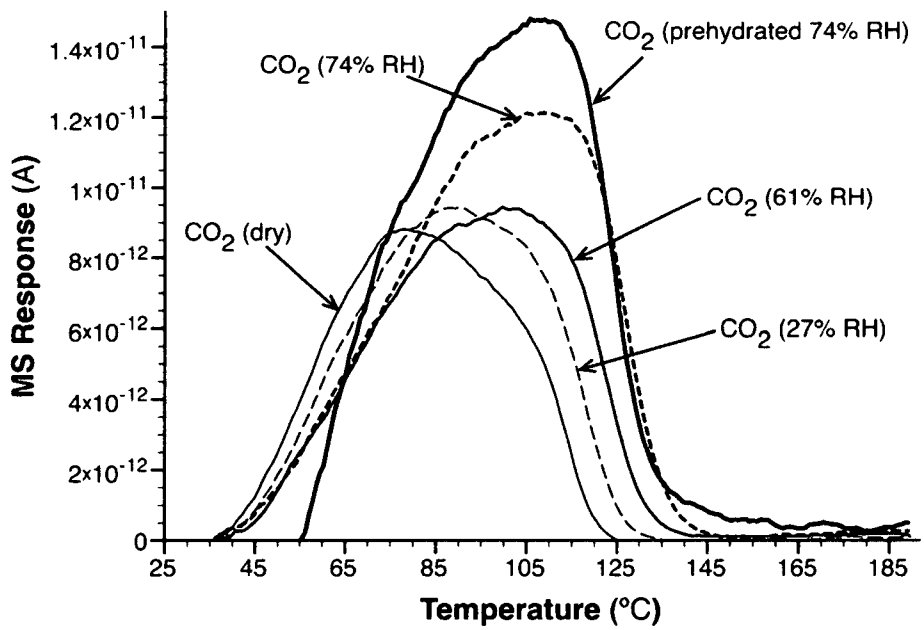

Figure 4.4 Temperature programmed desorption profiles of CO_2 after adsorption on MONO-PE-MCM-41

Table 4.2. Adsorption capacity for dry CO_2 on various amine-grafted porous materials

Support	CO_2 pressure (kPa)	Adsorption capacity (mmol g^{-1})	CO_2/N ratio	Reference
Silica gel	101	0.41	0.39	Leal et al, 1995
Xerogel	5	0.45	0.27	Huang et al., 2003
Xerogel	101	1.12	0.66	Huang et al., 2003
MCM-48	5	1.14	0.49	Huang et al., 2003
MCM-48	101	2.05	0.89	Huang et al., 2003
HMS	91	0.86	0.45	Knowles et al., 2005
Silica gel	91	0.68	0.60	Knowles et al., 2005
MCM-48 (dry grafting)	101	0.80	0.33	Kim et al., 2005
MCM-48 (water-aided grafting)	101	0.10	0.03	Kim et al., 2005
SBA-15 (dry grafting)	15	0.52	0.20	Hiyoshi et al., 2005
SBA-15 (water-aided grafting)	15	0.66	0.25	Hiyoshi et al., 2005
SBA 15	5	0.58	0.44	Wang et al., 2007
SBA-12	10	1.04	0.49	Zelenak et al., 2008
PE-MCM-41	5	2.05[a] (2.05)[b]	0.49	This work

[a] Obtained by MS

[b] Values in parenthesis obtained by gravimetry

Table 4.2 also presents the CO_2 adsorption performance of various silicas functionalized by primary amines reported in the literature. It should be noted that the CO_2 concentration used in such investigations varied from 5 to 100%. For a better illustration, values of CO_2/N ratios vs. CO_2 concentration were represented graphically in Figure 4.6. As discussed before, it is expected that at high CO_2 concentrations, in addition to chemisorption of CO_2 on amine groups, physisorption within the porous structure may also occur. This is likely the case of the results reported by Huang et al., [2003] and Knowles et al., [2005]

where the calculated CO_2/N ratio was higher than the stoichiometric ratio for carbamate formation. In the work of Knowles et al., [2005] for example, at 90% CO_2 concentration, the amount of CO_2 removed by the purely siliceous support was between 0.40 and 0.65 mmol g^{-1}, representing a significant contribution to the capacity of the functionalized material at such concentration. Yet, the adsorption data reported by Leal et al., [1995], Hiyoshi et al., [2005] and Kim et al., [2005], corresponded to CO_2/N ratios lower than 0.5, despite the high CO_2 concentration used in some cases. This unexpectedly low performance, however, is consistent with the fact that such adsorbents presented a significant loss of porosity after functionalization, which may hinder the accessibility of functional groups or give rise to severe diffusion limitations due to an unfavorable pore structure.

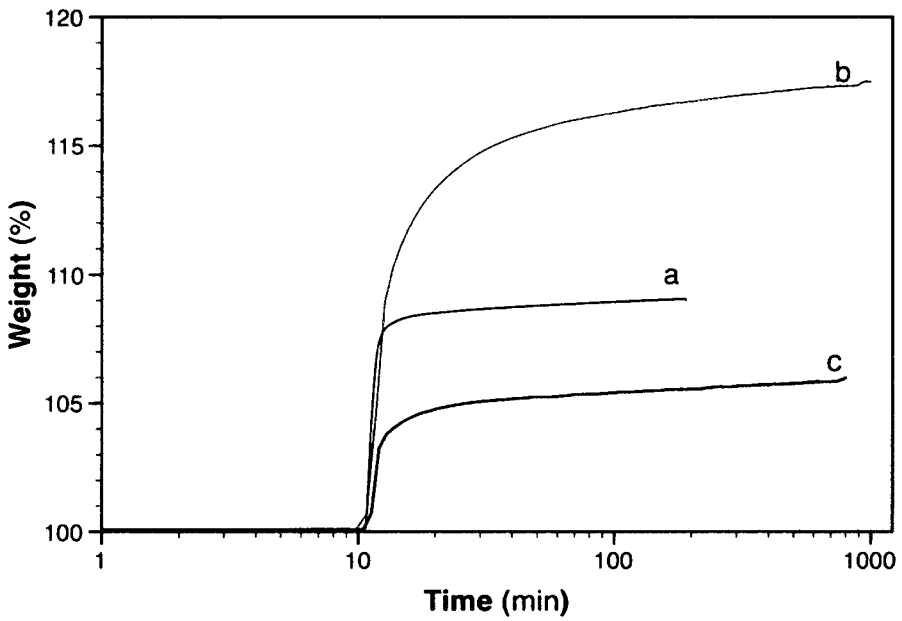

Figure 4.5 Weight gain for MONO-PE-MCM-41 under different conditions as recorded by TGA; (a) adsorption of dry CO_2; (b) coadsorption of CO_2 and water vapor; (c) adsorption of CO_2 at RH = 61% on material prehydrated at the same RH

The materials used by other workers that maintained a mesoporous nature [Huang et al., 2003; Wang et al., 2007; Zelenak et al., 2008], when used for adsorption at low concentration exhibited CO_2/N ratios close to the stoichiometric ratio, in agreement with the findings of the current investigation. It is worth mentioning that our MONO-PE-MCM-41

exhibited a clear advantage over the rest of the adsorbents presented in Table 4.2 in terms of adsorption capacity, attributed to its open porous structure and high amine loading. Moreover, it may be inferred that MONO-PE-MCM-41 will have a higher adsorption rate compared to materials with less open pore structure.

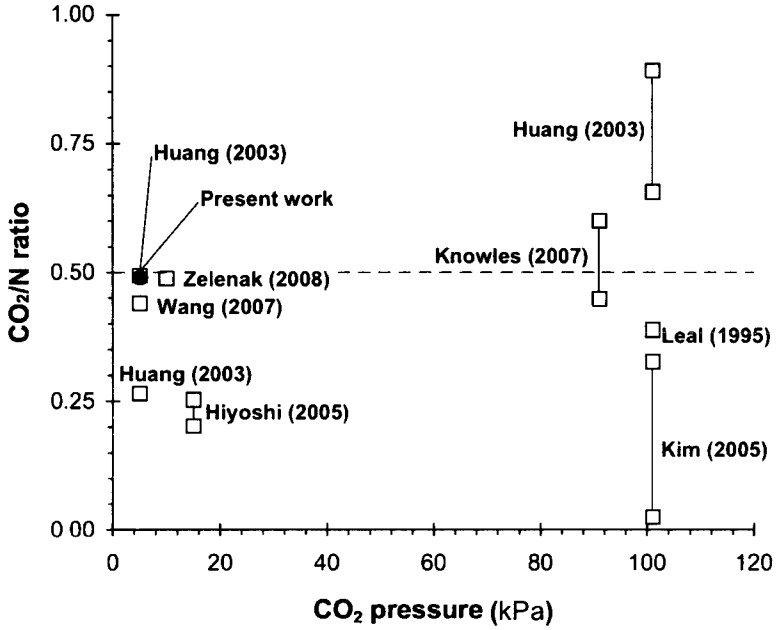

Figure 4.6 CO_2/N vs. CO_2 concentration ratio for amine-functionalized materials reported in the literature (squares) and in this work (circle) for dry adsorption

4.3.2 Adsorption of humid CO_2. Figure 4.5 shows typical TGA profiles for CO_2 adsorption in the presence of moisture. As can be seen, when a humid CO_2 stream is fed, the response of a gravimetric apparatus is a result of the overall weight gain without distinction between the contribution from water or from CO_2 uptake. Thus, a technique capable of discriminating between the two adsorbates, such as MS, is required. The adsorption capacity of MONO-PE-MCM-41 for CO_2 at different RH calculated from MS signals (Figure 4.4) is presented in Table 4.3. It is interesting to notice in Figure 4.4 that the maximum temperature for CO_2 desorption increases with the CO_2/N ratio (see Table 4.3), suggesting that bicarbonate is more stable than carbamate.

In all cases, the CO_2 adsorption capacity in humid streams was higher than that of dry CO_2. As the CO_2/N ratio was invariably higher than 0.5, the production of bicarbonate can be

inferred. Consistent with the current findings, Khatri et al., [2006] provided direct evidence on the formation of bicarbonate species by infrared spectroscopy during humid CO_2 adsorption on supported amines. However, within the range of vapor concentration used in this work, only partial production of bicarbonate occurred since the CO_2/N ratio was below 1. It is interesting to mention that at RH of 27% and 61%, the adsorption capacity underwent a modest increase of 16% and 22%, respectively compared to dry CO_2 adsorption. A more significant increase (i.e., 60%) was observed at RH = 74%, resulting in a CO_2/N ratio of 0.78. A reasonable explanation may be proposed based on the adsorption isotherm for water on MONO-PE-MCM-41 shown in Figure 4.7. At a RH of 74%, a sharp increase in water uptake took place, indicating the occurrence of capillary condensation. The large increase in CO_2 adsorption capacity could then be explained either by the presence of a large amount of water molecules available to react with the amine and CO_2 or as a result of an environment reminiscent of amines in solution.

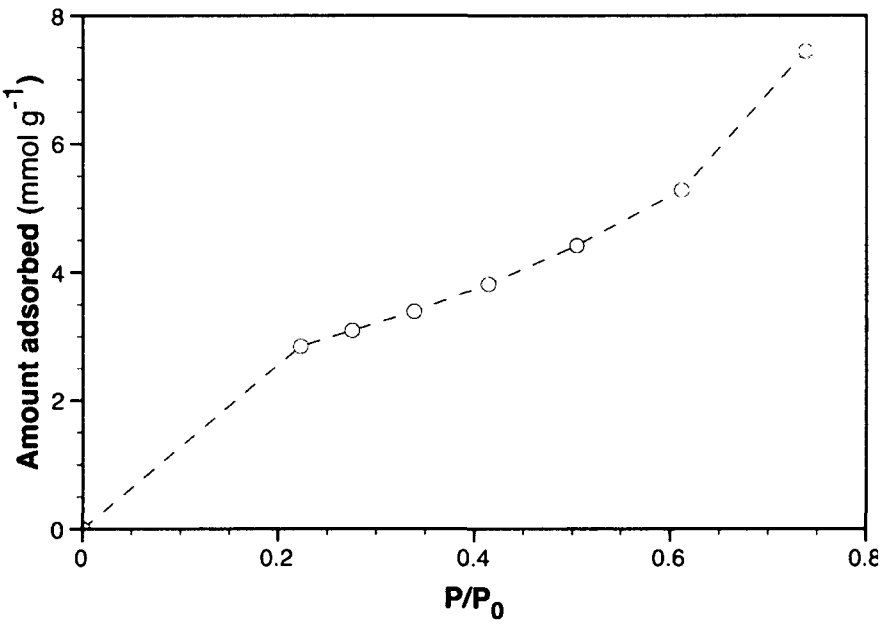

Figure 4.7 Water adsorption isotherm at 25 °C on MONO-PE-MCM-41

Based on the above observations, it may be inferred that as the pore filling of water occurs, a higher efficiency in the production of bicarbonate takes place and it is thus possible

that under extremely high RH, the theoretical CO_2/N ratio of 1 may be reached. Some values of adsorption capacity reported in the literature are presented in Table 4.3

Table 4.3 Adsorption capacity for humid CO_2 streams on amine-grafted porous materials

Support	CO_2 pressure (kPa)	RH (%)	Adsorption capacity (mmol g^{-1})	CO_2/N ratio	Method of analysis	Reference
Silica gel	101	98	0.89	0.74	TPD	Leal et al., [1995]
MCM-48	5	64	2.3	1	TPD	Huang et al., [2003]
HMS[a]	91	30	1.04	0.54	TGA	Knowles et al., [2005]
SBA-15 (dry grafting)[a]	15	61	0.5	0.20	Breakthrough curve	Hiyoshi et al., [2005]
SBA-15 (water-aided grafting)[a]	15	61	0.65	0.25		Hiyoshi et al., [2005]
SBA 15	10	100	0.40	0.21	Breakthrough curve	Hicks et al., [2008]
SBA-15[b]	10	100	3.11	0.44		Hicks et al., [2008]
PE-MCM-41	5	27	2.37	0.57	TGA - MS	This work
PE-MCM-41	5	61	2.51	0.60		This work
PE-MCM-41	5	74	3.27	0.78		This work
PE-MCM-41[a]	5	27	2.46 (1.58)[c]	0.63		This work
PE-MCM-41[a]	5	61	2.64 (1.31)[c]	0.63		This work
PE-MCM-41[a]	5	74	3.67 (1.90)[c]	0.88		This work

[a] Pre-hydrated samples

[b] Covalently tethered hyperbranched aminosilica

[c] Obtained by gravimetry

. The CO_2/N ratios along with the corresponding RH are shown in Figure 4.8, where, in line with the findings of the present study, the adsorbent of Huang et al., [2003] and Leal et al., [1995] presented high CO_2/N values at RH of 64 and 98%, respectively. On the other hand, although the capacity of amine-grafted SBA-15 reported by Hicks et al., [2008] was

determined at high RH, low CO_2/N ratios were observed. This may be associated with the use of a fixed bed column, and it is possible that the residence time was not long enough to reach equilibrium. Interestingly, the best performing material reported in that work, a hyperbranched aminosilica, presented a CO_2/N close to 0.5, suggesting that the faster carbamate production was the dominating reaction in the dynamic process.

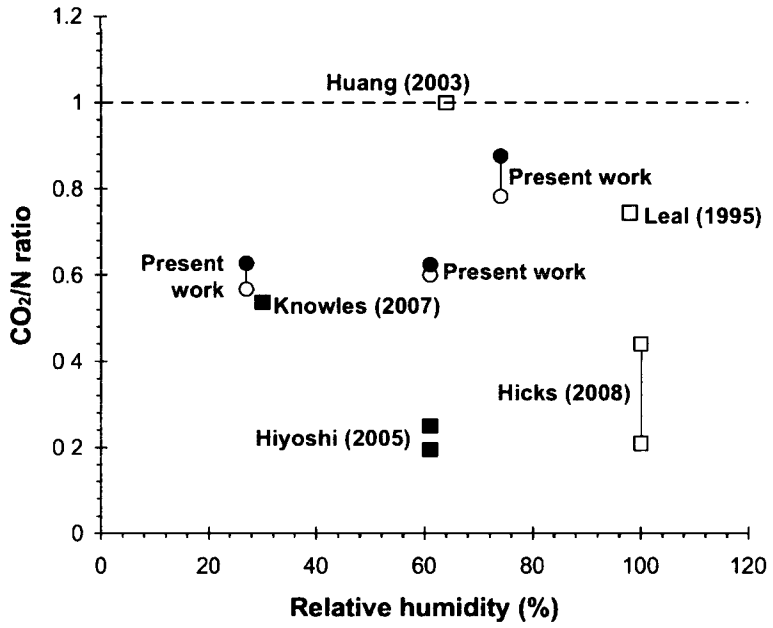

Figure 4.8 CO_2/N ratio vs. relative humidity for amine-functionalized materials reported in the literature and in this work (open symbols: fresh samples, closed symbols: pre-hydrated samples)

From the discussion above, it is inferred that the mechanism of CO_2 adsorption on supported amines is analogous to that of liquid amines. It is, however, of interest to further scrutinize the results obtained when pre-hydration of the adsorbent takes place. The adsorption capacities of samples pre-hydrated at different RHs are also presented in Table 4.3. As stated earlier, in all cases the calculated CO_2/N ratio was higher than 0.5, which suggests the production of bicarbonate. This is consistent with the observations by Chang et al., [2003] using infrared spectroscopy on pre-hydrated supported amines. It is also seen that the amount adsorbed on samples pre-hydrated at low RH is similar to the uptake of humid CO_2 by fresh samples, although a difference of ca. 10% was observed at RH = 74%.

However, it is important to point out that the adsorption capacities for pre-hydrated samples are severely underestimated when only TGA is used (Figure 4.5 and values in parentheses in Table 4.3), compared to the results obtained by mass spectrometry. It is possible that pre-adsorbed water is displaced during CO_2 adsorption, a phenomenon that would go undetected by gravimetry. Such a problem may also occur with other co-adsorbates. This could explain the apparent lack of consistency in the results reported by other authors using pre-hydrated adsorbents (Table 4.3). It is thus crucial, in the case of multicomponent adsorption, to use a technique that specifically discriminates between coadsorbates.

4.4 Conclusions

Under appropriate conditions, at least as far as primary monoamines are concerned, chemisorption of CO_2 using amine-functionalized materials is reminiscent of CO_2 scrubbing with ethanolamine solutions with maximum CO_2/N molar ratios of 0.5 and 1 for dry and humid streams corresponding to the formation of carbamate and bicarbonate, respectively. Using a silica support with a widely open pore structure such as PE-MCM-41 for propylamine grafting affords superior adsorbents with enhanced amine loading and quantitative adsorption of CO_2. It can be inferred that the reaction mechanisms governing the interaction between CO_2 and supported amines are analogous to that of amines in solution with the caveat that significant amounts of bicarbonate will form only when capillary condensation of water occurs. Depending on the concentration of CO_2 and RH of the feed, CO_2/N ratios that deviate from the stoichiometric ratios of 0.5 and 1 are often associated with experimental conditions (e.g., CO_2 pressure, RH) or accessibility of active sites. It was also demonstrated that gravimetry is not a reliable technique for the evaluation of CO_2 adsorption capacity in humid streams as it underestimates the total CO_2 uptake.

References

B. Arstad, R. Blom, O. Swang, CO_2 absorption in aqueous solutions of alkanolamines: mechanistic insight from quantum chemical calculations. J. Phys. Chem. A 111 (2007) 1222

A. Bahadori, H.B. Vuthaluru, S. Mokhatab, Rapid prediction of CO_2 solubility in aqueous solutions of diethanolamine and methyldiethanolamine, Chem. Eng. Technol. 31 (2008) 245

P. Birbara, T. Filburn, H. Michels, T. Nalette, Sorbent System and Method for Absorbing

Carbon Dioxide (CO_2) from the Atmosphere of a Closed Habitable Environment. US Patent 6,364,938, 2002

B. Bonenfant, M. Mimeault, R. Hausler, Determination of the structural features of distinct amines important for the absorption of CO_2 and regeneration in aqueous solution. Ind. Eng. Chem. Res. 42 (2003) 3179

W. Böttinger, M. Maiwald, H. Hasse, Online NMR spectroscopic study of species distribution in MEA–H_2O–CO_2 and DEA–H_2O–CO_2. Fluid Phase Equilib. 263 (2008) 131

F. Brandani, D.M. Ruthven, The effect of water on the adsorption of CO_2 and C_3H_8 on type X zeolites. Ind. Eng. Chem. Res. 43 (2004) 8339.

A.C.C. Chang, S.C.C. Chuang, M. Gray, Y. Soong, In-situ infrared study of CO_2 adsorption on SBA-15 grafted with γ-(Aminopropyl)triethoxysilane. Energy Fuels 17 (2003) 468

E.F. da Silva, H.F. Svendsen, Computational chemistry study of reactions, equilibrium and kinetics of chemical CO_2 absorption. Int. J. Greenhouse Gas Control 1 (2007) 151

M.L. Gray, K.J. Champagne, Y. Soong, T. Filburn, High Capacity Immobilized Amine Sorbents. US Patent 7,288,136, 2007

P.J.E. Harlick, A. Sayari,. Applications of pore-expanded mesoporous silica. 5. Triamine grafted material with exceptional CO_2 dynamic and equilibrium adsorption performance. Ind. Eng. Chem. Res. 46 (2007) 446.

J.C. Hicks, J.H. Drese, D.J. Fauth, M.L. Gray, G. Qi, C.W. Jones, Designing adsorbents for CO_2 capture from flue gas-hyperbranched aminosilicas capable of capturing CO_2 reversibly. J. Am. Chem. Soc. 130 (2008) 2902

N. Hiyoshi, K. Yogo, T. Yashima, Adsorption characteristics of carbon dioxide on organically functionalized SBA-15. Microporous Mesoporous Mater. 84 (2005) 357

H.Y. Huang, R.T. Yang, D. Chinn, C.L. Munson, Amine-grafted MCM-48 and silica xerogel as superior sorbents for acidic gas removal from natural gas. Ind. Eng. Chem. Res. 42 (2003) 2427

J.P. Jakobsen, J. Krane, H.F. Svendsen, Liquid-phase composition determination in CO_2-H_2O-alkanolamine systems: an NMR study. Ind. Eng. Chem. Res. 44 (2005) 9894

C.W. Jones, J.C. Hicks, D.J. Fauth, M. Gray, Structures for Capturing CO_2, Methods of Making the Structures and Methods for Capturing CO_2, US Patent application 20070149398, 2007

R.A. Khatri, S.C.C. Chuang, Y. Soong, M. Gray, Thermal and chemical stability of regenerable solid amine sorbent for CO_2 capture. Energy Fuels 20 (2006) 1514

S. Kim, J. Ida, V.V. Guliants, J.Y.S. Lin, Tailoring pore properties of MCM-48 silica for selective adsorption of CO_2. J. Phys. Chem. B 109 (2005) 6287

G.P. Knowles, J.V. Graham, S.W. Delaney, A.L. Chaffee, Aminopropyl-functionalized mesoporous silicas as CO_2 adsorbents. Fuel Process. Technol. 86 (2005) 1435

G.P. Knowles, S.W. Delaney, A.L. Chaffee, Diethylenetriamine[propyl(silyl)]-functionalized (DT) mesoporous silicas as CO_2 adsorbents. Ind. Eng. Chem. Res. 45 (2006) 2626

M. Kruk, M. Jaroniec, A. Sayari, A. Application of large pore MCM-41 molecular sieves to improve pore size analysis using nitrogen adsorption measurements. Langmuir 13 (1997) 6267

M. Kruk, M. Jaroniec, A. Sayari, A. New insights into pore-size expansion of mesoporous silicates using long-chain amines. Microporous Mesoporous Mater. 35-36 (2000) 545

O. Leal, C. Bolivar, C. Ovalles, J.J. Garcia, Y. Espediel, Reversible adsorption of carbon dioxide on amine surface-bonded silica gel. Inorg. Chim. Acta, 240 (1995) 183

X. Liu, L. Zhou, X. Fu, Y. Sun, W. Su, Y. Zhou, Adsorption and regeneration study of the mesoporous adsorbent SBA-15 adapted to the capture/separation of CO_2 and CH_4. Chem. Eng. Sci. 62 (2007) 1101

S. Ma'mun, H.F. Svendsen, K.A. Hoÿb, O. Juliussen, Selection of new absorbents for carbon dioxide capture. Energy Convers. Manage. 48 (2007) 251

G. Olah, A. Goepert, S. Meth, S. Prakash, Nano-Structure Supported Solid Regenerative Polyamine and Polyamine Polyol Adsorbents for the Separation of Carbon Dioxide from Gas Mixtures Including the Air. Int. Patent application WO/2007/US74615 20070727, 2008

B.A. Oyenekan, G.T. Rochelle, Alternative stripper configurations for CO_2 capture by aqueous amines. AIChE J. 53 (2007) 3144

J.P.K. Reynhardt, Y. Yang, A. Sayari, H. Alper, Polyamidoamine dendrimers prepared inside the channels of pore-expanded periodic mesoporous silica. Adv. Funct. Mater. 15 (2005) 1641

A. Sayari, M. Kruk, M. Jaroniec, I.L. Moudrakovski, New approaches to pore size engineering of mesoporous silicates. Adv. Mater. 10 (1998) 1376

A. Sayari, Y. Yang, M. Kruk, M. Jaroniec, Expanding the pore size of MCM-41 silicas: use

of amines as expanders in direct synthesis and postsynthesis procedures. J. Phys. Chem. B 103 (1999) 3651

A. Sayari, "Mesoporous materials" in The Chemistry of Nanostructured Materials, edited by Peidong Yang, World Scientific, Singapore (2003) pp. 39-68

A. Sayari, Amine Modified Adsorbent, its Preparation and Use for Dry Scrubbing of Acid Gases. International Patent application WO/2004/054708, 2004

A. Sayari, P.J.E. Harlick, Functionalized Adsorbent for Removal of Gases and Uses Thereof. International Patent application WO/2006/094411, 2006

R. Serna-Guerrero, A. Sayari, A. Applications of pore-expanded mesoporous silica. 7. adsorption of volatile organic compounds. Environ. Sci. Technol., 41 (2007) 4761

P.D. Vaidya, E.Y. Kenig, CO_2-alkanolamine reaction kinetics: a review of recent studies. Chem. Eng. Technol. 30 (2007) 1467

A. Veawab, P. Tontiwachwuthikul, A. Chakma, Corrosion behavior of carbon steel in the CO_2 absorption process using aqueous amine solutions. Ind. Eng. Chem. Res. 38 (1999) 3917.

L. Wang, L. Ma, A. Wang, Q. Liu, T. Zhao, CO_2 adsorption on SBA-15 modified by aminosilane. Chin. J. Catal. 28 (2007) 805

X. Xu, C. Song, J.M. Andresen, B.G. Miller, A.W. Scaroni, novel polyethylenimine-modified mesoporous molecular sieve of MCM-41 type as high-capacity adsorbent for CO_2 capture. Energy Fuels 16 (2002) 1463

H. Yang, Z. Xu, M. Fan, R. Gupta, R.B. Slimane, A.E. Bland, I. Wright, I. Progress in carbon dioxide separation and capture: A review. J. Environ. Sci. 20 (2008) 14

V. Zelenak, D. Halamova, L. Gaberova, E. Bloch, P. Llewellyn, Amine-modified SBA-12 mesoporous silica for carbon dioxide capture: Effect of amine basicity on sorption properties. Micropor, Mesopor. Mater. 116 (2008) 358

Chapter 5

Further investigations of CO_2 capture using triamine-grafted pore-expanded mesoporous silica

Chem. Eng. J. 158 (2010) 513-519

Abstract

A promising adsorbent for acid gas removal, referred to as TRI-PE-MCM-41, was produced by grafting a triamine-containing silane on an MCM-41 type mesoporous silica whose pores have been enlarged by post-synthesis hydrothermal treatment in the presence of a pore-expander, The CO_2 adsorption capacity was determined gravimetrically, and via column-breakthrough measurements. The tolerance of TRI-PE-MCM-41 to moisture in the feed was substantiated by measurements under both equilibrium and dynamic conditions. Using a combination of mass spectrometry and thermogravimetry, it was corroborated that the presence of moisture enhances the CO_2 uptake at equilibrium. Adsorption measurements using fixed bed columns showed that moisture does not affect negatively the CO_2 working adsorption capacity compared to dry streams. Furthermore, since the material hardly adsorbed any N_2 or O_2, the selectivity for CO_2 over N_2 and O_2 was practically infinitely high. Cyclic measurements of pure CO_2 and CO_2:N_2 = 10:90 mixture using different regeneration modes shed light on the stability of the material and the influence of adsorption/desorption operating conditions on its performance. It was found that the temperature swing regeneration mode is suitable for desorption above 120 °C, while regeneration under temperature-vacuum swing may be attractive at lower desorption temperatures.

5.1 Introduction

One of the most serious problems facing humanity is to prevent the release of excessive amounts of carbon dioxide, due to its impact on climate change. At present, gas absorption using liquid alkanolamine solutions is industry's preferred technology for CO_2 capture at low temperature, but suffers major drawbacks including high demand of energy and the corrosive nature of the absorbent [Audus, 1997; Meisen and Shuai, 1997; Aaron and Tsouris, 2005].

Adsorption separation is recognized as an efficient and economically attractive candidate to complement or replace the current CO_2 scrubbing processes as it is expected to combine high selectivity and productivity, while offering low energy requirements to regenerate the solid adsorbent [Aaron and Tsouris, 2005]. To be competitive, an ideal medium for CO_2 adsorption should combine a number of favorable attributes including: (i) high CO_2 dynamic adsorption capacity, (ii) high selectivity toward CO_2, (iii) low energy requirements for regeneration, (iv) stability to prolonged adsorption-desorption cycling including tolerance to oxidation, and (v) tolerance to the presence of moisture in the CO_2-containing feed.

Inspired by liquid amine scrubbing technology, a number of research groups developed solid-supported amines as adsorbents for CO_2 separation [Birbara et al., 2002; Gray et al., 2007; Harlick and Sayari, 2007; Jones et al., 2007; Olah et al., 2008]. Chief among the supports are ordered mesoporous silicas and organosilicas, which have proven to be promising materials in a wide variety of environmental applications. The possibility to incorporate functional groups on their internal surface or within their pore volume has produced highly efficient materials that could lead to alternative separation technologies, including the removal of acid gases from a variety of gas streams [Yue et al., 2006; Son et al., 2008; Yue et al., 2008; Belmabkhout and Sayari, 2009a; Belmabkhout and Sayari, 2009b; Belmabkhout et al., 2009; Choi et al., 2009; Ma et al., 2009; Belmabkhout et al, 2010].

Our research group developed a highly promising adsorbent for CO_2 and other acid gases [Harlick and Sayari, 2007; Belmabkhout and Sayari, 2009b]. This material, referred to as TRI-PE-MCM-41, consists of a triamine-functionalized pore-expanded MCM-41 silica. In our previous efforts, we focused on optimizing the conditions for the preparation of TRI-PE-MCM-41 through surface grafting of aminosilane [Harlick and Sayari, 2007] as well as its adsorptive properties using mostly 5% CO_2/N_2 gas mixture [Harlick and Sayari, 2007; Belmabkhout and Sayari, 2009b]. Limited work on the effect of moisture was also carried out using gravimetric measurements [Harlick and Sayari, 2007]. It was later demonstrated using a propylamine modified mesoporous silica that TGA may underestimate the actual CO_2 uptake in the presence of moisture [Serna-Guerrero et al., 2008]. To properly analyze the effect of moisture on CO_2 adsorption at equilibrium, a method coupling gravimetry and mass spectrometry (TGA-MS) was developed. The main purpose of the present work was to expand on our earlier findings to gain an in-depth understanding of amine-modified

mesoporous silicas as CO_2 adsorbents. Specifically, the current work deals with the following issues: (i) CO_2 adsorption in dry and humid streams at equilibrium using a TGA-MS method, (ii) CO_2 working adsorption capacity and selectivity under dynamic conditions using a fixed bed column, and (iii) behavior of the adsorbent through various adsorption-desorption cycles, studying the effects of adsorption temperature (T_A), desorption temperature (T_D) and desorption pressure (P_D). The adsorbent behavior throughout a number of cycles provided new insights on the stability of the material and its requirements for an efficient regeneration.

5.2 Experimental

5.2.1 Materials. Cab-O-Sil M-5 fumed silica from Cabot was used as the silica source. Cetyltrimethylammonium bromide (CTAB, Aldrich) and tetramethyl ammonium hydroxide (TMAOH, 25%, in water, Aldrich) were used as structure directing agent and for pH adjustment, respectively. The post-synthesis pore expander agent was dimethyldecylamine (DMDA, 97% purity, Aldrich). The grafting agent, obtained from Sigma-Aldrich, was 2-[2-(3-trimethoxysilylpropylamino)ethylamino]ethylamine (herein referred to as TRI-silane). Ultra high purity grade nitrogen, CO_2 grade 4 purity, and certified gas mixtures of CO_2 balance air were supplied by Linde Canada. All reagents and gases were used without further purification.

5.2.2 Synthesis of TRI-PE-MCM-41 adsorbent. The pore-expanded mesoporous support was prepared in two steps based on a procedure described elsewhere [Sayari et al., 1998; Kruk et al., 2000]. Briefly, MCM-41 type silica was synthesized at 100 °C using CTAB as structure directing agent in the presence of TMAOH. Pore expansion was achieved through a post-synthesis hydrothermal treatment in the presence of DMDA at 120 °C for 3 days [Sayari et al., 1998; Sayari et al., 1999; Serna-Guerrero and Sayari, 2007]. After removal of the surfactant template and the pore-expander by calcination, the obtained product was labeled PE-MCM-41.

Incorporation of the amine functionality was achieved via surface grafting following a procedure described elsewhere [Harlick and Sayari, 2007]. A sample of PE-MCM-41 was loaded into a multi-neck glass flask containing 150 mL of toluene. Once a homogeneous mixture was produced, 0.3 mL of distilled deionized water per gram of silica were added and

left stirring for at least 30 min. The glass flask was then submerged in a silicon oil bath set at 85 °C using a temperature controlled stirring hotplate with an external temperature probe. TRI-silane (3 mL per gram of PE-MCM-41) was subsequently added to the mixture and left stirring for 16 h. The material was filtered and washed with copious amounts of toluene, then pentane. Finally, the recovered solid was dried at 100 °C in a natural convection oven for 1 h and was labeled TRI-PE-MCM-41.

5.2.3. Characterization. The structural properties of PE-MCM-41 and TRI-PE-MCM-41 were determined by nitrogen adsorption at -196 °C using a Micromeritics ASAP 2020 volumetric apparatus. Prior to measurements, the samples were degassed under vacuum at 150 °C for 5 h. The surface area (S_{BET}) was determined by the BET method, whereas the pore size distribution was calculated using the Kruk-Jaroniec-Sayari (KJS) approach. [Kruk et al., 1997]. The pore volume (V_p) was determined as the amount of liquid nitrogen adsorbed at P/P_0 = ca. 1. The organic content in the sample was measured by thermogravimetric analysis (TGA) on a TA Instruments Q-500 apparatus under flowing nitrogen using a heating ramp of 10 °C min^{-1} up to 800 °C, followed by complete combustion of the organic material under air at the same heating rate up to 1000 °C. Only the weight loss above 200 °C was taken into account for the calculation of amine content [Harlick and Sayari, 2007].

Single component CO_2 adsorption equilibrium measurements were performed using a Rubotherm gravimetric-densimetric apparatus (Bochum, Germany). More details about the experimental set-up and procedure may be found elsewhere [Belmabkhout and Sayari, 2009b]. Briefly, the materials studied (MCM-41, PE-MCM-41 and TRI-PE-MCM-41) were activated at 150 °C under vacuum ($5x10^{-4}$ mbar) for at least 2 h. The temperature was subsequently reduced to ambient and the sample placed in contact with CO_2 under the desired pressure. Equilibration time was allowed until no significant change in the sample weight was observed.

5.2.4 Adsorption in humid streams. Two different approaches were used to study the performance of TRI-PE-MCM-41 in the presence of humid streams: measurements at equilibrium and measurements under dynamic conditions.

The CO_2 adsorption capacity at equilibrium was determined using the TGA instrument described in Section 5.2.3, coupled with a Pfeiffer Thermostar mass spectrometer. The experimental procedure involved the following steps: (i) activation of the adsorbent, (ii) adsorption of CO_2, (iii) temperature programmed desorption (TPD) of CO_2 and (iv) decomposition of the organic layer of the adsorbent to determine the amine content of the actual sample. A sample of TRI-PE-MCM-41 of ca. 30 mg was placed in the measurement pan of the TGA and pretreated under flowing N_2 at 150 °C since it has been demonstrated that the grafted amine species are stable up to 250 °C [Harlick and Sayari, 2007] and any CO_2 and moisture adsorbed from ambient air desorbs below 140 °C [Khatri et al., 2006]. In addition, non-hydrolyzed methoxy groups are also removed during the activation step [Harlick and Sayari, 2007]. After pretreatment, the temperature was decreased to 25 °C and the gas stream switched to a mixture of 5% CO_2 balance N_2. To control the relative humidity (RH) in the stream, the mixture of CO_2 in N_2 was bubbled through a glass saturator containing distilled deionized water located in a temperature controlled cooling bath before entering the measurement chamber of the TGA. The flow of 5% CO_2/N_2 mixture was maintained for at least 16 h to ensure that equilibrium was attained. The organic content in the sample was obtained by thermal decomposition as described above.

To properly quantify the amount of CO_2 adsorbed, particularly in the presence of moisture, mass spectrometry (MS) was used in combination with TGA [Serna-Guerrero et al., 2008], as it has been suspected that the commonly used TGA may underestimate the CO_2 uptake. The mass spectrometer was calibrated against CO_2 using the decomposition of known quantities of $CaCO_3$ under flowing nitrogen at a heating rate of 10 °C min^{-1} in the TGA instrument. After base line correction, a linear relationship between the area of the MS signal corresponding to 44 amu and the total amount of CO_2 was obtained. It was used to quantify the CO_2 released from the adsorbent during TPD.

In addition, breakthrough measurements were performed using the experimental set-up shown in Figure 5.1 to investigate the behavior of TRI-PE-MCM-41 in dynamic conditions. Line "A" is used to feed an inert gas, most commonly nitrogen, to activate the sample before each experiment, while line "B" feeds a mixture of 5% CO_2 balance air. The stainless steel column used had an inner diameter of 4.6 mm and a packed length of 120 mm. The column was packed with ca. 1 g of TRI-PE-MCM-41 particles of sizes 40 – 60 mesh

obtained by pressing TRI-PE-MCM-41 powder in a hydraulic press at 450 $kg_f\,cm^{-2}$, crushing the obtained pellets and sieving between nets with openings of 40 and 60 mesh. Notice that the pressure used was found to afford pellets without altering the structural properties of the material [Serna-Guerrero and Sayari, 2007]. The column effluent was monitored using a Pfeiffer Thermostar® mass spectrometer (MS), whose detection limit for CO_2 was estimated to be below 10 ppm. In a typical experiment, the adsorbent was treated at 150 °C for 2 h under a nitrogen flow of 50 mL min^{-1}, then cooled to room temperature and exposed to the CO_2-containing mixture at the same flow rate. The level of humidity was controlled in a similar manner as described for equilibrium measurements using distilled deionized water in a glass saturator submerged in a temperature-controlled cooling bath. The complete breakthrough of CO_2 and other species was indicated by the downstream gas composition reaching that of the feed gas.

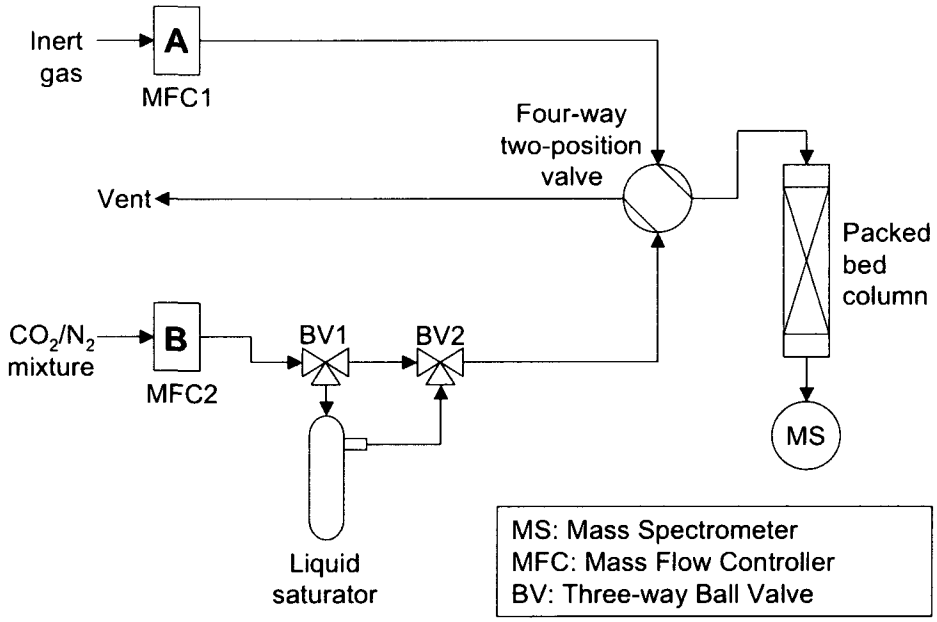

Figure 5.1 Experimental setup for dynamic adsorption measurements

The adsorption capacity was estimated from the breakthrough curves produced by the MS response using the following equation:

$$n_{adsi} = \frac{FC_{0i}t_{ni}}{W} \qquad (1)$$

where n_{adsi} is the dynamic adsorption capacity of any gas i, F is the total molar flow, C_{0i} is the concentration of the gas i entering the column, W is the mass of adsorbent loaded in the column, and t_{ni} is the stoichiometric time corresponding to gas i, which is estimated from the breakthrough profile according to Equation 2 [Geankoplis, 1993]:

$$t_{ni} = \int_0^t \left(1 - \frac{C_{Ai}}{C_{0i}}\right) dt \tag{2}$$

where C_{0i} and C_{Ai} are the concentrations of any gas i upstream and downstream the column, respectively.

5.2.5 Adsorption-desorption cycles. To assess the stability of the adsorbent, adsorption-desorption cyclic measurements were carried out on TRI-PE-MCM-41 at different conditions using temperature swing (TS) and temperature vacuum swing (TVS) regeneration conditions. Because the adsorption-desorption operating conditions may change from one application to another and may depend on the nature of the feed stream, six adsorption-desorption configurations were explored, as shown in Table 5.1, and were studied for streams containing pure CO_2 and a CO_2:N_2 = 10:90 mixture.

Table 5.1 Cyclic adsorption-desorption configurations[a]

Configuration	Conditions		
	Adsorption temperature (°C)	Desorption temperature (°C)	Desorption pressure (bar)
a	25	75	1
b	25	75	0.1
c	50	120	1
d	50	120	0.1
e	50	90	1
f	50	90	0.1

(a) Adsorption at atmospheric pressure

For example, configuration *a* represents the conditions that may be found in a TS operation, as desorption occurs under atmospheric pressure and 75 °C under purge gas flowing at 50 mL min^{-1}, whereas configuration *b* can be associated with a TVS adsorption since regeneration is performed with the aid of vacuum (i.e., P_D = 0.1 bar). The experimental procedure was as follows: a sample of ca. 1 g of TRI-PE-MCM-41 was loaded in the Rubotherm apparatus and was exposed to UHP nitrogen at 50 mL min^{-1} for 30 min at 75, 90 or 120 °C, either under atmospheric pressure or under vacuum (0.1 bar). Subsequently, the sample was cooled down to 25 or 50 °C at isobaric conditions and the feed gas was switched to either pure CO_2 or CO_2:N_2 = 10:90 mixture at 50 mL min^{-1}. The working adsorption capacity (non-equilibrium) was assumed to be the weight gain of the sample after 30 min exposure. The cycle of regeneration and CO_2 adsorption was repeated 10 times for the six sets of adsorption-desorption conditions.

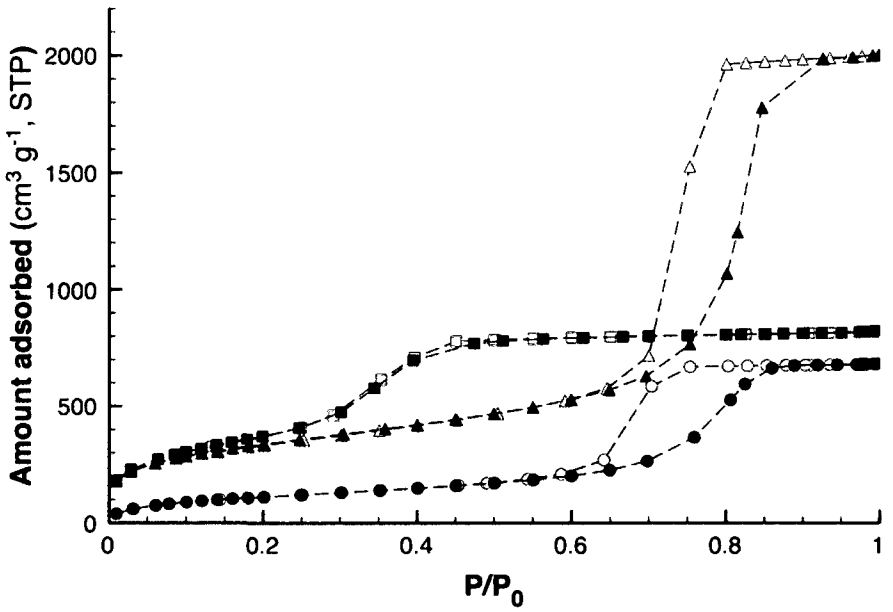

Figure 5.2 Nitrogen adsorption (closed symbols) and desorption (open symbols) isotherms for MCM-41 (squares), PE-MCM-41 (triangles) and TRI-PE-MCM-41 (circles) at 77 K

5.3 Results and discussion

5.3.1 Characterization of materials. The nitrogen adsorption isotherms of MCM-41, PE-MCM-41 and TRI-PE-MCM-41 are presented in Figure 5.2. All isotherms corresponded to

the IUPAC Type IV classification, characteristic of mesoporous materials. The structural properties determined by nitrogen adsorption measurements are shown in Table 5.2. The post-synthesis hydrothermal treatment of MCM-41 afforded a material with significantly larger mean pore diameter (d_p) and V_p without loss in surface area [Kruk et al., 2002]. The pore-expanded support exhibited a d_p of 11.7 nm and a S_{BET} of 1230 m^2 g^{-1}. After grafting, d_p decreased to 9.4 nm, consistent with the occurrence of organic species onto the internal surface. TRI-PE-MCM-41 maintained a relatively large S_{BET} (ca. 367 m^2 g^{-1}) and V_p (ca. 0.87 cm^3 g^{-1}). The widely open pore structure of surface-modified PE-MCM-41 has been associated with the efficient use of internal functional groups [Reynhardt et al., 2005; Harlick and Sayari, 2007].

Table 5.2 Structural properties of mesoporous materials

Materials	S_{BET} (m^2/g)	V_p (cm^3/g)	d_p (nm)
MCM-41	1490	0.99	3.3
PE-MCM-41	1230	3.09	11 7
TRI-PE-MCM-41	367	0.87	9.4

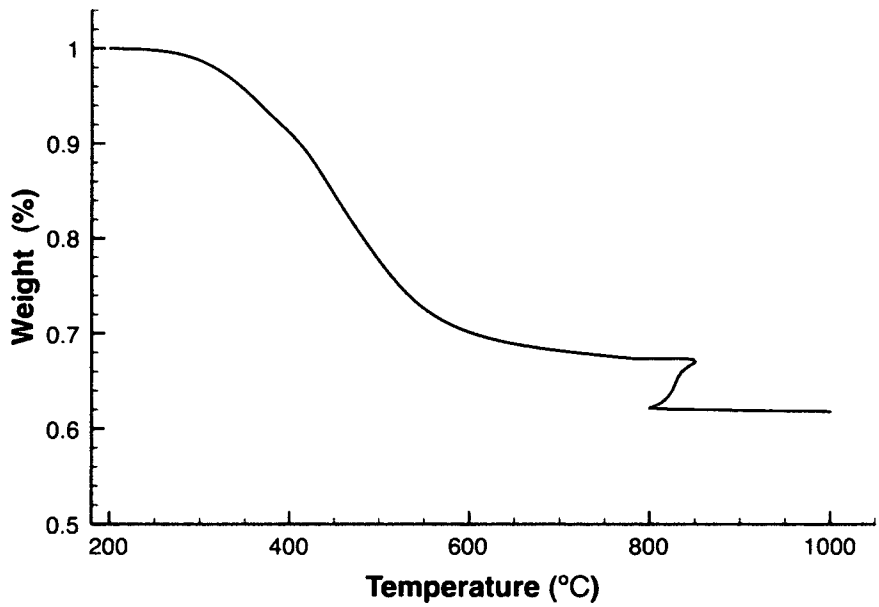

Figure 5.3 Thermogravimetric decomposition curve for TRI-PE-MCM-41

The TGA profile for TRI-PE-MCM-41 is presented in Figure 5.3. Since PE-MCM-41 did not undergo any weight loss under TGA up to 1000 °C (not shown), it was inferred that the weight loss for TRI-PE-MCM-41 is associated exclusively with the decomposition of the organic species. This event started at *ca.* 250 °C, indicating a reasonably high thermal stability. Notice that in some cases, a small weight loss was observed below 200 °C. This was demonstrated to be due to adsorbed water and/or alcohol associated with incomplete hydrolysis of the alkoxysilane [Harlick and Sayari, 2007]. Thus, it was previously established through comparison with elemental analysis, that only the weight loss beyond 200 °C corresponds to the decomposition of the amine-containing chain. Using this method, the amine loading was found to be 7.9 mmol g^{-1}.

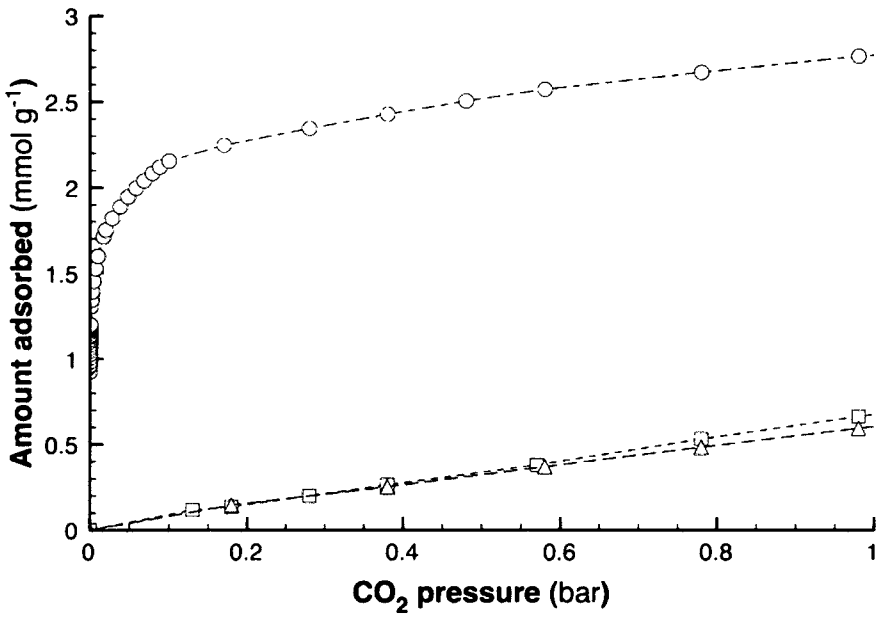

Figure 5.4 Adsorption isotherms of CO_2 on MCM-41 (squares), PE-MCM-41 (triangles), and TRI-PE-MCM-41 (circles) at 25 °C

Figure 5.4 shows the CO_2 adsorption isotherms for MCM-41, PE-MCM-41 and TRI-PE-MCM-41 materials at 25 °C and up to 1 bar. Within the range of CO_2 pressure studied, no significant difference in CO_2 capacity was observed as a result of the hydrothermal pore expansion of MCM-41. However, amine functionalization of the mesoporous silica had a strong impact on the performance of the adsorbent, particularly at very low CO_2 partial

pressure. Indeed, TRI-PE-MCM-41 exhibited a high CO_2 uptake in the low concentration range, as a result of the interaction of CO_2 with the surface amine sites. The adsorption capacity at 5% of dry CO_2 was 2.05 mmol g^{-1} for TRI-PE-MCM-41, while at the same concentration the capacity exhibited by the non-modified materials was only ca. 0.1 mmol g^{-1}.

5.3.2 Influence of moisture in the feed. In a previous contribution [Serna-Guerrero et al., 2008], it was demonstrated that gravimetric analysis often underestimates the CO_2 uptake by amine functionalized materials in humid streams. Thus, to properly assess the influence of moisture on the adsorption of CO_2 on TRI-PE-MCM-41 at equilibrium, mass spectrometry was used. The CO_2 adsorption capacity of TRI-PE-MCM-41 based on the intensity of the 44 amu signal during the TPD of CO_2 adsorbed in the presence of different moisture contents is shown in Figure 5.5.

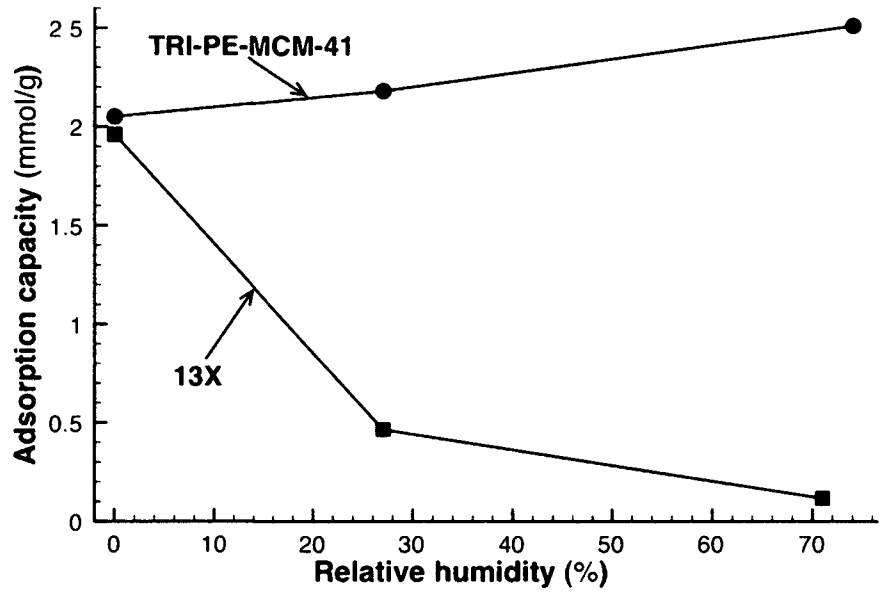

Figure 5.5 Adsorption capacity at equilibrium of 5% CO_2/N_2 on TRI-PE-MCM-41 and 13X zeolite at 25 °C in the presence of humidity

The amount of adsorbed CO_2 was found to increase with the concentration of moisture in the feed stream. The CO_2 adsorption capacity was 2.05, 2.19 and 2.51 mol g^{-1} for

0, 27 and 74% relative humidity (RH), respectively This behavior is in contrast to typical microporous CO_2 physical adsorbents such as 13X zeolite, whose adsorption capacity deteriorates dramatically, even at very low humidity levels (Figure 5 5) Enhancement of CO_2 adsorption capacity in wet streams may be explained on the basis of the generally accepted reaction mechanisms between CO_2 and amines, i e , formation of carbamate (CO_2/N = 0 5) under dry conditions and formation of bicarbonate (CO_2/N = 1) in the presence of moisture While this promoting effect had been inferred in the past through gravimetric methods, the use of TGA-MS confirms the tolerance of TRI-PE-MCM-41 to moisture, and quantifies the adsorption enhancement

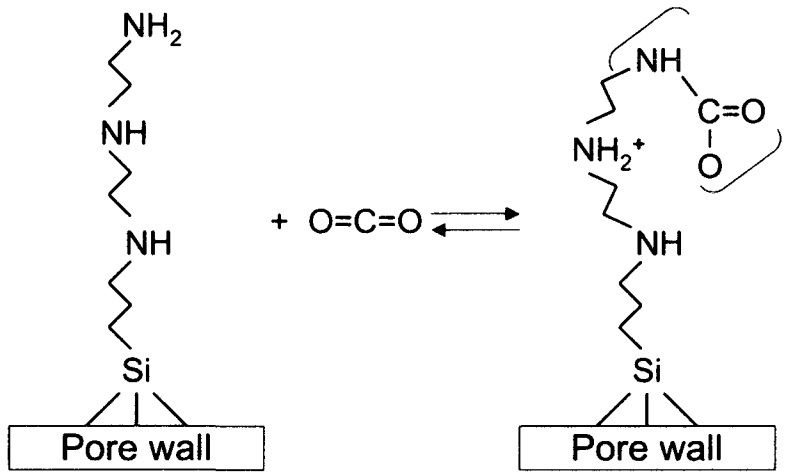

Scheme 5.1 Carbamate formation pathway on TRI-PE-MCM-41 The dotted line represents a hydrogen bond

It is worth mentioning that in dry conditions, the CO_2 to amine ratio (CO_2/N) in the case of TRI-PE-MCM-41 was ca 0 30, a lower value than the stoichiometric carbamate ratio of 0 5 obtained on grafted primary monoamine [Serna-Guerrero et al , 2008] A possible explanation to the lower values of CO_2/N ratio in this case may be associated with recent findings reported by da Silva et al [2006], and Kim et al [2007], who determined the most stable carbamate species formed between CO_2 and various amine molecules In general, CO_2 forms carbamate with amines that are in close proximity Further, if the organic species has more than two amine groups, hydrogen bonds may be formed between carbamate and the unreacted amines (Scheme 5 1), lowering the CO_2/N ratio Thus, for TRI-PE-MCM-41 two

amine groups are likely to react with CO_2 to form carbamate, while the third amine would be inhibited to react further either due to the formation of hydrogen bonds or by steric effects. Consequently, a CO_2/N ratio of 0.33 would be expected from a triamine molecule, a value close to that observed in our adsorbent at dry conditions. The increase of adsorption capacity in the presence of moisture is attributed to the partial formation of bicarbonate species.

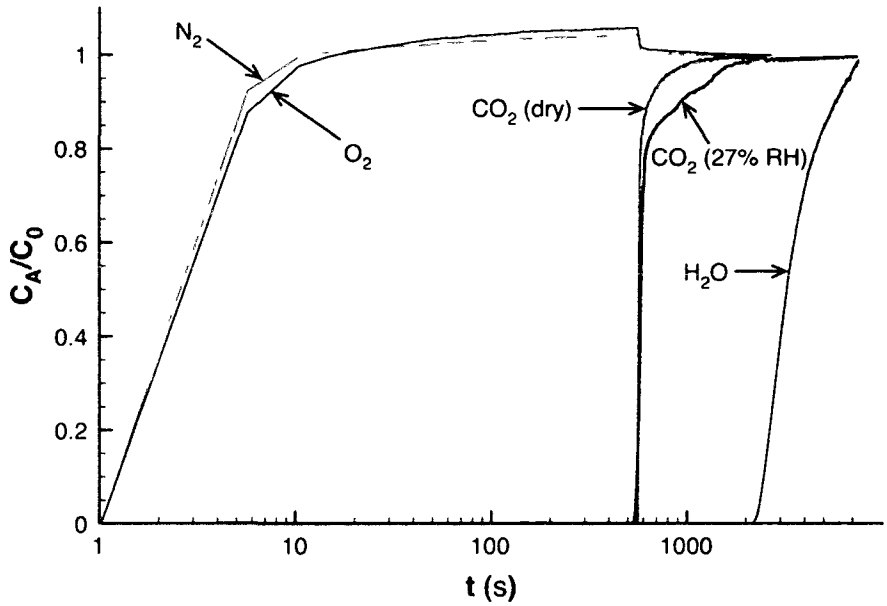

Figure 5.6 Column breakthrough curves of CO_2 (5% balance air) on TRI-PE-MCM-41 under dry and humid conditions

With respect to adsorption in packed bed columns, Figure 5.6 shows the breakthrough curves of CO_2 at a concentration of 5% balance air under dry conditions and in the presence of 27% RH. The amount of adsorbent was 1 g and the gas stream flow rate was 50 mL min^{-1}. In both cases, N_2 appeared in the column downstream almost immediately after the process has started, indicating a negligible adsorption capacity for N_2, in line with the gravimetric data [Belmabkhout and Sayari, 2009b]. This was also the case with O_2, whose breakthrough occurred immediately after the start of the adsorption process. No CO_2 was detected downstream the column up to ca. 500 s, demonstrating the high efficiency of TRI-PE-MCM-41 to separate CO_2. The breakthrough of CO_2 was steep and the complete saturation corresponded to a dry CO_2 adsorption capacity of 1.90 ± 0.19 mmol/g. The CO_2 dynamic

adsorption capacity is in good agreement with the gravimetric equilibrium capacity (2.05 mmol g^{-1}) at the same partial pressure, as reported in Figure 5.4. From these results, it is concluded that the selectivity of CO_2 over N_2 and O_2 is very high, approaching an infinite value. It is worth mentioning that such selectivity of TRI-PE-MCM-41 toward CO_2 is considerably higher than that exhibited by other typical CO_2 adsorbents like zeolites [Cavenati et al., 2004], activated carbon [Dreisbach et al., 1999] or MOFs [Yang et al., 2008].

Figure 5.6 also shows the breakthrough of water and CO_2 at a RH = 27% under otherwise the same conditions. The calculated dynamic adsorption capacity for CO_2 and water vapor were 1.98 and 2.3 mmol g^{-1}, respectively. As seen, water vapor did not adversely affect the CO_2 adsorption capacity. It is thus inferred that under non-equilibrium adsorption, as far as CO_2 removal is concerned, TRI-PE-MCM-41 is also highly tolerant to moisture. Nevertheless, the anticipated increase in CO_2 adsorption was not observed. As explained in detail in a previous contribution [Serna-Guerrero et al., 2008], this may be attributed to the comparatively slow kinetics associated with bicarbonate vs. carbamate formation. Thus, observation of enhanced CO_2 adsorption in the presence of water vapor requires a sufficiently long residence time. This requirement does not seem to be achieved under the current dynamic conditions.

5.3.3 Cyclic measurements. Figure 5.7 shows the cyclic adsorption measurements for pure CO_2 and CO_2:N_2 = 10:90 mixture using TS and TVS configurations *a* and *b*, respectively. The adsorption capacity was stable over the ten adsorption-desorption cycles for both pure CO_2 and CO_2:N_2 = 10:90 mixture. Using adsorption at 25 °C and desorption at 75 °C, the adsorption capacity using TVS was ca. 21% and ca. 35% higher than TS for pure CO_2 and CO_2:N_2 = 10:90 mixture, respectively. This may be explained by an incomplete regeneration of adsorption sites at 75 °C and atmospheric pressure. However, the combined effect of T_D = 75 °C and vacuum led to enhanced desorption, thus obtaining a higher CO_2 working capacity. The adsorption capacity of CO_2:N_2 = 10:90 mixture was ca. 40% lower than pure CO_2 using TS configuration *a*, but this difference was only ca. 28% in the TVS configuration *b*. Indeed, the incomplete activation using TS configuration *a*, resulted in less favorable working adsorption capacity than TVS configuration *b*. This clearly shows that TVS configuration *b* is

associated with better performances when adsorption and desorption are carried out at relatively low temperature.

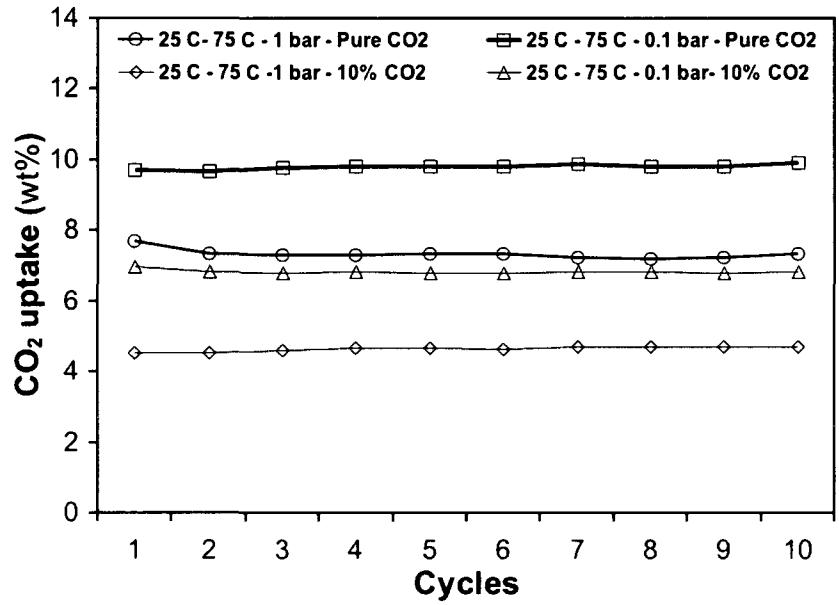

Figure 5.7 Adsorption-desorption cycles using TS and TVS configurations *a* and *b* for pure CO_2 and CO_2:N_2 = 10:90 mixture

Figure 5.8 shows the cyclic adsorption measurements for pure CO_2 and CO_2:N_2 = 10:90 mixture using TS and TVS configurations *c* and *d*, respectively. Adsorption over the ten cycles can be considered stable since the capacity in cycle 10 was within less than 5% with respect to cycle 1, although a slightly decreasing tendency was observed. With respect to the regeneration configurations, when using adsorption at 50 °C and desorption at 120 °C, the adsorption capacity using either TS or TVS was similar. Accordingly, 120 °C seems to be enough to completely regenerate the adsorbent, leading to a limited effect of vacuum when $T_D \geq 120$ °C is applied. It is important to notice that, although the T_A in configurations *c* and *d* was higher than in *a* and *b*, in terms of adsorption capacity, configurations *c* and *d* outperformed *a* and *b*. These results show that a competitive working adsorption capacity can be obtained even at temperatures higher than ambient if the appropriate regeneration conditions are met.

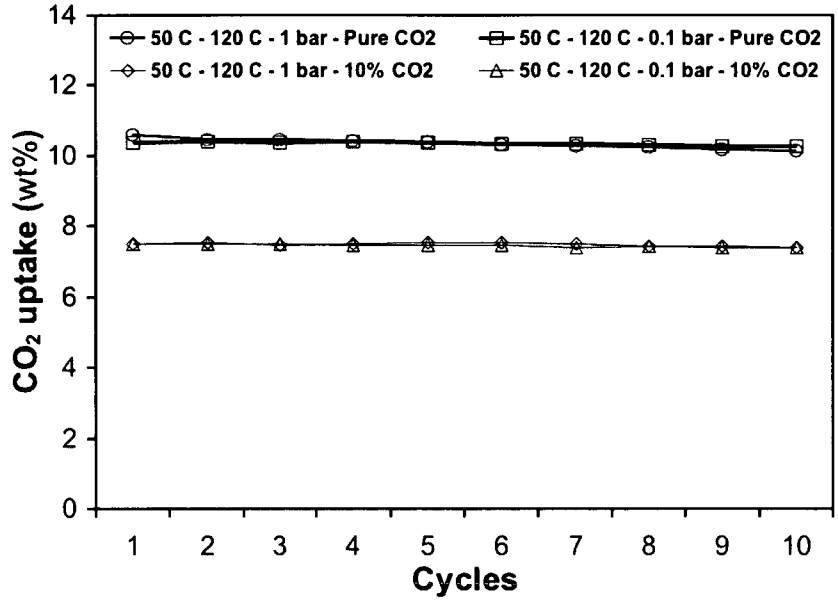

Figure 5.8 Adsorption-desorption cycles using TS and TVS regeneration configurations *c* and *d* for pure CO_2 and CO_2:N_2 = 10:90 mixture

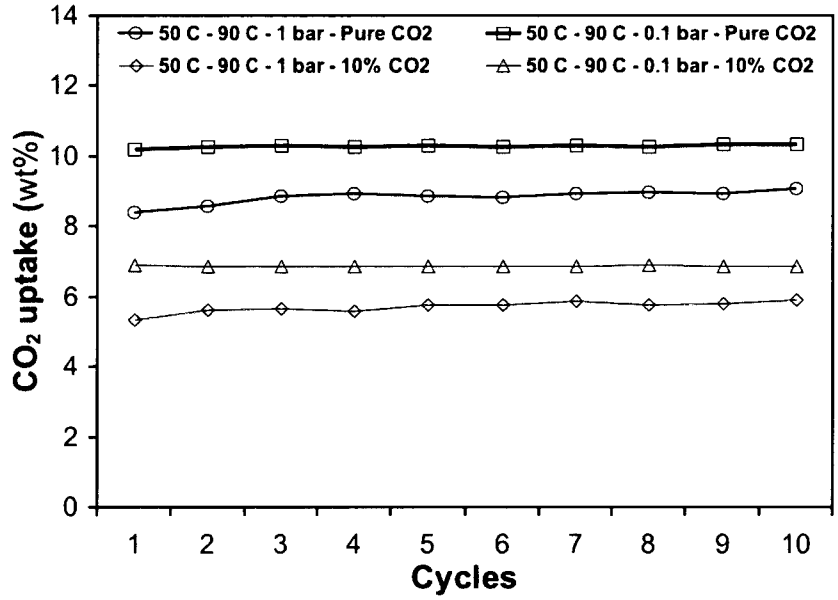

Figure 5.9 Adsorption-desorption cycles using TS and TVS regeneration configurations *e* and *f* for pure CO_2 and CO_2:N_2 = 10:90 mixture

To test the effect of T_D on the working capacity of TRI-PE-MCM-41, cyclic adsorption-desorption measurements using configurations *e* and *f* were performed. While T_A

was maintained at 50 °C, in these configurations T_D was decreased to 90 °C. The adsorption capacity throughout ten cycles is presented in Figure 5.9. A stable adsorption capacity was observed in all cases. However, the TVS regeneration resulted in a comparatively higher adsorption capacity than when using TS only. These observations are akin to those based on configurations *a* and *b*, suggesting that a comparative advantage of using vacuum during regeneration is only observed when T_D is 90 °C or lower. It is worth noting that configurations *d* and *f* produced very similar adsorption capacity despite the lower T_D used in the latter, particularly in the case of pure CO_2 streams. This suggests that the use of vacuum can lead to a competitive adsorption capacity at low T_D that may be attractive in cases where the use of heat is prohibitive.

Figures 5.7 - 5.9 show clearly that triamine surface-modified pore-expanded MCM-41 mesoporous silica exhibit different working CO_2 capture performances depending on the regeneration mode used (TS or TVS), T_A and T_D and the CO_2 concentration.

5.4 Conclusions

This work provides a broad picture of key CO_2 adsorption properties of amine-grafted pore-expanded mesoporous silica. It was demonstrated that, unlike most physical adsorbents, the CO_2 adsorption capacity of TRI-PE-MCM-41 is improved in the presence of moisture while maintaining an infinite selectivity towards CO_2 versus N_2. Adsorption-desorption cyclic measurements using pure CO_2 and CO_2:N_2 = 10:90 mixture showed that TRI-PE-MCM-41 exhibits excellent stability up to T_D = 120 °C. It was shown that optimum regeneration strategies for TRI-PE-MCM-41 depend on the temperature of adsorption and desorption, in addition to the adsorbate concentration specific to each intended application. For CO_2 removal at low T_D, for example, temperature-vacuum swing adsorption resulted in a better adsorption working capacity, while at higher T_D, temperature swing adsorption appeared to be a suitable approach.

References

D. Aaron, C. Tsouris, Separation of CO_2 from flue gas: a review. Sep. Sci. Technol. 40 (2005) 321

H. Audus, Greenhouse gas mitigation technology: an overview of the CO_2 capture and sequestration studies and further activities of the IEA Greenhouse Gas R&D Programme. Energy 22 (1997) 217

Y. Belmabkhout, A. Sayari, Adsorption of CO_2 from dry gases on MCM-41 silica at ambient temperature and high pressure. 2. Adsorption of CO_2/N_2, CO_2/CH_4 and CO_2/H_2 binary mixtures. Chem. Eng. Sci. 64 (2009a) 3729

Y. Belmabkhout, A. Sayari, Effect of pore expansion and amine functionalization of mesoporous silica on CO_2 adsorption over a wide range of conditions. Adsorption 15 (2009b) 318

Y. Belmabkhout, R. Serna-Guerrero, A. Sayari, Adsorption of CO_2 from dry gases on MCM-41 silica at ambient temperature and high pressure. 1: Pure CO_2 adsorption. Chem. Eng. Sci. 64 (2009) 3721

Y. Belmabkhout, R. Serna-Guerrero, A. Sayari, Adsorption of CO_2-containing gas mixtures over amine-bearing pore-expanded MCM-41 silica: applications for gas purification. Ind. Eng. Chem. Res. 49 (2010) 359

P. Birbara, T. Filburn, H. Michels, T. Nalette, Sorbent system and method for absorbing carbon dioxide (CO2) from the atmosphere of a closed habitable environment. US Patent 6,364,938, 2002

S. Cavenati, C.A. Grande, A.E. Rodrigues, Adsorption equilibrium of methane, carbon dioxide, and nitrogen on zeolites 13X at high pressures. J. Chem. Eng. Data 49 (2004) 1095

S. Choi, J. H. Drese, C. W. Jones. Adsorbent materials for carbon dioxide capture from large anthropogenic point sources. ChemSusChem 2 (2009) 796

E.F. da Silva, H.F. Svendsen, Study of the carbamate stability of amines using ab initio methods and free-energy perturbations. Ind. Eng. Chem. Res. 45 (2006) 2497

F. Dreisbach, R. Staudt, J.U. Keller, High pressure adsorption data of methane, nitrogen, carbon dioxide and their ternary mixture on activated carbon. Adsorption 5 (1999) 215

C.J. Geankoplis, Transport Processes and Unit Operations, third ed. Prentice-Hall, New Jersey, 1993

M.L. Gray, M.L. Champagne, K.J., Soong, Y., Filburn, T. High capacity immobilized amine sorbents. US Patent 7,288,136, 2007

P.J.E. Harlick, A. Sayari, Applications of pore-expanded mesoporous silica. 5. Triamine grafted material with exceptional CO_2 dynamic and equilibrium adsorption performance. Ind. Eng. Chem. Res. 46 (2007) 446

C.W. Jones, J.C. Hicks, D.J. Fauth, M. Gray, Structures for capturing CO_2, methods of making the structures and methods for capturing CO_2. US Patent application 20070149398, 2007

R.A. Khatri, S.C.C. Chuang, Y. Soong, M. Gray, Thermal and chemical stability of regenerable solid amine sorbent for CO_2 capture. Energy Fuels 20 (2006) 1514

I. Kim, H.F. Svendsen, Heat of absorption of carbon dioxide (CO_2) in monoethanolamine (MEA) and 2-(aminoethyl)ethanolamine (AEEA) solutions. Ind. Eng. Chem. Res. 46 (2007) 5803

M. Kruk, M. Jaroniec, A. Sayari, Application of large pore MCM-41 molecular sieves to improve pore size analysis using nitrogen adsorption measurements. Langmuir 13 (1997) 6267

M. Kruk, M. Jaroniec, A. Sayari, New insights into pore-size expansion of mesoporous silicates using long-chain amines. Micropor. Mesopor. Mater. 35-36 (2000) 545

M. Kruk, M. Jaroniec, V. Antochshuk, A. Sayari, Mesoporous silicate–surfactant composites with hydrophobic surfaces and tailored pore sizes J. Phys. Chem. B 106 (2002) 10096

X. Ma, X. Wang, C. Song, "Molecular basket" sorbent for separation of CO_2 and H_2S from various gas streams. J. Am. Chem. Soc. 131 (2009) 5777

A. Meisen, X. Shuai, Research and development issues in CO_2 capture. Energy Convers. Manage. 38 (1997) S37

G. Olah, A. Goepert, S. Meth, S. Prakash, Nano-structure supported solid regenerative polyamine and polyamine polyol adsorbents for the separation of carbon dioxide from gas mixtures including the air. Int. Patent Application WO2008/021700 A1, 2008

J.P.K. Reynhardt, Y. Yang, A. Sayari, H. Alper, Polyamidoamine dendrimers prepared inside the channels of pore-expanded periodic mesoporous silica. Adv. Funct. Mater. 15 (2005) 1641

A. Sayari, M. Kruk, M. Jaroniec, I. L. Moudrakovski, New approaches to pore size engineering of mesoporous silicates. Adv. Mater. 10 (1998) 1376

A. Sayari, Y. Yang, M. Kruk, M. Jaroniec, Expanding the pore size of MCM-41 silicas: use of amines as expanders in direct synthesis and postsynthesis procedures. J. Phys. Chem. B. 103 (1999) 3651

R. Serna-Guerrero, A. Sayari, Environ. Applications of pore-expanded mesoporous silica. 7. Adsorption of volatile organic compounds. Environ. Sci. Technol. Sci. Technol. 41 (2007) 4761

R. Serna-Guerrero, E. Da'na, A. Sayari, New Insights into the Interactions of CO_2 with amine-functionalized silica. Ind. Eng. Chem. Res. 47 (2008) 9406

W.J. Son, J.S. Choi, W.S. Ahn, Adsorptive removal of carbon dioxide using polyethyleneimine-loaded mesoporous silica materials. Micropor. Mesopor. Mater. 113 (2008) 31

Q. Yang, C. Zhong, J.F. Chen, Computational study of CO_2 storage in metal−organic frameworks. J. Phys. Chem. C 112 (2008) 1562

M.B. Yue, Y. Chun, Y. Cao, X. Dong, J.H. Zhu. CO_2 capture by as-prepared SBA-15 with an occluded template. Adv. Funct. Mater. 16 (2006) 1717

M.B. Yue, L.B. Sun, Y. Cao, Y. Wang, Z.J. Wang, J.H. Zhu, Efficient CO_2 capturer derived from as-synthesized MCM-41 modified with amine. Chem. Eur. J. 14 (2008) 3442

Chapter 6

Modeling CO_2 adsorption on amine-functionalized mesoporous silica: 1. A semi-empirical equilibrium model

Chem. Eng. J. 161 (2010) 173–181

Abstract

An equilibrium model capable of describing CO_2 adsorption isotherms on amine-grafted mesoporous silica using a semi-empirical method was developed. The proposed model is based on the assumption that adsorption of CO_2 occurs via two independent mechanisms: (i) chemical adsorption on the amine functional groups, and (ii) physisorption on the surface of the adsorbent. The CO_2 adsorption isotherms on triamine-grafted pore-expanded MCM-41 silica were measured at different temperatures and used to develop the proposed model. The equilibrium model was capable of describing CO_2 adsorption over a wide range of pressure, from 0.001 to 20 bar. Furthermore, when applied in a temperature-dependent form, it fitted experimental data at different temperatures between 25 and 55 °C. The adequacy of the model was reflected by the low values of the normalized standard deviations (< 8%) obtained at all temperatures. The model was also successfully used to fit experimental CO_2 isotherms of a triamine-grafted mesoporous silica with lower amine content and five varieties of monoamine-grafted SBA-15, as well as experimental data for H_2S adsorption at 25, 35 and 50 °C. Moreover, the heat of CO_2 and H_2S adsorption calculated using the temperature-dependent parameters of the proposed model was in excellent agreement with experimental data.

6.1 Introduction

As we enter the second decade in this new millennium, it has become evident that one of the major challenges faced by our generation is the reduction of contaminant emissions to the environment despite industrialization's unstoppable progress. The release of carbon dioxide (CO_2) poses a particular predicament: a product of the large consumption of fossil fuels, CO_2 is considered as a major anthropogenic contribution to climate change. As a result, various

methods to capture CO_2 in an efficient, cost-effective manner are currently under study. Among those alternatives, the technology considered nowadays as mature is CO_2 scrubbing using amine solutions. Unfortunately, several concerns are associated with liquid amine absorption, including high energy requirements for solvent regeneration, extensive corrosion of the equipment [Li, 2008; Feng et al., 2010] and, recently, the impact of the amine solutions life cycle on the surrounding ecosystems [Veltman et al., 2010]. Thus, several adsorption separation technologies are actively pursued, to develop a competitive, lower cost alternative.

Currently, vast efforts by the scientific community are underway to produce suitable adsorbents capable of handling the operating demands of CO_2 emitting sources, ranging from new approaches using well known adsorbents like zeolites [Lively et al., 2009; Su et al., 2010] and activated carbons [Plaza et al., 2009; Czakkel et al., 2009] to the exploration of new materials such as periodic mesoporous silicas [Huang et al., 2003; Hiyoshi et al., 2005; Knowles et al., 2005; Zheng et al., 2005; Yue et al., 2006; Knöfel et al., 2007; Liu et al., 2007; Wang et al., 2007; Hicks et al., 2008; Belmabkhout and Sayari, 2009a; Ma et al., 2009; Zukal et al., 2009] and metal organic frameworks (MOFs) [Couck et al., 2009; Hamon et al., 2009; Yazaydin et al., 2009]. Inspired by the current liquid amine CO_2 scrubbing technology, amine groups have been incorporated onto a number of solid supports for the removal of carbon dioxide (CO_2) from gaseous mixtures [Huang et al., 2003; Hiyoshi et al., 2005; Knowles et al., 2005; Zheng et al., 2005; Yue et al., 2006; Knöfel et al., 2007; Liu et al., 2007; Wang et al., 2007; Hicks et al., 2008; Belmabkhout and Sayari, 2009a; Couck et al., 2009; Ma et al., 2009; Zukal et al., 2009]. The objective of such effort was to exploit the efficient amine – CO_2 interactions, while preventing the aforementioned shortcomings of the liquid – gas systems. In particular, a variety of amine-bearing molecules have been incorporated into periodic mesoporous silicas (for a review, see Harlick and Sayari [2007] and Choi et al., [2009]). Due to their suitable structural characteristics, ordered mesoporous materials drew, in recent years, the attention of researchers in many fields, particularly in catalysis and adsorption. Typically, this class of materials exhibits large surface area and pore volume with narrow pore size distribution in the nanometer range [Sayari, 1997; Sayari, 2003]. Furthermore, the possibility to tailor their pore systems, including pore size, volume and connectivity [Sayari et al., 1998; Sayari et al., 1999; Selvam et al., 2001] and to

incorporate surface and/or framework functional groups [Stein et al., 2000; Sayari et al., 2001] makes them versatile materials that can be exploited for a wide range of applications. As far as amine-functionalized mesoporous silicas are concerned, it has been found that (i) up to a certain amine content, the CO_2 adsorption capacity increases with the content of functional groups attached on the surface, and (ii) only when the adsorbent maintains an open pore structure are the amines efficiently used, especially when adsorption occurs at temperatures close to ambient [Serna-Guerrero et al., 2008].

Because, in general, amine-functionalized mesoporous materials have proven to be promising in terms of adsorption capacity, kinetics and stability in some cases, it was deemed attractive to model the behavior of such systems for its subsequent simulation and interpretation. However, based on our own data [Serna-Guerrero et al., 2008; Belmabkhout and Sayari, 2009a] and on literature reports [Huang et al., 2003; Liu et al., 2007; Wang et al., 2007; Zukal et al., 2009], it was observed that for properly synthesized amine-functional mesoporous materials, the CO_2 adsorption isotherms exhibit an unusual shape, as represented schematically in Figure 6.1. Unlike a typical Langmuir isotherm, consistent with chemical adsorption, CO_2 adsorption isotherms for amine-functionalized mesoporous adsorbents do not exhibit a saturation plateau at high pressure. As shown in Figure 6.1, after a dramatic uptake of CO_2 at low concentration, the adsorption capacity kept increasing with the partial pressure of the adsorbate. Accordingly, the common isotherm models (e.g. Langmuir, Freundlich) seem adequate to describe the adsorption profile only within a small range of concentration, particularly at low CO_2 pressure. A plausible explanation to this shape is the occurrence of a second independent mechanism for CO_2 adsorption, in addition to the CO_2 capture by amine groups. In a previous contribution [Serna-Guerrero et al., 2008], it was suggested that the overall adsorption of CO_2 on amine-functionalized mesoporous silicas is the result of both chemical interactions with the amine groups and physisorption on the surface of the adsorbent. Since then, other authors exploring CO_2 capture on functionalized adsorbents have adopted this hypothesis as well [Su et al., 2010]. It has also been observed that the purely siliceous support had a small capacity for CO_2 at low partial pressure due to physical adsorption but, as the pressure of CO_2 increased, its uptake became significant [Belmabkhout and Sayari 2009b; Belmabkhout et al., 2009].

To the best of our knowledge, the shape of the CO_2 adsorption isotherm over amine-functionalized mesoporous materials has not been analyzed in depth before, nor fit to an appropriate isotherm model. Thus, in the first part of this series, a semi-empirical model to fit the CO_2 adsorption data on amine-functionalized mesoporous materials over a wide range of pressure and temperature is proposed. Because the adsorption of CO_2 on amine-grafted mesoporous materials can be a result of complex interaction mechanisms [Serna-Guerrero et al., 2008], our objective was to develop a model with a wide scope using characterization data routinely produced and a series of justifiable assumptions. Earlier, our group developed a material with characteristics suitable for the incorporation of large amounts of surface organic species [Sayari et al., 1999]. This material, referred to as PE-MCM-41, consisted of a mesoporous silica type MCM-41 whose pores have been enlarged by a post-synthesis hydrothermal expansion. PE-MCM-41 exhibited a readily accessible pore structure even after surface amine functionalization [Harlick and Sayari, 2007; Serna-Guerrero et al., 2008], making it suitable for generating high-quality CO_2 adsorption isotherms.

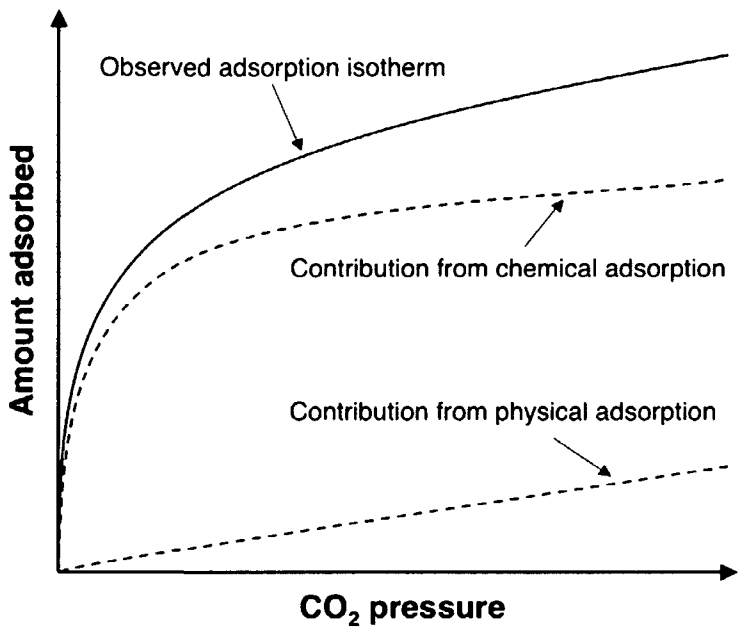

Figure 6.1 Schematic representation of CO_2 adsorption on amine-functionalized mesoporous adsorbents

6.1.1 Description of the proposed equilibrium model. The model considers a simultaneous uptake of adsorbate by physical and chemical interactions, thus consisting of the sum of two independent adsorption mechanisms, as expressed by Eq. 1:

$$q = q_{chem} + q_{phys} \tag{1}$$

where q is the total adsorption uptake, q_{chem} is the CO_2 uptake by amine groups and q_{phys} represents the CO_2 uptake by physisorption on the adsorbent surface. A dual-site model of this form assumes no interaction between the species adsorbed on each of the two types of adsorption sites. Such an assumption has been generally accepted when there are large differences between the adsorption energy of each type of site, resulting in a distinct preferential adsorption on one of them at low surface coverage [Do, 1998]. Indeed, this appears to be the case for CO_2 adsorption on amine-functional silica based on the observations that (i) amine functionalization enhances the adsorption capacity particularly at low concentrations [Serna-Guerrero et al., 2008; Belmabkhout and Sayari 2009a] and (ii) the measurements of heat of adsorption by calorimetry consistently reported high values associated to chemisorption at low surface coverage and approaching those of physisorption on pure silica at higher CO_2 loading [Knowles et al., 2005; Knöfel et al., 2007; Knofel et al., 2009].

The right-hand side terms of Eq. 1 can be represented using existing isotherm models with independent coefficients for each adsorption mechanism. In this work, we propose to use the Toth isotherm model to represent each of the adsorption mechanisms since it has a temperature-dependent form that makes it useful for modeling not only isothermal but also non-isothermal behavior [Do, 1998; Belmabkhout et al., 2009]. In addition, the Toth isotherm has a coefficient associated with the isosteric heat of adsorption at zero coverage (ΔH), which can provide further physical meaning to the proposed model.

Thus, the model can be represented as:

$$q = \left[\frac{n_s bP}{\left(1+(bP)^t\right)^{1/t}}\right]_{chem} + \left[\frac{n_s bP}{\left(1+(bP)^t\right)^{1/t}}\right]_{phys} \tag{2}$$

where P is the pressure of the adsorbate, n_s, b and t are the characteristic parameters of the Toth model, and the subscripts "*chem*" and "*phys*" denote the contribution from each of the mechanisms to the overall adsorption capacity. To express the Toth isotherm as a function of temperature, the model coefficients are represented in the form of Eq. 3-5:

$$b = b_0 \exp\left[\frac{\Delta H}{RT_0}\left(\frac{T_0}{T} - 1\right)\right] \tag{3}$$

$$t = t_0 + \alpha\left(1 - \frac{T_0}{T}\right) \tag{4}$$

$$n_S = n_{S0} \exp\left[\chi\left(1 - \frac{T}{T_0}\right)\right] \tag{5}$$

where ΔH is the heat of adsorption at a surface coverage close to zero, R is the universal gas constant, α and χ are the parameters of the temperature-dependent form of the Toth model and the subscript 0 refers to the parameters obtained under a reference temperature T_0.

The main challenge in the implementation of this model is to discriminate between the contributions of each adsorption mechanism in the overall CO_2 uptake measured experimentally. Thus, a proposed method is to calculate q_{phys} based on the adsorption data of CO_2 on the siliceous support before functionalization under the assumption that physical adsorption does not depend strongly on the nature of the surface whether it is the siliceous support or its functionalized counterpart. Due to the weak interactions involved in physisorption, this is a reasonable assumption. Nonetheless, further support to this supposition will be provided later in this work. Thus, as long as capillary condensation does not occur and the inner surface of the material is freely accessible, the CO_2 uptake by physical adsorption can be considered proportional to the surface area. Under such assumption, the amount of CO_2 physisorbed on the surface of the functionalized adsorbent at any given CO_2 pressure is related to the CO_2 uptake by the unmodified silica support under the same pressure and temperature conditions according to Equation 6:

$$q_{phys@P/P_0} = q_{support@P/P_0} \frac{S}{S_{support}} \quad (6)$$

where $q_{support}$ and $S_{support}$ are the CO_2 uptake and surface area of the purely siliceous mesoporous support, respectively, and S is the surface area of the amine-containing adsorbent.

Once the contribution from physical adsorption is established, it can be subtracted from the total CO_2 uptake to calculate the amount adsorbed due to the chemical interaction between CO_2 and amines. In this manner, the contribution from the amine groups (q_{chem}) can be fitted to an appropriate isotherm model and, when added to q_{phys}, will describe the overall CO_2 uptake due to the combined contributions of the two independent mechanisms.

To estimate the accuracy of the fit of the proposed model, an error function based on the normalized standard deviation was calculated as follows:

$$\Delta q(\%) = \sqrt{\frac{\sum\left[\left(q_{exp} - q_{mod}\right)/q_{exp}\right]^2}{N-1}} \quad (7)$$

where $\Delta q(\%)$ is the normalized standard deviation, q_{exp} and q_{mod} are the experimental and calculated amounts of CO_2 adsorbed, and N is the number of data points available in each isotherm.

6.2 Experimental

6.2.1 Synthesis of the adsorbent. The synthesis of the mesoporous adsorbent has been described in detail elsewhere and is represented in Figure 6.2 [Harlick and Sayari, 2007]. Briefly, MCM-41 silica was produced using cetyltrimethylammonium bromide ($CTMA^+Br^-$) as structure directing agent in basic conditions at 100 °C. The post-synthesis pore expansion procedure was performed at 120 °C for 3 days using dimethyldecylamine (DMDA) as expander agent. A sample of this material was calcined under nitrogen, then air at 550 °C for 5 h to obtain PE-MCM-41C (Figure 6.2). The amine groups were incorporated by grafting 2-[2-(3-trimethoxysilylpropylamino)ethylamino]ethylamine (TRI-silane) onto the silica surface as follows. PE-MCM-41C was suspended in 150 ml of toluene in a glass vessel, followed by

the addition of 0.3 ml of distilled, deionized water per gram of silica. After homogenization of the mixture, the temperature in the reactor was increased to 85 °C and 3 g of TRI-silane per gram of silica was added under vigorous stirring. The reaction proceeded for 16 h. The solid phase was then filtered and washed thoroughly with toluene, then pentane. Finally, the solid was dried in a natural convection oven at 100 °C for 1 h and the product was labeled TRI-PE-MCM-41. An adsorbent with lower amine loading, designated as TRI-PE-MCM-41(dry), was produced by grafting TRI-silane on PE-MCM-41C following the same procedure as described above, but without addition of water. Another material that will be considered in the upcoming discussion is PE-MCM-41E, where "E" stands for "extracted" (Figure 6.2). This material consisted of a cetyltrimethylammonium-bearing mesoporous silica produced by the selective extraction of the expander agent with ethanol [Serna-Guerrero and Sayari, 2007].

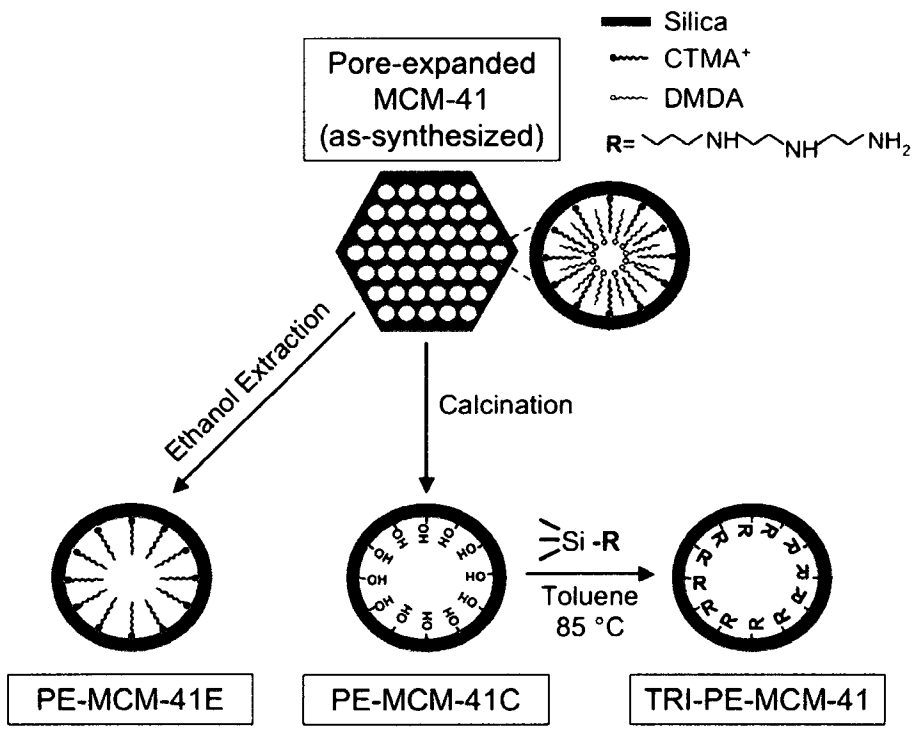

Figure 6.2 Schematic representation of the synthesis of mesoporous adsorbents

6.2.2 Characterization of the adsorbent. The structural properties of PE-MCM-41C, PE-MCM-41E, TRI-PE-MCM-41 and TRI-PE-MCM-41(dry) were determined by nitrogen

adsorption measurements at 77 K using a Micromeritics ASAP 2020 volumetric apparatus. The samples were degassed under vacuum at 150 °C for 5 h before adsorption measurements. The surface area was calculated using the BET method, while the pore volume was considered as the volume of liquid nitrogen adsorbed at a relative pressure close to 1. The pore size distribution was obtained using the KJS method [Kruk et al., 1997]. The organic content was determined by thermogravimeric analysis (TGA) using a TA Q-500 instrument, considering that only the weight lost beyond 200 °C is associated with the decomposition of covalently tethered amine-containing groups [Harlick and Sayari, 2007].

6.2.3 Adsorption measurements. Measurements of CO_2 adsorption at equilibrium on PE-MCM-41C, PE-MCM-41E, TRI-PE-MCM-41 and TRI-PE-MCM-41(dry) were performed on a Rubotherm microbalance with automated gas dosing system. This system allows the flow of gases at controlled pressures ranging from 0.001 to 60 bar at ambient temperature. In the current work, the adsorbent was pretreated under a flow of 50 ml min^{-1} ultra-high purity nitrogen at 150 °C for 2 h. The sample was subsequently cooled down to the desired temperature (i.e., 25, 35, 45 or 55 °C) before exposure to flowing CO_2 at the desired partial pressure. A minimum equilibration time of 2 h was used for each data point of the isotherm. After this time, the observed weight of the sample remained constant, inferring that equilibrium has been reached. The adsorption capacity was calculated from the weight change of the sample in the presence of CO_2 after accounting for the effect of buoyancy [Belmabkhout et al., 2009]. For each adsorption isotherm, a fresh sample was used. This procedure was also applied to measure the adsorption isotherms of H_2S on TRI-PE-MCM-41 and PE-MCM-41C at 25, 35 and 55 °C. Adsorption data at different temperatures allowed the calculation of the isosteric heat of adsorption (ΔH_{ISO}) using the Clausius-Clapeyron equation. The Toth isotherm parameters for q_{phys} and q_{chem} were obtained by non-linear regression using an iterative method with the aid of Microsoft Excel© software.

6.3 Results and discussion

The nitrogen adsorption isotherms obtained for PE-MCM-41C, PE-MCM-41E and TRI-PE-MCM-41 are presented in Figure 6.3. The calculated structural properties are shown in Table 6.1. As can be seen, all samples exhibited a Type IV isotherm according to the IUPAC

classification, characteristic of materials with mesoporous structure. After functionalization, smaller pore volume and surface area were observed, attributed to the occurrence of the organic molecules onto the channels' surface. The loading of amine species on the adsorbent was estimated as 7.27 mmol g^{-1} for TRI-PE-MCM-41 and 4.90 mmol g^{-1} for TRI-PE-MCM-41(dry). The surface area of TRI-PE-MCM-41 was of 429 m^2 g^{-1} and 539 m^2 g^{-1} for TRI-PE-MCM-41(dry), which represent 38% and 48% of the surface area of the purely siliceous support, respectively. The amount of organic species (i.e., $CTMA^+$) in PE-MCM-41E, measured by TGA was 1.13 mmol g^{-1}.

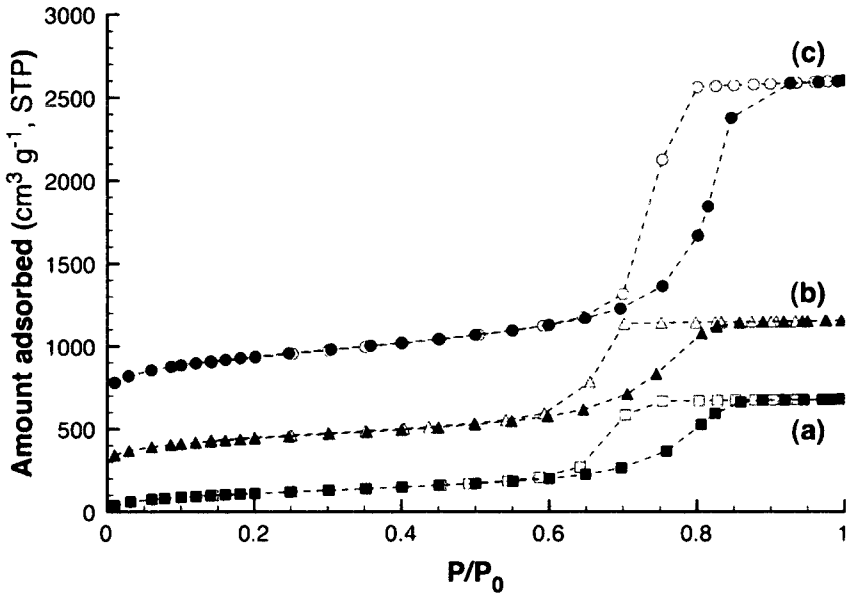

Figure 6.3 Nitrogen adsorption (closed symbols) and desorption (open symbols) isotherms for (a) TRI-PE-MCM-41, (b) PE-MCM-41E and (c) PE-MCM-41C. For clarity, isotherms (b) and (c) were shifted upward by 300 and 600 cm^3 g^{-1}, respectively

With respect to CO_2 adsorption on TRI-PE-MCM-41, Figure 6.4 shows the isotherms determined experimentally at different temperatures. All experimental data for CO_2 adsorption on TRI-PE-MCM-41 were included in Appendix A, Supporting Information Table 6.S1. The shape of these isotherms is in agreement with other isotherms reported in the literature [Huang et al., 2003; Liu et al., 2007; Wang et al., 2007; Serna-Guerrero et al., 2008; Belmabkhout and Sayari, 2009a; Zukal et al., 2009]. Indeed, a steep uptake of CO_2 was

observed at low CO_2 partial pressures followed by a small, but steady increase at high pressure.

Table 6.1 Structural properties of mesoporous materials

Sample	Surface area ($m^2\ g^{-1}$)	Mean pore size (nm)	Pore volume ($cm^3\ g^{-1}$)	Amine loading ($mmol_N\ g^{-1}$)	Reference
PE-MCM-41C	1134	10.88	2.26	-	This work
PE-MCM-41E	565	8.67	1.32	-	This work
TRI-PE-MCM-41	429	9.57	1.05	7.27	This work
TRI-PE-MCM-41(dry)	539	9.56	1.15	4.90	This work
SBA-15	582	9.2	0.95	-	Wang et al., 2007
APSBA15C	405	7.5	0.65	1.44	
APSBA15U(78C, 20h)	466	7.5	0.73	1.9	
APSBA15U(50C, 20h)	313	7.4	0.57	2.56	
SBA-15	883	6.2	0.93	-	Zukal et al., 2009
SBA15/AP1	562	5.8	0.79	1.1	
SBA15/AP2	460	5.6	0.68	2	

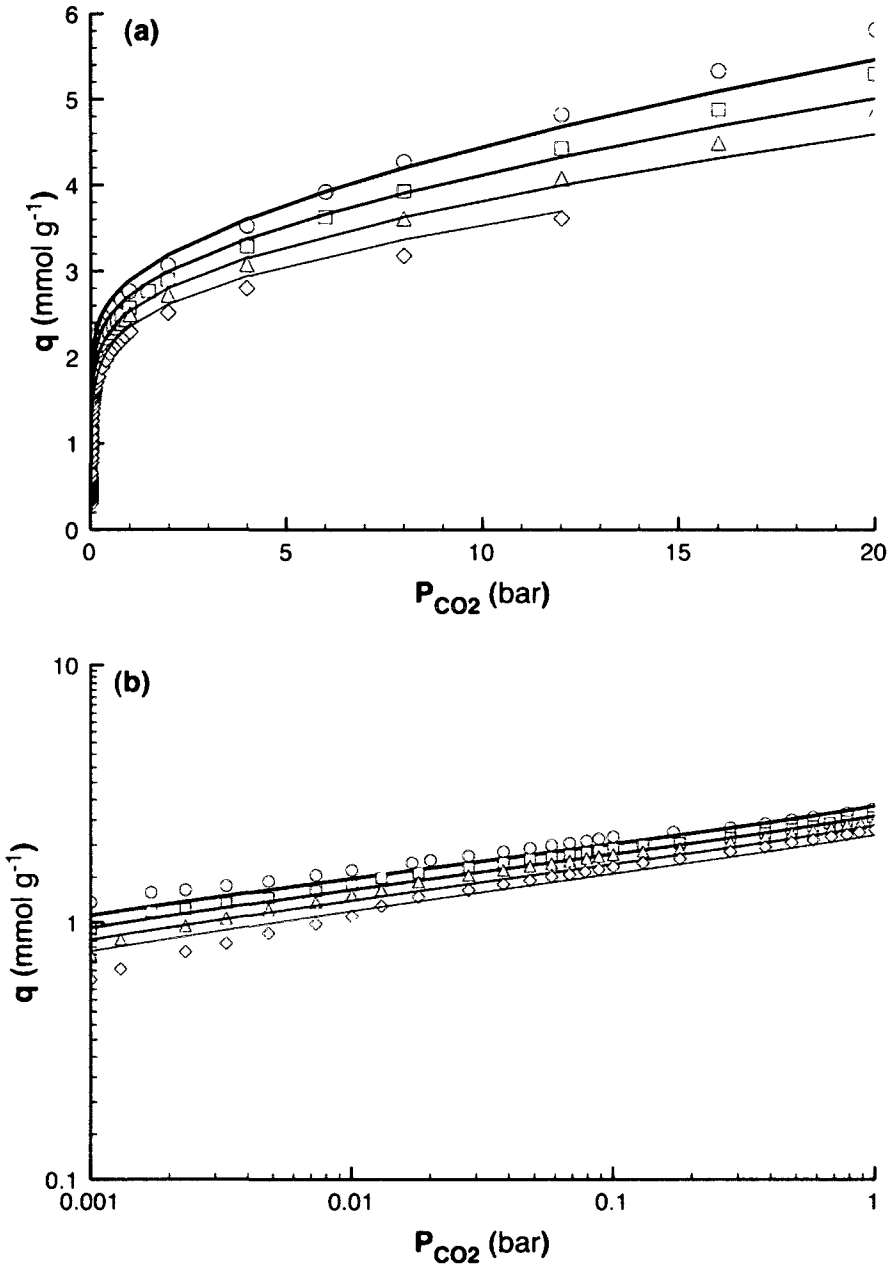

Figure 6.4 Adsorption isotherm of CO_2 on TRI-PE-MCM-41 in the (a) high and (b) low pressure range at 25°C (circles), 35° C (squares), 45° C (triangles) and 55° C (diamonds). The solid lines correspond to the equilibrium model proposed in this work

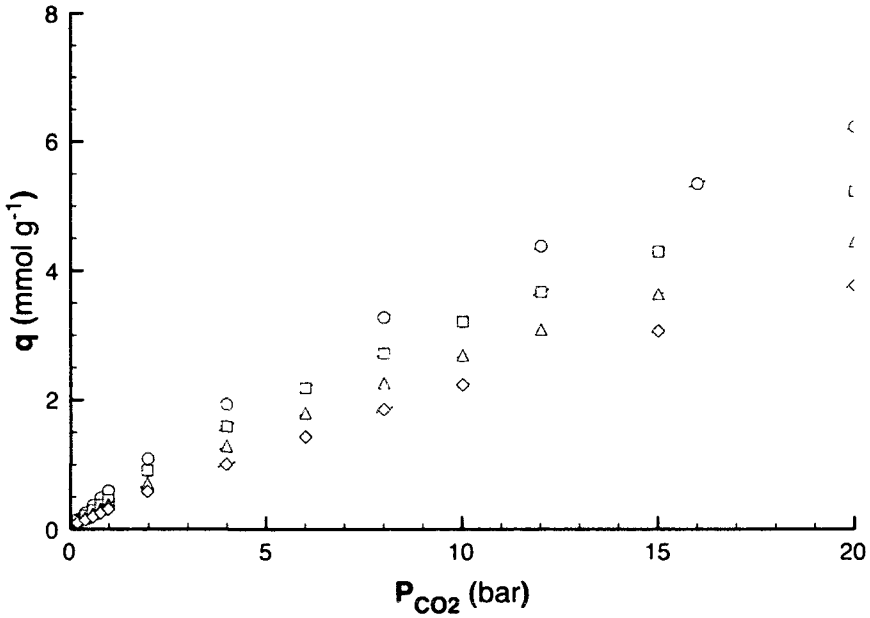

Figure 6.5 CO_2 adsorption isotherm for PE-MCM-41C at 25 °C (circles), 35 °C (squares), 45 °C (triangles) and 55 °C (diamonds)

Figure 6.5 shows the adsorption isotherms of CO_2 on PE-MCM-41C at different temperatures. Tabulated experimental data are available in Appendix A, Supporting Information, Table 6.S2. Within the range of pressures analyzed, there was no capillary condensation of CO_2. It should also be mentioned that the CO_2 uptake on PE-MCM-41C became significant, i.e., above 0.1 mmol g^{-1}, only when the CO_2 pressure reached ca. 0.2 bar. Below this pressure, no uptake could be measured reliably. Using the adsorption data for PE-MCM-41C, the corresponding values of q_{phys} for TRI-PE-MCM-41 at different temperatures were calculated taking into account the difference in surface areas, using Equation 6 (Figure 6.6, closed symbols). Data of q_{phys} thus obtained were fitted using the Toth model. The parameters of the Toth equation for the isotherms calculated for physisorption are presented in Table 6.2. Using data at 25 °C as reference, Figure 6.6 shows that the model fits adequately the adsorption data at all temperatures. After subtraction of the calculated contribution of physical adsorption from the total CO_2 uptake measured experimentally, the profile attributed to CO_2 uptake by amines (chemisorption) closely relates to a Type I isotherm (Figure 6.6, open symbols), consistent with adsorption due to chemical interactions. The Toth isotherm model was also applied to these data and the parameters obtained are

shown in Table 6.2. As seen, the temperature-dependent Toth model is a good fit to the experimental values of q_{chem}, although some limitations of the model were observed in the low CO_2 pressure range at 55 °C.

Table 6.2 Toth parameters of the temperature-dependent isotherm form for CO_2 adsorption on TRI-PE-MCM-41 using 25 °C as reference temperature

CO_2 uptake	n_{s0} (mmol g^{-1})	b_0 (bar^{-1})	t_0	χ	α	ΔH (kJ mol^{-1})
q_{phys}	6.98	2.74×10^{-1}	9.62×10^{-1}	5.35	0	19.2
q_{chem}	3.64	1.25×10^{5}	2.24×10^{-1}	0	6.05×10^{-2}	67.3

As presented in Figure 6.4, addition of q_{chem} and q_{phys} produced a model that closely matched the experimental values of q for TRI-PE-MCM-41 throughout the entire range of pressure and temperature analyzed. The calculated values of $\Delta q(\%)$ were 6.2, 5.7, 7.8 and 6.8% for the isotherms at 25, 35, 45 and 55 °C, respectively. Since the values of $\Delta q(\%)$ were less than 10% in all cases, it is inferred that the proposed methodology provides a suitable model to describe CO_2 adsorption isotherms over amine-functionalized silicas, and possibly other adsorption systems where both physisorption and chemisorption occur. It is worth noting that, although the Toth equation was used, this should not be regarded as a limitation of the proposed methodology. Since the separate contributions of physical and chemical adsorption correspond to Type I isotherms, other models could potentially be applied. However, the use of the Toth model in this work was found to be convenient to correlate the obtained parameters with physical and thermodynamic properties, such as ΔH, as will be discussed later. Another parameter of the Toth model that can provide physical meaning is n_s. The value of n_s is associated with the adsorbent uptake at saturation, in other words, the maximum amount that can possibly be adsorbed [Do, 1998]. According to the generally accepted mechanisms for adsorption of dry CO_2 on amines, the limiting stoichiometry for CO_2 removal via carbamate formation corresponds to 0.5 mol of CO_2 per mol of amine. Thus, the upper limit of q_{chem} should reflect such stoichiometry, being 3.65 mmol g^{-1} of CO_2 for an amine loading of 7.27 mmol g^{-1} and, as seen in Table 6.2, this is precisely the value

assigned to n_s. Furthermore, the parameter that governs the temperature dependence of n_s, i.e. χ, was found to be zero in the case of q_{chem}. This suggests that, at least within the range of temperatures analyzed, the mechanism for the chemical adsorption remains the same.

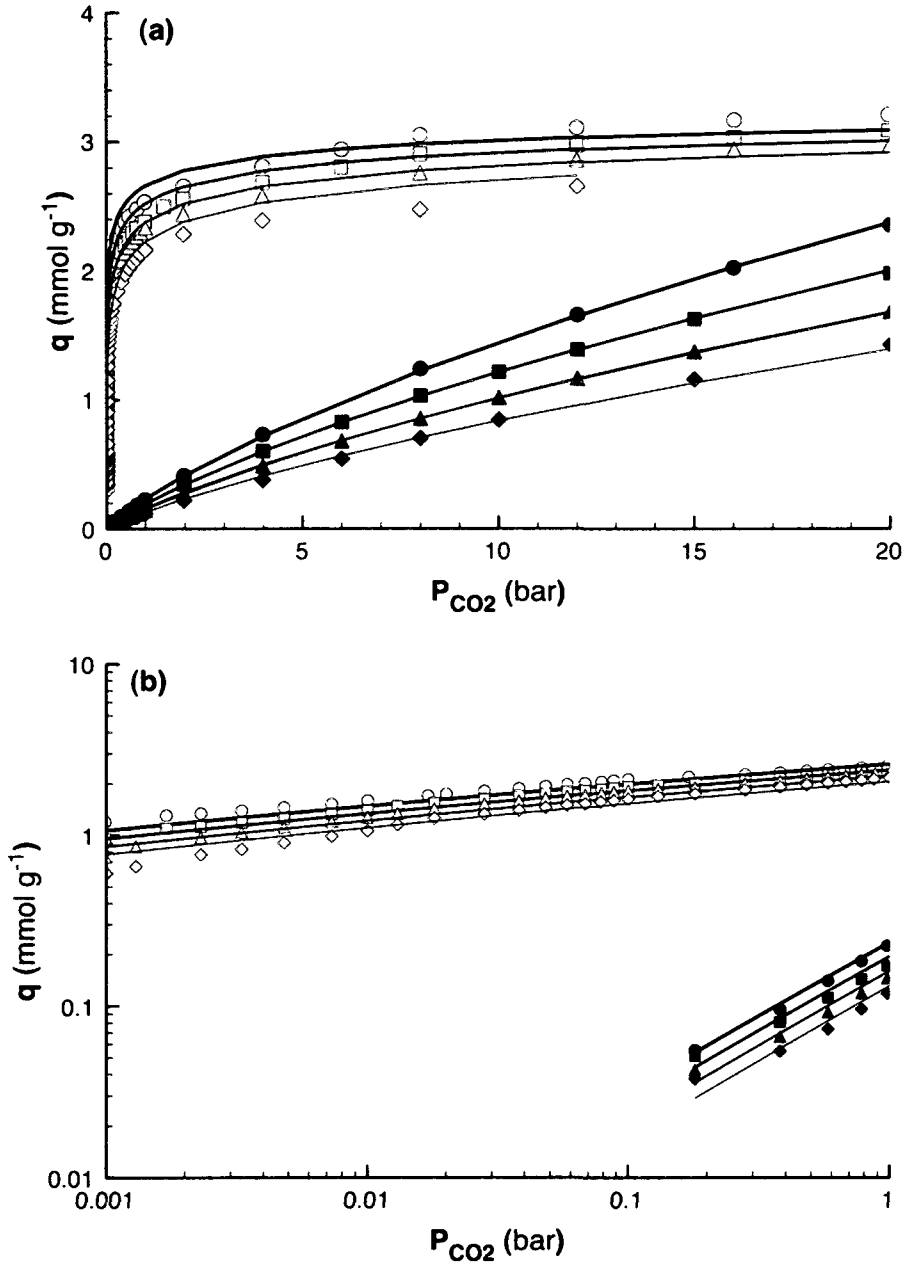

Figure 6.6 q_{chem} (open symbols) and q_{phys} (closed symbols) adsorbed CO_2 in TRI-PE-MCM-41 in the (a) high and (b) low pressure range at 25°C (circles), 35° C (squares), 45° C (triangles) and 55° C (diamonds). The lines correspond to the Toth isotherm model fit

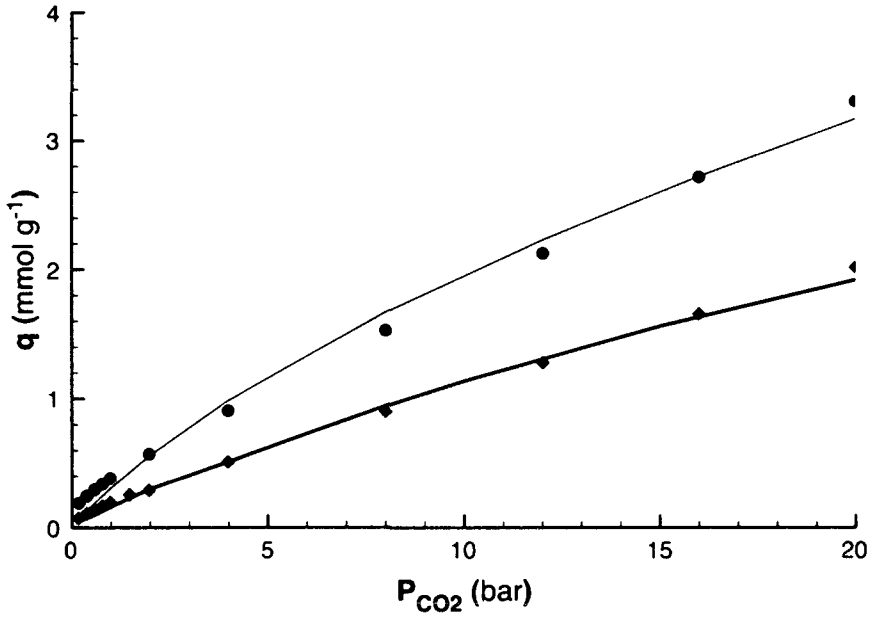

Figure 6.7 Adsorption isotherms of CO_2 for PE-MCM-41E at 25 °C (circles) and 55 °C (diamonds). The lines represent the isotherms predicted using Equation 6

One of the assumptions used in this work was that the surface of amine-functionalized adsorbent and the surface of the pristine mesoporous silica exhibit similar behavior with regard to CO_2 physical adsorption. While such assumption vastly simplified the determination of the contribution from physical adsorption, it may seem to be too simplistic. To provide further support to this contention, a mesoporous material containing linear alkyltrimethylammonium groups, namely PE-MCM-41E (Figure 6.2) was used as a reference material. PE-MCM-41E is an excellent candidate to mimic the physisorption of CO_2 on TRI-PE-MCM-41 as it contains a layer of organic groups with similar length as the triamine species, but without any amine functionality. Figure 6.7 shows the CO_2 adsorption isotherms at 25 and 55 °C obtained experimentally for PE-MCM-41E. The isotherms exhibited a similar shape as that of PE-MCM-41 (Figure 6.5), although at any given CO_2 pressure, the uptake was comparatively lower. Using the values of q for PE-MCM-41C and correcting for the difference in surface areas according to Equation 6, the adsorption isotherms for PE-MCM-41E were calculated. The predicted isotherms, included in Figure 6.7, show a remarkable agreement with the experimental values, particularly at high CO_2 pressures where the contribution of physisorption is more significant. This lends strong

support to the validity of the proposal to calculate q_{phys} using the more convenient silica support as a reference material for CO_2 physisorption.

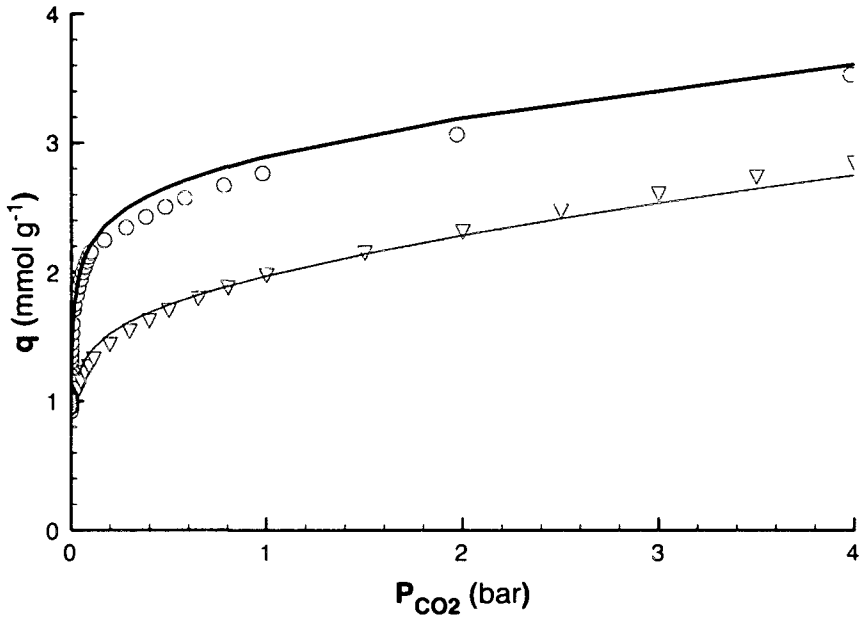

Figure 6.8 CO_2 adsorption isotherms at 25 °C for TRI-PE-MCM-41(dry) (triangles) and TRI-PE-MCM-41 (circles)

To provide further support to the wide applicability of the proposed methodology, CO_2 adsorption isotherms produced experimentally for a variety of amine-functionalized mesoporous adsorbents were fitted using the new model. We first considered a sample with the same triamine species and mesoporous support but lower amine content, i.e., TRI-PE-MCM-41(dry). The adsorption isotherm of CO_2 on TRI-PE-MCM-41(dry) at 25 °C is presented in Figure 6.8, along with the isotherm for TRI-PE-MCM-41 for comparison. As seen, the adsorption isotherm for TRI-PE-MCM-41(dry) also exhibits the characteristic shape described in Figure 6.1. From Figure 6.8, it is evident that the adsorption of CO_2 is strongly dependent on the amine content, as TRI-PE-MCM-41 has a higher adsorption capacity throughout the entire range of pressure. The methodology proposed in this work was applied to the CO_2 isotherm for TRI-PE-MCM-41(dry) and a model was produced that fits adequately the experimental data for TRI-PE-MCM-41(dry) (Figure 6.8, Table 6.3). Table 6.3 shows that n_s is the parameter whose value differs most significantly from those obtained

for TRI-PE-MCM-41. This parameter affects linearly the values of q_{chem} and q_{phys} and its variation is directly related to the surface area for physical adsorption (q_{phys}) and to the amine content for chemisorption (q_{chem}). Indeed, for q_{phys}, n_s was 26% higher for TRI-PE-MCM-41(dry), compared to TRI-PE-MCM-41, reflecting the ca. 26% difference between their surface areas. For q_{chem}, the value of the n_s parameter for TRI-PE-MCM-41(dry) was ca. 62% that of n_s calculated for TRI-PE-MCM-41, which is also the ratio of the amine loading in TRI-PE-MCM-41(dry) compared to TRI-PE-MCM-41.

Table 6.3 Toth parameters of the new isotherm model for CO_2 adsorption on various amine-grafted mesoporous materials at room temperature

	q_{phys}			q_{chem}		
Sample	n_s (mmol g^{-1})	b (bar^{-1})	t	n_s (mmol g^{-1})	b (bar^{-1})	t
TRI-PE-MCM-41(dry)	8.83	2.74×10^{-1}	9.62×10^{-1}	2.45	1.25×10^{5}	2.11×10^{-1}
APSBA15C	6.61	4.44×10^{-1}	9.20×10^{-1}	0.72	1.25×10^{5}	2.53×10^{-1}
APSBA15U(78C, 20h)	7.60	4.44×10^{-1}	9.20×10^{-1}	0.95	1.25×10^{5}	2.53×10^{-1}
APSBA15U(50C, 20h)	5.12	4.44×10^{-1}	9.20×10^{-1}	1.28	1.25×10^{5}	2.53×10^{-1}
SBA15/AP1	9.15	7.38×10^{-1}	9.30×10^{-1}	0.55	1.25×10^{5}	1.60×10^{-1}
SBA15/AP2	7.51	7.37×10^{-1}	9.30×10^{-1}	1.00	1.25×10^{5}	1.89×10^{-1}

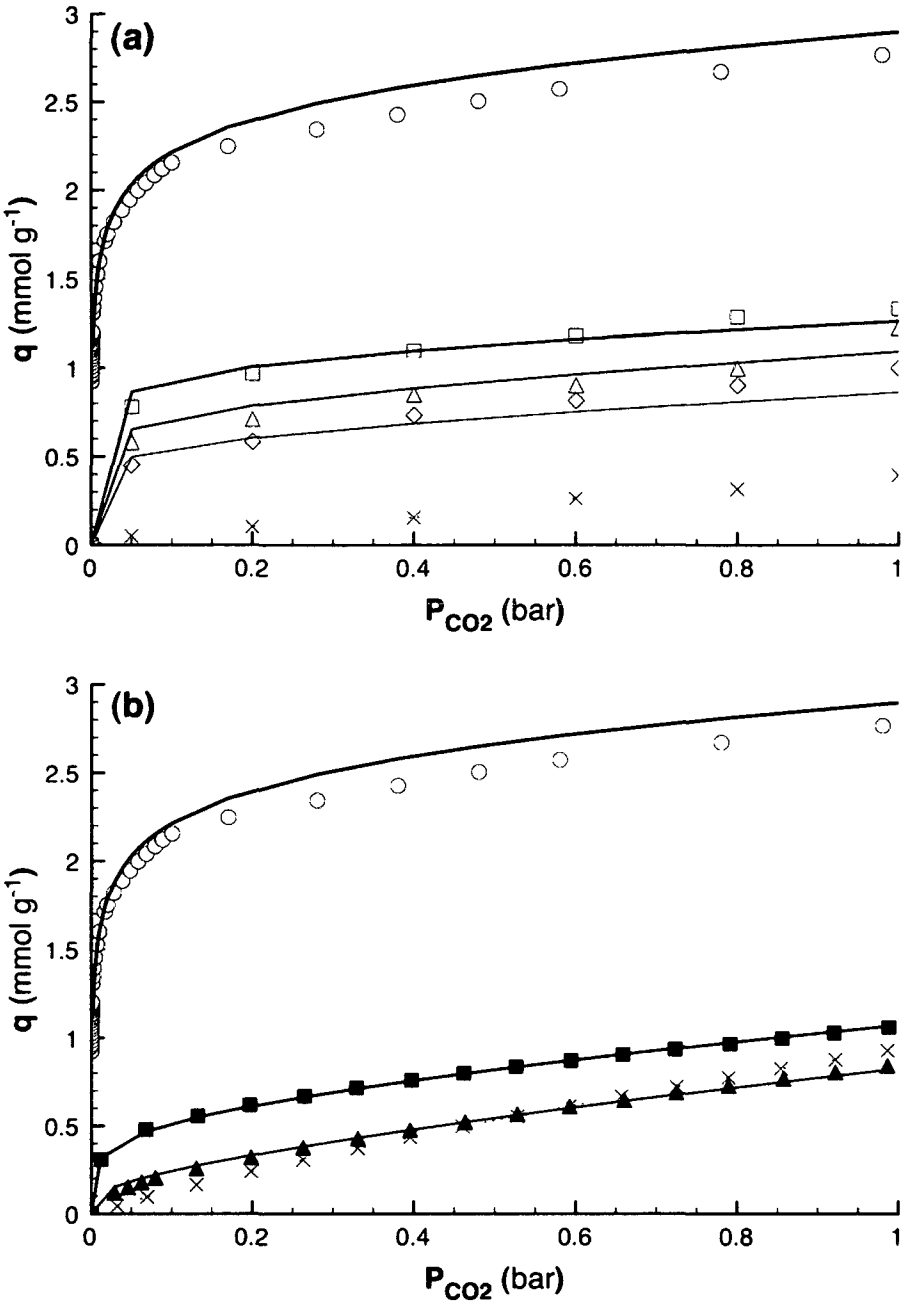

Figure 6.9 CO_2 adsorption isotherms on TRI-PE-MCM-41 (circles) and: (a) APSBA15(50C, 20h) (squares), APSBA15U(78C, 20h) (triangles), APSBA15C (diamonds) and SBA-15 (crosses) from Wang et al[15]; (b) SBA15/AP1 (triangles), SBA15/AP2 (squares) and SBA-15 (crosses) from Zukal et al[19]. The solid lines correspond to the equilibrium model proposed in this work

The next stage was to test the model on a family of propylamine-functionalized SBA-15 mesoporous silica reported by Wang et al. [2007]. This represents a challenge to the proposed methodology as these samples consisted of not only a different mesoporous support, but also a different functional group with a single primary amine group. Although details on the synthesis of these adsorbents can be found in the original work, it can be mentioned that APSBA15C was functionalized by grafting on calcined SBA-15, while APSBA15U(78C, 20h) and APSBA15U(50C, 20h) were functionalized by grafting on the as-synthesized SBA-15 via the so-called "one-step silylation" method, using the temperature and time indicated in parentheses. The structural properties and amine loadings of these samples are shown in Table 6.1. Figure 6.9a shows the adsorption isotherms for these amine-grafted SBA-15 materials with the isotherm fit obtained using the proposed model. The values of $\Delta q(\%)$ were of 7.58, 5.63 and 3.25% for APSBA15C, APSBA15U(78C, 20h) and APSBA15U(50C, 20h), respectively, reflecting the high accuracy of the model to describe the experimental data.

A particularly interesting finding is the trend observed for the Toth parameters associated with CO_2 adsorption on these samples (Table 6.3). Similar to TRI-PE-MCM-41, n_s was the only parameter that changed significantly from one sample to another. The values of n_s for q_{chem} were again a direct reflection of the amine content, while those for q_{phys} varied almost linearly with the surface area of the adsorbents, even when compared to our triamine-grafted adsorbent. For example, APSBA15C had a surface area and a value of n_s for q_{phys} of 94% with respect to TRI-PE-MCM-41, while the values of amine loading and n_s for q_{chem} are both ca. 20% of those for TRI-PE-MCM-41. This was a particularly important finding as it was possible to correlate the model with structural and chemical properties for a variety of amine-functionalized materials. Accordingly, it may be possible to predict the value of n_s for q_{phys}, as it was consistently equal to 0.016 mmol $m^{-2} \times S$.

Due to these successful applications, we proceeded to test another series of adsorbents, reported by Zukal et al., [2009], namely SBA-15/AP1 and SBA-15/AP2, consisting of propylamine-grafted SBA-15 with different amine loadings, as seen in Table 6.1. The experimental data for CO_2 adsorption reported, along with their corresponding isotherm fit are shown in Figure 6.9b. Once again, excellent correlations were obtained, with values of $\Delta q(\%)$ of 2.31% and 3.38% for SBA-15/AP1 and SBA-15/AP2, respectively. In

line with earlier observations, the parameter n_s changed proportionally with the surface area and amine content of each sample. Furthermore, in the case of q_{chem}, the values of the parameter b were remarkably close, not just between these samples, but also when compared to the samples described above (Table 6.3). In the case of q_{phys}, the parameter t remained almost constant within the various samples, with values close to 1. To provide a possible explanation to such variations, it is worth recalling the meaning of parameters b and t. Parameter b is associated with the strength of the adsorbate- adsorbent interactions [Do, 1998], for which its constant value reflects the similarity of the materials under study, i.e., in all cases q_{chem} is a result of chemical interaction of CO_2 with amine groups. The stronger bonds formed in the case of chemical adsorption are reflected in the considerably larger value of b for q_{chem} (1.25×10^5 bar^{-1}) compared to those of q_{phys}, (2.7×10^{-1} to 7.38 bar^{-1}). On the other hand, t is a parameter associated with the heterogeneity of the surface, with $t = 1$ for homogeneous surfaces [Do, 1998]. Since the values of t for q_{phvs} were in all cases close to unity, it shows that the model obtained interpreted the available sites for physisorption as homogeneously distributed, similarly to the silica support from which it was derived. For q_{chem}, it is reasonable to assume that, because of the particular type of amines and their accessibility for each adsorbent, they presented diverse distributions of adsorption sites, with the subsequent variation in t values.

Since the proposed isotherm model is based on a general assumption that functionalized mesoporous silica exhibit two independent adsorption mechanisms, the applicability of the model may extend to other acid gases. Consequently, the proposed isotherm model was applied to H_2S adsorption data on TRI-PE-MCM-41 as shown in Figure 6.10. Once again, the isotherm shape resembles that of Figure 6.1, which can be related to the dual adsorption mechanisms. The parameters obtained for the isotherm model are shown in Table 6.4. The associated values of $\Delta q(\%)$ were 6.63, 1.67 and 1.65% for the isotherms at 25, 35 and 50 °C, respectively. The excellent fit of the proposed model with H_2S adsorption data on amine-modified adsorbents is a strong indication that this methodology may apply to any adsorption system that combines independent chemisorption and physisorption sites.

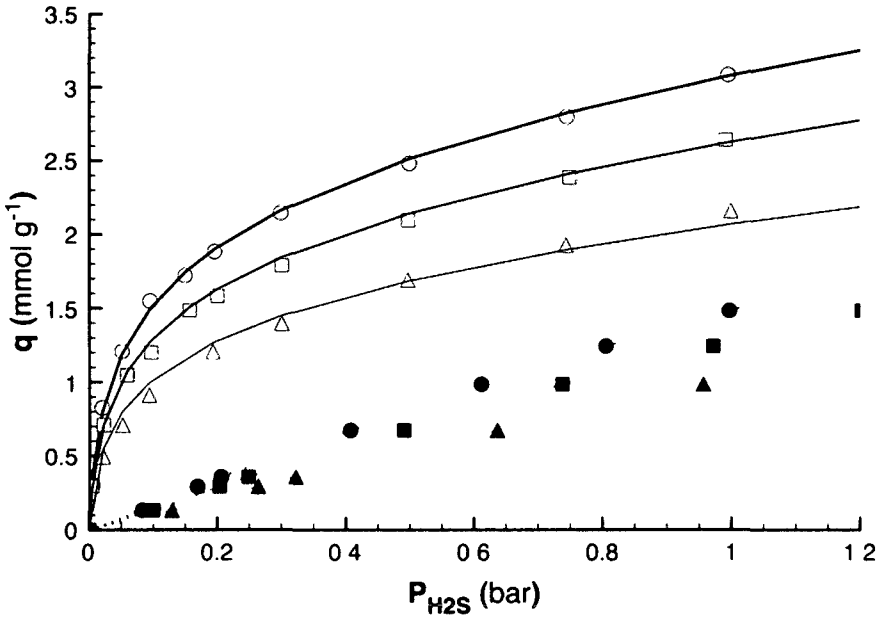

Figure 6.10 Adsorption isotherms of H_2S on TRI-PE-MCM-41 (open symbols) and PE-MCM-41 (closed symbols) at 25 °C (circles), 35 °C (squares) and 50 °C (triangles). The solid lines correspond to the equilibrium model proposed in this work

Table 6.4 Toth parameters of the temperature-dependent isotherm form for H_2S adsorption on TRI-PE-MCM-41 using 25 °C as reference temperature

H_2S uptake	n_{s0} (mmol g^{-1})	b_0 (bar^{-1})	t_0	χ	α	ΔH (kJ mol^{-1})
q_{phys}	3.42	1.98×10^{-1}	9.98×10^{-1}	4.06	0	14.3
q_{chem}	7.27	426	2.22×10^{-1}	0	1.00×10^{-5}	48.3

Figure 6.11 shows the values of ΔH_{ISO} calculated using the Clausius-Clapeyron equation on the experimental adsorption data for PE-MCM-41C (Figure 6.5) and TRI-PE-MCM-41 (Figure 6.4). It should be noted that the evolution of ΔH_{ISO} as a function of loading presented in this work for TRI-PE-MCM-41 and the corresponding silica support are consistent with the profiles reported by other authors [Knöfel et al., 2007; Knofel et al., 2009] using microcalorimetry for CO_2 adsorption on diamine-grafted SBA-15. High values of ΔH_{ISO} were observed in the low range of CO_2 pressure, in line with the strong interaction between CO_2 and amine groups and, as the CO_2 loading increased, ΔH_{ISO} decreased to values

similar to those associated with CO_2 adsorption on silica. This trend was also observed in the case of H_2S adsorption, although lower values were obtained compared to CO_2, suggesting that weaker interactions occur with this molecule. This provides further support to the proposed model based on a combination of two adsorption mechanisms.

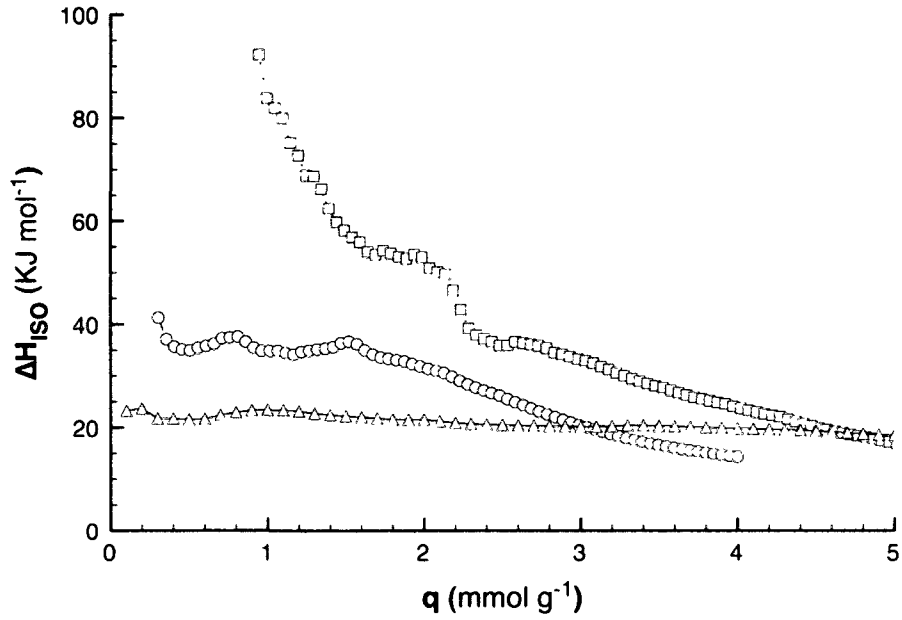

Figure 6.11 Isosteric heat of adsorption for CO_2 on PE-MCM-41C (triangles), CO_2 on TRI-PE-MCM-41 (squares) and H_2S on TRI-PE-MCM-41 (circles)

With respect to PE-MCM-41C, ΔH_{ISO} was found to be almost constant throughout the range of pressure studied. In addition, the value of ΔH (19.2 kJ mol^{-1}) calculated using the Toth parameter b for q_{phys}, corresponds closely to that of ΔH_{ISO} on the silica support (ca. 20 kJ mol^{-1}) and is comparable to the value reported by Knowles et al. [2005] and Knofel et al. [2009] using calorimetry for CO_2 adsorption on mesoporous silica (i.e., 28 kJ mol^{-1} and 20 kJ mol^{-1}, respectively). It is also worth mentioning that the values of ΔH_{ISO} obtained for PE-MCM-41C are just above the enthalpy of condensation of CO_2 (ca. 17 kJ mol^{-1}) [Knöfel et al., 2007], indicative of weak interactions. The high values of ΔH_{ISO} at low surface coverage (Figure 6.11) and the value of ΔH (67.3 kJ mol^{-1}) obtained using the Toth isotherm for the chemical interaction between CO_2 and amine groups lie within the range of values typical for chemisorption of CO_2. It is thus reasonable to assume that, in line with the model proposed,

the overall heat of adsorption observed for CO_2 on the amine-grafted adsorbent is mainly a result of the strong interactions between amine groups and CO_2 at low loadings and weak interactions of CO_2 with the adsorbent surface at higher surface coverage. Similarly to CO_2 adsorption, the heat of H_2S adsorption calculated using parameters of the temperature-dependent isotherm model (Table 6.4) was comparable to the isosteric heat of adsorption calculated based on experimental data at low loadings (Figure 6.11). Indeed, ΔH for q_{chem} was 48.3 kJ mol^{-1}, while ΔH_{ISO} at low H_2S uptake was ca. 42 kJ mol^{-1}.

6.4 Conclusions

Based on the observation that CO_2 adsorption on amine-functionalized mesoporous silicas occurs via two independent chemisorption and physisorption mechanisms, a semi-empirical adsorption isotherm model capable of fitting the experimental CO_2 adsorption isotherm over a wide range of pressure, from as low as 0.001 bar to 20 bar was developed using the Toth model in its temperature-dependent form. The heat of adsorption associated with chemisorption and physisorption, calculated using the parameters of the Toth model was consistent with experimental data, providing further physical meaning to the proposed model. The contribution of physisorption was calculated based on the assumption that at any CO_2 pressure, the amount of physisorbed CO_2 is the same as the CO_2 uptake by an equal surface area of silica support. This approach was validated using alkyltrimethylammonium-containing mesoporous silica as reference.

The model was successfully applied to different amine-functionalized materials and different adsorbates, providing strong evidence of its robustness. Moreover, the temperature-dependent form of the b parameter allowed accurate calculation of the heat of adsorption associated with chemisorption and physisorption. Another parameter, n_s, was found to be directly correlated with the surface area for physisorption and with amine content for chemisorption. Thus, within a series of related functionalized mesoporous materials the CO_2 adsorption isotherms may be predicted based on surface area and amine loading.

Supplementary Data

Tabulated experimental data points of CO_2 and H_2S adsorption on PE-MCM-41C and TRI-PE-MCM-41 at 25, 35, 45 and 55 °C can be found in Appendix A.

References

J. An, S.J. Geib, N.L. Rosi, Highly selective CO_2 uptake in a cobalt adeninate metal-organic framework exhibiting pyrimidine and amino-decorated pores. J. Am. Chem. Soc. 132 (2010) 38

Y. Belmabkhout, A. Sayari, Effect of pore expansion and amine functionalization of mesoporous silica on CO_2 adsorption over a wide range of conditions. Adsorption 15 (2009a) 318

Y. Belmabkhout, A. Sayari, Adsorption of CO_2 from dry gases on MCM-41 silica at ambient temperature and high pressure. 2. Adsorption of CO_2/N_2, CO_2/CH_4 and CO_2/H_2 binary mixtures. Chem. Eng. Sci. 64 (2009b) 3729

Y. Belmabkhout, R. Serna-Guerrero, A. Sayari, Adsorption of CO_2 from dry gases on MCM-41 silica at ambient temperature and high pressure. 1. Pure CO_2 adsorption. Chem. Eng. Sci. 64 (2009) 3721

S. Choi, J.H. Drese, C.W. Jones, Adsorbent materials for carbon dioxide capture from large anthropogenic point sources. ChemSusChem 2 (2009) 796

S. Couck, J.F.M. Denayer, G.V. Baron, T. Remy, J. Gascon, F. Kapteijn, An amine-functionalized MIL-53 metal-organic framework with large separation power for CO_2 and CH_4. J. Am. Chem. Soc. 131 (2009) 6326

O. Czakkel, G. Onyestyák, G. Pilatos, V. Kouvelos, N. Kanellopoulos, K. László, Kinetic and equilibrium separation of CO and CO_2 by impregnated spherical carbons. Micropor. Mesopor. Mater. 120 (2009) 76

D.D. Do, Adsorption Analysis: Equilibria and Kinetics. Imperial College Press: London, 1998.

B. Feng, M. Du, T.J. Dennis, K. Anthony, M.J. Perumal, Reduction of energy requirement of CO_2 desorption by adding acid into CO_2-loaded solvent. Energy Fuels 24 (2010) 213

L. Hamon, P.L. Llewellyn, T. Devic, A. Ghoufi, G. Clet, V. Guillerm, G.D. Pirngruber, G. Maurin, C. Serre, G. Driver, W. van Beek, E. Jolimaitre, A. Vimont, M. Daturi, G. Ferey, Co-adsorption and separation of CO_2-CH_4 mixtures in the highly flexible MIL-53(Cr) MOF. J. Am. Chem. Soc. 131 (2009) 17490

P.J.E. Harlick, A. Sayari, Applications of pore-expanded mesoporous silica. 5. Triamine grafted material with exceptional CO_2 dynamic and equilibrium adsorption performance. Ind. Eng. Chem. Res. 46 (2007) 446

J.C. Hicks, J.H. Drese, D.J. Fauth, M.L. Gray, G. Qi, C.W. Jones, Designing adsorbents for CO_2 capture from flue gas – hyperbranched aminosilicas capable of capturing CO_2 reversibly. J. Am. Chem. Soc. 130 (2008) 2902

N. Hiyoshi, K. Yogo, T. Yashima, Adsorption characteristics of carbon dioxide on organically functionalized SBA-15. Micropor. Mesopor. Mater. 84 (2005) 357

H.Y. Huang, R.T. Yang, D. Chinn, C.L. Munson, Amine-grafted MCM-48 and silica xerogel as superior sorbents for acidic gas removal from natural gas. Ind. Eng. Chem. Res. 42 (2003) 2427

C. Knöfel, J. Descarpentries, A. Benzaouia, V. Zelenak, S. Mornet, P.L. Llewelyn, V. Hornebecq, Functionalized micro-/mesoporous silica for the adsorption of carbon dioxide. Micropor. Mesopor. Mater. 99 (2007) 79

C. Knöfel, C. Martin, V. Hornebecq, P. Llewellyn, Study of carbon dioxide adsorption on mesoporous aminopropylsilane-functionalized silica and titania combining microcalorimetry and in situ infrared spectroscopy. J. Phys. Chem. C 113 (2009) 21726

G.P. Knowles, J.V. Graham, S.W. Delaney, A.L. Chaffee, Aminopropyl-functionalized mesoporous silicas as CO_2 adsorbents. Fuel Process. Technol. 86 (2005) 1435

M. Kruk, M. Jaroniec, A. Sayari, Application of large pore MCM-41 molecular sieves to improve pore size analysis using nitrogen adsorption measurements. Langmuir 13 (1997) 6267

M. Lanuza, D.B. Galloway, J.J. Low, R.R. Willis, Screening of metal-organic frameworks for carbon dioxide capture from flue gas using a combined experimental and modeling approach. J. Am. Chem. Soc. 131 (2009) 18198

Y. Li Study on corrosion and material selection for desulphurization unit in refinery. Petroleum Refinery Eng. 38 (2008) 24

R.P. Lively, R.R. Chance, B.T. Kelley, H.W. Deckman, J.H. Drese, C.W. Jones, W.J. Koros, Hollow adsorbents for CO_2 removal from flue gas. Ind. Eng. Chem. Res. 48 (2009) 7314-7324.

X. Liu, L. Zhou, X. Fu, Y. Sun, W. Su, Y. Zhou, Adsorption and regeneration study of the mesoporous adsorbent SBA-15 adapted to the capture/separation of CO_2 and CH_4. Chem. Eng. Sci. 62 (2007) 1101

X. Ma, X. Wang, C. Song, "Molecular basket" sorbents for separation of CO_2 and H_2S from various gas streams. J. Am. Chem. Soc. 131 (2009) 5777

M.G. Plaza, C. Pevida, B. Arias, M.D. Casai, C.F. Martin, J. Fermoso, F. Rubiera, J.J. Pis, Different approaches for the development of low-cost CO_2 adsorbents. J. Environ. Eng. 135 (2009) 426

A. Sayari, Periodic mesoporous materials: synthesis, characterization and potential applications. Stud. Surf. Sci. Catal. 102 (1996) 1

A. Sayari, M. Kruk, M. Jaroniec, I.L. Moudrakovski, New approaches to pore size engineering of mesoporous silicates. Adv. Mater. 10 (1998) 1376

A. Sayari, Y. Yang, M. Kruk, M. Jaroniec, Expanding the pore size of MCM-41 silicas: use of amines as expanders in direct synthesis and postsynthesis procedures. J. Phys. Chem. B, 103 (1999) 3651

A. Sayari, S. Hamoudi, Periodic mesoporous silica-based organic-inorganic nanocomposite materials. Chem. Mater. 13 (2001) 3151

A. Sayari, Mesoporous materials, in: P. Yang (Ed.), The Chemistry of Nanostructured Materials, World Scientific: Singapore, 2003, pp. 39-68.

P. Selvam, S.K. Bhatia, C.G. Sonwane, Recent advances in processing and characterization of periodic mesoporous MCM-41 silicate molecular sieves. Ind. Eng. Chem. Res. 40 (2001) 3237

R. Serna-Guerrero, A. Sayari, Applications of pore-expanded mesoporous silica. 7. Adsorption of volatile organic compounds. Env. Sci. Technol. 41 (2007) 4761

R. Serna-Guerrero, E. Da'na, A. Sayari, New insights into the interactions of CO_2 with amine-functionalized silica. Ind. Eng. Chem. Res. 47 (2008) 9406

A. Stein, B.J. Melde, R.C. Schroden, Hybrid inorganic-organic mesoporous silicates – nanoscopic reactors coming of age. Adv. Mater. 12 (2000) 1403

F. Su, C. Lu, S.C. Kuo, W. Zeng, Adsorption of CO_2 on amine-functionalized Y-type zeolites. Energy Fuels 24 (2010) 1441

K. Veltman, B. Singh, E.G. Hertwitch, Human and environmental impact assessment on postcombustion CO_2 capture focusing on emissions from amine-based scrubbing solvents to air. Env. Sci. Technol. 44 (2010) 1496

L. Wang, L. Ma A. Wang, Q. Liu, T. Zhang, CO_2 adsorption on SBA-15 modified by aminosilane. Chin. J. Catal. 28 (2007) 805

A.O. Yazaydin, R.Q. Snurr, T.H. Park, K. Koh, J. Liu, M.D. LeVan, A.I. Benin, P. Jakubczak, M.B. Yue, Y. Chun, Y. Cao, X. Dong, J.H. Zhu, CO_2 capture by as-prepared SBA-15 with an occluded organic template. Adv. Funct. Mater. 16 (2006) 1717

F. Zheng, D.N. Tran, B.J. Busche, G.E. Fryxell, R.S. Addleman, T.S. Zemanian, C.L. Aardahl, Ethylenediamine-modified SBA-15 as regenerable CO_2 sorbent. Ind. Eng. Chem. Res. 44 (2005) 3099

A. Zukal, I. Dominguez, J. Mayerov, J. Cejka, Functionalization of delaminated zeolite ITQ-6 for the adsorption of carbon dioxide. Langmuir 25 (2009) 10314

Chapter 7

Modeling adsorption of CO_2 on amine-functionalized mesoporous silica.

2. Kinetics and breakthrough curves

Chem. Eng. J. 161 (2010) 182–190

Abstract

The adsorption kinetics of CO_2 on amine-functionalized mesoporous silica at low concentrations was investigated. Experimental data of CO_2 uptake as a function of time at temperatures between 25 and 70 °C were fit to a series of kinetic models, namely Lagergen's pseudo-first and pseudo-second order and Avrami's kinetic models. The best fit was obtained using Avrami's model, as it provided a fractional reaction order (ca. 1.4), which has been associated with the occurrence of multiple adsorption pathways. In addition, simulations of CO_2 adsorption in a column packed with amine-grafted mesoporous silica using computational fluid dynamics were carried out to predict breakthrough curves. The simulation results were compared to experimental data produced at various flow rates of a stream containing 5% CO_2 balance nitrogen. In all cases, the predicted breakthrough time and the corresponding CO_2 uptake were in close agreement with the experimental data.

7.1 Introduction

The deleterious effects of greenhouse gases on the environment and the threat they pose on the sustainability of ecosystems have fuelled the search for novel technologies capable of minimizing their emissions into the atmosphere. In particular, being the main anthropogenic contributor to climate change, carbon dioxide (CO_2) emissions have prompted a wide range of corrective initiatives to mitigate their impact. In addition to CO_2 capture to address environmental concerns, the removal of CO_2 in gas streams is required in other applications including air purification in confined spaces [Satyapal et al., 2001; Hwang et al., 2008] and natural gas treatment, among others [Cavenati et al., 2004; Delgado et al., 2004]. Consequently, researchers are actively exploring more efficient CO_2 capture technologies [Song et al., 2006; Yang et al., 2008].

Among the alternatives currently investigated for CO_2 capture, adsorption separation technologies have drawn particular attention since they can produce high purity streams with low energy consumption. As a result, a wide variety of adsorbents have been studied in recent years for such purpose [Choi et al., 2009]. As reported elsewhere [Harlick and Sayari, 2007; Belmabkhout and Sayari 2009], our research group developed a promising CO_2 adsorbent, referred to as TRI-PE-MCM-41, which consists of triamine-bearing organic species grafted on a mesoporous MCM-41 silica, whose pores were enlarged by post-synthesis hydrothermal treatment. This material was engineered to accommodate high loadings of amine functional groups while minimizing diffusion limitations. Indeed, TRI-PE-MCM-41 exhibited high adsorption capacity with an unprecedentedly fast rate of adsorption compared to other amine-functionalized adsorbents reported in literature [Harlick and Sayari, 2007]. Furthermore, unlike typical commercial adsorbents such as zeolites, TRI-PE-MCM-41 is tolerant to moisture in the feed and is highly selective towards acid gases in mixtures with nitrogen, oxygen, hydrogen and methane even at very low concentrations [Belmabkhout and Sayari 2009; Belmabkhout et al., 2009; Serna-Guerrero et al., 2010a]. In addition, it was demonstrated in a recent contribution that TRI-PE-MCM-41 is stable over a series of adsorption-desorption cycles when appropriate regeneration conditions (e.g., 70 °C under vacuum) are used [Serna-Guerrero et al., 2010a]. Because of the excellent attributes offered by amine-functionalized CO_2 adsorbents in general, and TRI-PE-MCM-41 in particular, it is interesting to model their adsorption characteristics to gain a better understanding of their behavior and for the simulation of CO_2 capture processes using such materials.

In a separate contribution, an adsorption equilibrium model for CO_2 on amine-functionalized silicas was developed based on the occurrence of two independent adsorption mechanisms [Serna-Guerrero et al., 2010b]. The development of this model stems from earlier observations regarding the interactions of CO_2 with amine-grafted mesoporous silica under dry and humid conditions [Serna-Guerrero et al., 2008]. The data indicated that in the presence of dry gaseous feed, CO_2 interacts chemically with amine groups with a maximum CO_2/N ratio of 0.5, consistent with the formation of carbamate species, an observation that has been corroborated by other groups using infrared spectroscopy [Knofel et al., 2009; Wang et al., 2009]. In addition, CO_2 can also adsorb physically on the surface of the material, particularly at pressures beyond 0.05 bar at room temperature. The equilibrium model was

capable of describing the adsorption of CO_2 and H_2S over a wide range of concentrations and temperature on our material and others, while providing parameters for the prediction of adsorption capacity at equilibrium, based on the structural properties of the adsorbent and its amine loading.

To gain further insights into the CO_2 adsorption on amine-functionalized adsorbents and with the aim of building a strong basis for simulation, the current contribution was devoted to the development of a suitable kinetic model. To the best of our knowledge, no kinetic models for CO_2 adsorption on amine-functionalized mesoporous silica have been proposed so far. In addition, based on the proposed kinetic model and the equilibrium model developed in a separate contribution [Serna-Guerrero et al., 2010b], we were able to simulate the adsorption of CO_2 in a fixed bed column using computational fluid dynamics.

7.1.1 Kinetic models. Among the properties expected in a good adsorbent, fast adsorption kinetics is one of the most important, since the efficiency of an adsorbent in dynamic processes, e.g., adsorption in a fixed bed column, and its capacity to withstand large adsorbate flows are associated with its rate of adsorption. Currently, the literature provides a wide number of kinetic models. Because of the complexity involved in the prediction of kinetic parameters, a typical approach consists of fitting experimental data to a series of established models, and selecting the one that provides the best fit. In recent years, however, several researchers attempted to rationalize some of the most popular kinetic models [Ho and McKay, 1998; Rudzinski and Panczyk, 2000; Azizian, 2004], making it possible to deduce information regarding the adsorbent-adsorbate interactions. Three such models will be considered in this work, including two of the most widely applied kinetic models, namely, Lagergen's pseudo-first order and pseudo-second order kinetic models [Inglezakis and Poulopoulos, 2006]. A fractional order kinetic model was recently developed based on Avrami's kinetic model of particle nucleation [Lopes et al., 2003] and was applied to describe the adsorption of anionic dyes on an aminopropyl-functionalized silica [Cestari et al., 2006], making it attractive for our work. Table 7.1 shows the list of equations associated with the kinetic models explored in this work, where t is the time elapsed from the beginning of the adsorption process, q_t is the amount adsorbed at a given point in time, and q_e represents the amount adsorbed at equilibrium.

To determine the adequacy of each model, an error function based on the normalized standard deviation (Eq. 1) was applied:

$$Err(\%) = \sqrt{\frac{\sum\left[\left(q_{t(\exp)} - q_{t(\mathrm{mod})}\right)/q_{t(\exp)}\right]^2}{N-1}} \times 100 \qquad (1)$$

where Err(%) is the error function, $q_{t(exp)}$ is the amount adsorbed at a given time determined experimentally, $q_{t(mod)}$ is the amount adsorbed as predicted by the model and N is the total number of experimental points.

Table 7.1 Kinetic adsorption models

Kinetic model	Equation	Differential form
Pseudo-first order	$q_t = q_e\left[1-\exp\left(-k_f t\right)\right]$	$\frac{dq_t}{dt} = k_f\left(q_e - q_t\right)$
Pseudo-second order	$q_t = \frac{k_s q_e^2 t}{1+q_e k_s t}$	$\frac{dq_t}{dt} = k_s\left(q_e - q_t\right)^2$
Avrami	$q_t = q_e\left[1-\exp\left(-\left(k_A t\right)^{n_A}\right)\right]$	$\frac{dq_t}{dt} = {k_A}^n t^{n-1}\left(q_e - q_t\right)$

Accordingly, it is necessary to determine q_e to completely define a kinetic model. As mentioned earlier, we developed an equilibrium model to describe the adsorption over a wide range of CO_2 pressure at temperatures from 25 to 55 °C [Serna-Guerrero et al., 2010b]. Although CO_2 adsorption isotherms on TRI-PE-MCM-41 have already been reported, a typical adsorption isotherm for CO_2 on TRI-PE-MCM-41 is shown in Figure 7.1 for illustration. In addition, the model used to fit this data is expressed in Eq. 2:

$$q_e = \left[\frac{n_s bP}{\left(1+(bP)^t\right)^{1/t}}\right]_{chem} + \left[\frac{n_s bP}{\left(1+(bP)^t\right)^{1/t}}\right]_{phys} \qquad (2)$$

where n_s, b and t are the characteristic parameters of the model and the subscripts "chem" and "phys" denote the contribution of chemical and physical adsorption, respectively.

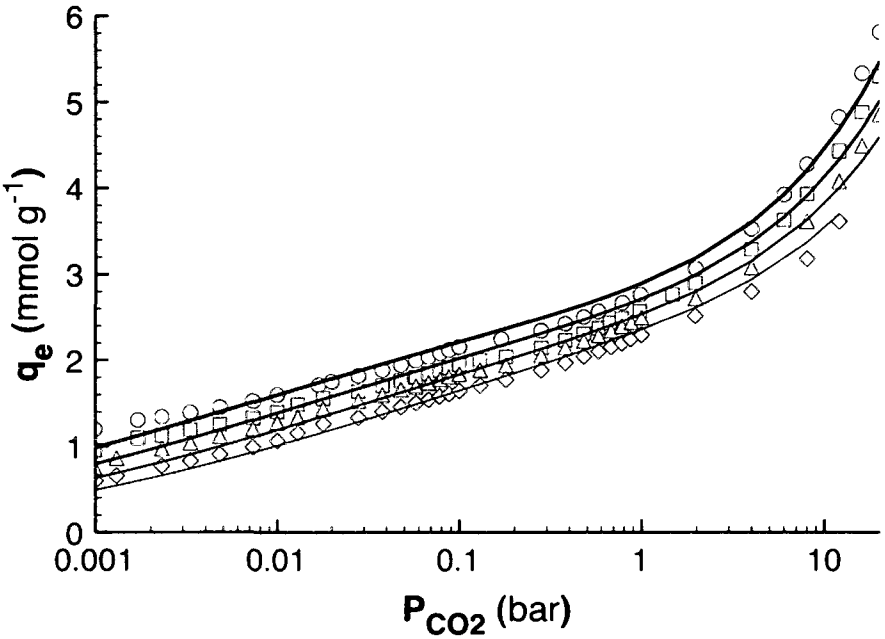

Figure 7.1 CO_2 adsorption isotherm on TRI-PE-MCM-41 at 25 (circles), 35 (squares), 45 (triangles) and 55 °C (diamonds). The solid lines represent the isotherm model fit

The temperature-dependent forms of the model coefficients are:

$$b = b_0 \exp\left[\frac{\Delta H}{RT_0}\left(\frac{T_0}{T} - 1\right)\right]$$

$$t = t_0 + \alpha\left(1 - \frac{T_0}{T}\right)$$

$$n_s = n_{s0} \exp\left[\chi\left(1 - \frac{T}{T_0}\right)\right]$$

where ΔH is the heat of adsorption at loadings close to zero, R is the universal ideal gas constant, α and χ are the parameters of the temperature-dependent form of the Toth model and the subscript 0 refers to the parameters obtained at a reference temperature T_0. The

values of the equilibrium model parameters for CO_2 adsorption using 25 °C as reference temperature are presented in Table 7 2

Table 7.2 Isotherm parameters for CO_2 adsorption on TRI-PE-MCM-41 using 25 °C as reference temperature

CO_2 uptake	n_{s0} (mmol g^{-1})	b_0 (bar^{-1})	t_0	χ	α	ΔH (kJ mol^{-1})
q_{phys}	6.98	2.74×10^{-1}	9.62×10^{1}	5.35	0	19.2
q_{chem}	3.64	1.25×10^{5}	2.24×10^{1}	0	6.05×10^{2}	67 3

7 1 2 Fixed bed column modeling The establishment of equilibrium and kinetic models contributes to the understanding of the adsorption phenomena, but one of their main objectives from an engineering standpoint is the description of a process for simulation and modeling. Using appropriate equilibrium and kinetic equations, the behavior of a fixed bed column can be predicted By comparison with experimental data, it is possible to validate the adequacy of the model proposed

For adsorption in a fixed bed column, the mass transfer in the gas phase can be modeled as a dispersed plug flow accounting for mixing in the axial direction. As a general rule, the difference of concentration in the radial direction is considered negligible when the ratio of the column-to-particle radius is sufficiently large, typically above 10 The general mass balance equation for an adsorption packed bed column is:

$$\varepsilon\left[D_L \frac{\partial^2 C_A}{\partial z^2}\right] - u_s \frac{\partial C_A}{\partial z} - (1-\varepsilon)\left[\rho_p (dq/dt)\right] = \varepsilon \frac{\partial C_A}{\partial t} \qquad (3)$$

where D_L is the axial dispersion of the adsorbate in the gas stream, z is the length in the axial direction, u_s is the superficial velocity of the gas mixture, ε is the bed void fraction, t is time, C_A is the concentration of the adsorbate in the gas phase and (dq/dt) is the rate of adsorption. In the present study, the term (dq/dt) was calculated from the kinetic models described in Section 7 1.1. The coefficients of the various kinetic models are lumped values representing

the various levels of gas phase diffusion onto the solid adsorbent until equilibration between the gas and adsorbed phases.

To solve the mass balance equation, the following assumptions and limits were used:

At $t < 0$: $C_A = 0$; $q = 0$

At $t > 0$: $C_{A\,@\,z=0} = C_0$; $(dC_A/dz)_{@\,z=L} = (dC_A/dz)_{@\,z=L-dz}$

At $t = \infty$: $C_A = C_0$

where C_0 is the concentration of the feed.

In this work, the inlet concentration of CO_2 was set at 5% balance nitrogen since this concentration is of interest for some potential applications, e.g., flue gas treatment and air purification in closed-circuit breathing systems. It is thus possible to consider the gas stream as a dilute solution, a condition under which the fluid velocity across the bed length is deemed constant. In addition, because of the low concentration of CO_2, an isothermal column operation was assumed. This assumption simplifies the model since the mass balance can be described without the use of an energy balance. While admittedly the operation of a real adsorption column is typically adiabatic, it should be mentioned that the experiments were performed in a column located inside a temperature-controlled enclosure, which might lend support to the approximation of isothermal conditions for this first attempt at modeling CO_2 adsorption on amine-grafted mesoporous silica.

The mass balance equation was solved by computational fluid dynamics using the finite volume method [Versteeg and Malalasekera, 1995]. This method permits the solution of partial differential equations by the discretization of the system into segments referred to as control volumes. It is assumed that concentration varies linearly within the limits of the control volume and the mass transfer at the limits of each control volume is continuous. The result is a series of simultaneous equations from which it is possible to calculate the concentration throughout discrete points of space and time. The accuracy of this method relies heavily on the size of control volumes, with smaller sizes providing a more accurate description of the system but with increased computational requirements. In this work, the convective – dispersive mass transfer was modeled using the hybrid scheme in which the influence of axial dispersion is considered significant only at Peclet numbers lower than 2.

The transient state was approximated with the totally implicit scheme, in which the change of adsorbate concentration in each control volume as a function of time is considered to be dependent only on the conditions of the previous step in time. An iterative solution routine was programmed using Microsoft Excel® Visual Basic for Applications.

7.2 Experimental section

7.2.1 Materials. Cab-O-Sil M-5 fumed silica from Cabot was used as the silica source. Cetyltrimethylammonium bromide (CTAB, Aldrich) and tetramethylammonium hydroxide (TMAOH 25%, balance water, Aldrich) were used as structure directing agent and for pH adjustment, respectively. The post-synthesis pore expander agent was dimethyldecylamine (DMDA 97% purity, Aldrich). The grafting agent 2-[2-(3-trimethoxysilylpropylamino)ethylamino]ethylamine (herein referred to as TRI-silane) and polyethyleneimine (PEI, M_n = 423) were obtained from Sigma-Aldrich. Ultra high purity grade nitrogen and certified gas mixture of 5% CO_2 balance N_2 were supplied by Linde Ltd., Canada. All reagents and gases were used without further purification.

7.2.2. Synthesis of adsorbent. Detailed description of the synthesis of the amine-functionalized mesoporous material used in the present work was reported by Harlick and Sayari [2007]. Briefly, MCM-41 type silica was produced at 100 °C in the presence of CTAB in basic conditions using TMAOH. Subsequently, the pore size of MCM-41 was increased by hydrothermal restructuring at 120 °C in the presence of DMDA [Sayari et al., 1999]. The surfactant template and pore expander agent were removed by calcination in nitrogen, then in air at 550 °C, and the resulting material was labeled PE-MCM-41. The amine functional groups were incorporated onto PE-MCM-41 by grafting in toluene at 85 °C in a 250 mL glass reactor. First, 0.3 mL of water per g of silica was added to a PE-MCM-41 silica suspension in toluene, followed by addition of TRI-silane (3 ml per g of silica). Grafting proceeded for 16 h, and then the product was filtered and washed with toluene and pentane. The solid obtained was dried in a natural convection oven at 100 °C for 1 h and labeled TRI-PE-MCM-41. Finally, as fine powder produces large pressure drops in packed bed columns, pellets were produced as follows. The powdered form of TRI-PE-MCM-41 was loaded in a dye and compressed under a load of 450 kg cm^{-2} using a hydraulic press. As reported earlier,

such a pressure did not affect significantly the structural properties of the adsorbent [Serna-Guerrero et al., 2007]. The particles thus produced were crushed and sieved between openings of 0.82 and 0.41 mm (i.e., 20 and 40 mesh, respectively). Another sample used in this investigation was prepared by dispersing PEI on PE-MCM-41, following the recipe by Xu et al. [2002]. An amount of 1 g of PEI was dispersed in methanol at room temperature followed by addition of 1 g PE-MCM-41 to the mixture under continuous stirring. The mixture was stirred overnight under ambient air until complete evaporation of the solvent. The resulting solid was labeled as PEI-PE-MCM-41.

7.2.3 Characterization. The structural properties of the adsorbent were determined by nitrogen adsorption measurements at 77 K using a Micromeritics ASAP 2020 volumetric instrument. The sample was treated under vacuum (i.e., 0.5 mmHg) at 100 °C for 5 h before adsorption measurements. Surface area was determined using the BET method, while the pore volume was considered as the volume of liquid nitrogen adsorbed at a relative pressure close to 1. The pore size distribution was obtained using the KJS method [Kruk et al., 1997]. Additionally, the organic content was determined by thermogravimetric analysis (TGA) using a TA Q-500 instrument. The sample was heated at 10 °C min^{-1} under flowing nitrogen up to 800 °C followed by decomposition in the presence of air at the same heating rate and up to 1000 °C.

7.2.4 CO_2 adsorption measurements. The uptake of CO_2 as a function of time was monitored using the TA instrument mentioned above. A sample of ca. 0.03 g of TRI-PE-MCM-41 was loaded in a platinum crucible with a depth of 5 mm. Once loaded, the sample was activated by heating at 10 °C min^{-1} up to 150 °C for TRI-PE-MCM-41 and up to 100 °C for PEI-PE-MCM-41 under flowing nitrogen for 2 h. It was then cooled to the desired temperature (i.e., 25, 40, 55 or 70 °C) and exposed to a flowing mixture of 5% CO_2 balance nitrogen at 100 mL min^{-1}. Previous studies showed that under such conditions, adsorption of nitrogen on TRI-PE-MCM-41 is negligible [Belmabkhout and Sayari, 2009]. According to the analysis presented by Barrie et al., [2004], for gravimetric measurements in a microbalance, when a shallow layer of adsorbent is combined with a sufficiently high adsorbate flow rate, the influence of axial dispersion through the adsorbent layer does not affect significantly the

experimental measurement. Furthermore, similarly to zero-length columns, it was proven that at low adsorbate concentration the operation could be considered isothermal despite the inherent release of heat associated with CO_2 adsorption. Since our experimental procedure meets these conditions, the assumptions of negligible axial dispersion and isothermal operation were considered adequate for the TGA measurements. The experimental CO_2 uptake as a function of time was fitted to each kinetic model listed in Table 7.1 using a regression on their linearized forms.

The experimental setup used for CO_2 adsorption studies in a packed bed column is represented schematically in Figure 7.2. A sample of ca. 0.45 g of TRI-PE-MCM-41 with 20 – 40 mesh particle size was loaded in a stainless steel column with inner diameter of 0.43 cm and 12 cm of packed height. Before each run, the adsorbent was activated for 2 h using a flow of 50 mL min^{-1} of helium, while maintaining the column at 150 °C using an electric oven with temperature control. The temperature was then lowered to 25 °C, and the flow was switched to a mixture of 5% CO_2 balance nitrogen at 50, 30 or 15 mL min^{-1}, equivalent to a contact time of 0.024, 0.04 and 0.08 min, respectively. The column downstream was continuously monitored using a Pfeiffer Thermostar mass spectrometer (MS). The experimental breakthrough curves of CO_2 were obtained from the MS signal corresponding to 44 amu.

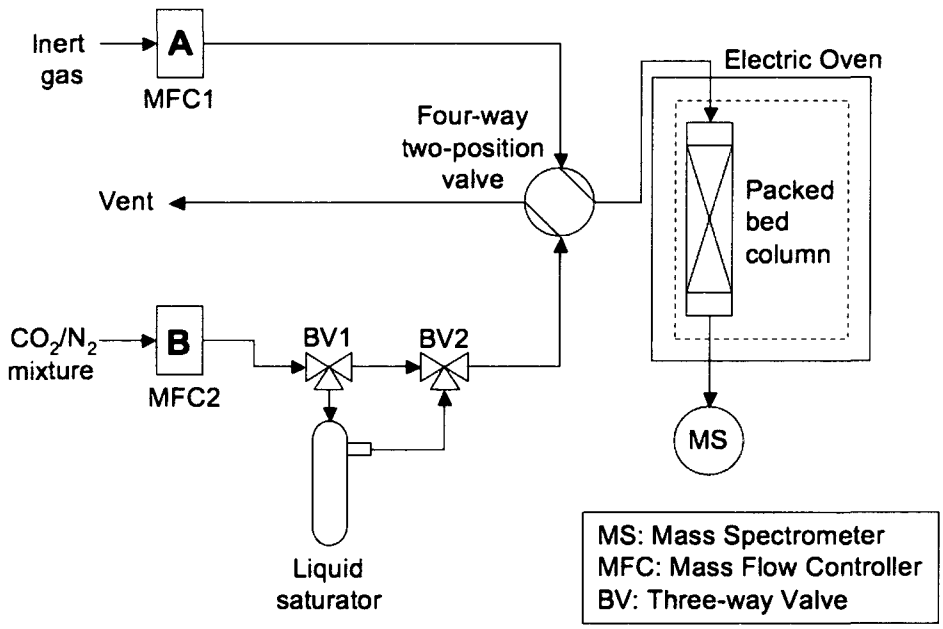

Figure 7.2 Experimental setup for CO_2 adsorption in a packed bed column

The dynamic adsorption capacity (q) of the column was calculated using Eq. 4:

$$q = \frac{FC_0 t_q}{W} \tag{4}$$

where F is the total molar flow, C_0 is the concentration of the adsorbate in the feed stream, W is the mass of adsorbent loaded in the column, and t_q is the stoichiometric time, which is estimated from the breakthrough profile according to Eq. 5 [Geankoplis, 1993]:

$$t_q = \int_0^{\infty} \left(1 - \frac{C_A}{C_0}\right) dt \tag{5}$$

where C_0 and C_A are the concentrations of the adsorbate upstream and downstream the column, respectively.

7.3 Results and discussion

Nitrogen adsorption-desorption isotherms for TRI-PE-MCM-41 and PE-MCM-41 are presented in Figure 7.3, while TGA profiles are shown in Figure 7.S1 (Appendix B, Supplementary Information). The structural properties deduced from nitrogen adsorption data are presented in Table 7.3. The shape of the nitrogen adsorption isotherms for PE-MCM-41 and TRI-PE-MCM-41 correspond to Type IV according to the IUPAC classification, which is associated with mesoporous materials. Figure 7.3 also shows that after impregnation of PEI on PE-MCM-41, most of its pore volume and surface area were lost, in agreement with observations by other workers studying PEI-loaded mesoporous silica with high organic content [Xu et al., 2002; Drage et al., 2008; Son et al., 2008; Chen et al., 2009; Ma et al., 2009]. Moreover, TRI-PE-MCM-41 maintained a mesoporous nature after the incorporation of functional groups, which is a key feature for an effective adsorbent [Serna-Guerrero et al., 2008]. Although incorporation of organic molecules resulted in a decreased surface area, in the case of TRI-PE-MCM-41 it remained relatively high (429 $m^2 g^{-1}$). The loading of amine groups for TRI-PE-MCM-41 was 7.27 mmol g^{-1}.

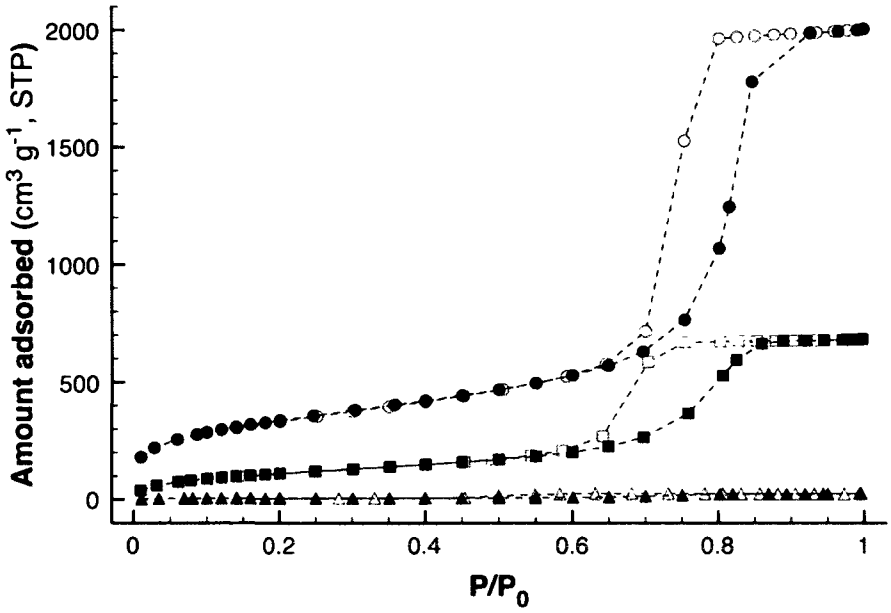

Figure 7.3 Nitrogen adsorption (closed symbols) and desorption (open symbols) isotherms for PE-MCM-41 (circles), TRI-PE-MCM-41 (squares) and PEI-PE-MCM-41 (triangles)

Table 7.3 Structural properties of mesoporous materials

	Surface area (m^2 g^{-1})	Pore volume (cm^3 g^{-1})	Mean pore size (nm)
PE-MCM-41	1134	2.62	10.9
TRI-PE-MCM-41	429	1.05	9.6
PEI-PE-MCM-41	21	0.04	8.2

7.3.1 Adsorption kinetics. Figure 7.4 shows the CO_2 uptake vs. time at 25, 40, 55 and 70 °C, and the corresponding profiles as predicted by the different kinetic models. In general, fast adsorption kinetics were observed with more than 80% of the total CO_2 uptake on TRI-PE-MCM-41 occurring within the first 40 s of contact time. Table 7.4 shows the values of the kinetic constants and the characteristic parameters of the kinetic models, along with the associated errors as calculated using Eq. 1.

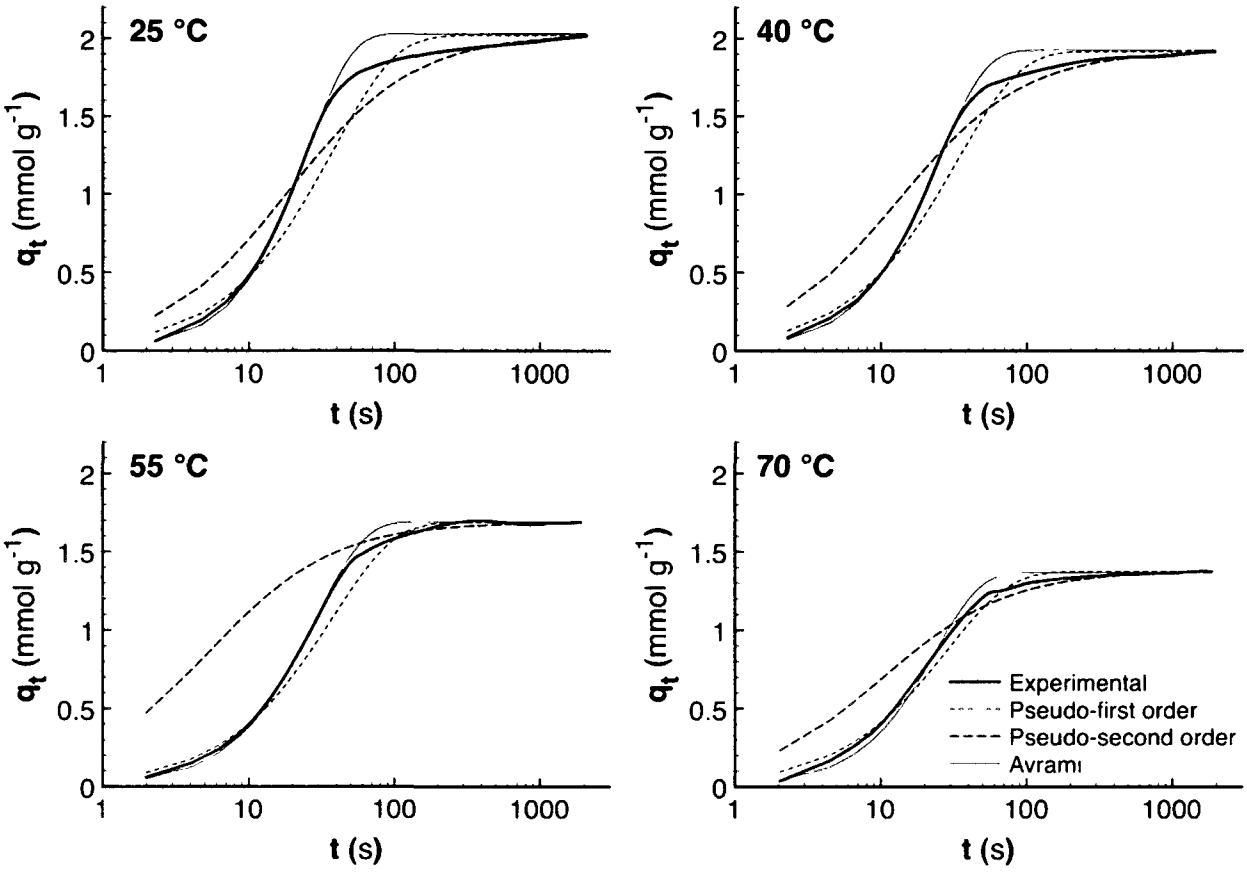

Figure 7.4 Experimental CO_2 uptake on TRI-PE-MCM-41 and corresponding fit to kinetic models

Table 7.4 Values of the kinetic model parameters for CO_2 adsorption on TRI-PE-MCM-41

		25 °C	40 °C	55 °C	70 °C
Pseudo-first	k_f (s^{-1})	3.61×10^{-2}	3.96×10^{-2}	4.01×10^{-2}	4.12×10^{-2}
	Err(%)	5.7	4.5	3.1	8.3
Pseudo-second	k_s (g mmol^{-1} s^{-1})	2.10×10^{-2}	3.11×10^{-2}	5.06×10^{-2}	5.63×10^{-2}
	q_e (mmol g^{-1})	2.06	1.95	1.71	1.40
	Err(%)	12.8	13.0	36.2	27.1
Avrami	k_A (s^{-1})	3.92×10^{-2}	4.02×10^{-2}	4.12×10^{-2}	4.21×10^{-2}
	n_A	1.46	1.36	1.41	1.41
	Err(%)	3.5	2.8	1.7	2.8

It was observed that the pseudo-first and pseudo-second order kinetic models presented some limitations with respect to the prediction of CO_2 adsorption on TRI-PE-MCM-41. At 25 °C for example, after a few seconds the pseudo-first order model underestimated the CO_2 uptake, up to ca. 100 s. After this time, the CO_2 adsorbed was consistently overestimated until the process approached equilibrium. On the other hand, the pseudo-second order appeared to fit the process accurately, but only beyond ca. 300 s. These results are in agreement with earlier reports, suggesting that the pseudo-first order kinetic model is applicable only under low surface coverage, and hence describes the early stages of adsorption [Ho and McKay, 1998; Ho, 2006]. It was also proposed that the pseudo-second order kinetic model represents adsorption at high adsorbate loadings. The adequacy of the pseudo-first order kinetic model at low surface coverage can be used to describe the behavior of CO_2 adsorption on purely siliceous MCM-41 and PE-MCM-41, for example. Indeed, because of the low adsorption capacity of non-functionalized mesoporous silica at CO_2 concentration of 5%, the surface coverage can be considered low, even at equilibrium. Hence, as previously reported by our group [Belmabkhout and Sayari, 2009], the pseudo-first order kinetics successfully described CO_2 adsorption on purely siliceous adsorbents. However, when applied to CO_2 adsorption on the functionalized adsorbent, this model presented some limitations, deviating significantly from the experimental data after the first few seconds of the adsorption process, presumably after the adsorbate surface coverage became high enough. This is clearly consistent with the plot of the linearized form of the kinetic model, available in the Supplementary Data (Figure 7.S2), where a deviation from linearity occurred after a few seconds of contact time. Nonetheless, for practical purposes, the values of k_f presented in Table 7.4 can be used within an acceptable degree of accuracy, since the calculated error within the range of temperature considered did not exceed 8%. The attractiveness in using the pseudo-first order kinetic model is twofold: (i), due to its simple mathematic expression, it has been widely applied for the study and modeling of adsorption systems, and (ii) it can be used to determine kinetic properties like micropore diffusion when the geometry of the particles is known [Roque-Malherbe, 2007]. For example, if interparticle diffusion is considered the rate-limiting step and the particles are assumed to be comprised of spheres with the same size, a diffusivity factor can be calculated using Eq. 6:

$$k_f = 15\frac{D_S}{r_p^2} \tag{6}$$

where D_S is the diffusivity in the solid and r_p is the radius of a particle.

It is also possible to obtain values of diffusivity from the experimental uptake profile using a Fickian diffusion model of the form [Inglezakis and Poulopoulos, 2006]:

$$\frac{q_t}{q_e} = 1 - \frac{6}{\pi^2}\sum_{n=1}^{\infty}\frac{1}{n^2}\exp\left(-n^2\pi^2\frac{D_S}{r_p^2}t\right) \tag{7}$$

Accordingly, the Fickian diffusion model was used to corroborate the values of D_S/r_p^2 calculated from the pseudo-first order model (Eq. 6). A value of D_S/r_p^2 can be obtained from the slope of a linearized form of Eq. 7. A plot of CO_2 uptake on TRI-PE-MCM-41 and its fit to the linearized form of Eq. 7 can be found in the Supporting Information, along with its corresponding linear regression parameters (Figure 7.S5 and Table 7.S1).

Table 7.5 D_S/r_p^2 (s^{-1}) values for CO_2 adsorption on TRI-PE-MCM-41 and NaY

	TRI-PE-MCM-41		NaY
			[Li and Tezel, 2007]
	Pseudo-first	Fickian	
25 °C	2.41×10^{-3}	2.66×10^{-3}	3.01×10^{-4}
40 °C	2.64×10^{-3}	2.96×10^{-3}	6.77×10^{-4}
55 °C	2.67×10^{-3}	2.98×10^{-3}	1.41×10^{-3}
70 °C	2.74×10^{-3}	3.06×10^{-3}	2.76×10^{-3}

Table 7.5 shows that the values of D_S/r_p^2 obtained using both approaches are within ca. 10% from each other. The closeness of D_S/r_p^2 values suggests that the first-order kinetic model parameters can be used with an acceptable level of confidence to describe the CO_2 uptake on TRI-PE-MCM-41. The difference between these values can be mainly attributed to the assumptions of particle shape and equal size used in Eq. 6, as deviations likely occurred. For comparison, Table 7.5 also shows values of D_S/r_p^2 reported in literature for CO_2

adsorption on NaY zeolite [Li and Tezel, 2007]. The relatively higher values of D_S/r_p^2 in the case of TRI-PE-MCM-41 represent lower diffusion limitations, which can be attributed to a larger pore size than NaY zeolite and could be translated into faster adsorption kinetics.

As seen in Figure 7.5, the pseudo-second order kinetic model fits the experimental data once the CO_2 uptake slows down. Although a good fit was obtained on the linearized form of the pseudo-second order model (Supporting Information, Figure 7.S3), the value of Err(%) was higher compared with the pseudo-first order model, the main source of error being its inability to fit the uptake at the beginning of the process. However, other characteristics of the pseudo-second order kinetic model may be useful. For example, this model does not require *a priori* determination of the amount adsorbed at equilibrium, as it can be deduced from the linear regression of the experimental data [Inglezakis and Poulopoulos, 2006]. The values of q_e reported in Table 7.4 reflected closely the experimental adsorption capacity at equilibrium. Nevertheless, as observed by Royer et al. [Royer et al., 2009], the value of k_s depends strongly on the initial concentration of the adsorbate.

The best fit to a kinetic model was obtained using Avrami's equation. The calculated order of this model was of ca. 1.4, and varied in less than 5% with respect to the adsorption temperature within the range studied. According to Lopes et al, [2003] and Cestari et al., [2006], the fractional order of this model stems from the complexity of the reaction mechanisms or the occurrence of more than one reaction pathway. It is thus possible that the excellent fit of Avrami's kinetic model resulted from its capacity to account for the CO_2 uptake by chemical and physical adsorption demonstrated earlier [Serna-Guerrero et al., 2008]. A further advantage of Avrami's equation is that the kinetic constant, expressed in s^{-1}, is independent of the initial concentration of the adsorbate [Royer et al., 2009].

Since the pseudo-first order kinetic model and Avrami's model were considered adequate, we used the corresponding kinetic coefficients at various temperatures (i.e., 25, 40, 55 and 75 °C) to calculate the parameters of an Arrhenius type equation (Eq. 8) by a linear regression on its linearized form:

$$k = A\exp\left(\frac{-E_a}{RT}\right) \tag{8}$$

where A is the Arrhenius preexponential factor, E_a is a term associated with the activation energy, R is the universal ideal gas constant, and T is temperature. Eq. 8 can be used to predict values of the kinetic constant (k) at a certain temperature, which can be useful to describe non-isothermal behavior.

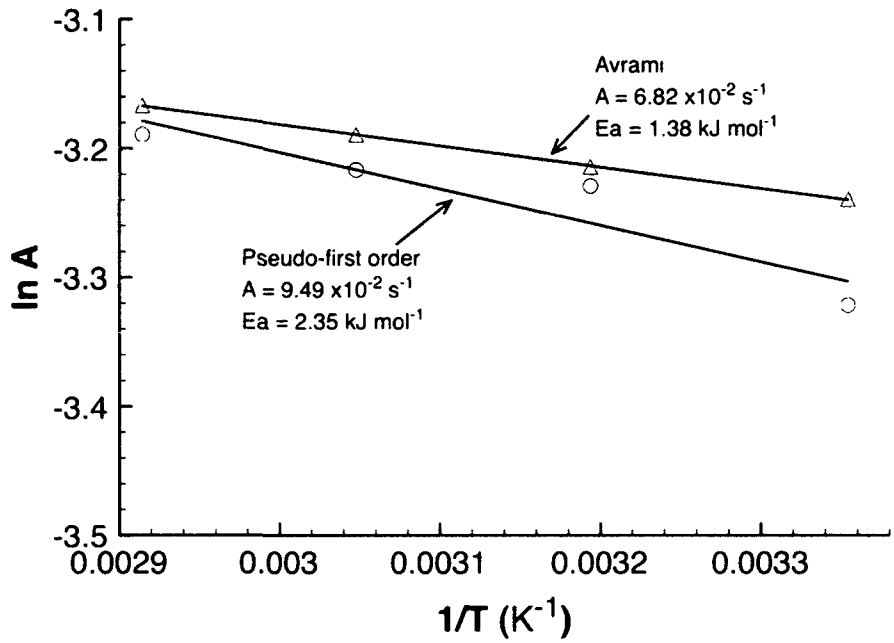

Figure 7.5 Arrhenius plots for the kinetic constants obtained by pseudo-first order and Avrami kinetic models

Figure 7.5 shows the plots of the linearized Arrehnius equation, along with the corresponding values of A and E_a. As seen, there is a discrepancy between the values of E_a for the different kinetic models. However, caution should be exercised when attempting to associate E_a with the actual activation energy in the case of models with a kinetic order other than one. For example, as demonstrated by Azizian et al., [2004], the value of k obtained from the pseudo-second order kinetic model is not the kinetic constant for adsorption in a strict sense, but rather a complex function involving different parameters such as the kinetic constant for desorption, the surface coverage at equilibrium and the change of adsorbate concentration during the process. In a similar manner, the fractional order in the Avrami model suggests that the value of k_A is an overall constant representing various reaction steps. The Arrhenius equation in these cases is useful to predict k at different temperatures,

although the adequacy of these semi-empirical models to determine thermodynamic parameters is still debatable.

Recent effort was devoted to the development of PEI-impregnated on mesoporous silica [Xu et al., 2002; Drage et al., 2008; Son et al., 2008; Chen et al., 2009; Ma et al., 2009] and carbon [Aroua et al., 2008; Plaza et al., 2009] as they reportedly exhibit high CO_2 adsorption capacity. Consequently, it was of interest to determine the kinetic properties of PEI-impregnated PE-MCM-41 silica for comparison with TRI-PE-MCM-41. Figure 7.6 shows profiles of CO_2 uptake on PEI-PE-MCM-41 at 25 °C and 70 °C. According to most of the reports presented in the literature, the optimum CO_2 uptake on PEI-impregnated materials, in terms of both adsorption capacity and kinetics, was observed at ca. 75 °C. However, this was not the case of the present study. While it was evident that PEI-PE-MCM-41 presented a slow uptake at room temperature, after a long contact time it exhibited a significantly high q_e. The adsorption capacity was lower at 75 °C, but its kinetic behavior was much more favorable, reaching an uptake of 80% of its total capacity after ca. 10 min of contact time. Thus, it is possible that either (i) the results at room temperature presented in previous studies were not at, or sufficiently close to, equilibrium due to the particularly slow kinetics, producing an apparently higher q_e at ca. 75 °C because of significantly improved kinetics, or (ii) the large pores of the support used in this work offered a comparative advantage permitting a better, albeit slow, access to amine groups even at room temperature.

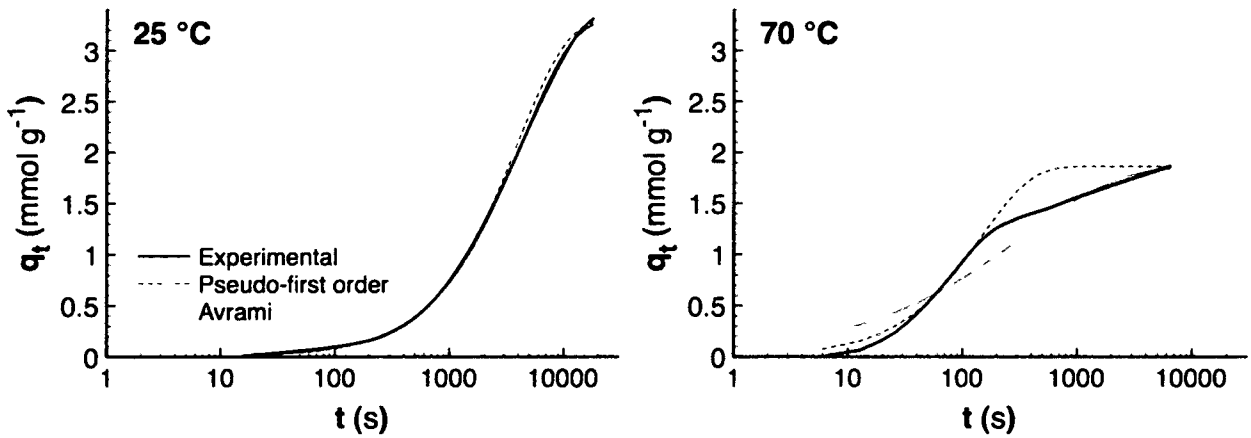

Figure 7.6 Experimental CO_2 uptake on PEI-PE-MCM-41 and corresponding fit to kinetic models

The unfavorable kinetics of PEI-impregnated materials at room temperature has been widely reported [Xu et al., 2002; Drage et al., 2008; Son et al., 2008; Chen et al., 2009; Ma et al., 2009], and a series of explanations have been put forth. In general, it is believed that PEI agglomerates in a bulk, liquid-like phase inside the pores, generating strong diffusion limitations to CO_2 leading to an inefficient use of amine groups. As temperature increases, diffusion through the PEI phase improves accompanied with a facilitated uptake of CO_2.

Table 7.6 Values of the kinetic model parameters for CO_2 adsorption on PEI-PE-MCM-41

		25 °C	70 °C
Pseudo-first	k_f (s^{-1})	2.53×10^{-4}	6.81×10^{-3}
	Err(%)	6.3	12.4
Avrami	k_A (s^{-1})	2.35×10^{-4}	2.96×10^{-3}
	n_A	0.97	0.52
	Err(%)	6.3	17.9

Table 7.6 shows the kinetic parameters obtained for PEI-PE-MCM-41 using the pseudo-first and Avrami's kinetic models. It was observed that the first-order kinetics provided an adequate description of the adsorption of CO_2 at 25 °C since the Err(%) value was small and even Avrami's model produced a kinetic order close to unity. This was not the case at 70 °C, as Avrami's kinetic order was a fractional value, suggesting a change in adsorption mechanisms, consistent with the hypothesis that a different physical state of PEI occurs at higher temperature. It was also evident that even at 70 °C, the kinetics of CO_2 adsorption on PEI-PE-MCM-41 is comparatively slower than that of TRI-PE-MCM-41. Since Avrami's model produced orders with different values, a fair comparison can be made based on k_f for the first-order kinetics model. As seen, PEI presented a k_f of 6.81×10^{-3} at 70 °C, while it was 4.12×10^{-2} for TRI-PE-MCM-41 under the same conditions. The comparison was more dramatic for adsorption at room temperature, where TRI-PE-MCM-41 had a kinetic constant two orders of magnitude higher than its PEI-impregnated counterpart. The combination of high amine loading and open pore structure represents a distinct advantage of TRI-PE-MCM-41 in terms of rate of adsorption. It is thus reasonable to conclude that,

although a high concentration of amine groups can be obtained by PEI impregnation on mesoporous silica, the favorable kinetics of TRI-PE-MCM-41 leads to more efficient CO_2 separation processes.

7.3.2 Fixed bed column adsorption. To predict breakthrough curves, we studied the adsorption of CO_2 in a fixed bed column packed with TRI-PE-MCM-41 pellets. The characteristics of the adsorption bed and the operating conditions are summarized in Table 7.7. A series of typical experimental breakthrough curves of CO_2 are presented in Figure 7.7. The steep nature of these curves is indicative of an efficient use of the adsorbent in dynamic processes, in line with high rate of adsorption. In actual applications, the adsorption columns are regenerated before breakthrough occurs, so one of the main uses of a simulation model is its capacity to predict the breakthrough time (t_b) and the corresponding uptake (q_b). In this work, t_b was defined somewhat arbitrarily as the time corresponding to C_A/C_0 = 10%, although this value may vary according to the specific requirements of each application. In accordance with the generally accepted behavior of a packed bed column, q_b under the smallest flow rate (15 mL min^{-1}) was the closest to q_e, as a result of increased contact time and a shorter mass transfer zone. As seen in Table 7.8, q_b for TRI-PE-MCM-41 decreased from 1.89 mmol g^{-1} at a flow rate of 15 mL min^{-1} to 1.56 mmol g^{-1} at 50 mL min^{-1}. Considering the particularly short retention time at 50 mL min^{-1}, it can be said that the adsorbent is remarkably efficient as its q_b represents more than 75% of its q_e.

Table 7.7 Adsorption bed characteristics and operating conditions for fixed bed adsorption experiments

Packed bed length (z)	12 cm
Inner column diameter	0.42 cm
Bed porosity (ε)	0.38
Particle density (ρ_P)	880 mg cm^{-3}
Feed gas composition	5% CO_2; 95% N_2
Total pressure	1 atm
Axial dispersion coefficient (D_L)	0.167 cm^2 s^{-1}*

**Source:* Geankoplis, 1993

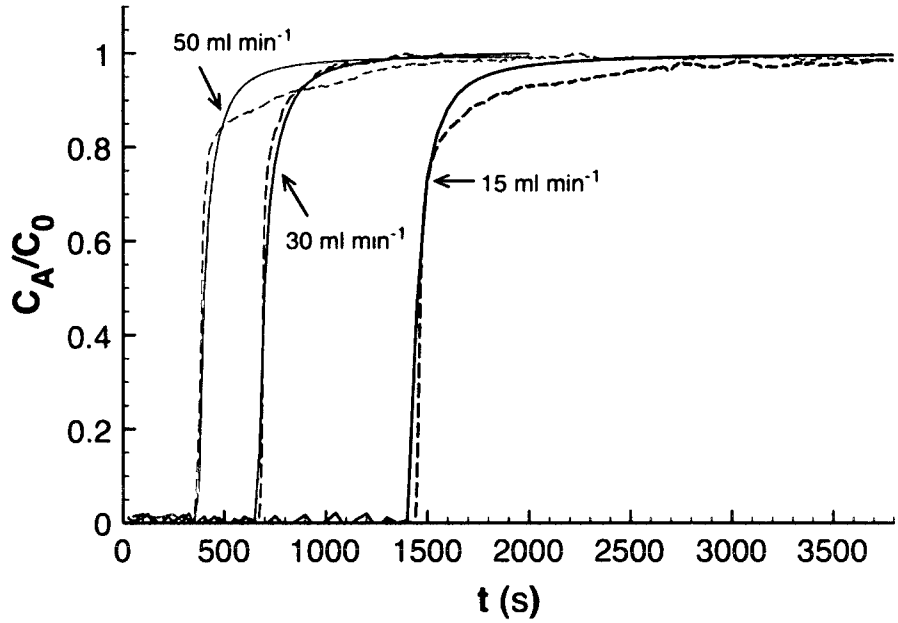

Figure 7.7 Experimental (dashed lines) and predicted (solid lines) breakthrough curves of 5% CO_2 balance N_2 on TRI-PE-MCM-41

Because of the excellent behavior of Avrami's kinetic model, it was chosen for the modeling of CO_2 adsorption in a fixed bed column. The concentration of CO_2 downstream the column predicted by the model is also presented in Figure 7.7, where it can be compared with the experimental data. Although not shown, a preliminary study to determine the appropriate size of control volumes and time steps was performed by systematically decreasing their values. It was found that under the conditions used in this study, no significant change was observed when the time steps were of 0.01 s or smaller combined with control volumes of less than 1/20 of the total length of the column. All the simulations presented herein were obtained using these values.

As seen in Table 7.8, the predicted t_b was in all cases close to the experimental data. It is particularly interesting to notice that the breakthrough curve generated by the model reproduced the asymmetry observed in the experimental curve, with a slower increase of downstream concentration beyond C_A/C_0 of ca. 0.60. These results corroborate the utility of the fixed bed column model used to predict CO_2 adsorption on TRI-PE-MCM-41, reflecting the adequacy and usefulness of the proposed kinetic and equilibrium models. Some

differences between the predicted breakthrough curves and the experimental data presented in Figure 7.7 were observed when C_A/C_0 approached 1, particularly in the breakthrough curves corresponding to 15 and 50 mL min^{-1}. Indeed, some experimental signals showed a slower than expected approach to saturation. However, this behavior did not occur in all cases, indicating that it is most likely attributable to experimental errors, related to either the accuracy of the instrument and/or to a slightly drifting baseline.

Table 7.8 Experimental and predicted values of t_b and q_b

	Experimental*		Model	
F (mL min^{-1})	t_b (s)	q_b (mmol g^{-1})	t_b (s)	q_b (mmol g^{-1})
15	1524 ±28	1.89 ±0.03	1450	1.80
30	714 ±23	1.77 ±0.06	675	1.67
50	380 ±24	1.56 ±0.09	375	1.54

*Average values of three experimental runs

Although a small discrepancy (i.e., less than 10%) was observed between the experimental and predicted values of q_b, as shown in Table 7.8, the latter were consistently lower, suggesting the occurrence of a systematical error. This error might be a result of the assumptions made to solve the fixed bed model, in addition to those of the kinetic and equilibrium models. Nonetheless, considering all the potential sources of error, the level of accuracy observed is a strong indication that the proposed models provide an acceptable representation of the behavior of CO_2 adsorption in a fixed bed column containing amine-functionalized mesoporous silica.

7.4 Conclusions

This study presented for the first time a kinetic analysis of CO_2 adsorption on amine functionalized materials at low adsorbate concentrations and an attempt at modeling the behavior of a fixed bed column. The adsorption kinetics of CO_2 on TRI-PE-MCM-41, an amine-grafted mesoporous adsorbent, was successfully described using Avrami's kinetic model with a reaction kinetic order of 1.4. This was attributed to the ability of Avrami's model to describe complex adsorption mechanisms as a result of its fractional order. This

model was capable of describing the uptake of CO_2 in the temperature range of 25 to 75 °C, with a standard deviation of less than 3.5%. It was also demonstrated that TRI-PE-MCM-41 offers more favorable kinetics than PEI-impregnated pore expanded MCM-41 silica. The kinetic model developed herein, in conjunction with the equilibrium model proposed in a previous work, was applied to describe the adsorption of CO_2 in a fixed bed column. By solving the mass balance equation of a fixed bed adsorption column using computational fluid dynamics, t_b was accurately predicted for different flow rates. Moreover, the shape of the breakthrough curve as predicted by the model was in close agreement with the experimental data. This suggests that computational fluid dynamics can be used to describe CO_2 adsorption on amine-containing materials and that the equilibrium and kinetic models developed for the adsorption of CO_2 on TRI-PE-MCM-41 are adequate.

Supplementary Data

TGA profiles of TRI-PE-MCM-41 and PEI-MCM-41, along with plots of the linearized forms of kinetic models and their corresponding regression parameters can be found in Appendix B.

References

M.K. Aroua, W.M.A.W. Daud, C.Y. Yin, D. Adinata, Adsorption capacities of carbon dioxide, oxygen, nitrogen and methane on carbon molecular basket derived from polyethyleneimine impregnation on microporous palm shell activated carbon. Sep. Purif. Technol. 62 (2008) 609

S. Azizian, Kinetic models of sorption: a theoretical analysis. J. Colloid Interface Sci. 276 (2004) 47

P.J. Barrie, C.K. Lee, L.F. Gladden, Adsorption and desorption kinetics of hydrocarbons in FCC catalysts studied using a tapered element oscillating microbalance (TEOM). Part 2: numerical simulations. Chem. Eng. Sci. 59 (2004) 1139

Y. Belmabkhout, A. Sayari, Effect of pore expansion and amine functionalization of mesoporous silica on CO_2 adsorption over a wide range of conditions. Adsorption 15 (2009) 318

Y. Belmabkhout, R. Serna-Guerrero, A. Sayari, Adsorption of CO_2-containing gas mixtures over amine-bearing pore-expanded MCM-41 silica: application for gas purification. Ind. Eng. Chem. Res. 49 (2010) 359

S. Cavenati, C.A. Grande, A.E. Rodrigues, Adsorption equilibrium of methane, carbon dioxide, and nitrogen on zeolites 13X at high pressures. J. Chem. Eng. Data 49 (2004) 1095

A.R. Cestari, E.F.S. Vieira, G.S. Vieira, L.E. Almeida, The removal of anionic dyes from aqueous solutions in the presence of anionic surfactant using aminopropylsilica - a kinetic study. J. Hazard. Mater. B 138 (2006) 133

C. Chen, S.T. Yang, W.S. Ahn, R. Ryoo, Amine-impregnated silica monolith with a hierarchical pore structure: enhancement of CO_2 capture capacity. Chem. Commun. 24 (2009) 3627

S. Choi, J.H. Drese, C.W. Jones, Adsorbent materials for carbon dioxide capture from large anthropogenic point sources. ChemSusChem 2 (2009) 796

J.A. Delgado, M.A. Uguina, J.L. Sotelo, B. Ruiz, M.R. Rosario, Separation of carbon dioxide/methane mixture by adsorption on a basic resin. Adsorption 13 (2007) 373

T.C. Drage, A. Arenillas, K.M. Smith, C.E. Snape, Thermal stability of polyethylenimine based carbon dioxide adsorbents and its influence on selection of regeneration strategies. Microporous Mesoporous Mater. 116 (2008) 504

C.J. Geankoplis, Transport Processes and Unit Operations, third ed. Prentice-Hall, New Jersey, 1993

P.J.E. Harlick, A. Sayari, Applications of pore-expanded mesoporous silica. 5. Triamine grafted material with exceptional CO_2 dynamic and equilibrium adsorption performance. Ind. Eng. Chem. Res. 46 (2007) 446

Y.S. Ho, G. McKay, The kinetics of sorption of basic dyes from aqueous solution by sphagnum moss peat. Can. J. Chem. Eng. 76 (1998) 882

Y.S. Ho, Review of second-order models for adsorption systems. J. Hazard. Mater. B 136 (2006) 681

H.T. Hwang, A. Harale, P.K.T. Liu, M. Sahimi, T.T. Tsotsis, A membrane-based reactive separation system for CO_2 removal in a life support system. J. Membr. Sci. 315 (2008) 116

V.J. Inglezakis, S.G. Poulopoulos, Adsorption, Ion Exchange and Catalysis: Design of Operations and Environmental Applications. Elsevier, Amsterdam, 2006

C. Knofel, C. Martin, V Hornebeq, P L. Llewellyn, Study of carbon dioxide adsorption on mesoporous aminopropylsilane-functionalized silica and titania combining microcalorimetry and in situ infrared spectroscopy J. Phys. Chem. C 113 (2009) 21726

P. Li, H. Tezel, Equilibrium and kinetic analysis of CO_2-N_2 adsorption separation by concentration pulse chromatography J. Colloid. Interf. Sci 313 (2007) 12

E.C.N. Lopes, F.S.C. dos Anjos, E.F S. Vieira, A.R. Cestari, An alternative Avrami equation to evaluate kinetic parameters of the interaction of Hg(II) with thin chitosan membranes. J Colloid Interface Sci. 263 (2003) 542

X. Ma, X. Wang, C. Song, "Molecular basket" sorbents for separation of CO_2 and H_2S from various gas streams. J. Am. Chem Soc 131 (2009) 5777

M.G. Plaza, C Pevida, B. Arias, M.D. Casal, C F Martin, J Fermoso, F Rubiera, J J Pis, Different approaches for the development of low-cost CO2 adsorbents. J. Environ. Eng. 135 (2009) 426

R M A Roque-Malherbe, Adsorption and Diffusion in Nanoporous Materials CRC Press, Florida, 2007

B. Royer, N F Cardoso, E.C. Lima, J C P Vaghetti, N.M. Simon, T. Calvete, R. Cataluña Veses, Applications of Brazilian pine-fruit shell in natural and carbonized forms as adsorbents to removal of methylene blue from aqueous solutions—Kinetic and equilibrium study. J. Hazard. Mater 164 (2009) 1213

W. Rudzinski, T. Panczyk, Kinetics of isothermal adsorption on energetically heterogeneous solid surfaces. a new theoretical description based on the statistical rate theory of interfacial transport. J. Phys Chem. B 104 (2000) 9149

S. Satyapal, T. Filburn, J. Trela, J. Strange, Performance and properties of a solid amine sorbent for carbon dioxide removal in space life support applications. Energy Fuels 15 (2001) 250

A. Sayari, Y. Yang, M. Kruk, M. Jaroniec, Expanding the pore size of MCM-41 silicas· use of amines as expanders in direct synthesis and postsynthesis procedures. J. Phys. Chem B. 103 (1999) 3651

R. Serna-Guerrero, A. Sayari, Applications of pore-expanded mesoporous silica. 7 Adsorption of volatile organic compounds. Environ Sci. Technol 41 (2007) 4761

R. Serna-Guerrero, E Da'na, A. Sayari, New insights into the interactions of CO_2 with amine-functionalized silica. Ind Eng Chem. Res 47 (2008) 9406

R Serna-Guerrero, Y. Belmabkhout, A. Sayari, Further investigations of CO_2 capture using triamine-grafted pore-expanded mesoporous silica. Chem Eng. J. 158 (2010a) 513

R. Serna-Guerrero, Y Belmabkhout, A. Sayari, Modeling CO_2 adsorption on amine-functionalized mesoporous silica. 1. A semi-empirical equilibrium model. Chem. Eng. J. 161 (2010b) 173

W.J. Son, J.S Choi, W.S Ahn, Adsorptive removal of carbon dioxide using polyethyleneimine-loaded mesoporous silica materials. Microporous Mesoporous Mater 113 (2008) 31

C Song, Global challenges and strategies for control, conversion and utilization of CO_2 for sustainable development involving energy, catalysis, adsorption and chemical processing. Catal Today 115 (2006) 2

H.K. Versteeg, W Malalasekera, An Introduction to Computational Fluid Dynamics The Finite Volume Method Prentice Hall, England, 1995

X Wang, V. Schwartz, J.C. Clark, X. Ma, S H Overbury, X Xu, C Song, Infrared study of CO_2 sorption over "molecular basket" sorbent consisting of polyethyleneimine-modified mesoporous molecular sieve J Phys Chem. C 113 (2009) 7260

X. Xu, C. Song, J.M. Andersen, B.G Miller, A. Scaroni, Novel polyethylenimine-modified mesoporous molecular sieve MCM-41 type as high-capacity adsorbent for CO_2 capture. Energy Fuels 16 (2002) 1463

H. Yang, Z. Xu, M. Fan, R. Gupta, R.B. Slimane, A.E Bland, I. Wright, Progress in carbon dioxide separation and capture: A review J. Environ. Sci. 20 (2008) 14

Chapter 8

Influence of regeneration conditions on the cyclic performance of amine-grafted mesoporous silica for CO_2 capture: an experimental and statistical study

Chem. Eng. Sci. 65 (2010) 4166–4172

Abstract

This work deals with the behavior of an amine-grafted mesoporous silica (referred to as TRI-PE-MCM-41) throughout adsorption-desorption cycles in the presence of 5% CO_2/N_2 using various regeneration conditions in batch experiments. The criteria proposed to determine the optimum regeneration conditions are the working adsorption capacity, the rate of desorption and the change of adsorption capacity between consecutive cycles. Using a 2^3 factorial design of experiments, the impact on the performance of the adsorbent of different levels of temperature, pressure and flow rate of purge gas during desorption was determined. It was found that all the parameters under study have a statistically significant influence on the working adsorption capacity, but only temperature is influential with respect to desorption rate. Regeneration using temperature swing was found to be attractive, as the highest CO_2 adsorption capacity (1.95 mmol g^{-1}) and the fastest desorption rate (9.82 $\times 10^{-4}$ mmol g^{-1} s^{-1}) occurred when desorption was carried out at 150 °C. However, if vacuum is applied, regeneration can be achieved at a temperature as low as 70 °C with only a 13 % penalty in terms of working adsorption capacity. It was also demonstrated that under the proper regeneration conditions, TRI-PE-MCM-41 is stable over 100 adsorption-desorption cycles.

8.1 Introduction

The currently strong interest in the development of adsorption separation technologies for carbon dioxide (CO_2) capture is associated with their high efficiency, low energy requirements, and often ease of regeneration and recycling. However, the most common adsorbents, such as activated carbon and zeolites, require exhaustive control of humidity in the feed stream because of the competitive adsorption of water and CO_2 [Brandani and Ruthven, 2004; Santos et al., 2008]. This represents a major penalty in terms of size and

complexity of the equipment, which is particularly unfavorable for non-stationary systems. Inspired by the well known CO_2 scrubbing using aqueous amine solutions, new adsorbents have been developed by incorporating amine groups on porous supports [Birbara et al., 2002; Gray et al. 2007; Jones et al., 2007; Olah et al., 2008, Serna-Guerrero et al., 2008; Couck et al., 2009; Ma et al., 2009]. Specifically, ordered mesoporous materials offer structural characteristics that are attractive for adsorption separation applications such as high surface area, large pore volume, and nanometer-size pores with a narrow size distribution. They can also be readily modified into amine-functionalized adsorbents with high CO_2 adsorption capacity [Gray et al., 2008; Hicks et al., 2008].

Our group developed a family of amine-bearing adsorbents for acid gas removal, such as CO_2, with high efficiency in terms of adsorption capacity, rate and selectivity [Harlick and Sayari, 2007; Serna-Guerrero et al., 2008]. One of such materials, referred to as TRI-PE-MCM-41, consists of a mesoporous silica support type MCM-41 whose pores have been enlarged by hydrothermal post-synthesis treatment followed by surface grafting of 2-[2-(3-trimethoxysilylpropylamino)ethylamino]ethylamine (TRI-silane). Because of the extra-large pore size of the support material (ca. 9-15 nm), the obtained adsorbent exhibits an open pore structure and a high surface density of readily accessible amine groups. In the presence of gas mixtures containing up to ca. 5% CO_2, TRI-PE-MCM-41 presented higher adsorption capacity and rate than benchmark microporous adsorbents, including zeolites [Harlick and Sayari, 2007; Belmabkhout and Sayari, 2009]. Moreover, TRI-PE-MCM-41 is tolerant to moisture in the feed and recyclable with low energy requirements. Recently, our group reported the adsorption capacity at equilibrium and the isosteric heat for the adsorption of CO_2 on TRI-PE-MCM-41 [Belmabkhout and Sayari, 2009]. This work showed that TRI-PE-MCM-41 exhibits high CO_2 uptake at low partial pressures, e.g., 2.05 mmol g^{-1} at a CO_2 pressure of 0.05 bar. Moreover, the calculated heat of adsorption (ca. 90 kJ mol^{-1}) at minimum loading, was consistent with the occurrence of predominantly chemical adsorption of CO_2 at low pressures. In addition, it was demonstrated that, unlike typical microporous adsorbents, the adsorption of nitrogen (N_2) at room temperature is negligible even at pressures above atmospheric. This results in a selectivity that can be considered infinite towards CO_2 in mixtures with N_2.

The viability of amine-functionalized materials for CO_2 adsorption rests on efficient regeneration and recycling. Although a large number of investigations have been devoted to amine-grafted mesoporous silicas (for a review see Harlick and Sayari (2007) and Serna-Guerrero et al. (2008)), little attention was paid to the influence of regeneration conditions on their performance. Currently, the main strategies applied for recycling consist on heating the adsorbent (i.e., temperature swing adsorption) and decreasing the operating pressure (i.e., pressure or vacuum swing adsorption) throughout the regeneration step. Also, a sweeping gas can be used to promote desorption, in which case the outcome during regeneration is not a pure stream of adsorbate but, ideally, a highly concentrated mixture. Some studies involving cyclic CO_2 adsorption reported regeneration by temperature swing [Xu et al., 2002; Franchi et al., 2005; Wang 2007; Drage et al., 2008; Hicks et al., 2008; Yue et al., 2008] or pressure swing [Liu et al., 2007; Chaffee et al., 2007], but no critical analysis of the benefits and shortcomings of each strategy was presented. An interesting work, published by Chaffee et al. [2008] for example, studied vacuum swing adsorption (VSA) cycles in columns packed with amine-grafted SBA-15. In it, a synergistic effect was observed on the purity of the product when the column operated at higher feed temperatures, but since this work focused on VSA, the impact of desorption temperature was not analyzed. In another study, Schladt et al. [2007], reported a thorough analysis on the influence of various regeneration parameters on the performance of amines supported on poly(methyl methacrylate). However, as the amine-bearing species were dispersed on, but not chemically attached to the polymeric support, the temperature used for regeneration was limited to a maximum of 60 °C to prevent evaporation of the supported organic species. Furthermore, there was no analysis of the impact of regeneration conditions on the rate of desorption, an issue of major significance in the design of adsorption systems.

The objective of the present work was to examine the behavior of TRI-PE-MCM-41 as adsorbent for CO_2 at low concentration (i.e. 5%) and ambient temperature over a number of cycles as a function of regeneration conditions. A CO_2 concentration of 5% was chosen to represent some potential applications such as flue gas treatment and closed-circuit breathing systems. This preliminary screening on regeneration conditions using batch experiments can provide a better understanding of the adsorbent on which to build a proper regeneration strategy for dynamic adsorption using fixed bed columns. With the intention to study the

main regeneration strategies mentioned above, the influence of desorption pressure (P_D), desorption temperature (T_D), purge gas flow (F_D), and their corresponding interactions on the performance of the adsorbent was determined by means of a statistical analysis using a 2^3 factorial design [Montgomery, 1983]. With the aid of a statistical model, the extent of the influence of each parameter can be determined in an objective fashion, while permitting the analysis of the interactions between the parameters, which may not be evident from experimental observations. The criteria chosen for the analysis of regeneration conditions were: (i) working adsorption capacity (q) for CO_2, which corresponds to the actual CO_2 uptake in a full cycle when a specific set of regeneration conditions is used, (ii) rate of desorption, a parameter that is critical in the design of adsorption systems as it shows how fast the material is regenerated and, thus, has direct impact on the number and/or size of columns required to achieve a desired productivity, and (iii) the change in adsorption capacity between consecutive cycles, which is associated with the stability of the material under a set of regeneration conditions. While it is acknowledged that the selection of a regeneration configuration in industrial size packed bed adsorption columns depends on a variety of economic and equipment design factors, the rationalization of the influence of operating conditions on the adsorbent performance provides a starting point for such decision. This work is thus a contribution toward the development of a suitable strategy for the regeneration of porous, amine-grafted silica adsorbents, mainly in applications involving low CO_2 partial pressures and adsorption at temperatures close to ambient.

8.2 Materials and Methods

8.2.1 Synthesis and characterization of the adsorbent. The material used in this investigation, namely TRI-PE-MCM-41, consisted of pore-expanded mesoporous silica type MCM-41 (PE-MCM-41) whose surface has been modified through grafting of TRI-silane. The preparation of TRI-PE-MCM-41 has been described in detail elsewhere [Harlick and Sayari, 2007]. Briefly, PE-MCM-41 was prepared in three steps, consisting of (i) synthesis of conventional MCM-41 at 100 °C, followed by (ii) pore expansion via hydrothermal treatment in the presence of dimethyldecylamine at 120 °C for 3 days and (iii) removal of organic template and expander agent by calcination in air at 550 °C for 5h. Surface functionalization was achieved using the following procedure. After drying 1 g of PE-MCM-41 in a vacuum oven

at 120 °C, the material was poured into 150 mL of toluene at 85 °C, subsequently adding 0.3 mL of water and 3 mL of TRI-silane and leaving the mixture under vigorous stirring for 16 h. The solid was then filtered, washed thoroughly with toluene and pentane, and dried in a natural convection oven for 1 h at 100 °C.

The structural properties of TRI-PE-MCM-41 were determined by nitrogen adsorption at -196 °C using a Micromeritics ASAP 2020 volumetric apparatus. Before adsorption, the sample was degassed under vacuum at 150 °C for 5 h. The surface area was calculated using the BET method in the range of relative pressure between 0.05 and 0.3. The pore size distribution was determined using the KJS approach [Kruk et al., 1997], while the pore volume was calculated as the volume of liquid nitrogen adsorbed at a pressure close to $P/P_0 = 1$. The amine content was determined by thermogravimetric analysis (TGA) on a TA Instruments Q-500 apparatus using the weight loss above 200 °C [Harlick and Sayari, 2007].

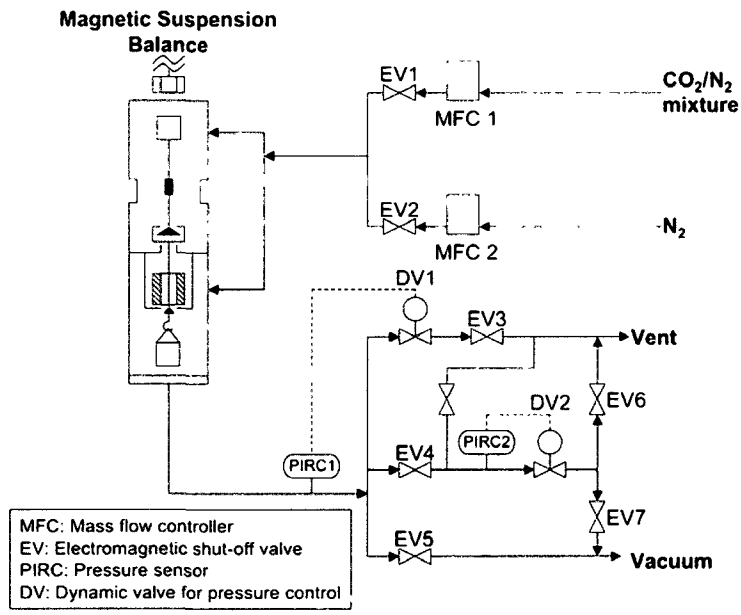

Figure 8.1 Schematic representation of the Rubotherm magnetic microbalance and automated gas dosing system

The adsorption isotherm of CO_2 at room temperature was measured by gravimetry using a Rubotherm magnetic microbalance with automated gas dosing and pressure control. A sample of ca. 1 g of fresh TRI-PE-MCM-41 was loaded and prepared under a flow of UHP

N_2 at 200 °C for 2 h. Subsequently, the temperature of the adsorbent was decreased to 25 °C and the gas flow was switched to pure CO_2 grade 4 at the desired pressure. Enough equilibration time was allowed until no significant change in weight was recorded, being typically 2 h. In an analogous manner, the adsorption isotherm of N_2 at room temperature was measured.

8.2.2 Cyclic adsorption of CO_2. Cyclic adsorption and desorption measurements of CO_2 on TRI-PE-MCM-41 were performed using a Rubotherm magnetic microbalance with automated gas dosing, represented schematically in Figure 8.1. This setup allows a gas stream to be directed to a 150 mL measurement chamber under controlled conditions of flow and pressure. Additionally, the temperature of the sample chamber was controlled via a heating system. In a typical experiment, the sample was first exposed to UHP nitrogen at 10 or 50 mL min^{-1} at 70 or 150 °C. Subsequently, the sample was cooled to 25° C and the feed gas was switched to a mixture of 5% CO_2 balance nitrogen flowing at 50 mL min^{-1}. The value of q was measured from the weight gain of the sample after a 2 h exposure to the CO_2 mixture, since preliminary studies showed that, after this time, no weight change is observed and, thus, equilibrium can be assumed. Notice that it was established in separate experiments that the amount of nitrogen adsorbed by TRI-PE-MCM-41 under these conditions (i.e., 1 atm total pressure at 25 °C) is negligible [Belmabkhout and Sayari, 2009]. The sample was then regenerated for 2 h in the presence of nitrogen under a desired set of conditions as listed in Table 8.1. This procedure was repeated over 5 CO_2 adsorption-regeneration cycles for each set of regeneration conditions. The weight change profile recorded by the instrument also allowed the determination of desorption rate, defined as the change of CO_2 desorbed from the sample with respect to time. The arithmetic mean of the values of q over the five cycles was considered as the average adsorption capacity (q_{AVG}), and used in the statistical analysis. Similarly, averages of the maximum rate of desorption (r_{AVG}) and the variation of adsorption capacity between consecutive cycles (Δq_{AVG}) were calculated.

The statistical analysis was performed using a factorial design varying the parameters P_D, T_D and F_D whose upper and lower level values were set based on the following considerations: (i) to avoid thermal degradation of the adsorbent, the upper level of T_D was set at 150 °C as preliminary studies using TGA showed that degradation of the organic

species starts at ca. 250 °C, (ii) the lower level value of P_D was set at 0.1 bar to mimic typical industrial vacuum swing adsorption processes, and (iii) the upper level value of F_D = 50 mL min^{-1}, representing a feed/purge gas flow ratio of 1. Under these extreme upper values of T_D and F_D, it is expected to make evident the influence, if any, of each parameter. Although not included in the statistical analysis, it should be mentioned that in the case of regeneration at 1 bar, additional experiments were performed using a value of F_D = 10 mL min^{-1} (feed/purge gas flow ratio of 5) in order to provide a small driving force to remove the desorbing CO_2.

Data analysis was performed using a linear model to describe the influence of each regeneration condition and their interactions on the observed response. Such model has the following form:

$$Y = \beta_0 + \beta_1 T_D + \beta_2 P_D + \beta_3 F_D + \beta_4 T_D P_D + \beta_5 T_D F_D + \beta_6 P_D F_D \quad (1)$$

where Y is the measured response, i.e., q_{AVG}, r_{AVG} or Δq_{AVG} and the values of β represent the coefficients of the linear model. For the present analysis, the null hypothesis (H_0) has the form:

$$H_0: \beta_0=0,\ \beta_1=0,\ \beta_2=0,\ \beta_3=0,\ \beta_4=0,\ \beta_5=0,\ \beta_6=0$$

where H_0 represents a negligible influence of all regeneration conditions and their interactions. To establish whether a parameter is significant, a p-value test with a 95% level of confidence was applied on the experimental results. The statistical analysis was performed using MiniTab® v.15.1 statistical software. It should be noted that the statistical model produced is not meant to model an adsorption-desorption process but to determine the impact of each β coefficient on the adsorbent performance.

Since the statistical analysis showed that T_D was the most dominant factor affecting q_{AVG} and r_{AVG} (*vide infra*), an additional set of experiments using P_D = 0.1 bar and F_D = 50 mL min^{-1} under various regeneration temperatures ranging from 25 to 150 °C was carried out. The purpose of these experiments was to analyze specifically the effect of temperature on the performance of the material.

Table 8.1 Factorial design for the analysis of regeneration conditions and values of q_{AVG}, r_{AVG} and Δq_{AVG}

Experiment	T_D (°C)	P_D (bar)	F_D (mL min^{-1})	q_{AVG} (mmol g^{-1})	r_{AVG} (mmol g^{-1} s^{-1})	Δq_{AVG} (mmol g^{-1})
1	70	0.1	0	0.54 ± 0.06	$1.62 \times 10^{-4} \pm 1.4 \times 10^{-5}$	2.81×10^{-2}
2	150	0.1	0	1.91 ± 0.03	$9.61 \times 10^{-4} \pm 3.8 \times 10^{-5}$	1.77×10^{-2}
3	70	1	0	0.00	0.00	0.00
4	150	1	0	0.03	0.00	0.00
5	70	0.1	50	1.69 ± 0.02	$3.06 \times 10^{-4} \pm 2.4 \times 10^{-5}$	0.95×10^{-2}
6	150	0.1	50	1.95 ± 0.04	$9.82 \times 10^{-4} \pm 1.1 \times 10^{-5}$	2.00×10^{-2}
7	70	1	50	1.05 ± 0.01	$1.97 \times 10^{-4} \pm 3.7 \times 10^{-5}$	0.27×10^{-2}
8	150	1	50	1.94 ± 0.01	$9.75 \times 10^{-4} \pm 5.5 \times 10^{-5}$	0.55×10^{-2}

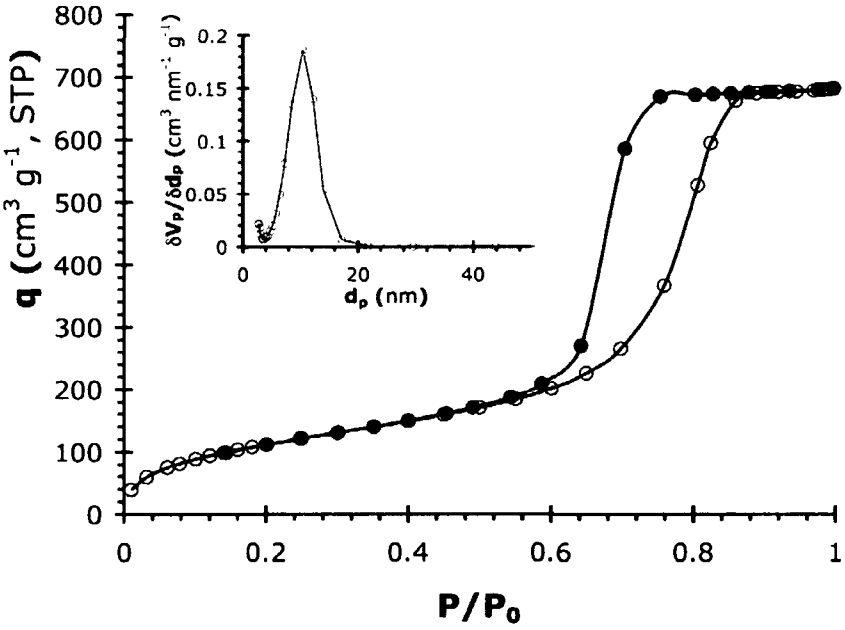

Figure 8.2 Nitrogen adsorption (open symbols) and desorption (closed symbols) isotherm and pore size distribution (inset) for TRI-PE-MCM-41

8.3 Results and Discussion

As shown in Figure 8.2, the nitrogen adsorption isotherm for TRI-PE-MCM-41 was of Type IV according to the IUPAC classification, which is characteristic of mesoporous

materials. TRI-PE-MCM-41 maintained a porous structure after incorporation of amines with a mean pore size of 9.6 nm and a pore volume of 1.05 cm^3 g^{-1}. In addition, the sample exhibited a surface area of 429 m^2 g^{-1}. These structural properties are highly desirable, as the occurrence of open pore structure has been associated with high rates of adsorption and efficient use of the functional amine groups [Harlick and Sayari, 2007; Serna-Guerrero et al., 2008]. The content of amine groups as determined by TGA was ca. 7.8 mmol per gram of adsorbent. Such high amine content, in combination with a favorable pore structure, produced a material with promising characteristics for CO_2 capture.

Figure 8.3 shows the adsorption isotherms of CO_2 and N_2 on TRI-PE-MCM-41 at 25 °C. The adsorbent offers a high CO_2 uptake at low pressures, likely as a result of the strong compatibility between CO_2 and the amine functional groups and the accessibility of such functional groups due to the aforementioned open pore structure. With respect to N_2, its uptake can be considered negligible, as the adsorption capacity recorded was below the accuracy limits of the instrument. It is thus reasonable to say that there is no competitive adsorption between the components of the streams used in this work.

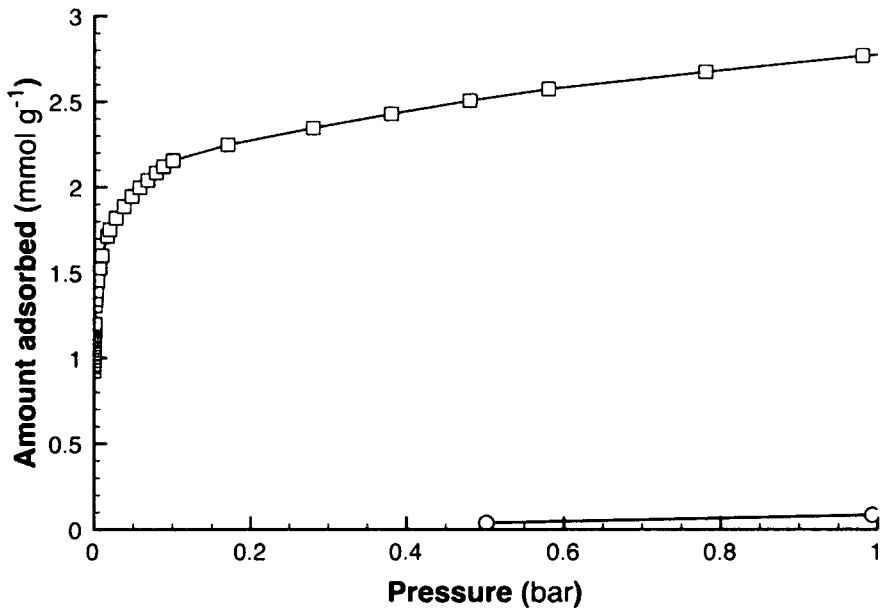

Figure 8.3 CO_2 (squares) and N_2 (circles) adsorption isotherms on TRI-PE-MCM-41 at 25 °C

8.3.1 Influence of regeneration parameters. As an illustrative example, Figure 8.4 shows a typical profile of weight change with respect to time as recorded by the Rubotherm microbalance under regeneration at T_D = 150 °C, P_D = 1 bar and F_D = 50 mL min^{-1}. A steep weight increase during the adsorption step was observed, indicative of a fast adsorption. Figure 8.4 also shows the derivative of weight as a function of time, from which the rates of adsorption and desorption can be monitored throughout the process. The high rate of adsorption has already been discussed in previous contributions [Harlick and Sayari, 2007; Serna-Guerrero et al., 2008; Belmabkhout and Sayari, 2008] where it was attributed to a combination of high amine loading and an open-pore structure, resulting in a large number of readily available functional groups. Table 8.1 shows the values of q_{AVG}, r_{AVG} and Δq_{AVG} determined from such measurements and used in the statistical analysis.

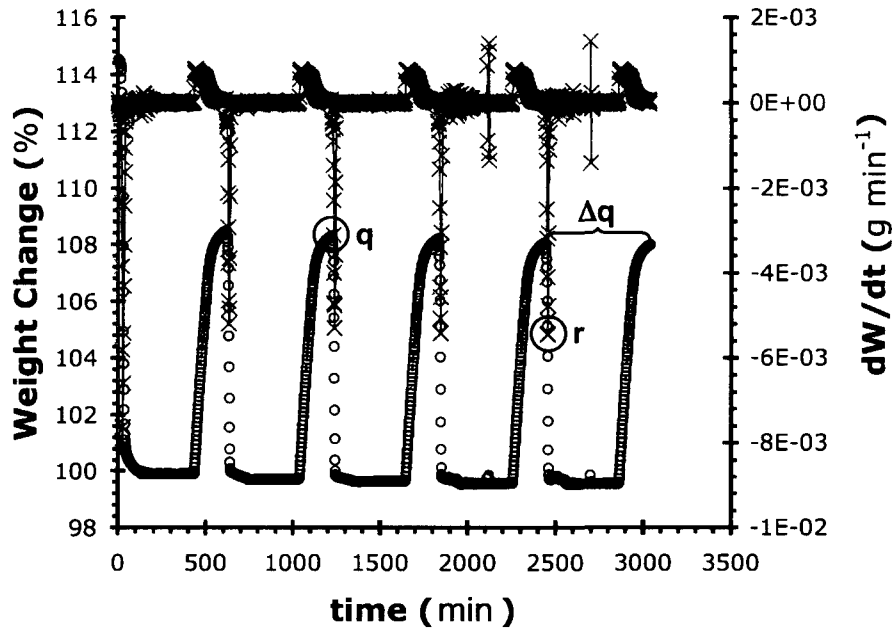

Figure 8.4 Weight change (circles) and weight derivative (crosses) profiles as a function of time for regeneration at T_D = 150 °C, P_D = 1 bar and F_D = 50 mL min^{-1}

Figure 8.5 shows the values of q for each cycle under the different regeneration conditions listed in Table 8.1. It is seen that, within the range of conditions studied, the regeneration of TRI-PE-MCM-41 at 150 °C resulted in the highest values of q. Further, the values of q were remarkably constant at 1.9 mmol g^{-1} whenever the upper T_D level was used,

regardless of the levels of P_D and F_D, the only exception being at P_D = 1 bar and F_D = 0. This is an interesting finding since the use of vacuum is commonly associated with improved regeneration efficiency, but under high T_D, there was no apparent benefit when low P_D is used. A possible explanation is that the energy provided by heating at 150 °C is sufficient to effectively regenerate the adsorbent, hence making the use of an additional driving force, such as vacuum, unnecessary. In contrast, at the lower level of T_D (i.e. 70 °C), values of q ranging from ca. 0.5 to ca. 1.7 mmol g^{-1} were observed for different levels of P_D and F_D. At T_D = 70 °C, the values of q obtained under vacuum regeneration with no purge flow were comparatively lower than the case where F_D = 50 mL min^{-1}, showing a positive impact of purge gas on q. It is also seen that only when desorption occurs at 70 °C, regeneration under vacuum offered a comparative advantage, specifically when used in combination with the upper level of purge gas flow. Indeed, under such conditions, the adsorption capacity obtained was only about 13% lower than that obtained under regeneration at 150 °C.

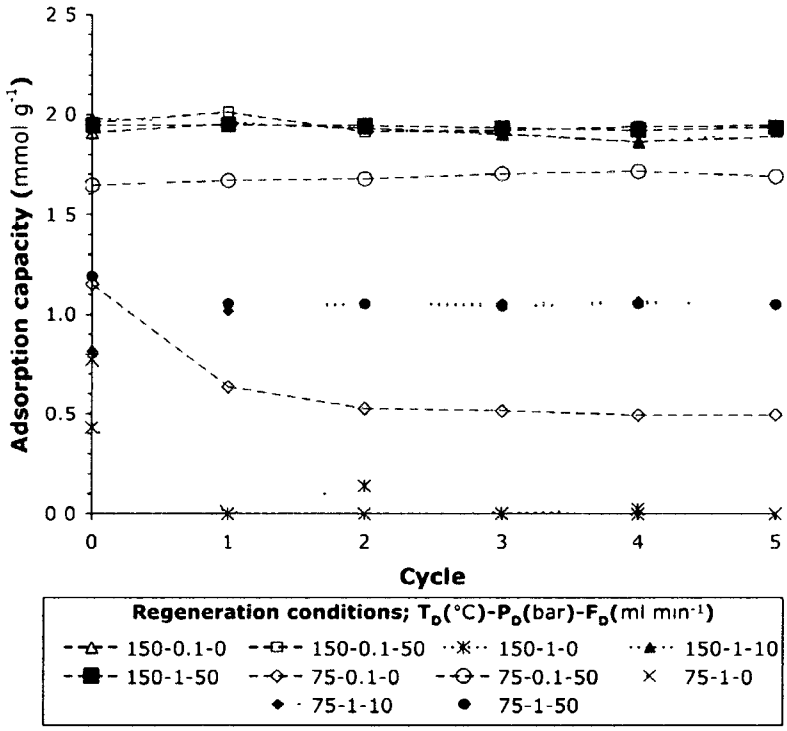

Figure 8.5 Working adsorption capacity of TRI-PE-MCM-41 for 5% CO_2 over several cycles under various regeneration conditions

A special case occurred when P_D = 1 bar and F_D = 0, as q decreased significantly after the first cycle, likely as a result of an incomplete regeneration due to the absence of a driving force capable of removing any desorbed CO_2. Nevertheless, it was also found that, as long as a minimum flow of purge gas was used (e.g. 10 mL min^{-1}), q was hardly dependent on the nitrogen flow rate, suggesting that efficient regeneration may occur even at low sweeping gas flow.

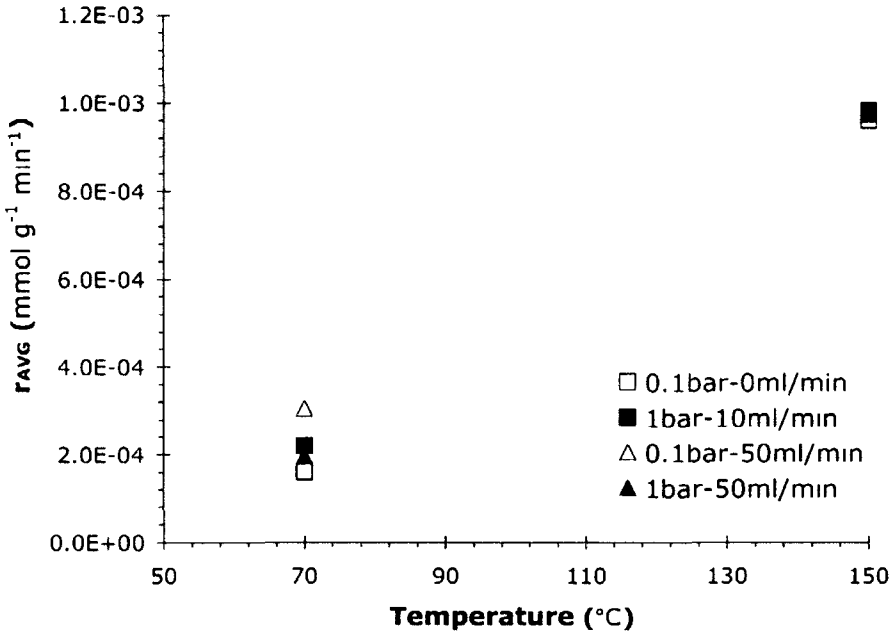

Figure 8.6 Maximum average rate of desorption of CO_2 from TRI-PE-MCM-41 under various regeneration conditions

Figure 8.6 shows r_{AVG} as a function of temperature for the different sets of regeneration conditions used. As seen, r_{AVG} is considerably higher when the adsorbent is regenerated at 150 °C vs. 70 °C. It is interesting to observe that, similarly to q, at T_D = 150 °C, the two other regeneration conditions, i.e., P_D and F_D, did not seem to have a significant impact on r_{AVG}. At 70 °C, the values of r_{AVG} are somewhat scattered, which suggests that, at low T_D the influence of the other parameters may become considerable, in an analogous manner as observed for q. Using a statistical analysis will determine whether any of these variations is actually related to the levels of the parameters chosen.

To shed further light on the observations presented above, a statistical analysis of the results was applied, in order to provide an unbiased assessment on the importance of each parameter. The values of the coefficients for the statistical model obtained for each response are presented in Table 8.2. The positive β_i values associated with T_D in the cases of q_{AVG} and r_{AVG} are consistent with the above-mentioned finding that the use of heat results in higher values of q_{AVG} and faster desorption rates. On the other hand, the β_i coefficients associated with P_D were negative, indicating that q_{AVG} and r_{AVG} tend to increase when regeneration is performed under vacuum. With respect to the statistical model for Δq_{AVG}, it is seen that the coefficient associated with F_D has a negative value, indicating that low purge gas flows can potentially affect the stability of the adsorbent, perhaps due to incomplete regeneration, as was observed when $F_D = 0$.

Table 8.2 Values of the β_i coefficients for the statistical model of q_{AVG}, r_{AVG} and Δq_{AVG} as a function of the regeneration parameters T_D, P_D and F_D and their interactions

	q_{AVG}		r_{AVG}		Δq_{AVG}	
Term	β_i[(a)]	P-value[(b)]	β_i[(a)]	P-value[(b)]	β_i[(a)]	P-value[(b)]
Constant	-1.3751	0.005	-6×10^{-4}	0.021	0.0128	0.222
T_D	0.5533	0.013	4.34×10^{-4}	0.029	0.0027	0.663
P_D	-0.1494	0.048	-0.02×10^{-4}	0.920	-0.0060	0.419
F_D	0.2821	0.025	0.74×10^{-4}	0.165	-0.0341	0.598
T_D*P_D	0.1472	0.048	0.65×10^{-4}	0.185	0.0027	0.663
T_D*F_D	0.2679	0.027	0.11×10^{-4}	0.664	0.0006	0.923
P_D*F_D	0.0135	0.442	0.33×10^{-4}	0.343	0.0007	0.907

(a) β_i refers to the coefficients associated with the parameters or combinations thereof in Equation (1)

(b) A p-value of less than 0.05 represents a statistically relevant term.

The p-values in Table 8.2 provide a simple mean to compare the importance of the variables under study and their interactions. As the confidence level was set to 95%, a p-value of 0.05 represents the limit on whether the effect of a regeneration condition is significant or not, i.e., when the value of the standardized effect is lower than 0.05, it is deemed significant, while higher values represent a variable that is not statistically relevant. Analysis of q_{AVG} shows that T_D is the most influential parameter, followed by F_D. Thus, under the conditions used in this study, heating can be regarded as the main condition required for desorption, prompting an efficient release of adsorbed CO_2, particularly at the high level of T_D. The influence of purge gas flow on q is associated with the need of a sweeping gas to provide a driving force for the removal of the desorbing CO_2, particularly when P_D = 1 bar since the adsorption capacity was lost when F_D = 0. The flow of sweeping gas was also useful during regeneration under vacuum, as it evidently enhanced the values of q at T_D = 70 °C. It should be noted, however, that a low sweeping gas flow may suffice, since the values of q observed with the upper value of F_D were similar to those corresponding to F_D = 10 mL min^{-1}.

Interestingly, it is seen that the standardized effect of P_D is close to the limit set for relevance, suggesting that, although small, under certain conditions (e.g., low T_D) it has an impact on the working adsorption capacity of the material. These results show that the vacuum level used in this work provided only a limited driving force to remove the CO_2 adsorbed on TRI-PE-MCM-41, most likely attached by strong chemical bonds. This analysis is particularly important if PSA is considered, since q_{AVG} was enhanced to a lesser extent when regenerating at low P_D compared to high T_D and thus, decisions over the process design should depend on whether it is more expensive to heat a column during regeneration and obtain a high productivity or to provide vacuum and have a smaller production of high purity gas. It is interesting to notice that the interaction between P_D and T_D was also statistically significant, representing a synergistic effect when vacuum and heat are applied. From an operating point of view, this interaction can be exploited to improve the adsorbent performance by using vacuum when regeneration is carried out at low T_D. For example, it is conceivable to use a T_D lower than 150 °C to decrease the heating energy consumption, combined with regeneration under vacuum to improve the working adsorption capacity.

Table 8.2 also shows that, as far as r_{AVG} is concerned, the only parameter whose influence can be considered important is T_D. This is consistent with data shown in Figure 8.6, where it appears evident that when T_D = 150 °C, a much higher r_{AVG} was obtained. On the other hand, the aforementioned scattering of r_{AVG} values at the lower level of T_D does not appear to have a statistically relevant correlation with any parameter.

The last factor to be analyzed is the stability of the adsorbent, represented by the average change of the working adsorption capacity between consecutive cycles (Δq_{AVG}). From the values of q for various adsorption-desorption cycles presented in Figure 8.5, there is no apparent variation of Δq_{AVG} regardless of regeneration conditions. The statistical analysis provides further support to whether the variation of adsorption capacity is significant and if a particular factor affects the stability of the material. As seen in the p-test value in Table 8.2, none of the parameters under study exhibited a significant effect on Δq_{AVG}. Indeed, the standardized effects of all parameters are far above the established limit of significance. The negligible influence of F_D, P_D or T_D on the adsorbent stability is a positive finding, suggesting that the regeneration conditions used in this study may be applied for more extensive cycling processes.

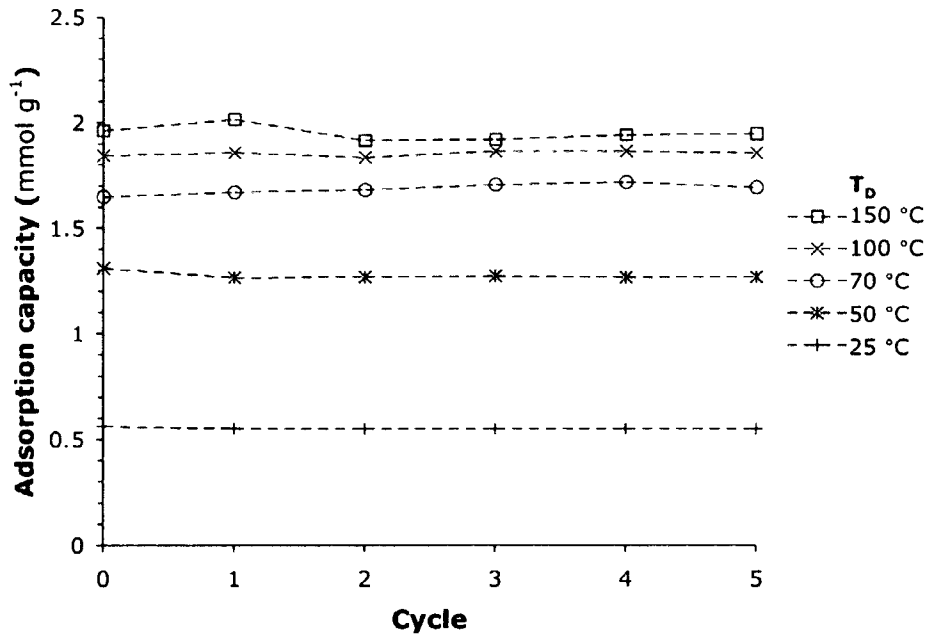

Figure 8.7 Working adsorption capacity of TRI-PE-MCM-41 for 5% CO_2 over various cycles under different regeneration temperatures with P_D = 0.1 bar and F_D = 50 mL/min

8.3.2 Further studies on the influence of T_D. Since T_D was found to be the most influential parameter in the performance of the adsorbent, it was of interest to explore in more depth the effect of this parameter on the behavior of TRI-PE-MCM-41. Hence, a series of experiments were performed using desorption temperatures of 25, 50, 70, 100 and 150 °C. The values of P_D and F_D in these experiments were 0.1 bar and 50 mL min^{-1}, respectively, as this combination afforded the most favorable q_{AVG} in the above described experiments using T_D = 70 °C. Figure 8.7 shows values of q along various cycles for the different regeneration temperatures confirming that T_D is a determining factor. Under these conditions, regeneration at 25 °C is equivalent to using pressure swing regeneration conditions alone and it is seen to result in a considerably low q. This suggests that vacuum is not sufficient and additional energy is required to properly regenerate TRI-PE-MCM-41, probably as a result of strong CO_2-amine interactions, making a TVSA-configuration more appropriate. Moreover, quite similarly to the previous results, q does not seem to be notably affected throughout the adsorption-desorption cycling.

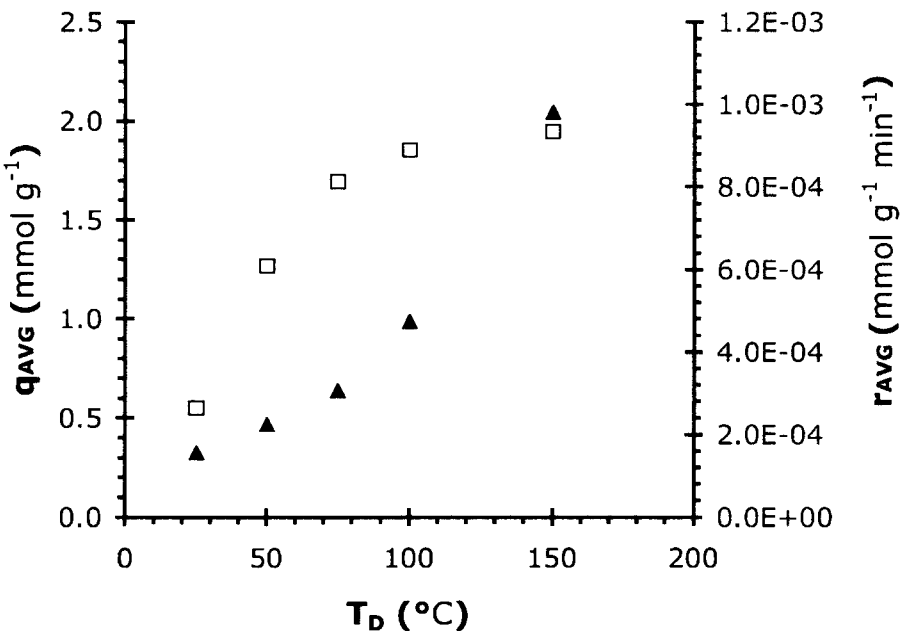

Figure 8.8 Average working adsorption capacity (squares) and average maximum rate of desorption (triangles) of CO_2 on TRI-PE-MCM-41 as a function of T_D

Although it was found that T_D has an important effect on q_{AVG} (Figure 8.8), it appears less dramatic within the range of 70 to 150 °C than at lower regeneration temperatures. Indeed, q_{AVG} after regeneration at 70 and 150 °C was of 1.69 and 1.95 mmol g^{-1}, respectively, corresponding to a ca. 13% variation. This is an interesting finding as it shows that TRI-PE-MCM-41 can be efficiently regenerated using temperatures as low as 70 °C, while zeolites typically require higher temperatures for regeneration, particularly when moisture is present.

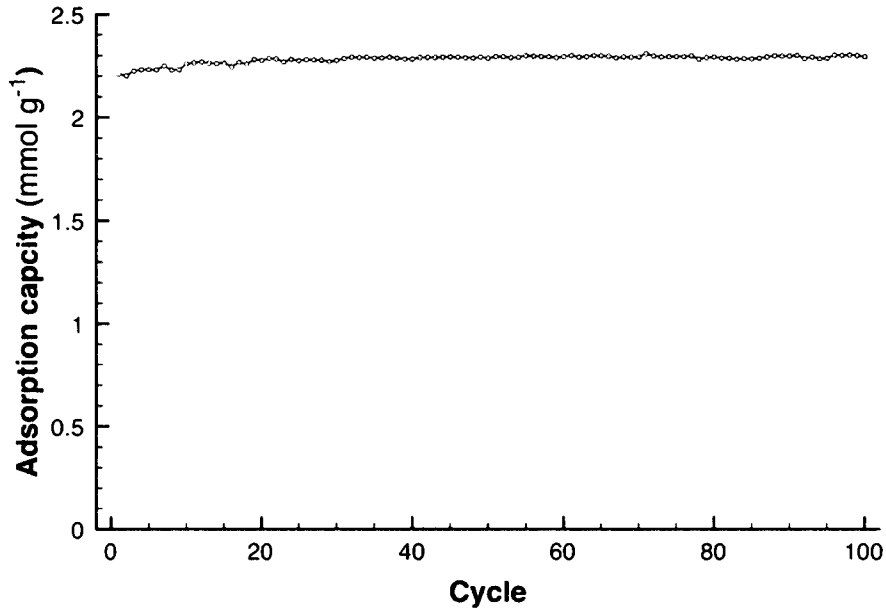

Figure 8.9 Working adsorption capacity of TRI-PE-MCM-41 for pure CO_2 over various cycles under regeneration with T_D = 70 °C, P_D = 0.1 bar and F_D = 50 mL min^{-1}

In contrast to q_{AVG}, r_{AVG} decreased considerably between 150 and 100 °C from 9.82×10^{-4} to 4.75×10^{-4} mmol g^{-1} min^{-1}, and even less at lower T_D, as can be observed in Figure 8.7. This is in line with the strong influence of T_D on r_{AVG} predicted by the statistical analysis. Based on these results, it is inferred that, in addition to its consistently higher q, a determining factor supporting the use of temperature swing regeneration conditions is the favorable desorption kinetics. As we reported in earlier contributions [Serna-Guerrero et al., 2008; Belmabkhout and Sayari, 2009], chemical adsorption on TRI-PE-MCM-41 is dominant at low CO_2 concentrations, while at higher partial pressures physical adsorption also occurs.

Because of the occurrence of a different adsorption mechanism at higher pressure, our findings may apply only at low CO_2 concentrations, where chemical interactions between CO_2 and the amine functionality are predominant.

To further demonstrate the high stability of TRI-PE-MCM-41, we carried out 100 adsorption-desorption cycles. The regeneration was carried out under vacuum at 70 °C since this combination afforded a relatively high q, with low heating requirements. Figure 8.9 shows that TRI-PE-MCM-41 exhibits a remarkable stability, as the value of q corresponding to a q_{AVG} of 2.28 mmol g^{-1}, remained constant within 1% over the entire series of 100 cycles.

8.4 Conclusions

This study provided a first screening of the performance of TRI-PE-MCM-41 as an adsorbent for CO_2 under different regeneration conditions (i.e., T_D, P_D and F_D) over several cycles. While the statistical analysis suggests that all the parameters studied have an influence on the CO_2 working adsorption capacity at room temperature, T_D had the strongest impact, likely as a result of the prevailing chemical interaction between CO_2 and amine groups. More specifically, at high T_D, e.g. 150 °C, the desorption temperature becomes the dominant factor, with little effect for P_D and F_D. Quite importantly, TRI-PE-MCM-41 was found to be stable under all the conditions used in this study. Regeneration using vacuum only does not appear as an attractive approach, particularly when no purge gas flow and low temperature are used during regeneration. In contrast, the use of regeneration temperatures of 70 °C and higher seems appropriate, as high T_D not only produced the highest capacity for CO_2, but also resulted in a significantly faster desorption.

References

Y. Belmabkhout, M. Frère, G. De Weireld, High-pressure adsorption measurements. A comparative study of the volumetric and gravimetric methods. Measur. Sci. Technol. 15 (2004) 848

Y. Belmabkhout, A. Sayari, Effect of Pore Expansion and Amine Functionalization of Mesoporous Silica on CO_2 Adsorption over a wide range of conditions. Adsorption 15 (2009) 318

F. Brandani, D.M. Ruthven, The Effect of Water on the Adsorption of CO_2 and C_3H_8 on Type X Zeolites. Ind. Eng. Chem. Res. 43 (2004) 8339

P. Birbara, T. Filburn, H. Michels, T. Nalette, Sorbent System and Method for Absorbing Carbon Dioxide (CO_2) from the Atmosphere of a Closed Habitable Environment. US Patent 6,364,938, 2002

A.L. Chaffee, G.P. Knowles, Z. Liang, J. Zhang, P. Xiao, P.A. Webley, CO_2 capture by adsorption: materials and process development. Int. J. Greenhouse Gas Control 1 (2007) 11

S. Couck, J.F.M. Denayer, G.V. Baron, T. Rémy, J. Gascon, F. Kapteijn, An amine-functionalized MIL-53 metal-organic framework with large separation power for CO_2 and CH_4. J. Am. Chem. Soc. 131 (2009) 6326

T.C. Drage, A. Arenillas, K.M. Smith, C.E. Snape, Thermal stability of polyethylenimine based carbon dioxide adsorbents and its influence on selection of regeneration strategies. Micropor. Mesopor. Mater. 116 (2008) 504

R.S. Franchi, J.P.E. Harlick, A. Sayari, Applications of pore-expanded mesoporous silica. 2. Development of a high-capacity, water-tolerant adsorbent for CO_2. Ind. Eng. Chem. Res. 44 (2005) 8007

M.L. Gray, K.J. Champagne, Y. Soong, T. Filburn, High Capacity Immobilized Amine Sorbents. US Patent 7,288,136, 2007

M.L. Gray, K.J. Champagne, D. Fauth, J.P. Baltrus, H. Pennline, Performance of Immobilized Tertiary Amine Solid Sorbents for the Capture of Carbon Dioxide. Int. J. Greenhouse Gas Control 2 (2008) 3

J.C. Hicks, J.H. Drese, D.J. Fauth, M.L. Gray, G. Qi, C.W. Jones, Designing adsorbents for CO_2 capture from flue gas-hyperbranched aminosilicas capable of capturing CO_2 reversibly. J. Am. Chem. Soc. 130 (2008) 2902

P.J.E. Harlick, A. Sayari, Applications of pore-expanded mesoporous silica. 5. Triamine grafted material with exceptional CO_2 dynamic and equilibrium adsorption performance. Ind. Eng. Chem. Res. 46 (2007) 446

C.W. Jones, J.C. Hicks, D.J. Fauth, M. Gray, Structures for Capturing CO_2, Methods of Making the Structures and Methods for Capturing CO_2. US Patent application 20070149398, 2007

M. Kruk, M. Jaroniec, A. Sayari, Application of large pore MCM-41 molecular sieves to improve pore size analysis using nitrogen adsorption measurements. Langmuir 13 (1997) 6267

X. Liu, L. Zhou, X. Fu, Y. Sun, W. Su, Y. Zhou, Adsorption and Regeneration Study of the Mesoporous Adsorbent SBA-15 Adapted to the Capture/Separation of CO_2 and CH_4, Chem. Eng. Sci. 62 (2007) 1101

X. Ma, X. Wang, C. Song, "Molecular basket" sorbents for separation of CO_2 and H_2S from various gas streams. J. Am. Chem. Soc. 131 (2009) 5777

D.C. Montgomery, Design and Analysis of Experiments, 2nd ed. John Wiley and sons New York, 1983

G. Olah, A. Goepert, S. Meth, S. Prakash, Nano-Structure Supported Solid Regenerative Polyamine and Polyamine Polyol Adsorbents for the Separation of Carbon Dioxide from Gas Mixtures Including the Air. Int. Patent application WO 2008/021700 A1, 2008

J.C. Santos, F.D. Magalhaes, A. Mendes, Contamination of zeolites used in oxygen production by PSA: effects of water and carbon dioxide. Ind. Eng. Chem. Res. 47 (2008) 6197

M.J. Schladt, T.P. Filburn, J.J. Helble, Supported amine sorbents under temperature swing absorption for CO_2 and moisture capture. Ind. Eng. Chem. Res. 46 (2007) 1590

R. Serna-Guerrero, E. Da'na, A. Sayari, New Insights into the interactions of CO_2 with amine-functionalized silica. Ind. Eng. Chem. Res. 47 (2008) 9406

L. Wang, L. Ma, A. Wang, Q. Liu, T. Zhang, CO_2 adsorption on SBA-15 modified by aminosilane. Chinese J. Catal. 28 (2007) 805

X. Xu, C. Song, J.M. Andresen, B.G. Miller, A.W. Scaroni, Novel polyethylenimine-modified mesoporous molecular sieve of mcm-41 type as high-capacity adsorbent for CO_2 capture. Energy Fuels 16 (2002) 1463

M.B. Yue, L.B. Sun, Y. Cao, Y. Wang, Z.Y. Wang, J.H. Zhu, Efficient CO_2 capturer derived from as-synthesized mcm-41 modified with amine. Chem. Euro. J. 14 (2008) 3442

Chapter 9

Triamine-grafted pore-expanded mesoporous silica for CO_2 scrubbing in closed-circuit breathing systems

Abstract

This work presents for the first time a study on the application of triamine-grafted mesoporous silica, referred to as TRI-PE-MCM-41, for metabolic CO_2 scrubbing in closed-circuit breathing systems. In the first place, a comparative study with a benchmark absorbent, namely soda lime, is presented. CO_2 uptake in a fixed bed column was measured at various flow rates and compositions. It was found that the presence of a volatile anesthetic molecule probe did not affect significantly the CO_2 removal capacity for either TRI-PE-MCM-41 or soda lime. Although soda lime presented a significantly higher CO_2 uptake than TRI-PE-MCM-41, it was negatively affected by high flow rates, being reduced from 12.7 to 6.6 mmol g^{-1} under flow rates of 15 and 50 mL min^{-1}, respectively. On the other hand, under a stream of 10% CO_2 balance air, TRI-PE-MCM-41 presented capacities of 2.49 to 1.89 mmol g^{-1} corresponding to flow rates of 15 and 50 mL min^{-1}, respectively. The comparatively lower impact of high flow rates to the working adsorption capacity of TRI-PE-MCM-41 was associated with its fast adsorption kinetics. In addition, the performance of TRI-PE-MCM-41 in a commercial closed-circuit breathing system under real operating conditions is presented. Under the current configuration, lower than expected adsorption capacities were measured. A discussion regarding potential reasons for such underperformance, along with suggestions for future improvement are included.

9.1 Introduction

Closed-circuit breathing systems (CCBSs) are setups used to supply breathing gases in confined spaces or hazardous environments. The main objective of CCBSs is to recycle unused and exhaled gases for cost saving and size reduction, as the human respiratory system uses only a fraction of the oxygen inhaled. Currently, CCBSs find various applications, including life support in confined spaces such as aerospace and submarine transportation [Filburn et al., 2001; Filburn et al, 2005; Hwang et al., 2008], breathing equipment for

mining, diving and rescue [Moore 2007] and medical instruments such as anesthesia delivery apparatuses [Baum 1996]. To make use of the recycled gases, it is necessary to remove any exhaled CO_2 from the breathing loop, as it may quickly reach life-threatening concentrations. CO_2 scrubbing in CCBS is nowadays performed using a variety of solid absorbents, among which soda lime is probably the most popular [Baum and Woehlck 2003]. Soda lime consists mainly of calcium hydroxide often mixed with strong bases such as sodium and potassium hydroxide, with compositions depending on each proprietary formulation. The reaction pathway between soda lime and CO_2 whose net result is the transformation of calcium hydroxide into calcium carbonate with CO_2 fixation, is presented in Scheme 9.1, a process leading to the formation of calcium carbonate as byproduct. Such a transformation is mediated by the strong alkaline bases due to their high reactivity.

$$CO_2 + H_2O \longrightarrow H_2CO_3$$
$$H_2CO_3 + 2NaOH \text{ (or KOH)} \longrightarrow Na_2CO_3 \text{ (or } K_2CO_3) + 2H_2O$$
$$Na_2CO_3 \text{ (or } K_2CO_3) + Ca(OH)_2 \longrightarrow CaCO_3 + 2NaOH \text{ (or KOH)}$$

Scheme 9.1 Reaction pathway of CO_2 with soda lime

Although CO_2 scrubbing in CCBSs with soda lime has been in use for several decades, its popularity is mainly attributed to its low cost, while some concerns about its application have been raised in recent years. From an environmental point of view, for example, its use represents large amounts of solid waste since exhausted soda lime is discarded after a single use. From the operating point of view, it has been reported to present an inadequate response to erratic or high breathing rates, such as those experienced by users under stressful conditions. With respect to its application in anesthesia delivery units (ADU), further concerns have been raised as it was observed that the strong bases contained in soda lime promote the degradation of some volatile anesthetics into toxic compounds, including carbon monoxide [Baxter et al., 1998; Wissing et al., 2001; Keijzer et al., 2007] and a potentially hazardous derivative known as Compound A (i.e., pentafluoroisopropenyl fluoromethyl) [Frink et al., 1996; Bito et al., 1998; Baum and Woehlck 2003; Keijzer et al., 2007]. To prevent anesthetics degradation, novel formulations of soda lime without strong

bases have been marketed, although they reportedly present a comparatively lower absorption capacity than typical soda lime [Kharasch et al., 2002; Kobayashi et al., 2004].

To address the aforementioned drawbacks, a number of alternatives have been proposed, among which adsorption separation has attracted particular attention due to its potential to produce high purity air streams while being considered a low energy demanding process. One of the main challenges of adsorption separation technologies is finding a reusable adsorbent with high capacity and selectivity. In the past, some commercial adsorbents such as molecular sieves have been proposed, since their relatively high CO_2 adsorption capacity at low partial pressure is appropriate for CCBS applications [McNeirney, 2007]. However, it has been demonstrated that molecular sieves adsorb moisture preferentially, resulting in a drastic decrease in adsorption capacity even at low relative humidity (RH) [Brandani and Ruthven, 2004]. Thus, zeolites require an intensive dehydration of the gas streams, adding complexity to CCBS. Addition of a dehydration step would likely result in a larger size of the setup and, if a non-reusable drier were used, further production of solid waste.

In recent years, efforts have been placed on using amine-functionalized materials as CO_2 adsorbents, inspired by the widely used CO_2 scrubbing process using liquid amine solutions. As a result, a variety of amines dispersed on polymethylmethacrylate beads have been proposed as CO_2 adsorbents in breathing systems [Filburn et al., 2001; Filburn et al, 2005]. While amine-dispersed adsorbents reportedly offer a high adsorption capacity and tolerance to moisture, their stability throughout several adsorption-desorption cycles is limited, as the amine-functional groups are not strongly attached to the solid support. In order to produce a more stable adsorbent, amine-bearing molecules can be incorporated via chemical binding. In particular, amine-grafted mesoporous silica exhibited promising characteristics in terms of CO_2 adsorption capacity and rate of adsorption. Our research group developed an amine-functionalized mesoporous adsorbent, namely TRI-PE-MCM-41 with promising characteristics for the removal of CO_2 at concentrations relevant to CCBS applications [Harlick and Sayari, 2007; Belmabkhout and Sayari, 2009]. TRI-PE-MCM-41 offers high amine loading accompanied by large pore sizes, resulting in a high concentration of readily available amine groups. It has also been demonstrated that the reaction mechanisms between CO_2 and supported amines are analogous to those of liquid amine

solutions (Scheme 9.2), resulting in an enhanced capacity in humid streams due to a more favorable stoichiometry [Serna-Guerrero et al., 2008]. Additionally, this material presents a high selectivity toward CO_2 in mixtures including nitrogen, methane, hydrogen and air [Belmabkhout et al., 2010; Serna-Guerrero et al, 2010a]. TRI-PE-MCM-41 has also shown a high cyclic stability and can be regenerated under mild conditions, suggesting that its use is economically feasible [Sayari and Belmabkhout, 2010; Serna-Guerrero et al., 2010a; Serna-Guerrero et al., 2010b].

$$2(RNH_2) + CO_2 \longleftrightarrow \underset{\text{carbamate}}{RNHCO_2^- \; RNH_3^+}$$

$$RNH_2 + CO_2 + H_2O \longleftrightarrow \underset{\text{bicarbonate}}{RNH_3^+ \; HCO_3^-} \xleftrightarrow{RNH_2} \underset{\text{carbonate}}{(RNH_3^+)_2 \; CO_3^{2-}}$$

Scheme 9.2 Reaction mechanisms of CO_2 with amines in dry and humid streams

Due to the aforementioned characteristics of TRI-PE-MCM-41, it is of interest to evaluate its performance as CO_2 scrubber in CCBS. This work presents a study of CO_2 adsorption on TRI-PE-MCM-41 under conditions relevant to CCBS applications and offers a comparative study with soda lime. In addition, we present for the first time an evaluation of CO_2 capture with amine-grafted materials using a commercial-scale CCBS, i.e., an anesthesia delivery unit.

9.2 Experimental

9.2.1 Materials. The silica source used for the synthesis of PE-MCM-41 support was Cab-O-Sil M-5 fumed silica from Cabot. Cetyltrimethylammonium bromide (CTAB, Aldrich) and tetramethylammonium hydroxide (TMAOH 25%, balance water, Aldrich) were used as structure directing agent and for pH adjustment, respectively. The post-synthesis pore-expander agent was dimethyldecylamine (DMDA 97% purity, Aldrich). The grafting agent 2-[2-(3-trimethoxysilylpropylamino)ethylamino]ethylamine (herein referred to as TRI-silane) was obtained from Sigma-Aldrich. Translucent Liquid Sculpey® from Polyform was used as binder. Sodasorb© soda lime manufactured by Grace Ltd. was used as a benchmark commercial absorbent. Ultra high purity grade nitrogen, certified gas mixture of 5% CO_2 balance N_2 and medical grade oxygen (O_2) were supplied by Linde Ltd. Chloroform (99%

purity, Aldrich) was used as probe molecule instead of an actual volatile anesthetic. All reagents and gases were used without further purification.

9.2.2 Synthesis. The synthesis of TRI-PE-MCM-41 was carried out in two steps based on the recipe published previously by Harlick and Sayari [2007]. In the first place, MCM-41 type silica was produced at 100 °C using CTAB and TMAOH in aqueous solution with the following molar composition: 1 SiO_2: 0.29 TMAOH: 0.41 CTAB: 60 H_2O. To enlarge its pore size, as-synthesized MCM-41 underwent hydrothermal restructuring at 120 °C in the presence of DMDA at 130 °C for 2 days [Sayari et al., 1999]. Subsequently, both surfactants were removed by heating at 550 °C under flowing nitrogen, then air for 5 h. The resulting material was labeled PE-MCM-41. The amine functional groups were incorporated onto PE-MCM-41 by grafting using an 8 L stainless steel reactor. An amount of 300 g of PE-MCM-41 were dispersed in 5 L of toluene under vigorous stirring, followed by the stepwise addition of 75 mL of distilled water. Subsequently, 900 mL of TRI-silane (3 ml per g of silica) was added to the mixture. The stainless steel reactor was sealed and left stirring in an electric oven maintained at 85 °C. Grafting proceeded for 16 h, then the product was filtered and washed with toluene and pentane. The solid obtained was dried in a natural convection oven at 100 °C for 1 h and labeled TRI-PE-MCM-41.

To prevent severe pressure drops that would occur by using fine powder in a fixed-bed column, agglomerates were produced as follows. For laboratory-scale fixed bed-column experiments, TRI-PE-MCM-41 powder was loaded in a dye and compressed under a load of 450 kg cm^{-2} using a hydraulic press. As reported earlier, such a pressure did not affect significantly the structural properties of the adsorbent [Serna-Guerrero and Sayari, 2007]. The particles thus produced were crushed and sieved between openings of 20 and 40 mesh (i.e., 0.82 and 0.41 mm, respectively). Since commercial soda lime pellets have a larger size, for a fair comparison in fixed bed column experiments they were also crushed and sieved to produce particles of comparable size to TRI-PE-MCM-41. For evaluation in a commercial-scale CCBS, TRI-PE-MCM-41 powder was mixed with a polymeric ceramic binder to allow processing larger amounts of TRI-PE-MCM-41 and to produce agglomerates of larger size. Typically, 2 mL of ethanol were added per gram of TRI-PE-MCM-41 to produce a wet paste. Subsequently, the binder was added to the paste in a ratio of 250 mg per gram of TRI-PE-

MCM-41 and mixed mechanically. The wet paste was then extruded into rods with openings of ¼ in of diameter and cut into ca. 1 cm length. The wet extrudates were transferred into a vacuum oven at 140 °C for 30 min for evaporation of excess ethanol and curing of the binder. The pellets of TRI-PE-MCM-41 produced by addition of the binder will be referred to as TRI-PE-MCM-41B.

9.2.3 Characterization. The structural properties of the adsorbents were determined by nitrogen adsorption measurements at 77 K using a Micromeritics ASAP 2020 volumetric instrument. Before adsorption measurements, the sample was treated under vacuum (ca., 7×10^{-4} bar) at 100 °C for 5 h. Surface area was determined using the BET method, while the pore volume was considered as the volume of liquid nitrogen adsorbed at a relative pressure close to 1. The pore size distribution was obtained using the KJS method [Kruk et al., 1997]. Additionally, the organic content was determined by thermogravimetric analysis (TGA) using a TA Q-500 instrument. The sample was heated at 10 °C min^{-1} under flowing nitrogen up to 800 °C followed by decomposition in the presence of air at the same heating rate and up to 1000 °C.

9.2.4 CO_2 adsorption in laboratory-scale fixed bed column. Adsorption in a fixed bed column was carried out to determine the working adsorption capacity (q_b) of TRI-PE-MCM-41 at various flow rates and CO_2 concentrations and to determine the impact of the presence of volatile organic anesthetics on its performance, if any. In this work, q_b is defined as the CO_2 uptake before downstream CO_2 concentration reached 1%, in accordance with the limits established for clinical operation. Measurements of q_b were performed using a stainless steel column packed with particles of TRI-PE-MCM-41 (0.45 g) or soda lime (1.35 g) with sizes of 20-40 mesh. The column used had a diameter of 0.43 cm and a 12 cm packed length, and was located in a temperature-controlled enclosure. Before each experiment, the sample was treated by flowing helium at 50 mL min^{-1} at 150 °C for 2 h, time after which the temperature was decreased to 25 °C. A mixture of 5% or 10% CO_2 balance air flowing at the desired rate (i.e., 15, 30 or 50 ml min^{-1}) was fed to the column. Whenever required, the CO_2-air mixture was bubbled through a glass saturator containing chloroform at a temperature of -15 °C with the aid of a temperature-controlled bath in order to produce a mixture with a 3% chloroform

composition. The column downstream was monitored with a Pfeiffer Thermostar mass spectrometer. q_b values were calculated using Eq. 1:

$$q_b = \frac{FC_0 t_q}{W} \tag{1}$$

where F is the total molar flow, C_0 is the concentration of the adsorbate in the feed stream, W is the mass of adsorbent loaded in the column, and t_q is the stoichiometric time, which is estimated from the breakthrough profile according to Eq. 2 [Geankoplis, 1993]:

$$t_q = \int_0^\infty \left(1 - \frac{C_A}{C_0}\right) dt \tag{2}$$

where C_A is the concentration of the adsorbate upstream at the column inlet.

9.2.5 In-vitro studies in an anesthesia delivery system. After measurements in a laboratory-scale fixed bed column, a further step toward commercial application of TRI-PE-MCM-41 consisted in its evaluation under real operating conditions. To that aim, we performed a series of experiments in an Ohmeda Excel 310 anesthesia delivery system (ADS) by loading its scrubber canister with TRI-PE-MCM-41. A schematic representation of the ADS breathing circuit is presented in Figure 9.1. This setup included an automatic gas flow control for the breathing circuit and in-line sampling ports for CO_2 analysis of the exhaled (C_{ex}) and inhaled (C_{in}) streams. TRI-PE-MCM-41B was activated by heating at 90 °C under vacuum for 2 h. After cooling, ca. 400 g of TRI-PE-MCM-41B was loaded directly into the 2 L canister of the anesthesia machine. The patient's breathing was mimicked by a 2 L latex rebreathing bag connected to a continuous supply of CO_2, whose flow was regulated to provide a CO_2 concentration of 5% in the expiratory limb. Breathing rate was set at 12 breaths per minute for a total gas flow rate (F) of 5 or 8 L min^{-1} to simulate breathing under normal and stressful conditions. Medical grade oxygen was supplied as fresh gas at a rate of 1 to 2 L min^{-1}. Temperature was monitored at three evenly distributed points inside the canister from the

feed in the radial direction, i.e. at the "front" of the canister (T_{front}), at its "center" (T_{middle}) and at its "back" (T_{back}).

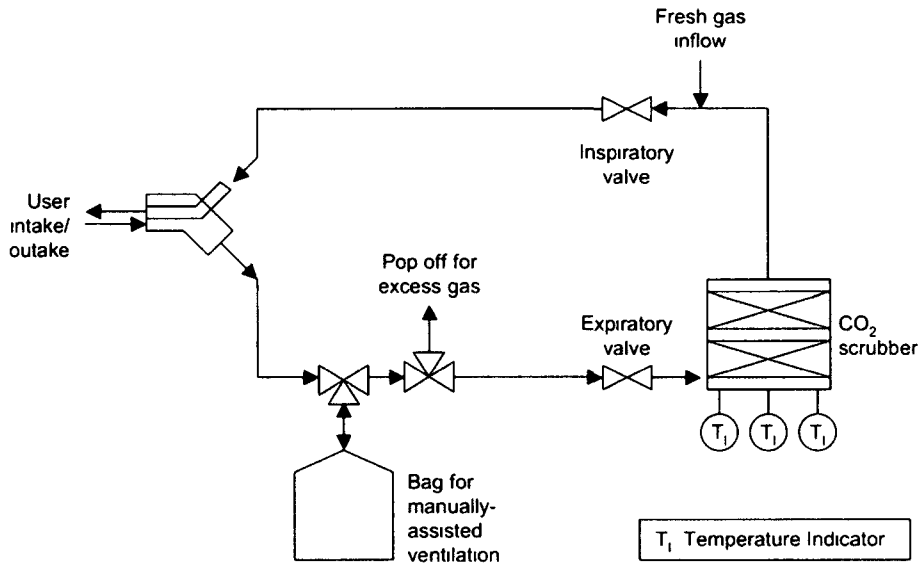

Figure 9.1 Schematic representation of anesthesia delivery system

9.3 Results and Discussion

Nitrogen adsorption isotherms of PE-MCM-41, TRI-PE-MCM-41 and TRI-PE-MCM-41B are presented in Figure 9.2. All samples presented a Type IV isotherm according to the IUPAC classification, characteristic of mesoporous materials. This implies that the mesoporous structure was maintained after the amine grafting and agglomeration procedures used in this work. The mesoporous structure is particularly attractive as it has been associated with an efficient use of amine functionalities [Serna-Guerrero et al., 2008; Belmabkhout and Sayari, 2009]. Table 9.1 shows values of structural properties determined by nitrogen adsorption. The loss of surface area and pore volume of TRI-PE-MCM-41 compared to PE-MCM-41 can be attributed to the space occupied by the organic moiety. With respect to TRI-PE-MCM-41B, a further decrease of surface area and pore volume was expected, as the binder is not a porous material and hence its contribution to these structural properties was negligible. Nonetheless, TRI-PE-MCM-41B still offered open pores with sizes in the mesoporous range, the most important characteristics for accessibility of amine groups.

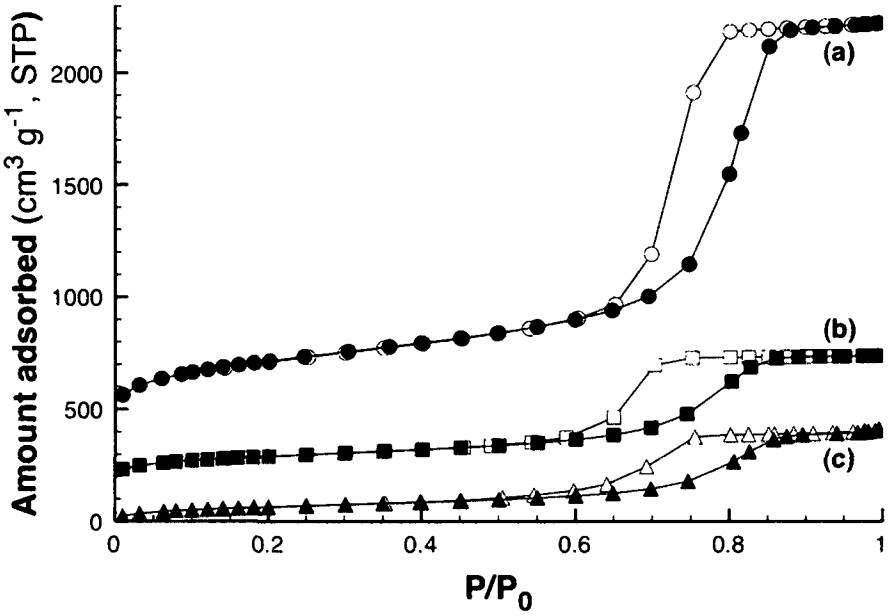

Figure 9.2 Nitrogen adsorption (closed symbols) and desorption (open symbols) isotherms for (a) PE-MCM-41, (b) TRI-PE-MCM-41 and (c) TRI-PE-MCM-41B; for clarity, isotherms (a) and (b) were shifted upwards by 400 and 200 $cm^3\ g^{-1}$, respectively

Table 9.1 Structural properties of PE-MCM-41 and TRI-PE-MCM-41

Sample	S_A ($m^2\ g^{-1}$)	V_p ($cm^3\ g^{-1}$)	d_p (nm)
PE-MCM-41	1134	2.62	10.8
TRI-PE-MCM-41	350	0.83	9.3
TRI-PE-MCM-41B	245	0.62	10.0

9.3.1 Adsorption in a fixed bed column. Adsorption of CO_2 in fixed bed columns was performed to explore the behavior of TRI-PE-MCM-41 in dynamic conditions at various flow rates and compositions. For illustration, Figure 9.3 shows typical breakthrough profiles of CO_2 on TRI-PE-MCM-41 and soda lime produced for experiments with 10% CO_2 concentration in air in the presence of chloroform. The first observation is that both soda lime and TRI-PE-MCM-41 have a negligible uptake of N_2, since its MS signal appeared immediately after the mixture was fed to the column. This translates into a high selectivity toward CO_2, most likely as a result of strong chemical interactions between CO_2 and the

scrubbing materials. The breakthrough curves of TRI-PE-MCM-41 under all flow rates presented a steep profile, associated with an efficient use of the column.

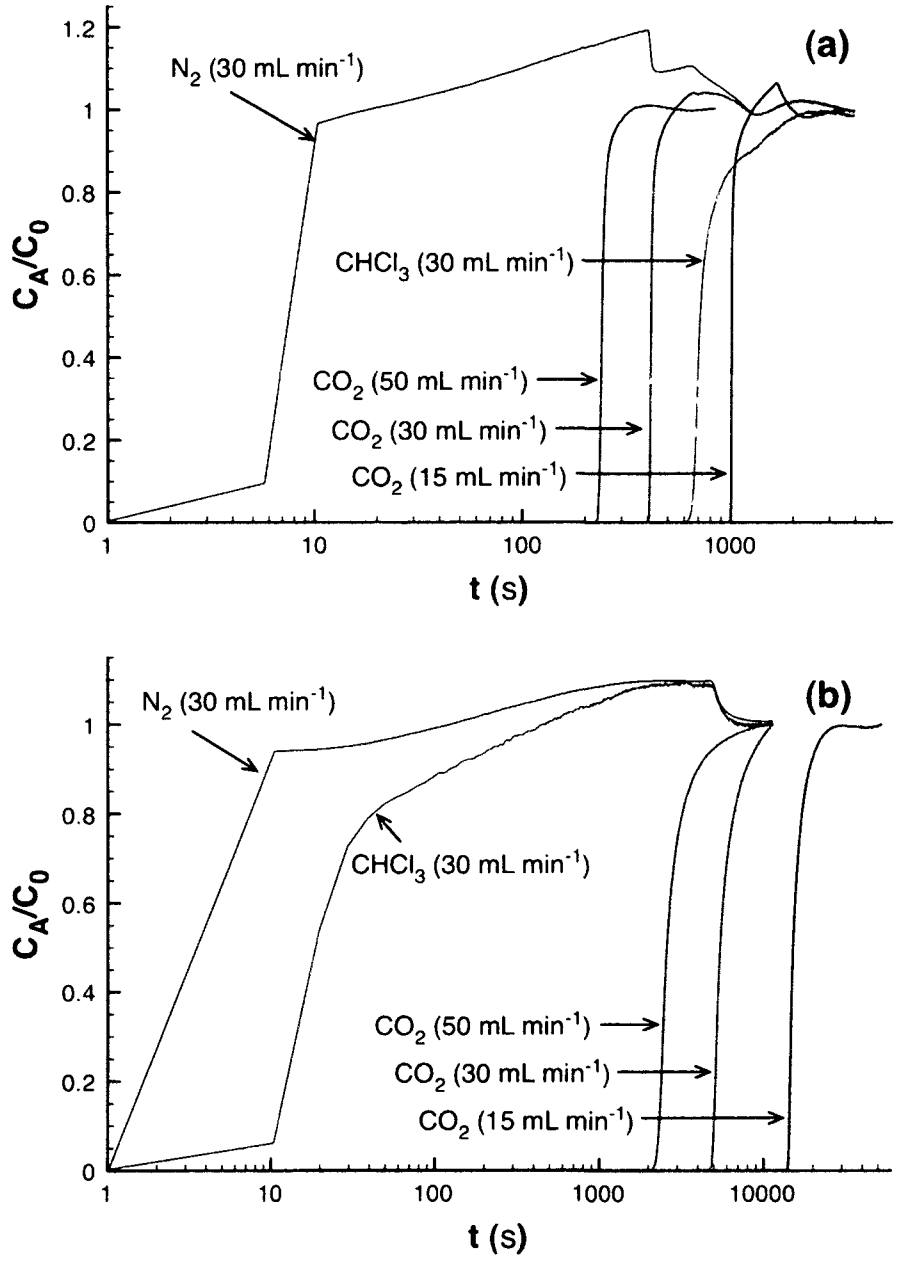

Figure 9.3 Typical breakthrough curves of streams containing 10% CO_2, 2% $CHCl_3$, balance N_2 on (a) TRI-PE-MCM-41 and (b) soda lime

An appreciably different behavior between scrubbing materials was observed with respect to chloroform, a volatile organic compound used as probe molecule to represent anesthetics. While there was no significant uptake of chloroform by soda lime, it was found that TRI-PE-MCM-41 adsorbed ca. 1.20, 0.93 and 0.78 mmol g^{-1} of it under a flow of 15, 30 and 50 mL min^{-1}, respectively. The uptake of chloroform by TRI-PE-MCM-41 is probably a result of its porosity and the presence of an organic moiety. Indeed, as was previously demonstrated [Serna-Guerrero et al., 2007], PE-MCM-41 has the capacity to adsorb volatile organic compounds, including $CHCl_3$. Typically, anesthetics are fed to an anesthesia delivery unit at a concentration of 2-3%, similar to that of the flow used in this study. Since these anesthetics are partially consumed by the user, it is likely that the actual concentration reaching the scrubber will be lower than 3%. However, the highest possible concentration of $CHCl_3$ was used with the purpose of making evident the influence of this adsorbate on the CO_2 capacity and selectivity of TRI-PE-MCM-41.

Figure 9.4 summarizes the values of q_b obtained under different gas compositions as a function of flow rate. As seen, there was no apparent variation of q_b when $CHCl_3$ was present. In the case of soda lime, this is in agreement with the negligible uptake of $CHCl_3$ previously mentioned. For TRI-PE-MCM-41, this means that CO_2 and $CHCl_3$ adsorbed non-competitively. It is possible that, since the amine groups are reactive with acid gases only, the removal of $CHCl_3$ occurs on adsorption sites of a different nature. It is thus inferred that the mechanisms for CO_2 removal using TRI-PE-MCM-41 or soda lime are not affected by the presence of volatile anesthetics.

It was also observed that for both scrubbing materials, q_b was a function of flow rate (Figure 9.4), a trend that can be explained since higher flow rates represent shorter contact time. However, the impact of flow rate on q_b was evidently more dramatic in the case of soda lime. Indeed, when F = 50 mL min^{-1}, the value of q_b for soda lime was ca. 50% of that obtained at 15 mL min^{-1}. On the other hand, q_b at 50 mL min^{-1} for TRI-PE-MCM-41 decreased by only 20% compared to its value at F = 15 mL min^{-1}. The adequate response of TRI-PE-MCM-41 to high flow rates is attributable to favorable kinetics. It is well established that when fast kinetics occur, an acceptable performance can be achieved at short retention times. In practice, this represents a more efficient use of TRI-PE-MCM-41 than soda lime under stressful operating conditions. It was also observed that only in the case of TRI-PE-

MCM-41 the CO_2 uptake were dependent on C_0, in agreement with its adsorption isotherm reported earlier [Serna-Guerrero et al., 2010c].

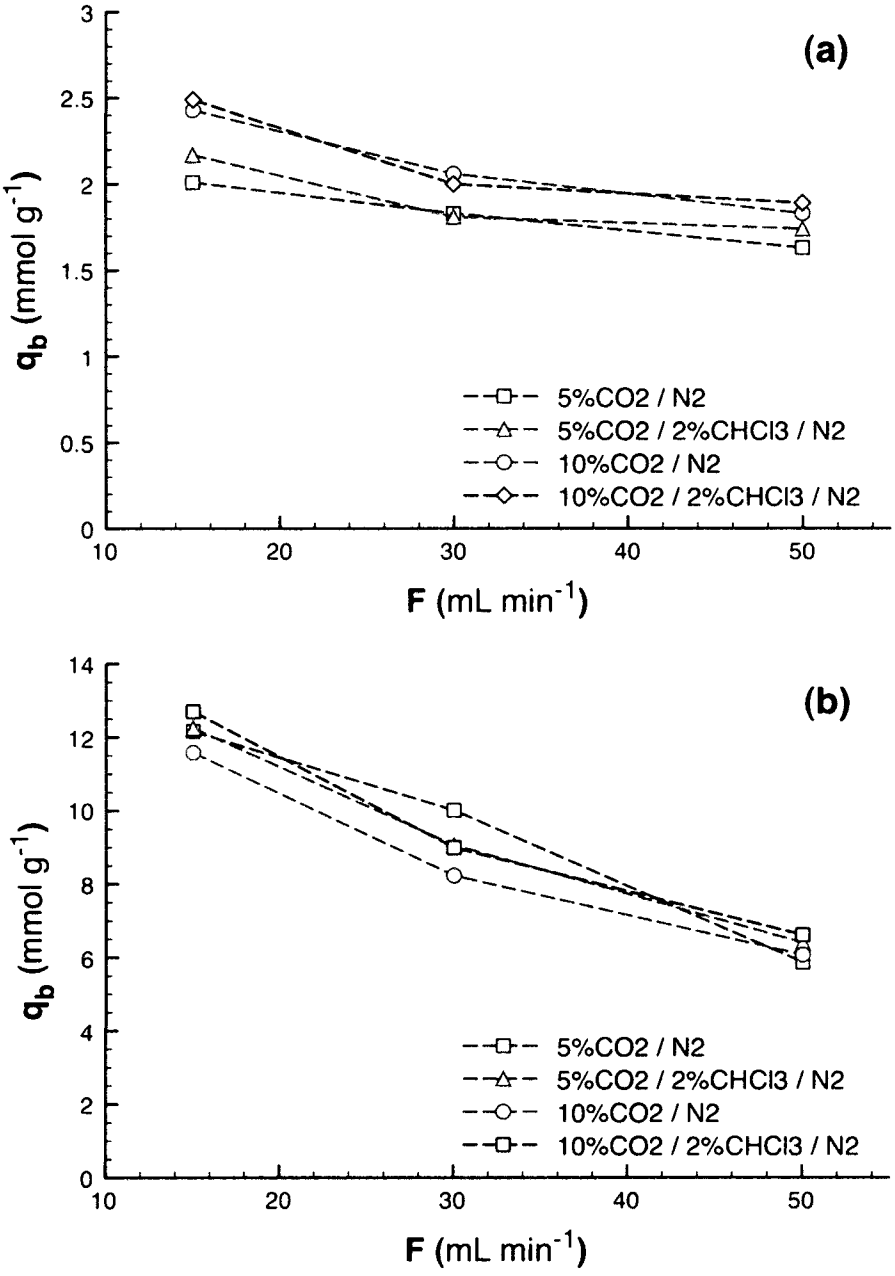

Figure 9.4 CO_2 uptake under various operating conditions on (a) TRI-PE-MCM-41 and (b) soda lime

Although the CO_2 removal capacity of soda lime was in all cases higher than TRI-PE-MCM-41, it must be kept in mind that the former is a single-use material. The CO_2 uptake on soda lime was ca. 5 times higher that that of TRI-PE-MCM-41 at each set of operating conditions used. Therefore, TRI-PE-MCM-41 should be regenerated many times to be competitive. In a recent report [Serna-Guerrero et al., 2010b], we carried out a series of adsorption-desorption experiments and demonstrated the impact of regeneration conditions on q_b. It was established that using a temperature-swing configuration at 150 °C, a high q_b could be maintained throughout several cycles. Furthermore, using a temperature-vacuum swing configuration at 70 °C and 0.1 bar, it was possible to reutilize TRI-PE-MCM-41 for over 100 cycles without any significant loss of capacity. Later, it was demonstrated that TRI-PE-MCM-41 can be regenerated over hundreds of cycles (ca. 700), under a set of well established conditions [Sayari and Belmabkhout, 2010] including temperature lower than 200 °C, preferably in the presence of moisture. Although it offers a comparatively lower q_b than soda lime, its ability to be recycled and its favorable kinetics make TRI-PE-MCM-41 a promising alternative for CO_2 scrubbing.

9.3.2 CO_2 Adsorption in an anesthesia delivery apparatus. As TRI-PE-MCM-41 demonstrated promising characteristics for CO_2 scrubbing in CCBS, the next step consisted on evaluating its performance in a commercial setup. To that aim, TRI-PE-MCM-41B was loaded into an anesthesia delivery system, and q_b was calculated under flow rates representing both typical and stressful operating conditions i.e., 5 and 8 L min^{-1}, respectively. Figure 9.5 shows a representation of CO_2 concentration at the inspiratory (C_{in}) and expiratory (C_{ex}) limbs of the breathing loop. As seen in Figure 9.5, it was not possible to read a C_{in} higher than 3% since the equipment is programmed to trigger an alarm at this concentration as a safety measure. Nevertheless, for this application, the main interest was measuring q_b at C_{in} values of 1% and lower. The adsorption capacity calculated before the clinical limit of 1% CO_2 was of 1.31 mmol g^{-1} at a flow of 5 L min^{-1}, with a slight decrease to 1.28 mmol g^{-1} when the flow rate increased to 8 L min^{-1}. It is worth noting that even at high flow rate, the value of C_{in} was low, denoting the high purity streams that can be obtained with TRI-PE-MCM-41B. This is as a particularly positive aspect about the use of TRI-PE-MCM-41, as

CO_2 rebreathing as a result of erratic or stressful user breathing is unlikely to occur before the adsorbent is fully exhausted.

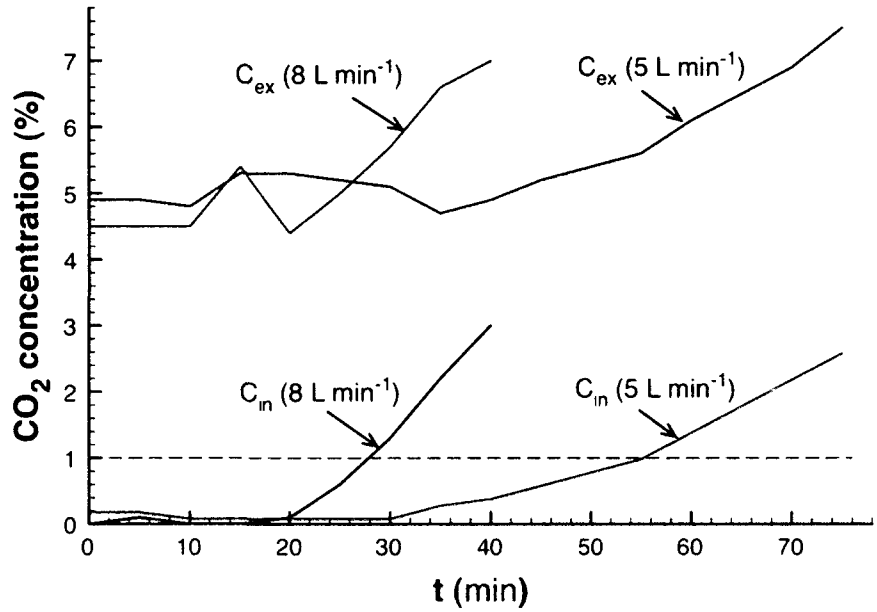

Figure 9.5 CO_2 concentration in anesthesia delivery unit loaded with TRI-PE-MCM-41 as scrubber

It was observed that the values of q_b measured in the anesthesia machine were smaller than those expected according to the fixed bed column studies reported above. Several reasons may be at the origin of this behavior. Since the binder's CO_2 uptake is negligible, a decrease in capacity proportional to the content of inert solids (i.e., ca. 10%) is expected. However, the main discrepancies between the values of q_b in laboratory-scale fixed-bed columns and commercial ADS can be attributed to the operating differences between methods. Figure 9.6 shows values of temperature measured at various points of the canister during operation under a 5 L min^{-1} flow. Unlike the fixed bed column described above, the canister was not maintained at a controlled temperature and so, its operation was completely adiabatic. The absence of temperature control and the high gas flow resulted in a significant temperature increase in the canister, reaching 54 °C at its highest point. While such temperature is attractive from a clinical point of view as it is considered antiseptic, it has been established that the adsorption capacity of TRI-PE-MCM-41 is reduced at higher

temperature [Serna-Guerrero et al, 2010c]. Indeed, while the capacity at equilibrium for TRI-PE-MCM-41 at room temperature is of 2.05 mmol g^{-1}, at the maximum values of T_{front}, T_{middle} and T_{back} it is of 1.80, 1.46 and 1.66 mmol g^{-1}, respectively.

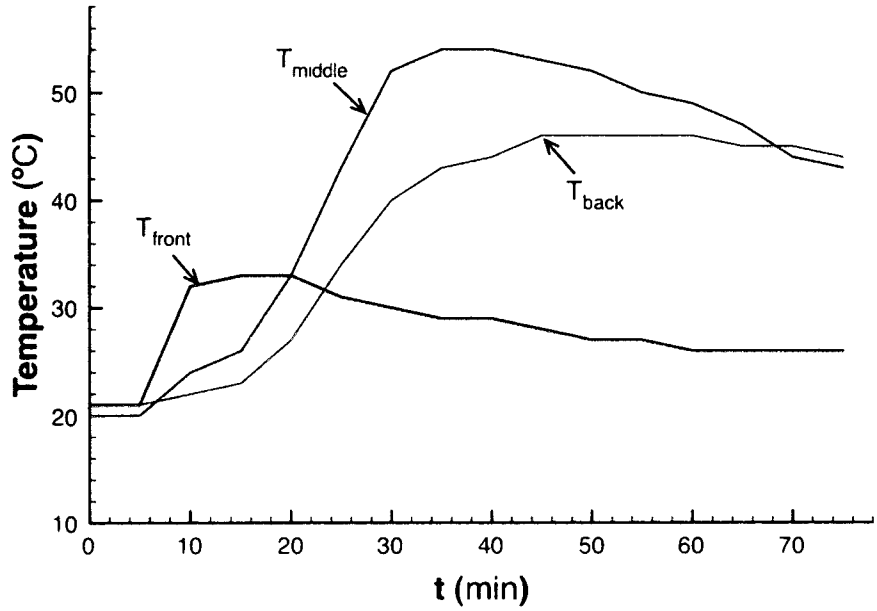

Figure 9.6 Temperature profiles of TRI-PE-MCM-41-loaded canister during CO_2 adsorption

Finally, it is possible that the remaining loss in capacity is associated with the current design of the scrubbing systems in ADS. Because of the well-documented production of dust in soda-lime canisters, gases are fed into the CO_2 scrubber in a radial direction at the bottom of the canister, to prevent contamination of the breathing limb and accidental ingestion of the absorbent by the user. This, however, is an unlikely configuration for adsorption in fixed beds, since they are typically fed axially, providing a more even distribution of gas flow with a subsequently efficient contact of gases with all the packed material. A common practice when designing fixed bed columns, for example, consists in adding a distributor at the feeding point of the column to promote turbulence and hence a more even gas flow. An indirect way to determine whether an uneven distribution of flow occurred can be based on the profiles in Figure 9.6. It was observed that the temperature measured closest to the entrance of the canister (T_{front}) rises quickly at the beginning of the process, as it is the first point of contact of CO_2 with the adsorbent. T_{front} decreases after the first few minutes,

indicating that adsorption no longer occurs around this point. As the temperature at the entrance decreases, T_{middle} and T_{back} start rising, reaching significantly higher values than that at the entrance. Considering the comparatively lower heat released at the inlet, it can be said that a significantly lower number of adsorption sites are being used in this section of the canister. This trend suggests that gases flow preferentially through the middle and back sections of the canister, while various adsorption sites close to the front are not reached. Thus, an inefficient use of the loaded adsorbent occurs, explaining the lower capacity observed during operation with the current configuration of ADS. Although not shown, a similar behavior was observed under a flow of 8 L min^{-1}.

9.4 Conclusions

The present study showed some of the advantages and limitations presented by TRI-PE-MCM-41 for removal of metabolic CO_2 in CCBS. The fast adsorption kinetics of TRI-PE-MCM-41 provided an efficient operation in fixed bed columns, as evidenced by steep breakthrough curves and a comparatively smaller decrease in q_b when operating at high flow rate compared to soda lime. It was also found that while TRI-PE-MCM-41 has the ability to adsorb organic compounds, it is not done competitively with CO_2. The high reactivity of the amine groups in TRI-PE-MCM-41 was also proven advantageous for CO_2 capture under real operating conditions in a commercial ADS. Indeed, TRI-PE-MCM-41 produced streams with a high degree of purity even at flows representing stressful operation. These positive observations, in conjunction with the previously proven stability of TRI-PE-MCM-41 throughout extensive adsorption-desorption cycling, are indications of its potential as an alternative scrubbing material to the currently used solid absorbents. During this first exploratory study of TRI-PE-MCM-41 performance in a commercial anesthesia machine, a lower-than-expected q_b was observed. However, this was partly associated with the current configuration of anesthesia delivery machines and hence, there is potential for improvement on CO_2 scrubbing using TRI-PE-MCM-41 by engineering a more efficient gas distribution in the scrubbing canister.

References

Jan A. Baum, Low Flow Anesthesia, Butterworth Heinemann, Oxford 1996

Pamela J. Baxter, Kyle B.S. Garton, Evan D. Kharasch, Mechanistic Aspects of Carbon Monoxide Formation from Volatile Anesthetics, Anesthesiology, 84 (1998) 929

Y. Belmabkhout, A. Sayari, Effect of pore expansion and amine functionalization of mesoporous silica on CO_2 adsorption over a wide range of conditions, Adsorption 15 (2009) 318

Y. Belmabkhout, R. Serna-Guerrero, A. Sayari, Adsorption of CO_2-Containing Gas Mixtures over Amine-Bearing Pore-Expanded MCM-41 Silica: Application for Gas Purification. Ind. Eng. Chem. Res. 49 (2010) 359

P. Birbara, T. Filburn, H. Michels, T. Nalette, Sorbent system and method for absorbing carbon dioxide (CO_2) from the atmosphere of a closed habitable environment. USPatent 6,364,938, 2002

H. Bito, Y. Ikeuchi, K. Ikeda, Effects of water content of soda lime on Compound A concentration in the anesthesia circuit in sevoflurane anesthesia. Anesthesiology 88 (1998) 66-71

F. Brandani, D.M. Ruthven, The effect of water on the adsorption of CO_2 and C_3H_8 on type X zeolites. Ind. Eng. Chem. Res. 43 (2004) 8339

E.J. Frink, W.B. Green, E.A. Brown, M.M.S. Malcomson, L.C. Hammond, F.G. Valencia, B.R. Brown, Anesthesiology 84 (1996) 566

T. Filburn, J.J. Helble, R.A. Weiss, Development of supported ethanolamines and modified ethanolamines for CO_2 capture. Ind. Eng. Chem. Res. 44 (2005) 1542

C.J. Geankoplis, Transport Processes and Unit Operations, third ed., Prentice-Hall, New Jersey, 1993

P.J.E. Harlick, A. Sayari, Applications of pore-expanded mesoporous silica. 5. Triamine grafted material with exceptional CO_2 dynamic and equilibrium adsorption performance, Ind. Eng. Chem. Res. 46 (2007) 446

H.T. Hwang, A. Harale, P. K.T. Liu, A membrane-based reactive separation system for CO_2 removal in a life support system. Journal of Membrane Science 315 (2008) 116

C. Keijzer, R.S.G. M. Perez, J.J. de Lange, Compound A and carbon monoxide production from sevoflurane and seven different types of carbon dioxide absorbent in a patient model. Acta Anaesthesiol. Scand. 51 (2007) 31

E.D. Kharasch, K.M. Powers, A.A. Artru, Comparison of Amsorb, Sodalime, and Baralyme Degradation of Volatile Anesthetics and Formation of Carbon Monoxide and Compound A in Swine *In Vivo*. Anesthesiology 96 (2002) 173

S. Kobayashi, H. Bito, K. Morita, T. Katoh, S. Sato, Amsorb Plus and Dragersorb Free, two new-generation carbon dioxide absorbents that produce a low compound A concentration while providing sufficient CO_2 absorption capacity in simulated sevoflurane anesthesia. J. Anesth. 18 (2004) 277

M. Kruk, M. Jaroniec, A. Sayari, Application of large pore MCM-41 molecular sieves to improve pore size analysis using nitrogen adsorption measurements. Langmuir 13 (1997) 6267

J.C. McNeirney, Removal of carbon dioxide and carbon monoxide from patient expired gas during anesthesia. Patent No. US 7,246,621, 2007

P. Moore, Miner protection, Mining Magazine 196, 5 (2007) 35

S Satyapal, T. Filburn, J. Trela, J. Strange, Performance and properties of a solid amine sorbent for carbon dioxide removal in space life support applications. Energy Fuels 15 (2001) 250

A. Sayari, Y. Yang, M. Kruk, M. Jaroniec, Expanding the pore size of MCM-41 silicas: use of amines as expanders in direct synthesis and postsynthesis procedures, J. Phys. Chem. B. 103 (1999) 3651

A. Sayari, Y. Belmabkhout, Stabilization of amine-containing CO_2 adsorbents: dramatic effect of water vapor. J. Am. Chem. Soc. 132 (2010) 6312

R. Serna-Guerrero, A. Sayari, Applications of pore-expanded mesoporous silica. 7. Adsorption of volatile organic compounds. Environ. Sci. Technol. 41 (2007) 4761

R. Serna-Guerrero, E. Da'na, A. Sayari, New insights into the interactions of CO_2 with amine-functionalized silica, Ind. Eng. Chem. Res. 47 (2008) 9406

R. Serna-Guerrero, Y. Belmabkhout, A. Sayari, Further investigations of CO_2 capture using triamine-grafted pore-expanded mesoporous silica. Chem. Eng. J. 158 (2010a) 513

R. Serna-Guerrero, Y. Belmabkhout, A. Sayari, Influence of regeneration conditions on the cyclic performance of amine-grafted mesoporous silica for CO_2 capture: An experimental and statistical study. Chem. Eng. Sci. (2010b) 4166

R. Serna-Guerrero, Y. Belmabkhout, A. Sayari, Modeling CO2 adsorption on amine-functionalized mesoporous silica: 1. A semi-empirical equilibrium model. Chem Eng. J. 161 (2010c) 173

H. Wissing, I. Kuhn, U. Warnken, R. Dudziak, Carbon monoxide production from desflurane, enflurane, halothane, isoflurane, and sevoflurane with dry soda lime. Anesthesiology, 95 (2001) 1205

Chapter 10

General Discussion and Conclusions

To talk about CO_2 capture technologies nowadays cannot be done without discussing climate change, considered by many as the most important environmental challenge of our generation. Even without a pessimistic approach, it can be acknowledged that the widespread use of fossil fuels has impacted negatively our planet. It is not exaggerated to say that we live in a very unique point of history, as we are slowly becoming aware of the environmental effects associated with a fossil fuel-based economy. The 20th century was witness to a vast, perhaps often uncontrolled, industrial growth along with technological advances far beyond anyone's expectations, however without hindsight on industrialization's long-term consequences. As a result, governments and population alike have only recently gained awareness of the potential damage inflicted to our ecosystem by unsustainable practices and thus, efforts are currently being placed on preventing an environmental disaster that could jeopardize the survival of our and other species.

It was in the spirit of providing a contribution to solving the problem of climate change that our research group decided to explore novel materials for adsorption of pollutants, among them CO_2, to which this thesis was devoted. Fossil fuel combustion is the main source of anthropogenic CO_2 emissions [Figueroa et al., 2008; Choi et al., 2009]. Unfortunately, despite the active search for cheap clean energy, fossil fuels will remain the main source of energy for decades to come [Figueroa et al., 2008; Liu et al., 2009]. Admittedly, adsorption separation is not the only solution explored for CO_2 capture, as efforts are also underway to further improve well established technologies such as liquid amine solution scrubbing [Ma'mun et al., 2007; Lepaumier et al., 2009], and chemisorption on metal oxides [Lee et al., 2008]. It is thus encouraging to know that a global, collective effort is taking place that could eventually produce reliable processes to truly overcome the effect of greenhouse gases.

With respect to adsorption separation technologies for CO_2 capture, amine functionalized materials have drawn particular attention in recent years, mainly due to their high selectivity toward CO_2 and their tolerance to moisture. Indeed, the efforts placed by

numerous research groups on the development of supported amines has resulted in a continuous improvement of such adsorbents, particularly in terms of adsorption capacity [Choi et al., 2009].

In general, a suitable adsorbent material must offer properties such as high adsorption capacity, fast rate of adsorption, selectivity and stability. The adsorbent developed by our research group, namely TRI-PE-MCM-41 was designed specifically to offer such characteristics when capturing acid gases [Harlick and Sayari, 2007; Belmabkhout and Sayari, 2009]. Consequently, this thesis was devoted to exploring in depth the adsorptive performance of this material for CO_2 capture, while gaining fundamental understanding on the performance of amine-functional materials and setting the basis for its potential application at a commercial scale. Along the way, the relevance of parameters such as rate of adsorption and selectivity was evidenced, in contrast to other researchers who have designed adsorbents focusing only on improving the adsorption capacity at equilibrium. It can be said that the results produced in this thesis consistently showed that, when properly designed, amine functional adsorbents offer features that make them promising alternatives for efficient CO_2 capture.

10.1 Summary of the main findings in this thesis

1. A recipe for incorporation of amine functionalities on mesoporous silica in the hundreds-of-gram scale as a key step for commercial scale production. Based on the previously optimized production of TRI-PE-MCM-41 in 1 g batches, a procedure for grafting amine-bearing silane on ca. 300 g of PE-MCM-41 batches was developed. The adsorbent obtained presented structural and chemical characteristics similar to those of adsorbents prepared in small-scale.

2. Direct evidence of the existence of interaction mechanisms between supported amines and CO_2 analogous to liquid amines, with the formation of carbamate in dry streams and bicarbonate in the presence of moisture. Before this work, it had only been speculated that the presence of moisture would enhance CO_2 uptake on amine-functionalized adsorbents as dictated by the reaction mechanisms generally accepted for reaction with liquid amine solutions. However, the results reported in the literature did not always corroborate this hypothesis with some cases even contradicting it. By a carefully designed experimental

setup, this work provided quantitative measurements of the increase in adsorption capacity under humid streams. It was observed that stoichiometric CO_2/N ratios close to 0.5 were obtained in dry streams with 0.05-0.1 bar partial pressure of CO_2 when the adsorbent maintained a mesoporous structure. To achieve the stoichiometric CO_2/N ratio of 1 expected in humid streams, it is necessary to have a sufficiently high relative humidity and a long enough contact time, since the formation of bicarbonate is a comparatively slow process.

3. Evidence that CO_2 adsorption on amine-functionalized mesoporous silica occurs via physical and chemical interactions. As part of the study of CO_2 interaction with amine-functionalized adsorbents, it was consistently found on data produced in this work and reported in the literature that, at high CO_2 partial pressure, the adsorption capacity exceeded the expected CO_2/N stoichiometric limit. At high CO_2 partial pressure, a continuous increase of adsorption capacity was measured, with slopes similar to those observed for non-modified silica supports. Careful analysis of literature data and our findings suggested that CO_2 adsorption occurs by strong chemical adsorption on the amine functional groups and by physical adsorption on the adsorbent surface. The chemical adsorption produces an enhanced adsorption capacity at low CO_2 concentration, while the contribution of physical interactions in the overall CO_2 capture becomes evident at high partial pressure of the adsorbate.

4. Evidence of a practically infinite selectivity of amine-functionalized adsorbents toward CO_2 over the main components of air (i.e., N_2 and O_2) in fixed bed operation under dry and humid streams. A particularly important characteristic of any adsorbent is its selectivity toward the adsorbate of interest. As presented in Chapter 5, in a fixed bed column packed with TRI-PE-MCM-41 using CO_2/air mixture, it was demonstrated that the uptake of N_2 ad O_2 was negligible. Furthermore, the same behavior was observed with humid streams, while CO_2 working adsorption capacity was enhanced.

5. A semi-empirical isotherm model for the adsorption of CO_2, H_2S and potentially other acid gases on amine-functionalized mesoporous silica over a wide range of pressure. For the first time, an adsorption isotherm model for amine-functionalized mesoporous materials was developed. The need for such a model stems from to the particular shape of CO_2 isotherms on amine-grafted mesoporous silica reported in the literature and obtained experimentally in this work. Such profile was attributed to the simultaneous occurrence of physical and chemical adsorption. The model was based on the following

assumptions that have been well justified: (i) chemical and physical adsorption were considered to be independent, (ii) chemical adsorption is a function of amine loading and (iii) physical adsorption depends on surface area. With this semi-empirical model, it was possible to describe CO_2 adsorption on amine-grafted materials over a wide range of pressure and temperature.

6. Kinetic parameters for the description of CO_2 uptake on amine-functionalized mesoporous materials at low concentrations. After exploring a series of models, it was determined that a kinetic model with fractional order, namely Avrami, was the most appropriate to describe CO_2 uptake on TRI-PE-MCM-41 as a function of time. Although a first-kinetic order model was comparatively less accurate, it still offered an acceptable degree of error. Based on the kinetic parameters obtained, TRI-PE-MCM-41 was compared with zeolites (NaY) and polyethyleneimine-impregnated mesoporous silica, demonstrating that TRI-PE-MCM-41 is a superior CO_2 adsorbent in terms of kinetics.

7. Simulation of CO_2 capture in a fixed bed column to predict breakthrough curves using the finite volume method. After establishing of equilibrium and kinetic models, it was feasible to attempt a simulation of CO_2 adsorption in a fixed bed column packed with TRI-PE-MCM-41. A numerical method (i.e., the finite volume method) was used to solve the simultaneous differential equations describing mass transfer, successfully predicting CO_2 breakthrough curves. This provided further support to the equilibrium and kinetic models proposed.

8. Objective assessment of the influence of regeneration parameters on the working performance of amine-functionalized materials during adsorption and regeneration. In the search of the optimum conditions for regeneration of TRI-PE-MCM-41, an exploratory work studying the impact of regeneration conditions on the performance of the adsorbent was conducted. Among the three conditions studied, i.e., temperature, pressure and purge gas flow, it was determined that the regeneration temperature had the strongest influence on adsorption capacity and rate of desorption. It was also demonstrated that vacuum affected the adsorption capacity, particularly when regeneration occurred at moderate temperatures, and that the sweeping gas was necessary to regenerate the adsorbent although only a small flow rate was required.

9. Stability of TRI-PE-MCM-41 over extensive cycling. To support the potential of the adsorbent for use in commercial applications, it was necessary to demonstrate its ability to withstand intensive recycling. Consequently, CO_2 adsorption on TRI-PE-MCM-41 was investigated using a temperature-vacuum swing configuration with regeneration at 70 °C and 0.1 bar for over 100 cycles. Under such conditions, no appreciable changes on its adsorptive behavior were observed.

10. A comparative study between amine-functionalized adsorbent and soda lime, demonstrating the advantages of the fast adsorption kinetics of the former in terms of column efficiency. As one of the potential applications of TRI-PE-MCM-41 involves CO_2 scrubbing in closed-circuit breathing systems, a direct comparison with the absorbent currently used, namely, soda lime was performed. Running a series of experiments in fixed-bed columns packed with TRI-PE-MCM-41 and soda lime, some similarities of these materials, such as a negligible uptake of N_2 were observed. It was also found that high flow rates have a more drastic impact on the working adsorption capacity of soda lime, losing almost half of its capacity at high flow rates, while under the same operating conditions, TRI-PE-MCM-41 presented only a loss of ca. 20% of its capacity at equilibrium. The superior efficiency of the column packed with TRI-PE-MCM-41 was attributed to the favorable kinetics offered by this adsorbent.

11. Evaluation of amine-functionalized mesoporous adsorbents in a commercial-scale CCBS setup, addressing the current limitations of this technology for future improvement. A step toward a competitive application of TRI-PE-MCM-41 in real life operations was achieved with the study of CO_2 capture in a commercial anesthesia delivery unit. In-vitro studies were performed mimicking typical surgical operation conditions, after loading TRI-PE-MCM-41 pellets in the scrubber canister. These experiments produced invaluable data on which to build strategies to optimize the use of the material for this particular application. Although a lower than expected working adsorption capacity was measured, this was attributed to the current design of the anesthesia machine, as the gas was fed in a radial direction to the canister, resulting in an uneven distribution of the flow.

10.2 Publications

The work performed in this thesis resulted in the publication of 5 articles in peer-reviewed journals, whose manuscripts are included here as Chapters 4 – 8. Another manuscript (Chapter 9) will be submitted shortly for publication. Further work performed by the author to complement parallel projects regarding adsorption on PE-MCM-41 and TRI-PE-MCM-41 has been included in three additional articles, published in Chemical Engineering Science [Belmabkhout et al., 2009; Belmabkhout et al., 2010a], and Industrial and Engineering Chemistry Research [Belmabkhout et al., 2010b].

10.3 Recommendations and future work

Based on the findings of this thesis, a series of recommendations can be made to improve the performance of the material in future efforts in research and development:

- Recovering and recycling chemicals can further optimize the synthesis of TRI-PE-MCM-41. In particular, TRI-silane is of interest, since not only it is used in large excess but it is the most expensive ingredient. The development of proper recovery processes could have an excellent impact on the overall economics of the adsorbent production.
- One of the typical variables currently explored in the design of amine-functionalized adsorbents is the type of amine-bearing molecule used as functional group. There are a wide variety of amine-bearing silanes, beside those studied in this thesis (i.e., MONO-silane and TRI-silane). However, the literature published so far mainly present synthesis via dry grafting, seldom using supports with pore sizes as large as that of PE-MCM-41. Considering the reported advantages of using a pore-expanded support and wet grafting, it could be of interest to explore other amine-bearing silanes, which may produce adsorbents with interesting properties after optimization of synthesis conditions.
- Although an acceptable agglomeration procedure, suitable for laboratory-scale experiments was found, efforts could be placed to further optimize this procedure, particularly with respect to the agglomerates size and shape. It is known that the various pellet shapes in a packed bed column provide different contact area and resistance to flow. Hence, each particular application may be improved using pellets with specific shape and dimensions.

- As for the material characterization, electron microscopy could be used to determine the shape and size of TRI-PE-MCM-41 particles. The morphology of the particles is of interest as it can be used to model adsorption within the particle at the microscopic scale.
- Based on the results observed during operation in the anesthesia delivery unit using TRI-PE-MCM-41, it is recommended to redesign the canister in order to provide a more even distribution of the flow to promote a more efficient use of the adsorbent bed.
- In current medical practice, the exhausted absorbent is disposed of and replaced with fresh soda lime periodically. As TRI-PE-MCM-41 would be regenerated for reuse, ideally a canister could be designed so that the material is regenerated directly inside the canister, i.e., without the need for exposure to ambient air or direct manipulation by the user. Depending on the engineering solution chosen, it will be necessary to establish protocols for canister replacement and regeneration. Another possibility to be explored is to redesign the CCBSs with a multiple fixed bed configuration and permit regeneration in situ without the need for canister replacement. Admittedly, this option would only be attractive for CCBSs not intended for personal equipment (e.g., breathing masks for mining or rescue), as this would likely result in a more complex system with subsequent increase in size and weight.
- Further analysis of TRI-PE-MCM-41 using commercial anesthesia machines should consist in performing *in vitro* testing with gas streams containing typical volatile anesthetics and monitoring the components downstream the canister. If the absence of decomposition or toxic byproducts is corroborated, studies *in vivo* could proceed.

References

Y. Belmabkhout, A. Sayari, Effect of pore expansion and amine-functionalization of mesoporous silica on CO_2 adsorption over a wide range of conditions, Adsorption 15 (2009) 318

Y. Belmabkhout, R. Serna-Guerrero, A. Sayari, Adsorption of CO_2 from dry gases on MCM-41 silica at ambient temperature and high pressure. 1: Pure CO_2 adsorption. Chem. Eng. Sci. 64 (2009) 3721

Y. Belmabkhout, R. Serna-Guerrero, A. Sayari, Amine-bearing mesoporous silica for CO_2 removal from dry and humid air. Chem. Eng. Sci. 65 (2010a) 3695

Y. Belmabkhout, R. Serna-Guerrero, A. Sayari, Adsorption of CO_2-containing gas mixtures over amine-bearing pore-expanded MCM-41 silica: Application for gas purification. Ind. Eng. Chem. Res. 49 (2010b) 359

S. Choi, J.H. Drese, C.W. Jones, Adsorbent materials for carbon dioxide capture from large anthropogenic point sources. ChemSusChem, 2 (2009) 796

P.J.E. Harlick, A. Sayari, Applications of pore-expanded mesoporous silicas. 5. Triamine grafted material with exceptional CO_2 dynamic and equilibrium adsorption performance, Ind. Eng. Chem. Res. 46 (2007) 446

J.D. Figueroa, T. Fout, S. Plasynski, H. McIlvried, R.D. Srivastava, Advances in CO_2 capture technology - The U.S. Department of Energy's carbon sequestration program. Int. J. Greenhouse Gas Control 2 (2008) 9

K.B. Lee, M.G. Beaver, H.S. Caram, S. Sircar, Reversible chemisorbents for carbon dioxide and their potential applications. Ind. Eng. Chem. Res. 47 (2008) 8048

H. Lepaumier, D. Picq, P.L. Carrette, New amines for CO_2 capture. I. Mechanisms of amine degradation in the presence of CO_2. Ind. Eng. Chem. Res. 48 (2009) 9061

W. Liu, D. King, J. Liu, B. Johnson, Y. Wang, Z. Yang, Critical material and process issues for CO_2 separation from coal-powered plants. JOM 61 (2009) 36

S. Ma'mun, H.F. Svendsen, K.A. Hoff, O. Juliussen, Selection of new absorbents for carbon dioxide capture, Energy Convers. Manage. 48 (2007) 251

Appendix A

Supplementary Data for Chapter 6

Table 6.S1 Experimental data for CO_2 uptake on TRI-PE-MCM-41

25°C		35°C		45°C		55°C	
P (bar)	n (mmol g^{-1})	P (bar)	n (mmol g^{-1})	P (bar)	n (mmol g^{-1})	P (bar)	n (mmol g^{-1})
0.0010	1.20	0.0010	0.95	0.0010	0.75	0.0010	0.60
0.0017	1.31	0.0017	1.10	0.0013	0.86	0.0013	0.66
0.0023	1.34	0.0023	1.13	0.0023	0.97	0.0023	0.77
0.0033	1.39	0.0033	1.19	0.0033	1.04	0.0033	0.83
0.0048	1.45	0.0048	1.25	0.0048	1.12	0.0048	0.91
0.0073	1.53	0.0073	1.33	0.0073	1.20	0.0073	0.99
0.010	1.60	0.010	1.40	0.010	1.28	0.01	1.06
0.017	1.71	0.013	1.49	0.013	1.34	0.013	1.16
0.020	1.75	0.018	1.56	0.018	1.44	0.018	1.26
0.028	1.82	0.028	1.64	0.028	1.53	0.028	1.34
0.038	1.89	0.038	1.71	0.038	1.60	0.038	1.41
0.048	1.95	0.048	1.77	0.048	1.66	0.048	1.46
0.058	2.00	0.058	1.80	0.058	1.70	0.058	1.51
0.068	2.04	0.068	1.84	0.068	1.74	0.068	1.54
0.079	2.08	0.079	1.88	0.079	1.78	0.078	1.58
0.088	2.12	0.088	1.91	0.088	1.81	0.088	1.61
0.1	2.16	0.1	1.95	0.1	1.84	0.1	1.65
0.17	2.25	0.13	2.00	0.13	1.89	0.13	1.71
0.28	2.34	0.18	2.04	0.18	1.94	0.18	1.77
0.38	2.43	0.28	2.14	0.28	2.06	0.28	1.89
0.48	2.51	0.38	2.23	0.38	2.15	0.38	1.97
0.58	2.57	0.48	2.31	0.48	2.23	0.48	2.05
0.78	2.67	0.58	2.37	0.58	2.29	0.58	2.10

Table 6.S1 Experimental data for CO_2 uptake on TRI-PE-MCM-41 (cont'd)

25°C		35°C		45°C		55°C	
P (bar)	n (mmol g^{-1})	P (bar)	n (mmol g^{-1})	P (bar)	n (mmol g^{-1})	P (bar)	n (mmol g^{-1})
0.98	2.77	0.67	2.44	0.68	2.34	0.68	2.16
1.97	3.07	0.78	2.49	0.78	2.40	0.78	2.20
3.98	3.53	0.98	2.57	0.88	2.44	0.87	2.25
6	3.93	1.47	2.77	1	2.50	1	2.30
8	4.28	1.96	2.90	1.97	2.72	1.97	2.52
12.01	4.83	3.98	3.29	3.98	3.08	3.98	2.80
16.01	5.33	5.99	3.63	8	3.62	8	3.18
20.02	5.82	8	3.93	12.01	4.08	12.01	3.62
		12.01	4.43	16.01	4.49		
		16.01	4.88	20.01	4.86		
		20	5.30				

Table 6.S2 Experimental data for CO_2 uptake on PE-MCM-41

25°C		35°C		45°C		55°C	
P (bar)	n (mmol g^{-1})	P (bar)	n (mmol g^{-1})	P (bar)	n (mmol g^{-1})	P (bar)	n (mmol g^{-1})
0.18	0.15	0.18	0.13	0.18	0.11	0.18	0.10
0.38	0.25	0.38	0.21	0.38	0.18	0.38	0.14
0.58	0.37	0.58	0.30	0.58	0.24	0.58	0.19
0.78	0.48	0.78	0.38	0.78	0.31	0.78	0.25
0.98	0.60	0.98	0.45	0.98	0.38	0.98	0.31
1.97	1.09	1.97	0.91	1.97	0.71	1.97	0.58

Table 6.S2 Experimental data for CO_2 uptake on PE-MCM-41 (cont'd)

25°C		35°C		45°C		55°C	
P (bar)	n (mmol g^{-1})	P (bar)	n (mmol g^{-1})	P (bar)	n (mmol g^{-1})	P (bar)	n (mmol g^{-1})
3.98	1.93	3.98	1.59	3.98	1.29	3.98	1.00
8	3.28	6	2.19	6.00	1.80	6	1.43
12.01	4.38	8	2.72	8.00	2.26	8	1.85
16.01	5.35	10.01	3.21	10.01	2.69	10.01	2.24
20.01	6.23	12.01	3.67	12.01	3.09	15.01	3.07
25.02	7.29	15.01	4.30	15.01	3.64	20.01	3.77
30.05	8.36	20.01	5.23	20.01	4.45		

Appendix B

Supplementary Data for Chapter 7

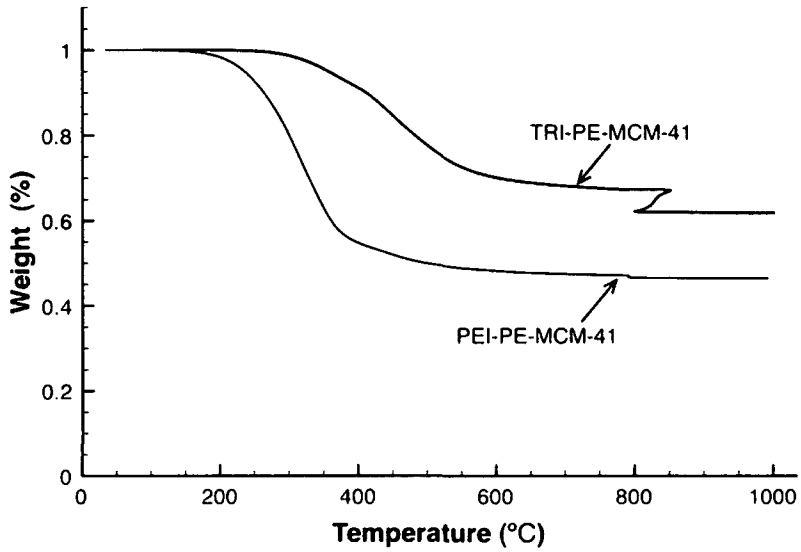

Figure 7.S1 Thermogravimetric analysis profiles of TRI-PE-MCM-41 and PEI-PE-MCM-41

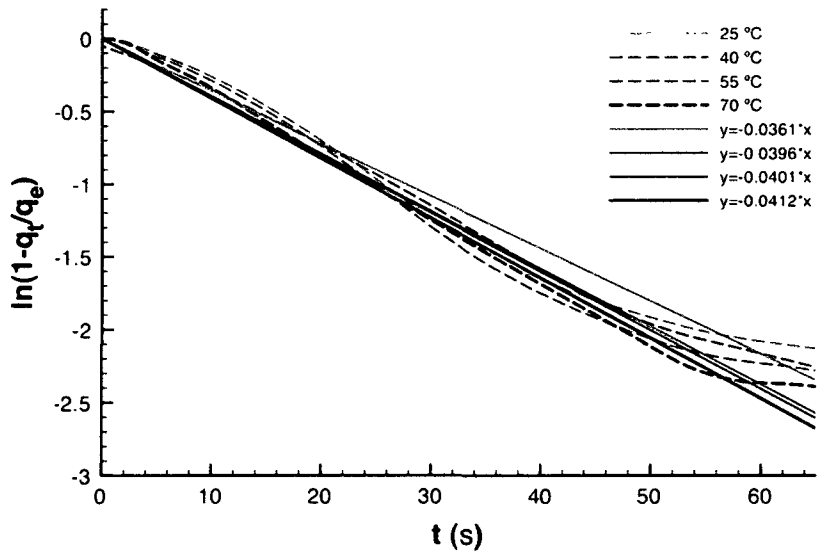

Figure 7.S2 Experimental data (dotted lines) and linear regression (solid lines) for pseudo-first kinetic model for adsorption of CO_2 on TRI-PE-MCM-41

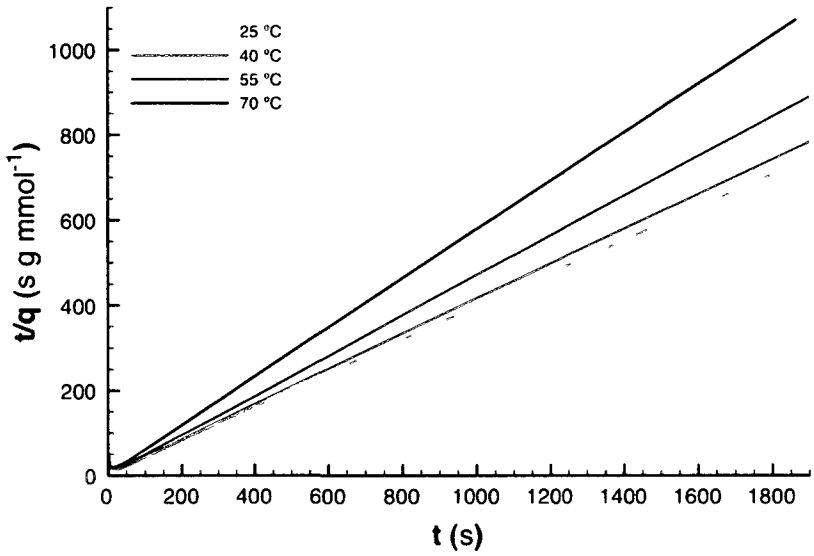

Figure 7.S3 Experimental data (dotted lines) and linear regression (solid lines) for pseudo-second kinetic model for adsorption of CO_2 on TRI-PE-MCM-41

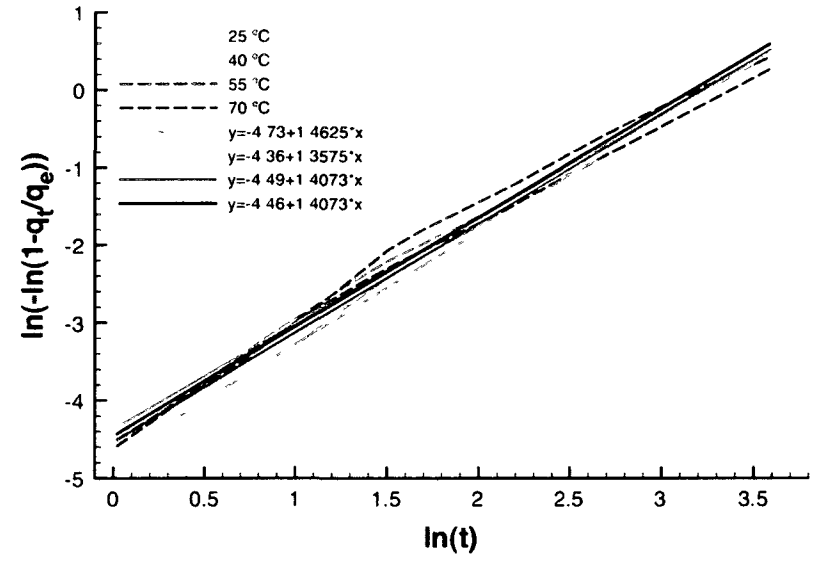

Figure 7.S4 Experimental data (dotted lines) and linear regression (solid lines) for Avrami's kinetic model for adsorption of CO_2 on TRI-PE-MCM-41

Table S1. Linear regression parameters of kinetic data for CO_2 adsorption on TRI-PE-MCM-41

		25 °C	40 °C	55 °C	70 °C
Pseudo-first	Slope	-3.61×10^{-2}	-3.96×10^{-2}	-4.01×10^{-2}	-4.12×10^{-2}
	R^2	0.809	0.899	0.984	0.984
Pseudo-second	Slope	3.90×10^{-1}	4.10×10^{-1}	4.67×10^{-1}	5.72×10^{-1}
	Intercept	7.21	5.40	2.41	5.81
	R^2	0.999	1	0.999	1
Avrami	Slope	1.46	1.36	1.41	1.41
	Intercept	-4.73	-4.36	-4.49	-4.46
	R^2	0.996	0.998	0.991	0.979
Fickian	Slope	-2.63×10^{-2}	-2.92×10^{-2}	-2.94×10^{-2}	-3.02×10^{-2}
	Intercept	-0.5	-0.5	-0.5	-0.5
	R^2	0.924	0.928	0.870	0.926

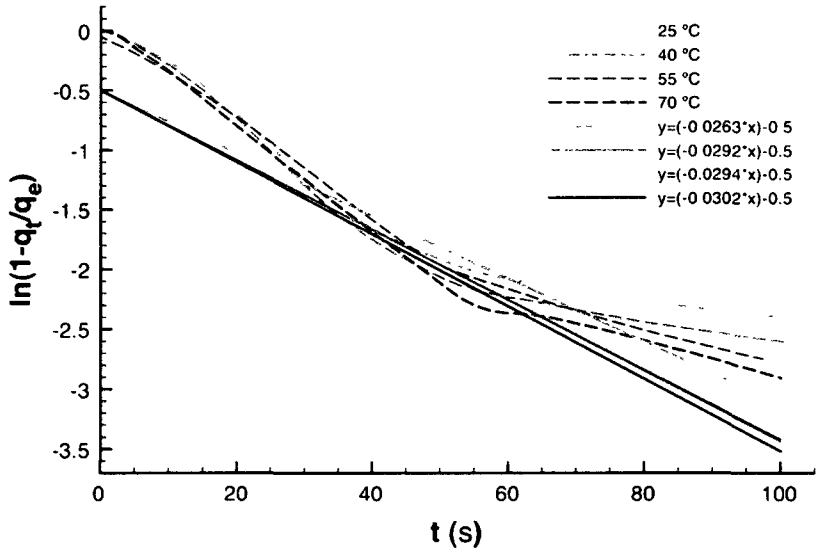

Figure 7.S5 Experimental data (dotted lines) and linear regression (solid lines) of Fickian diffusion model for adsorption of CO_2 on TRI-PE-MCM-41